MORGAN & CLAYPOOL PUBLISHERS

Fundamentals of Electronics: Book 3

Active Filters and Amplifier Frequency Response

Thomas F. Schubert, Jr.
Ernest M. Kim

Synthesis Lectures on Digital Circuits and Systems

Mitchell A. Thornton, *Series Editor*

VISIT…

Fundamentals of Electronics

Book 3

Active Filters and Amplifier Frequency Response

Synthesis Lectures on Digital Circuits and Systems

Editor
Mitchell A. Thornton, ***Southern Methodist University***

The *Synthesis Lectures on Digital Circuits and Systems* series is comprised of 50- to 100-page books targeted for audience members with a wide-ranging background. The Lectures include topics that are of interest to students, professionals, and researchers in the area of design and analysis of digital circuits and systems. Each Lecture is self-contained and focuses on the background information required to understand the subject matter and practical case studies that illustrate applications. The format of a Lecture is structured such that each will be devoted to a specific topic in digital circuits and systems rather than a larger overview of several topics such as that found in a comprehensive handbook. The Lectures cover both well-established areas as well as newly developed or emerging material in digital circuits and systems design and analysis.

Fundamentals of Electronics: Book 3 Active Filters and Amplifier Frequency Response
Thomas F. Schubert, Jr. and Ernest M. Kim
2016

Bad to the Bone: Crafting Electronic Systems with BeagleBone and BeagleBone Black, Second Edition
Steven F. Barrett and Jason Kridner
2015

Fundamentals of Electronics: Book 2 Amplifiers: Analysis and Design
Thomas F. Schubert and Ernest M. Kim
2015

Fundamentals of Electronics: Book 1 Electronic Devices and Circuit Applications
Thomas F. Schubert and Ernest M. Kim
2015

Applications of Zero-Suppressed Decision Diagrams
Tsutomu Sasao and Jon T. Butler
2014

Modeling Digital Switching Circuits with Linear Algebra
Mitchell A. Thornton
2014

Arduino Microcontroller Processing for Everyone! Third Edition
Steven F. Barrett
2013

Boolean Differential Equations
Bernd Steinbach and Christian Posthoff
2013

Bad to the Bone: Crafting Electronic Systems with BeagleBone and BeagleBone Black
Steven F. Barrett and Jason Kridner
2013

Introduction to Noise-Resilient Computing
S.N. Yanushkevich, S. Kasai, G. Tangim, A.H. Tran, T. Mohamed, and V.P. Shmerko
2013

Atmel AVR Microcontroller Primer: Programming and Interfacing, Second Edition
Steven F. Barrett and Daniel J. Pack
2012

Representation of Multiple-Valued Logic Functions
Radomir S. Stankovic, Jaakko T. Astola, and Claudio Moraga
2012

Arduino Microcontroller: Processing for Everyone! Second Edition
Steven F. Barrett
2012

Advanced Circuit Simulation Using Multisim Workbench
David Báez-López, Félix E. Guerrero-Castro, and Ofelia Delfina Cervantes-Villagómez
2012

Circuit Analysis with Multisim
David Báez-López and Félix E. Guerrero-Castro
2011

Microcontroller Programming and Interfacing Texas Instruments MSP430, Part I
Steven F. Barrett and Daniel J. Pack
2011

Microcontroller Programming and Interfacing Texas Instruments MSP430, Part II
Steven F. Barrett and Daniel J. Pack
2011

Pragmatic Electrical Engineering: Systems and Instruments
William Eccles
2011

Pragmatic Electrical Engineering: Fundamentals
William Eccles
2011

Introduction to Embedded Systems: Using ANSI C and the Arduino Development Environment
David J. Russell
2010

Arduino Microcontroller: Processing for Everyone! Part II
Steven F. Barrett
2010

Arduino Microcontroller Processing for Everyone! Part I
Steven F. Barrett
2010

Digital System Verification: A Combined Formal Methods and Simulation Framework
Lun Li and Mitchell A. Thornton
2010

Progress in Applications of Boolean Functions
Tsutomu Sasao and Jon T. Butler
2009

Embedded Systems Design with the Atmel AVR Microcontroller: Part II
Steven F. Barrett
2009

Embedded Systems Design with the Atmel AVR Microcontroller: Part I
Steven F. Barrett
2009

Embedded Systems Interfacing for Engineers using the Freescale HCS08 Microcontroller II: Digital and Analog Hardware Interfacing
Douglas H. Summerville
2009

Designing Asynchronous Circuits using NULL Convention Logic (NCL)
Scott C. Smith and JiaDi
2009

Embedded Systems Interfacing for Engineers using the Freescale HCS08 Microcontroller I: Assembly Language Programming
Douglas H.Summerville
2009

Developing Embedded Software using DaVinci & OMAP Technology
B.I. (Raj) Pawate
2009

Mismatch and Noise in Modern IC Processes
Andrew Marshall
2009

Asynchronous Sequential Machine Design and Analysis: A Comprehensive Development of the Design and Analysis of Clock-Independent State Machines and Systems
Richard F. Tinder
2009

An Introduction to Logic Circuit Testing
Parag K. Lala
2008

Pragmatic Power
William J. Eccles
2008

Multiple Valued Logic: Concepts and Representations
D. Michael Miller and Mitchell A. Thornton
2007

Finite State Machine Datapath Design, Optimization, and Implementation
Justin Davis and Robert Reese
2007

Atmel AVR Microcontroller Primer: Programming and Interfacing
Steven F. Barrett and Daniel J. Pack
2007

Pragmatic Logic
William J. Eccles
2007

PSpice for Filters and Transmission Lines
Paul Tobin
2007

PSpice for Digital Signal Processing
Paul Tobin
2007

PSpice for Analog Communications Engineering
Paul Tobin
2007

PSpice for Digital Communications Engineering
Paul Tobin
2007

PSpice for Circuit Theory and Electronic Devices
Paul Tobin
2007

Pragmatic Circuits: DC and Time Domain
William J. Eccles
2006

Pragmatic Circuits: Frequency Domain
William J. Eccles
2006

Pragmatic Circuits: Signals and Filters
William J. Eccles
2006

High-Speed Digital System Design
Justin Davis
2006

Introduction to Logic Synthesis using Verilog HDL
Robert B.Reese and Mitchell A.Thornton
2006

Microcontrollers Fundamentals for Engineers and Scientists
Steven F. Barrett and Daniel J. Pack
2006

Copyright © 2014 by Morgan & Claypool

All rights reserved. No part of this publication may be reproduced, stored in a retrieval system, or transmitted in any form or by any means—electronic, mechanical, photocopy, recording, or any other except for brief quotations in printed reviews, without the prior permission of the publisher.

Fundamentals of Electronics: Book 3 Active Filters and Amplifier Frequency Response

Thomas F. Schubert, Jr. and Ernest M. Kim

www.morganclaypool.com

ISBN: 9781627055666 paperback
ISBN: 9781627055673 ebook

DOI 10.2200/S00712ED1V03Y201603DCS049

A Publication in the Morgan & Claypool Publishers series
SYNTHESIS LECTURES ON DIGITAL CIRCUITS AND SYSTEMS

Lecture #49
Series Editor: Mitchell A. Thornton, *Southern Methodist University*
Series ISSN
Print 1932-3166 Electronic 1932-3174

Fundamentals of Electronics
Book 3
Active Filters and Amplifier Frequency Response

Thomas F. Schubert, Jr. and Ernest M. Kim
University of San Diego

SYNTHESIS LECTURES ON DIGITAL CIRCUITS AND SYSTEMS #49

MORGAN & CLAYPOOL PUBLISHERS

ABSTRACT

This book, *Active Filters and Amplifier Frequency Response*, is the third of four books of a larger work, *Fundamentals of Electronics*. It is comprised of three chapters that describe the frequency dependent response of electronic circuits. This book begins with an extensive tutorial on creating and using Bode Diagrams that leads to the modeling and design of active filters using operational amplifiers. The second chapter starts by focusing on bypass and coupling capacitors and, after introducing high-frequency modeling of bipolar and field-effect transistors, extensively develops the high- and low-frequency response of a variety of common electronic amplifiers. The final chapter expands the frequency-dependent discussion to feedback amplifiers, the possibility of instabilities, and remedies for good amplifier design.

Fundamentals of Electronics has been designed primarily for use in an upper division course in electronics for electrical engineering students and for working professionals. Typically such a course spans a full academic year consisting of two semesters or three quarters. As such, *Active Filters and Amplifier Frequency Response*, and the first two books in the series, *Electronic Devices and Circuit Applications*, and *Amplifiers: Analysis and Design*, form an appropriate body of material for such a course.

KEYWORDS

active filters, frequency response, Bode plot, filter, Butterworth, low-pass, high-pass, band-pass, band-stop, Chebyshev, switched capacitor, gain margin, phase margin, cutoff frequency, high frequency transistor modeling, Miller's theorem, capacitive coupling, Cascode, Darlington, multipole feedback frequency response, Nyquist stability, dominant pole compensation, compensation networks

Contents

Preface . . . . . **xv**

9 Active Filters **649**

9.1 Bode Plots 650
9.1.1 Bode Plots of the Factors 652
9.2 Filter Characteristics 667
9.3 Butterworth Filters 670
9.3.1 Alternate Definitions: 674
9.3.2 High-pass Butterworth Characterization: 675
9.4 OpAmp Realizations of Butterworth Filters 676
9.4.1 Low-pass OpAmp Filters: 677
9.4.2 High-pass OpAmp Filters: 682
9.4.3 Band-pass and Band-stop OpAmp Filters 685
9.5 Resonant Band-pass Filters 689
9.5.1 *RLC* Realization 691
9.5.2 *RC* Realization 692
9.5.3 Resonant Bandstop Filters 695
9.6 Chebyshev Filters 697
9.6.1 OpAmp Realization of Chebyshev Filters 707
9.7 Comparison of Filter Types 714
9.8 Switched-Capacitor Filters 715
9.8.1 MOS Switch 715
9.8.2 Simple Integrator 719
9.8.3 Gain Stage 720
9.8.4 Low-Pass Filters 722
9.9 OpAmp Limitations 722
9.9.1 Frequency Response of OpAmps 724
9.9.2 OpAmp Slew Rate 726
9.10 Concluding Remarks 728
References 741

10 Frequency Response of Transistor Amplifiers 743

10.1 Frequency Distortion 744
10.1.1 Gain and Phase Response 745
10.1.2 Step and Pulse Response 746
10.2 Dominant Poles 753
10.2.1 Low Cutoff Frequency (High Pass) 753
10.2.2 Low-Pass Response 755
10.3 Effect of Bias and Coupling Capacitors on Low-frequency Response 757
10.3.1 BJT Low-Frequency Response 757
10.3.2 FET Low-Frequency Response 766
10.4 High-Frequency Models of the BJT 768
10.4.1 Modeling a p-n Junction Diode at High Frequencies 770
10.4.2 Modeling the BJT at High Frequencies in the Forward-Active Region 772
10.5 Miller's Theorem 775
10.6 High-Frequency Response of Simple BJT Amplifiers 778
10.6.1 Common-Emitter Amplifier High-Frequency Characteristics 779
10.6.2 Exact Common-emitter High-frequency Characteristics 782
10.6.3 Common-Collector Amplifier High-Frequency Characteristics 786
10.6.4 Common-Base Amplifier High-Frequency Characteristics 789
10.6.5 Common-Emitter with Emitter Degeneration ($CE + R_e$) Characteristics 791
10.7 High-Frequency Models of the FET 795
10.7.1 Dynamic Models for the FET 795
10.8 High-Frequency Response of Simple FET Amplifiers 800
10.8.1 Common-source Amplifier High-Frequency Characteristics 800
10.8.2 Exact Common-Source High-Frequency Characteristics 802
10.8.3 Common-Drain High-Frequency Characteristics 803
10.8.4 Common-Gate High-Frequency Characteristics 804
10.8.5 Common-Source with Source Degeneration ($CS + Rs$) Characteristics 806
10.9 Multistage Amplifiers 810
10.9.1 Capacitor Coupling between Stages 811
10.9.2 DC (Direct) Coupling between Stages 816
10.9.3 Darlington Pair 818
10.9.4 Cascode Amplifier 820
10.10 Concluding Remarks 822

10.11 Problems 831
References 851

11 Feedback Amplifier Frequency Response 853

11.1 The Effect of Feedback on Amplifier Bandwidth (Single-Pole Case) 854
11.2 Double Pole Feedback Frequency Response 857
11.2.1 Frequency Response 859
11.2.2 Step Response 866
11.3 Multipole Feedback Frequency Response 869
11.4 Stability in Feedback Circuits 873
11.4.1 Gain and Phase Margins 874
11.4.2 Nyquist Stability Criterion 879
11.5 Compensation Networks 883
11.5.1 Dominant Pole (Lag) Compensation 884
11.5.2 Lag-Lead (Pole-Zero) Compensation 889
11.5.3 Lead Compensation (Equalizer) 894
11.5.4 Phantom Zero Compensation 898
11.6 Concluding Remarks 899
11.7 Problems 903
References 921

Authors' Biographies 923

Preface

In the previous two books of this series, all electronic circuit operation was considered to be either at near-zero frequency or in the "midband" region of operation. The midband range of frequencies, vitally important to amplifier discussions, is characterized by two basic simplifying assumptions:

- The midband frequencies are large enough so that discrete circuit capacitors appear to have negligible impedance with respect to the resistances in the circuit, and
- The midband frequencies are small enough so that the active elements (transistors, OpAmps, etc.) appear to have frequency-invariant properties.

It is the purpose of this book to explore the variation of circuit behavior over the entire range of frequencies. In addition to exploring frequency dependence, the time domain equivalence of these effects is explored.

A review of the characteristics of ideal filters and frequency response plots leads into the design of active filters. Active Butterworth and Chebyshev filter design is discussed in this section using OpAmps as the active circuit elements. Discussion of passive filters and filters with other active elements is saved until the chapter in Book 4 on communication circuits. The frequency response limitations of OpAmps provide an introduction to limitations common in other devices.

Transistor amplifier frequency response is first discussed through the effects of coupling and bypass capacitors. Once those principles are mastered, modified models for the diode, BJT and FET are introduced to model the high-frequency limitations of common devices and the result of these limitations on the frequency response of amplifier circuits. The effect of feedback on frequency response is initially presented as a special case of stabilization: here stabilization against variation in element value change due to frequency. Feedback effects on pole migration is emphasized. Compensation against possible instabilities or oscillations is explored extensively.

In this book, amplifier oscillations are considered an undesirable condition. In the next book of this series, these instabilities are explored in the design of linear oscillators.

Thomas F. Schubert, Jr. and Ernest M. Kim
March 2016

CHAPTER 9

Active Filters

An electronic filter is defined as a device that separates, passes, or suppresses an electronic signal (or group of signals) from a mixture of signals. Most common among all possible filters are those that separate signals according to the signal frequency content. This type of filter is found in virtually every common electronic device. As an example, consider a radio receiver. The antenna system for a radio receiving system receives a wide range of frequencies associated with many distinct radio stations. A radio receiver attached to that antenna system can be tuned to receive any particular station: its input filter section passes only those frequencies associated with that station and blocks all other frequencies. Of interest in this chapter are the characterization and design of such frequency-selective filters

Electronic frequency-selective filters are divided into two major groups based on the circuit elements making up the filter: passive filters and active filters. Passive electronic filters are commonly constructed using the basic passive building blocks familiar to all electrical engineers: resistors, capacitors, and inductors. These filters are of great value particularly in high power and high frequency applications.[1] In low frequency applications, the high-value inductances required in passive filter designs present several problems. Large value inductors are physically large, heavy, non-linear, and usually have a relatively large loss factor. In addition, the magnetic fields they generate are a source of electromagnetic interference. In many designs one or more of these features is undesirable. It is therefore often necessary to design filters that contain only resistors and capacitors. The addition of another common building block, the operational amplifier, allows for the design of these lower frequency filters as efficient and cost effective devices. The inclusion of an active device in the design has led to calling these filters, "active filters."

The approach to active filter design and characterization developed in this chapter begins with a review of frequency response characterization in the form of Bode plots. This form of graphical representation of filter response leads to a presentation of the four basic ideal types of frequency-selective filters: high-pass, low-pass, bandpass, and bandstop. Since ideal filter response is not achievable in the real world, several common, realistic filter response approximations are discussed and compared. The design process necessary to realize the four basic filter types using OpAmps, resistors, and capacitors is developed and explored.

Resistor size, weight, and power dissipation can also present problems to the filter designer. In integrated circuits, one low-frequency solution to the problem is switched-capacitor filters.

[1] A discussion of the uses of passive filters in communication circuits can be found in Chapter 15 (Book 4). Of particular interest is the discussion of tradeoffs between active and passive filters.

These filters are closely related to standard active filters where the resistors are replaced by rapidly switched capacitors. A discussion of this variation of active filters is found in Section 9.7.

Although OpAmps are highly useful electronic building blocks, they do have limitations. Most significant in filter design is the degradation in the voltage gain with frequency. The chapter ends with a discussion of the limitations of active filters designed with the use of OpAmps.

9.1 BODE PLOTS

Characterization of electronic systems in the frequency domain is directly related to time-domain system response. The response of a linear time-invariant system, $x_o(t)$, to an arbitrary input, $x_i(t)$, can be characterized, in the time-domain, by its impulse response, $h(t)$:

$$x_o(t) = \int_0^t h(t-\tau)x_i(\tau)\,d\tau. \tag{9.1}$$

While the convolution integral of Equation (9.1) has great utility in many situations,[2] a frequency-domain characterization of the system is more typical. The frequency-domain response of a system can be obtained by taking the Fourier Transform of the output quantity, $x_o(t)$:

$$X_o(\omega) = \mathfrak{F}\{x_o(t)\} = \int_{-\infty}^{\infty} x_o(t)e^{-j\omega t}\,dt \tag{9.2}$$

which reduces to

$$X_o(\omega) = H(\omega)X_i(\omega). \tag{9.3}$$

The spectrum of the output quantity, $X_o(\omega)$, is the product of the input quantity spectrum, $X_i(\omega)$, and the transfer function of the system, $H(\omega)$. The impulse response and the transfer function of a system are related by the Fourier Transform:

$$H(\omega) = \mathfrak{F}\{h(t)\}. \tag{9.4}$$

This frequency-domain transfer function is most typically characterized by its fundamental parts in polar form:

- $|H(\omega)|$—the magnitude response, and
- $\angle H(\omega)$—the phase response.

One of the most useful representations of these two quantities is a pair of plots. The typical format for these plots is the magnitude (on either a linear or a decibel scale) or the phase (in either degrees or radians) as the ordinate and frequency (on a logarithmic scale) as the abscissa. While

[2]Time-domain characteristics of electronic circuits and the relationship of these characteristics to the frequency-domain characteristics are discussed in Chapters 10 and 11 in Book 3 and Chapters 12 and 13 in Book 4.

many computer simulation programs exist for the efficient creation of such plots, much insight into the functioning of a filter (or any electronic circuit) and the dependence of the responses to circuit parameter variation can be gained by the manual creation of simple straight-line approximations to these magnitude and phase plots. Plots of the magnitude of the transfer function, in decibels, and the phase of the transfer function are called *Bode plots*.[3] The two plots together form a *Bode diagram*.

Mathematical Derivations

The response of a linear system to sinusoidal inputs can be described as the ratio of two polynomials in frequency, ω:

$$H(\omega) = K_o \frac{Z_m(\omega)}{P_n(\omega)}. \tag{9.5}$$

Here $Z_m(\omega)$ is an mth order polynomial whose roots identify the m zeroes of the response. The roots of $P_n(\omega)$ identify the n poles. For all real electronic systems, the response must not increase as frequency becomes infinite; thus the number of poles must be equal to or larger than the number of zeroes, $n \geq m$. Equation (9.5) can be expanded to be of the form:

$$H(\omega) = K_o \frac{1 + (j\omega)a_1 + (j\omega)^2 a_2 + \ldots + (j\omega)^m a_m}{1 + (j\omega)b_1 + (j\omega)^2 b_2 + \ldots + (j\omega)^n b_n}. \tag{9.6}$$

The numerator and denominator polynomials, $Z_m(\omega)$ and $P_n(\omega)$ respectively, can each be written as a factored product of multiples of four types of simple function, hereafter identified as *factors*, $\{F(\omega)\}$:

1. K_o — a constant
2. $j\omega$ — a root at the origin
3. $1 + \frac{j\omega}{\omega_o}$ — a simple root at $\omega = \omega_o$
4. $1 + 2\zeta\frac{j\omega}{\omega_o} + \left(\frac{j\omega}{\omega_o}\right)^2$ — a complex conjugate root pair.

Each of these four simple functions has a straight-line approximate Bode representation. The use of decibels (a logarithmic function) as a vertical scale for the magnitude plot and a linear scale for phase converts the product of the factors into the *sum* of the factor magnitudes (in dB) and the *sum* of the factor phases: division becomes subtraction. Therefore the total system response plot becomes the algebraic sum of the plots of the individual simple factors describing the system.

[3]Named for Hendrik Wade Bode (1905–1982). One early reference is his book Network Analysis and Feedback Design, Van Nostrand, New York, 1945.

9.1.1 BODE PLOTS OF THE FACTORS

The Bode *magnitude* straight-line representation of each of the four simple factors is unique. The Bode *phase* straight-line representation is unique for two of the factors (a constant and a root at the origin) and universally standardized for a third (a simple root). However, a variety of approximate representations for the phase of a complex conjugate root pair exists in the literature. The representation for a constant and for a root at the origin is exact: the other two factor representations are asymptotic in the case of magnitude and approximate in the case of phase. A discussion of each Bode representation follows. A summary can be found in Table 9.1.

A constant:
The most simple of the factors is a constant.

$$F_C(\omega) = K. \tag{9.7}$$

Here the magnitude is constant at $20\log|K|$. The phase plot is also constant at $\theta = 0°$ or $\theta = 180°$ depending on the mathematical sign of K. Each plot is an exact representation of the factor.

A pole or zero at zero frequency:
A pole or zero at the origin also has a simple Bode representation. The factor is of the form:

$$F_0(\omega) = j\omega. \tag{9.8}$$

The magnitude plot is a straight line on a logarithmic frequency scale:

$$|F_0(\omega)|_{\text{dB}} = 20\log|j\omega| = 20\log(\omega). \tag{9.9}$$

If the factor is in the numerator (indicating a zero), this straight line has a slope of $+20$ dB/decade:[4] denominator factors (poles) have a slope of -20 dB/decade. In each case the line passes through the point {0 dB, 1 rad/s).

The factor phase is constant at $\theta = 90°$ (or π radians). Consequently, the phase plot for zeroes will be at $+90°$ and at $-90°$ for poles.

A simple pole or zero at $\omega = \omega_o$:
Single poles and zeroes not at the origin have more complex plots. The factor form for a simple pole is:

$$F_1(\omega, \omega_o) = 1 + \frac{j\omega}{\omega_o}, \tag{9.10}$$

[4]A decade is a change in frequency by a factor of ten (10). A slope of 20 dB/decade is also identified in some sources as 6 dB/octave, where an octave is a frequency change by a factor of two (2).

where ω_o is the pole (zero) frequency. The magnitude of the factor (in dB) is given by:

$$|F_1(\omega, \omega_o)|_{\text{dB}} = 20\log\sqrt{1+\left(\frac{\omega}{\omega_o}\right)^2} = 10\log\left(1+\left(\frac{\omega}{\omega_o}\right)^2\right). \tag{9.11}$$

The phase is given by:

$$\angle F_1(\omega, \omega_o) = \tan^{-1}\left(\frac{\omega}{\omega_o}\right). \tag{9.12}$$

These two components of the simple factor are shown in Figure 9.1 as if the factor were in the denominator (representing a pole). Also shown in the figure are the Bode straight-line approximate plots.

The Bode plot of the magnitude is an asymptotic approximationand is made up of two intersecting straight lines that form a piecewise continuous plot. If $\omega \ll \omega_o$, $F(\omega) \approx 1$ and the magnitude plot is constant at 0 dB. If $\omega \gg \omega_o$,

$$|F_1(\omega, \omega_o)|_{\text{dB}} \approx 10\log\left(\left(\frac{\omega}{\omega_o}\right)^2\right) = 20\log(\omega) - 20\log(\omega_o). \tag{9.13}$$

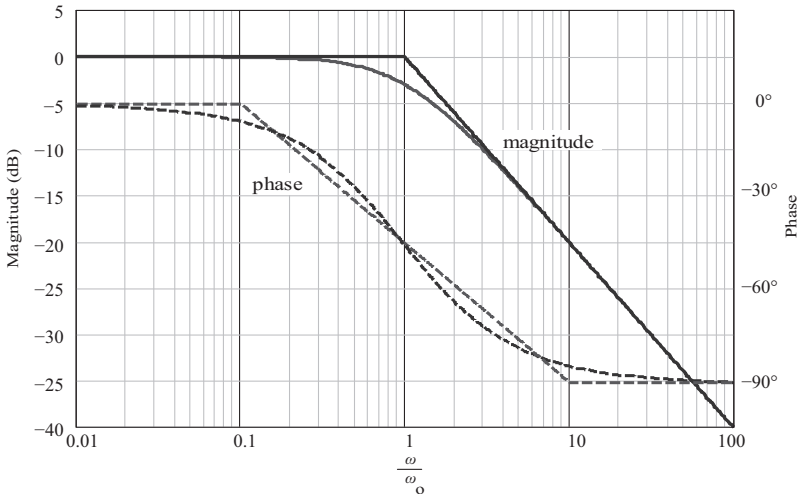

Figure 9.1: A simple pole Bode diagram.

The asymptote is a straight line with slope of 20 dB/decade that intersects the 0 dB line at $\omega = \omega_o$. The Bode approximation transitions between the two asymptotic lines at the root frequency where the approximation has its greatest error ($20\log(2) \approx 3.01$ dB).

As can be seen in Figure 9.1, the factor phase never exceeds 90° and essentially all phase change takes place within ±one decade of ω_o($\angle F_1(0.1\omega_o, \omega_o) = 5.71°$ and $\angle F_1(10\omega_o, \omega_o) = 84.29°$). Beyond one decade from the root, ω_o, the phase is approximated by a constant:

$$\omega < 0.1\omega_o \qquad —\angle F_1(\omega, \omega_o) = 0°$$
$$\omega > 10\omega_o \qquad —\angle F_1(\omega, \omega_o) = 90°.$$

Within ± decade of ω_o, the phase can be approximated by a straight line of slope 45°/decade:

$$0.1\omega_o < \omega < 10\omega_o \qquad —\angle F(\omega) = 45°\{\log(10\omega/\omega_o)\}.$$

This straight-line Bode approximation has a maximum error of ∼ 5.71°.

The error introduced by the Bode straight-line approximations has distinct symmetry about ω_o (Figure 9.2). Any corrections to the plots, if necessary, are accomplished by interpolation and comparison to standard plots. Some data points that are helpful in making accurate corrections are:

- Magnitude plot
  - The magnitude error at ω_o is 3.01 dB
  - The magnitude error at ± one octave ($0.5\omega_o$ and $2\omega_o$) is 0.97 dB
- Phase plot
  - Slope at ω_o is ≈ 66°/decade
  - The phase error is zero at $0.159\omega_o$, ω_o, and $6.31\omega_o$
  - The phase error at ± one decade is ±5.71°

Complex conjugate pole or zero pairs

A complex conjugate root pair presents a more complex relationship. The appropriate form of the factor is given by:

$$F_2(\omega, \omega_o, \zeta) = 1 + 2\zeta\frac{j\omega}{\omega_o} + \left(\frac{j\omega}{\omega_o}\right)^2 \tag{9.14}$$

where ω_o is identified as the resonant frequency and ζ is the damping factor.[5] A plot of the magnitude and phase response for a complex pair of poles with the damping factor as a parameter ($0.2 \leq \zeta \leq 0.9$ in increments of 0.1) is shown in Figure 9.3.

The variation of the plot with damping coefficient makes straight-line approximations near the resonant frequency questionable. Still, at about a third of a decade or larger from the resonant frequency, reasonable approximations of the magnitude plot can be made. Once again, if

[5]The damping factor lies in the range, $0 \leq \zeta < 1$, for complex conjugate root pairs.

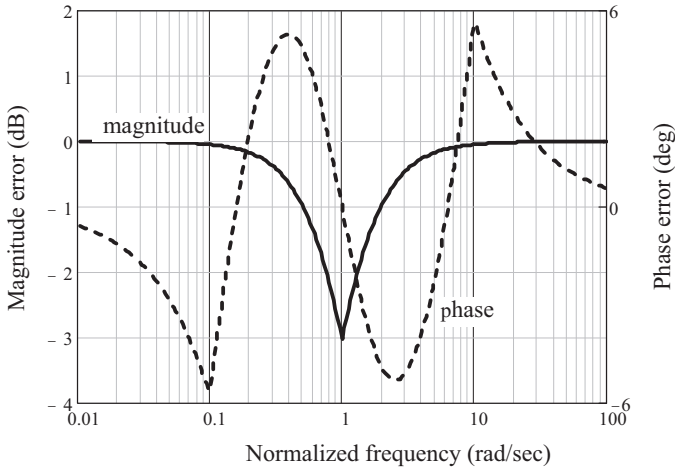

Figure 9.2: Bode straight-line approximation error: simple root.

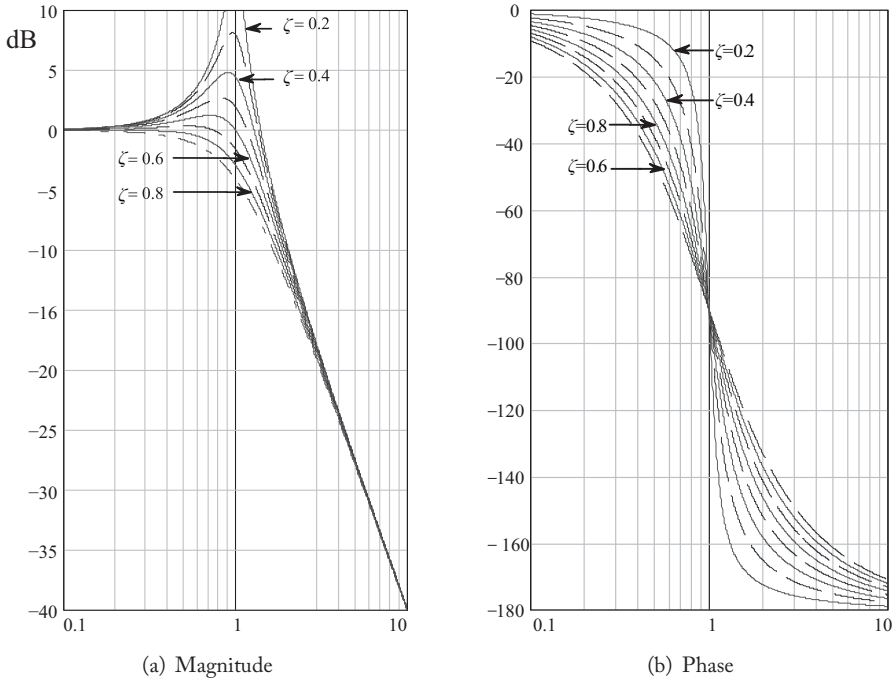

Figure 9.3: Complex conjugate pair pole frequency response.

$\omega \ll \omega_o$, $F(\omega) \approx 1$ and the approximate magnitude plot is constant at 0 dB. If $\omega \gg \omega_o$,

$$|F_2(\omega, \omega_o, \zeta)|_{\text{dB}} \approx 20 \log \left| \left(\frac{j\omega}{\omega_o} \right)^2 \right| = 40 \log(\omega) - 40 \log(\omega_o). \tag{9.15}$$

In this region the magnitude has a slope of 40 dB/decade with an intercept of the 0 dB axis at $\omega = \omega_o$. Near the resonant frequency, there can be a large difference between the approximate Bode magnitude plot and the true magnitude plot. Depending on the application, corrections to the curve may be necessary. These corrections can usually be accomplished with the addition of only a few data points and interpolation. Two helpful data points are the magnitude at the resonant frequency and the magnitude of the peak in the curve (if one exists). The magnitude at the resonant frequency is given by:

$$|F_2(\omega_o, \omega_o, \zeta)|_{\text{dB}} = 20 \log(2\zeta). \tag{9.16}$$

For damping coefficients less than, a $1/\sqrt{2}$ valley occurs in the magnitude of the factor. This valley will occur at the maximum difference between the true magnitude plot and the Bode straight line approximation (Figure 9.4). Interesting, this valley in the factor magnitude plot is usually encountered with the factor in the denominator and is consequently identified in the literature as a "peak." If only the factor is considered, the valley (peak) occurs at a frequency somewhat lower than the resonant frequency:

$$\omega_{peak} = \omega_o \sqrt{1 - 2\zeta^2}, \tag{9.17}$$

and has value,

$$\left|F_2(\omega_{peak}, \omega_o, \zeta)\right|_{\text{dB}} = 20 \log\left(2\zeta\sqrt{1 - \zeta^2}\right). \tag{9.18}$$

In cases where a complex-conjugate pair of poles cancels lower frequency zeroes so that the asymptotic plot is a constant for frequencies higher than the resonant frequency, the peak, necessarily of the same magnitude, occurs at a frequency somewhat higher than the resonant frequency:

$$\omega_{peak} = \frac{\omega_o}{\sqrt{1 - 2\zeta^2}}. \tag{9.19}$$

The Bode phase plot for a complex root pair is also simplified into a three-segment, straight-line plot. However, the damping coefficient complicates the location of the transition between segments. At frequencies much lower than the resonant frequency, the phase is near constant at 0°: at frequencies much higher than ω_o, the phase is near constant at 180°. Near ω_o the Bode approximate curve is a straight line joining the other segments.

The location of the transition points between the segments of the approximate Bode phase plot is not uniformly described in the literature: a ζ-independent approximation and at least two approximations that depend on the value of ζ are to be found. The ζ-independent approximation

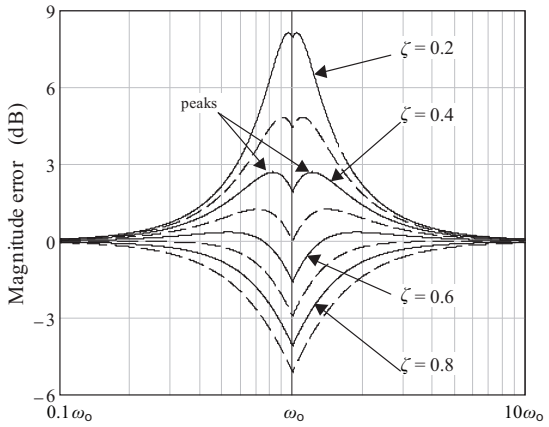

Figure 9.4: Bode straight-line magnitude error: complex conjugate root pair.

chooses a transition points at ± one decade, while the most prevalent of the ζ-dependent approximations vary the transition points (as a fraction of a decade) linearly with damping coefficient, ζ.

Of the ζ-dependent approximations found in the literature, it has been shown that the decade-fraction approximation more closely approximates the phase plot variation with damping coefficient under a variety of criteria. The decade-fraction approximation identifies the transition frequencies as lying $\pm\zeta$ decades from the resonant frequency. The constant phase regions are a function of ζ and are described as:

$$\begin{aligned} \omega < \omega_o 10^{-\zeta} \qquad & -\angle F_2(\omega, \omega_o, \zeta) = 0^\circ \\ \omega > 10^{\zeta}\omega_o \qquad & -\angle F_2(\omega, \omega_o, \zeta) = 180^\circ. \end{aligned}$$

The phase between the two constant phase regions is approximated by a straight line of slope $(90/\zeta)^\circ$/decade passing through the point $\omega_o, 90^\circ$:

$$\omega_o 10^{-\zeta} < \omega < 10^{\zeta}\omega_o \qquad -\angle F_2(\omega, \omega_o, \zeta) = \frac{90^\circ}{\zeta}\left(\log\left(\frac{\omega}{\omega_o}\right)\right) + 90^\circ$$

was the case in first order factors, the error introduced by the Bode straight-line approximations has distinct symmetry about ω_o. Any corrections to the plots, if necessary, are accomplished by interpolation and comparison to standard plots. Some data points that are helpful in making accurate corrections to the phase plot are:

- Phase plot slope at ω_o is $\approx (132/\zeta)^\circ$/decade

- The phase error goes to zero at:
  - $\omega = \omega_o$
  - $\omega = 10^{\pm(0.3\zeta^2+0.49\zeta+0.01)}$.
- The magnitude of the phase error at the transition points ($\omega = \omega_o 10^{\pm\zeta}$) is:
  - $\approx -15.8\zeta + 27.2 \quad$ for $\zeta \geq 0.4$
  - $= 10\zeta^3 - 22.8\zeta^2 - 0.7\zeta + 23.5 \quad$ (all values of ζ).

The decade-fraction ζ-dependent Bode phase approximation is shown in Figure 9.5 for two values of ζ along with the actual phase plots. Helpful data points, as identified above, are marked with a "+" sign.

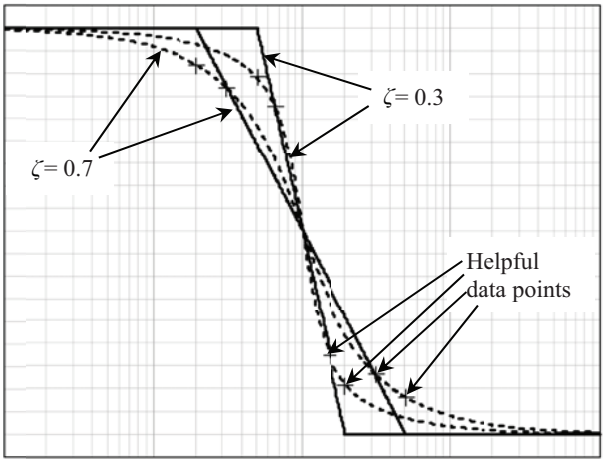

Figure 9.5: The decade-fraction ζ-dependent Bode phase approximation.

The Bode approximate plots for each of the four factors are summarized in Table 9.1 as if the factors are in the denominator. Factors in the numerator will have *positive* slopes and mathematical signs but otherwise be similar in shape. Total Bode plots are the sum of the plots of the factors.

Time delay

Systems with an inherent time delay, t_d, will experience a fifth factor: a phase shift that is linear with frequency:

$$F_D(\omega) = e^{-j\omega t_d}.$$

The delay factor has a Bode magnitude plot that is constant at zero dB: the system Bode magnitude plot is unchanged by the factor. Unfortunately the phase is linear with frequency $\{\phi = -t_d\omega\}$ and

does not have a "nice" plot on a logarithmic frequency scale: each decade in frequency experiences ten times the phase variation of the decade directly lower in frequency. Typically, any system delay is treated separately from the Bode phase plots: in systems where the time delay is small compared to the period of the highest frequency present, delay effects are usually considered insignificant and consequently ignored. A Bode diagram of the delay factor is shown in Figure 9.6.

Table 9.1: Bode factor magnitude and phase plots

Factor	Bode Magnitude Plot	Bode Phase Plot
K	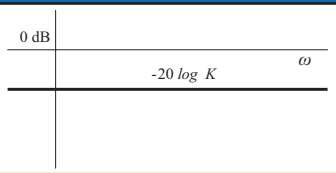	
$j\omega$	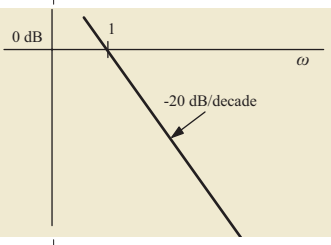	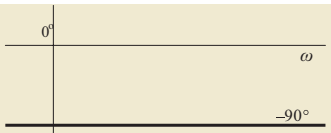
$1+\frac{j\omega}{\omega_o}$	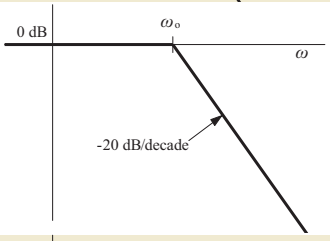	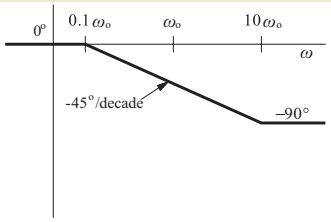
$1+2\zeta\frac{j\omega}{\omega_o}+\left(\frac{j\omega}{\omega_o}\right)^2$	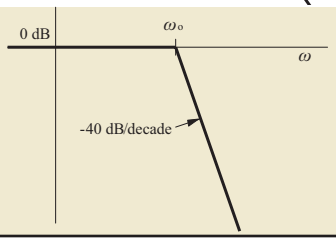	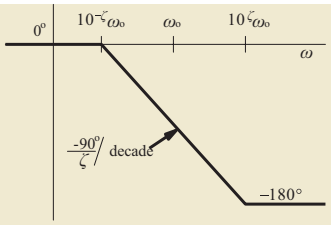

Temporal frequency vs. angular frequency

Theoretical derivations of Bode factors tend to utilize angular frequency (ω: rad/s). However, in the real world, it is likely that systems will be described using temporal frequency (f: Hz).

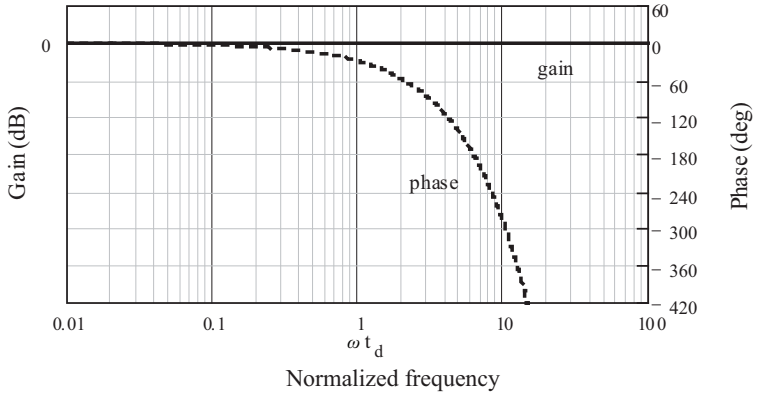

Figure 9.6: Time delay factor Bode diagram.

The functional form of the response, $H(\omega)$ or $H(f)$, is identical and conversions can be made using $\omega = 2\pi f$. The only other difference appears in a difference in the constant factor F_C for a particular system. If there are simple roots at the origin ($F_0 = j\omega$), the constant terms in $H(\omega)$ and $H(f)$ for the system {K_ω and K_f respectively} will differ by a factor:

$$K_f = (2\pi)^{m-n} K_\omega.$$

Where $m - n$ is the number of simple roots at the origin in the numerator minus those in the denominator.

Example 9.1 (Drawing Bode plots)
Draw the Bode diagram for the following transfer function:

$$H(\omega) = \frac{\left[0.836 \times 10^{-3}\right][j\omega]^2}{\left[1 + \frac{j\omega}{150}\right]\left[1 + \frac{j\omega}{800}\right]\left[1 + \frac{j\omega}{625 \times 10^3} + \frac{(j\omega)^2}{250 \times 10^9}\right]}.$$

Solution:
The Bode diagram consists of the Bode magnitude plot and the Bode phase plot. The given transfer function contains all of the primary factor types:

- a constant
- two zeroes at the origin
- two simple poles

- a complex conjugate pair of poles

The Bode magnitude plot for the constant is a horizontal line at:

$$20\log\left(0.836\times10^{-3}\right)=-61.56\,\text{dB}.$$

The Bode magnitude plot for the two zeroes at the origin has slope of +40 dB/decade (2 × 20 dB/decade) and passes through (0 dB, 1 rad/sec). The simple poles each introduce a slope increment of −20 dB/decade beginning at the pole frequencies:

$$\omega_{p1}=150\,\text{rad/sec}\quad\text{and}\quad\omega_{p2}=800\,\text{rad/sec}.$$

The complex pair of poles will introduce a slope increment of −40 dB/decade at the resonant frequency:

$$\omega_o^2=250\times10^9\qquad\Rightarrow\qquad\omega_o=500\times10^3\,\text{rad/sec}.$$

The pole pair damping coefficient is calculated to be:

$$\frac{2\zeta}{\omega_o}=\frac{1}{625\times10^3}\qquad\Rightarrow\qquad\zeta=0.4.$$

The magnitude at the resonant frequency can then be (optionally) corrected by determining:

$$|F_2\left(\omega_o,\omega_o,0.4\right)|=2\times0.4=0.8\qquad\Rightarrow\qquad-1.94\,\text{dB}.$$

Since the damping coefficient is less than $1/\sqrt{2}$ and the factor cancels out lower frequency zeroes, a peak in the magnitude response exists above the resonant frequency at:

$$\omega_{peak}=\omega_o\sqrt{1-2\zeta^2}=400\times10^3(0.825)=329.9\times10^3\,\text{rad/sec}.$$

Consequently, the other optional correction point has value:

$$\left|F_2\left(\omega_{peak},\omega_0,0.4\right)\right|=2(0.4)\sqrt{1-0.4^2}=0.733\qquad\Rightarrow\qquad-2.70\,\text{dB}.$$

Since the complex conjugate pair are poles, the factor lies in the denominator, the slope is −40 dB/decade, and the signs of the magnitude corrections are reversed (making them both, in this case, positive).

The magnitude plot is constructed as follows:

- A low-frequency starting point is found where the sum of all factors is known and below any pole (or zero) frequencies (other than those at the origin). Here $\omega=10$ is a good choice (evaluate the constant and the zeroes at the origin): $|H(10)|\approx-61.56+20\,\text{dB}+20\,\text{dB}=-21.56\,\text{dB}$.
- The slope of the plot at the above point is 20 dB/decade × (number of poles at origin), i.e., 40 dB/decade.

- The pole and zero frequencies are located and marked: Simple poles (down) and zeroes (up) by an arrow. Similarly, complex conjugate pairs are marked by a double arrow.
- The plot slope is incremented at the arrow frequencies by 20 dB/decade in the direction of the arrow. Multiple arrows at the same frequency indicate a multiplicative change in slope.
- Any higher order corrections are then made (if desired).

The resultant uncorrected Bode straight-line magnitude plot, four optional correction points (marked by "+"), and the exact magnitude plot for this system are shown in Figure 9.7.

The Bode phase plot for the constant and each of the zeroes at the origin are simple horizontal lines at 0° and 90° respectively. Each simple pole will increment the phase by −45°/decade at one decade below the pole frequency and decrement the phase by the same quantity one decade above the pole frequency. For the complex conjugate pair phase plot, the frequency range where the phase changes must be calculated by determining the quantity:

$$10^{\zeta} = 10^{0.4} = 2.51.$$

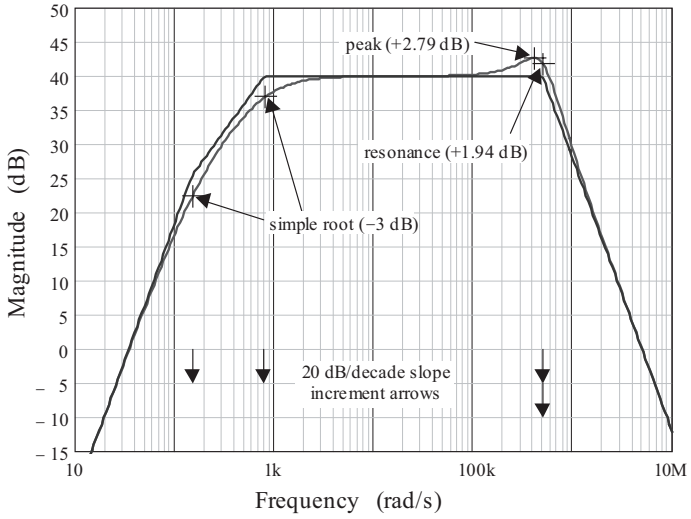

Figure 9.7: Magnitude of the frequency response for Example 9.1 with the Bode approximation overlay.

The transition frequencies for the phase change are then determined:

$$\frac{\omega_o}{2.51} < \omega < 2.51\omega_o \qquad \Rightarrow \qquad 199 \times 10^3 < \omega < 1.26 \times 10^6.$$

Since the factor is in the denominator, the phase plot between the transition frequencies has a slope increment of:

$$\frac{-90}{\zeta} = -225^\circ/\text{decade}.$$

The phase plot is constructed as follows:

- A low-frequency starting point is found where the sum of all factors is known and at least one decade below any pole (or zero) frequencies (other than those at the origin): here $\omega = 0.1$ is a good choice: $\angle H(0.1) \approx 0^\circ + 90^\circ + 90^\circ - 0^\circ - 0^\circ - 0^\circ = 180^\circ$.
- The phase plot transition frequencies are located and marked. Simple poles and zeroes by opposing arrow pairs at one tenth and ten times the pole or zero frequency (15 & 1500; 80 & 8000): complex conjugate root pairs by opposing arrow pairs at the calculated slope transition frequencies (199×10^3 & 1.26×10^6).
- The phase plot slope is changed at the arrow frequencies by the appropriate amount in the direction of the arrow.
- Any higher order corrections are then made (if desired).

The system uncorrected Bode straight-line approximate phase plot and the exact phase plot are shown in Figure 9.8. Six optional correction points (marked by "+") are also shown. Note that while these optional correction points improve the curve in regions where roots are far apart, in regions where the root transition regions overlap (i.e., at 80 and 1500 rad/s), their use may not improve the overall curve.

Example 9.2 (Drawing Bode plots—alternate method)
Draw the Bode diagram for the following transfer function:

$$H(\omega) = \frac{-1.25 \times 10^{-3}[j\omega]^2}{\left[1 + \frac{j\omega}{100}\right]\left[1 + \frac{j\omega}{800}\right]\left[1 + \frac{j\omega}{100 \times 10^3}\right]\left[1 + \frac{j\omega}{600 \times 10^3}\right]}.$$

Solution:

The Bode diagram consists of the Bode magnitude plot and the Bode phase plot. The given transfer function contains three of the primary factor types:

- a constant

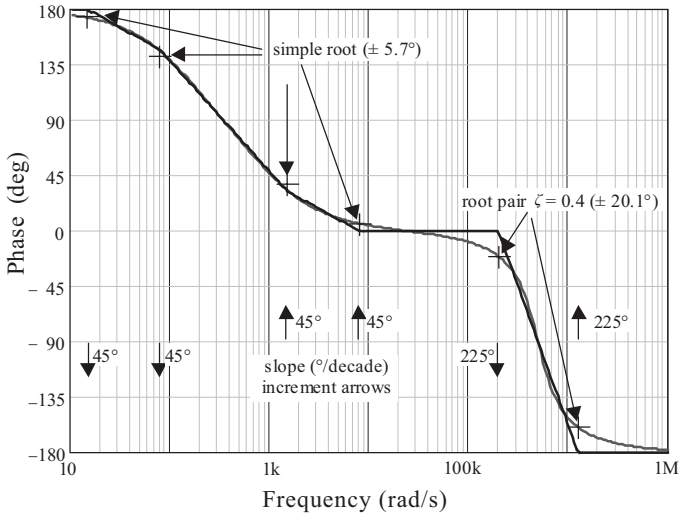

Figure 9.8: Phase of the frequency response for Example 9.1 with the Bode approximation overlay.

- two zeroes at the origin
- four simple poles
  - two at low frequencies (100 and 800 rad/sec)
  - two at high frequencies (100 and 600 krad/sec)

This particular form of the transfer function is quite common in electronic applications. Low-frequency poles (in this case, two) are canceled by the same number of zeroes at the origin resulting in a middle range of frequencies (the midband region) where the transfer function is essentially constant, and regions of decreasing gain as frequency varies from the midband region for both higher and lower frequencies. Similarly, the phase is relatively constant in the midband region. In such a situation, the Bode plot can be begun in the midband region and progress outwards. One should note that this method is not dependent on the poles being simple: the presence of complex conjugate pole pairs does not change the method described as long as there is a midband region of essentially constant gain or phase.

The value of the transfer function in the midband region can be determined by assuming a midband frequency, ω_{mid}, that is conceptually much larger than the largest of the low-frequency poles, but much smaller than the smallest of the high-frequency poles. Under that assumption, the pole factors take on a simpler form and result in an approximate transfer function value in the

midband region:

$$H\left(\omega_{mid}\right) \approx \frac{-1.25 \times 10^{-3}\left[j\omega_{mid}\right]^2}{\left[\frac{j\omega_{mid}}{100}\right]\left[\frac{j\omega_{mid}}{800}\right][1][1]} = -100.$$

The Bode magnitude plot for this example in the midband region becomes a horizontal line at: $20\log|-100| = 40\,\text{dB}$.

The magnitude plot is constructed as follows:

- The plot begins in the midband region with a horizontal line at the midband gain value: here, 40 dB.
- The pole and zero frequencies are located and marked: Simple poles (down) and zeroes (up) by an arrow. Similarly, complex conjugate pairs are marked by a double arrow.
- The plot slope is incremented at the arrow frequencies by 20 dB/decade in the direction of the arrow. Multiple arrows at the same frequency indicate a multiplicative change in slope.
- Any higher order corrections are then made (if desired).

The resultant uncorrected Bode straight-line magnitude plot and the exact magnitude plot for this system are shown below in Figure 9.9.

The Bode phase plot can be similarly constructed from the midband outward. The phase plot is constructed as follows:

- The plot begins in the midband with a horizontal line at the midband phase value: here, $\angle H(\omega_{mid}) \approx \angle(-100) = \pm 180°$.

  Since poles introduce negative angles, $-180°$ is more commonly chosen.
- The phase plot transition frequencies are located and marked. Simple poles and zeroes by opposing arrow pairs at one tenth and ten times the pole or zero frequency: complex conjugate root pairs by opposing arrow pairs at the calculated slope transition frequencies with the appropriate slope increment noted.
- The phase plot slope is changed at the arrow frequencies by the appropriate amount in the direction of the arrow.
- Any higher order corrections are then made (if desired).

The system uncorrected Bode straight-line approximate phase plot and the exact phase plot are shown as the second plot (Figure 9.10).

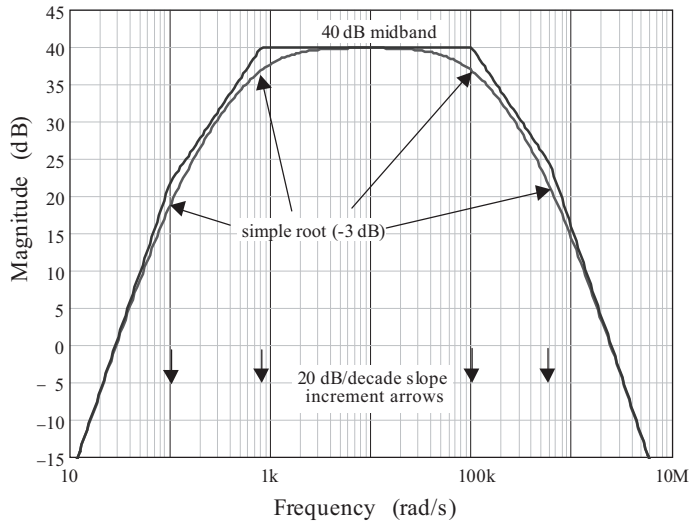

Figure 9.9: Magnitude of the frequency response for Example 9.2 with the Bode approximation overlay.

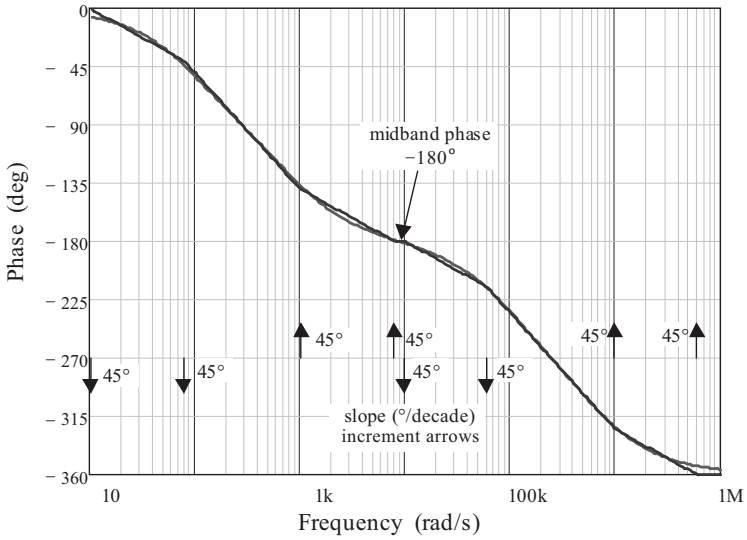

Figure 9.10: Phase of the frequency response for Example 9.2 with the Bode approximation overlay.

9.2 FILTER CHARACTERISTICS

Filters are classified according to the function that they perform. Ideal frequency selective filters have three fundamental design goals:

- To have no attenuation of input signals over a range of frequencies, called the *passband*.
- Over another, distinct range of frequencies, called the *stopband*, to have complete attenuation of input signals.
- To have no distortion of signals whose frequency content lies within the passband.

The relative frequency location of the passband and the stopband give rise to the four most common types of filters: low-pass, high-pass, band-pass, and band-stop. The magnitude of the ideal frequency response characteristics of these four filter types is depicted in Figure 9.11.

An ideal low-pass transfer characteristic is shown in Figure 9.11a with the passband extending from zero frequency to a cutoff frequency, $\omega = \omega_c$, and the stopband extending from ω_c to infinite frequency. The filter gain in the passband is unity and zero in the stopband. The ideal high-pass filter of Figure 9.11b is the inverse of the low-pass filter: the stopband extends from zero frequency to $\omega = \omega_c$ and the passband from ω_c to infinite frequency. A band-pass filter (Figure 9.11c) has a single passband extending in the frequency range, $\omega_1 < \omega < \omega_2$, while all other frequencies are stopped. Band-stop filters (Figure 9.11d) have a single stopband extending in the frequency range, $\omega_1 < \omega < \omega_2$, while all other frequencies are passed. Band-stop filters are often called band-elimination filters or notch filters.

The requirement for constant magnitude of the frequency response in the passband is a consequence of the need to pass signals whose frequency content lies within the passband without distortion. In order that a signal pass through a filter without distortion, the output of the filter must be an amplified duplicate of the input signal possibly delayed by a time lag, t_d:[6]

$$x_o(t) = K_o x_i(t - t_d). \tag{9.20}$$

The frequency domain equivalent of Equation (9.20) is obtained through the use of the Fourier Transform:

$$X_o(\omega) = \mathfrak{F}\{x_o(t)\} = \int_{-\infty}^{\infty} x_o(t) e^{-j\omega t}\, \mathrm{dt}. \tag{9.21}$$

Here $X_o(\omega)$ is the spectrum of $x_o(t)$. Replacing $x_o(t)$ by its definition (Equation (9.20)) yields the frequency domain relationship between the input signal spectrum and the undistorted output signal spectrum:

$$X_o(\omega) = K_o e^{-j\omega t_d} X_i(\omega). \tag{9.22}$$

[6]The time lag for many low-frequency filters can be approximated as $t_d \approx 0$. As frequencies become large, the physical size of an electronic filter and the internal capacitance of its elements can make time lag a significant property of the filter.

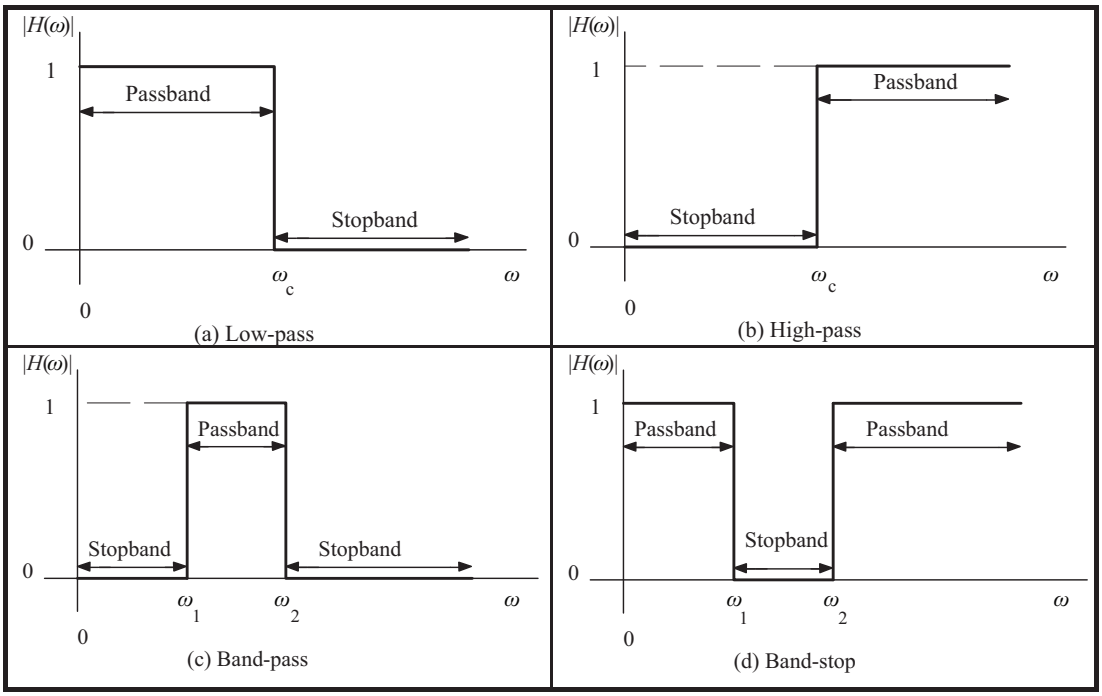

Figure 9.11: Filter idealized characteristics.

The transfer characteristic of the non-distorting filter, $H(\omega)$, is interpreted from Equation (9.22) to be the multiplier of the input signal spectrum:

$$H(\omega) = K_o e^{-j\omega t_d}. \tag{9.23}$$

The properties of a non-distorting filter are apparent. It is necessary that, over the range of frequencies contained in the input signal, the magnitude of the filter transfer function be constant with respect to frequency and the phase shift induced by the filter be linear with respect to frequency:

$$|H(\omega)| = K_o \quad \text{and} \quad \angle H(\omega) = -\omega t_d. \tag{9.24}$$

Notice that for zero time delay, $t_d = 0$, the phase shift induced by the filter is also zero.[7]

Real filters can only approximate the ideal transfer relationships depicted in Figure 9.11. The abrupt transition between the passband and the stopband of the various types of ideal filters is, unfortunately, impossible to achieve with a finite number of real circuit elements. In addition,

[7]Often a constant phase shift of $\pm 180°$ ($\pm\pi$ radians) is also acceptable: constant $\pm 180°$ phase shift is a simple inversion of the signal when passing through the filter.

zero gain in the stopband and no variation in gain in the passband are, at best, difficult to achieve. It is necessary to relax the design goals for these filters in order to be able to design and fabricate practical, real filters. A realistic set of *practical* design goals for frequency-selective filters is:

- In the *passband*, to have relatively small attenuation (or a gain) of input signals over a range of frequencies. The variation in gain over the passband is specified by a maximum variation value, $\gamma_{\max}$.
- Over the *stopband*, to have relatively large attenuation of input signals specified by a minimum attenuation value, $\gamma_{\min}$.
- To have a *transition region* lying between passband and stopband specified by a passband cutoff frequency, ω_c and a stopband edge, ω_s.
- To have minimal distortion of signals whose frequency content lies within the passband.

Figure 9.12 is a graphical representation of these design goals applied to a low-pass filter. Here the separation of the passband and the stopband by a transition band is apparent. The ration of the frequencies that specify the transition band, ω_c/ω_s, is called the selectivity factor and indicates the "sharpness" of the filter. The shaded areas represent tolerances in the passband and stopband gains: one of many possible filter responses that meet the design goals is presented as an arbitrary example.

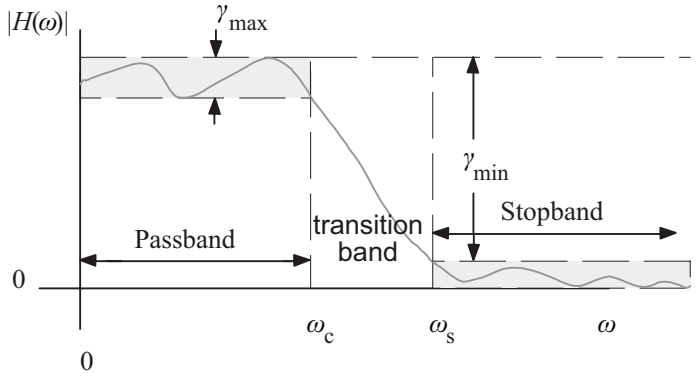

Figure 9.12: Realistic low-pass filter design goals and one possible solution.

As the tolerances for a filter are reduced, ($\gamma_{\max}$ reduced, $\gamma_{\min}$ increased, and ω_c/ω_s increased) the filter approaches ideal characteristics. While this goal may seem worthwhile in all cases, reducing tolerances increases the complexity of the circuitry involved to accomplish the more stringent design goals. Good design involves a balance between constraints and complexity.

There are several families of filters that meet the practical design goals of realistic filters in an efficient manner. Each family meets the goals in a unique manner. Two of the families that are common and will be discussed at length in this chapter are:

- Butterworth Filters
- Chebyshev Filters

Butterworth Filters are smooth filters. There is no ripple in the response in either the passband or the stopband and the transition between bands is monotonic. The edge of the passband is the frequency at which the magnitude of the filter transfer function. $|H(\omega)|$ drops by $\gamma_{\max}$. The edge of the stopband occurs at the frequency at which $|H(\omega)|$ drops by $\gamma_{\min}$ below the nominal passband gain. Chebyshev Filters have ripple in either the passband or in the stopband: once out of the region of ripple they are monotonic. Chebyshev filters can achieve a smaller transition region as compared to an equivalent-complexity Butterworth filter.

All real filters introduce some phase shift. In good filters this shift is reasonably linear with frequency throughout most of the passband: it can be interpreted as a time delay between the input and the output. As the order of the filter increases, the delay typically increases as well. Near the junction between the passband and the transition region the phase shifts become increasingly non-linear: frequencies near the edge of the passband suffer from phase distortion, as well as magnitude distortion. Discussion of filter design criteria in the following sections will be based primarily on the magnitude of the filter frequency response.

9.3 BUTTERWORTH FILTERS

Butterworth filters, often called maximally flat filters, are arguably the most common type of electronic filter. They meet the realistic goals of filters presented in the last section in a unique manner: they are *smooth* filters that transition monotonically from the passband to the stop band. The polynomials that characterize the Butterworth response are functions of only two parameters: the order of the filter, n, and the 3 dB frequency, ω_o. The response of an nth order low-pass Butterworth filter is an all-pole response characterized by the nth Butterworth polynomial, $B_n(\omega)$:

$$A_V(\omega) = \frac{A_{V0}}{B_n(\omega)}. \tag{9.25}$$

The magnitude of the nth Butterworth polynomial applied to low-pass filters is given by:

$$|B_n(\omega)| = \sqrt{1 + \left(\frac{\omega}{\omega_o}\right)^{2n}}. \tag{9.26}$$

There are several interesting properties of the Butterworth polynomials. At $\omega = \omega_o$ the magnitude of every Butterworth polynomial is:

$$|B_n(\omega_o)| = \sqrt{1 + (1)^{2n}} = \sqrt{2}. \tag{9.27}$$

Thus, ω_o is the frequency at which the output signal of the filter (a voltage or current) is reduced by a factor of $\sqrt{2}$ or, equivalently, the output power is reduced to one-half its passband value. The half-power frequency, here ω_o, is also commonly called the 3 dB frequency:

$$20\log\left(\sqrt{2}\right) = 3.01030\,\text{dB} \approx 3\,\text{dB}. \tag{9.28}$$

Since all Butterworth filters have a response that is reduced by 3 dB at the resonant frequency, it is often common to specify Butterworth filters with $\gamma_{\max} = 3\,\text{dB}$.

The slope of the filter magnitude response at $\omega = 0$ is zero, and at high frequencies, $\omega >> \omega_o$, is $-20n$ dB/decade. Thus, the order of the filter will determine the magnitude of the response in the stopband. The magnitude frequency response plot for the first six orders of Butterworth low-pass filter is presented in Figure 9.13. Butterworth polynomials are generated in order to achieve a smooth filter. In Section 9.1 it was demonstrated that the response of a system is determined only by the roots of the transfer characteristic equation. For a Butterworth filter, the roots of an nth order polynomial are chosen so that the first $2n-1$ derivatives of the magnitude of the response are zero at $\omega = 0$. These roots can easily be derived to be:

$$r_{k,n} = \omega_o e^{\left[\frac{j(2k+n-1)\pi}{2n}\right]}, \quad k = 1, 2, \ldots, n, \tag{9.29}$$

where $r_{k,n}$ is the kth root of the nth order Butterworth polynomial.

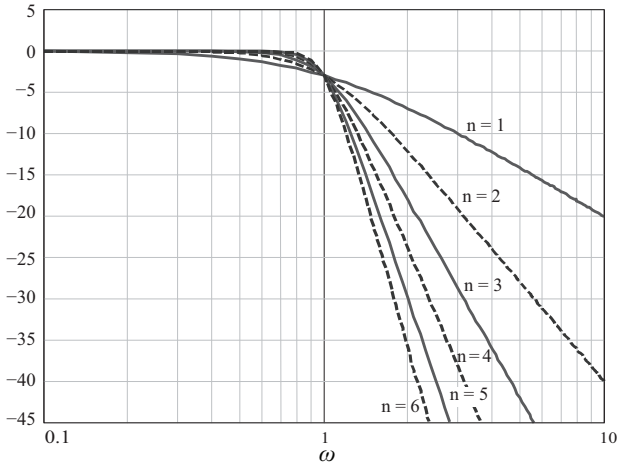

Figure 9.13: Butterworth filter frequency response.

The Butterworth polynomial roots lie in the complex plane on a circle of radius, ω_o, and are separated by an angle of by π/n. Odd order Butterworth polynomials have one real root at $-\omega_o$ and $(n-1)/2$ complex conjugate pairs. Even order polynomials have $n/2$ complex conjugate pairs

and no real roots. the location of the roots of the fifth and sixth Butterworth polynomials is shown in Figure 9.14.

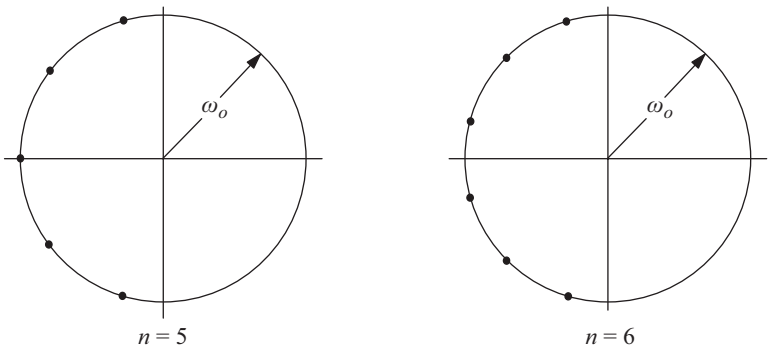

Figure 9.14: Butterworth polynomial pole locations.

A Butterworth polynomial can therefore be characterized by ω_o and the damping coefficient associated with each of the complex conjugate pairs. These damping coefficients can be calculated simply as:

$$\zeta_{i,n} = \left|\cos\left(\frac{(2i+n-1)\pi}{2n}\right)\right|, \qquad i = 1, 2, \ldots, n/2 \tag{9.30}$$

where $\zeta_{i,n}$ is the ith damping coefficient of the nth order Butterworth polynomial. While computation of the damping coefficients is quite simple, repetitive use of the same quantities makes a table of the first several order coefficients useful: the damping coefficients for the first eleven Butterworth polynomials are listed in Table 9.2. It is important to remember that *odd order Butterworth polynomials also have a real root*.

Example 9.3
A low-pass Butterworth filter is to be designed to meet the following design criteria:

Passband

nominal gain, $A_{Vo} = 1$
$\gamma_{\max} = 3\,\text{dB}$ at frequency, $f_{3\,\text{dB}} = 3\,\text{kHz}$

Stopband

$f_s = 20\,\text{kHz}$
$\gamma_{\min} = 40\,\text{dB}$ minimum.

Table 9.2: Butterworth filter damping coefficients

Filter Order	Damping Coefficients, ζ				
1					
2	0.7071				
3	0.5000				
4	0.3827	0.9239			
5	0.3090	0.8090			
6	0.2588	0.7071	0.9660		
7	0.2225	0.6235	0.9010		
8	0.1951	0.5556	0.8315	0.9808	
9	0.1736	0.5000	0.7660	0.9397	
10	0.1564	0.4540	0.7071	0.8910	0.9877
11	0.1423	0.4154	0.6549	0.8413	0.9595

Determine the order of filter necessary to achieve the design goals and the filter transfer function, $H(\omega)$.

Solution:

The resonant frequency of the filter response is

$$\omega_o = 2\pi f_{3\text{dB}} = 18.85 \times 10^3.$$

The order of the filter can be determined with Equation (9.26):

$$|B_n(\omega)| = \sqrt{1 + \left(\frac{\omega}{\omega_o}\right)^{2n}} \quad \Rightarrow \quad 10^{\left(\frac{40}{20}\right)} = \sqrt{1 + \left(\frac{2\pi f_s}{2\pi f_o}\right)^{2n}}.$$

Which can be rearranged to solve for n:

$$n = \frac{\log\left(10^{\frac{40}{10}} - 1\right)}{2\log\left(\frac{f_s}{f_o}\right)} = 2.427.$$

Since fractional order filters are not realistic, a *third-order filter is necessary* to accomplish the design goals. A third-order filter is characterized by a real pole and a single complex conjugate pair with damping coefficient (from Table 9.2), $\zeta = 0.5$.

The filter transfer function is given by ($\omega_o = 18.85 \times 10^3$):

$$H(\omega) = \frac{1}{\left(1 + \frac{j\omega}{\omega_o}\right)\left(1 + \frac{j\omega}{\omega_o} + \left(\frac{j\omega}{\omega_o}\right)^2\right)}.$$

9.3.1 ALTERNATE DEFINITIONS:

The definition of the Butterworth polynomials as given in Equation (9.26) is extremely useful for the particular (and common) case where the edge of the passband is defined by the 3 dB frequency. There are, however many cases where the edge of the passband must be defined by a variation in the gain, $\gamma_{\max}$. In those situations a slight variation in definition is necessary. The Butterworth polynomials can be defined with a third degree of freedom:

$$|B_n(\omega)| = \sqrt{1 + \varepsilon^2 \left(\frac{\omega}{\omega_c}\right)^{2n}}. \tag{9.31}$$

Here ω_c is the edge frequency of the passband. At $\omega = \omega_c$, the magnitude of all Butterworth polynomials is:

$$|B_n(\omega)| = \gamma_{\max} = \sqrt{1 + \varepsilon^2}. \tag{9.32}$$

Notice that $\varepsilon = 1$ relates to the standard definition of Butterworth polynomials given previously. The order of the filter is determined from Equation (9.31) using the attenuation necessary in the stopband. Once n and ε are known the resonant frequency of the filter can be determined:

$$\omega_o = \frac{\omega_c}{\sqrt[n]{\varepsilon}}. \tag{9.33}$$

Example 9.4
A low-pass Butterworth filter is to be designed to meet the following design criteria:

Passband

nominal gain, $A_{Vo} = 1$
passband edge, $f_c = 3\,\text{kHz}$ $\gamma_{\max} = 1\,\text{dB}$ maximum

Stopband

$f_s = 15\,\text{kHz}$ $\gamma_{\min} = 40\,\text{dB}$ minimum

Determine the Butterworth design parameters.

Solution:

A 1 dB variation in gain in the passband sets the value of ε (Equation (9.32)):

$$\sqrt{1+\varepsilon^2} = 10^{\frac{1}{20}} \qquad \Rightarrow \qquad \varepsilon = 0.50885.$$

The order of the filter can now be obtained by solving Equation (9.31):

$$|B_n(\omega)| = \sqrt{1+\varepsilon^2\left(\frac{\omega}{\omega_c}\right)^{2n}} \qquad \Rightarrow \qquad 10^{\frac{40}{20}} = \sqrt{1+0.50885^2\left(\frac{2\pi f_s}{2\pi f_c}\right)^{2n}}.$$

This has a solution $n = 3.28$: a fourth-order filter is necessary.

The resonant frequency of the filter is given by Equation (9.33):

$$\omega_o = \frac{\omega_c}{\sqrt[n]{\varepsilon}} = \frac{2\pi\,(3000)}{\sqrt[4]{0.50885}} = 22.318 \times 10^3 \text{ rad/s} \qquad f_o = 3.552\,\text{kHz}.$$

The design goals of this filter can be met by a fourth-order Butterworth filter with resonant frequency 3.552 kHz. The fourth-order Butterworth polynomial has two pairs of complex conjugate poles with damping coefficients 0.3827 and 0.9329.

9.3.2 HIGH-PASS BUTTERWORTH CHARACTERIZATION:

High-pass Butterworth filters are characterized by Butterworth polynomials with the quantities ω and ω_o interchanged. This interchange has the effect of adding two zero-frequency zeroes to the transfer function. The magnitude of the Butterworth polynomials applied to high-pass filters is given by:

$$|B_n(\omega)| = \sqrt{1+\left(\frac{\omega_o}{\omega}\right)^{2n}} = \sqrt{1+\varepsilon^2\left(\frac{\omega_c}{\omega}\right)^{2n}}. \tag{9.34}$$

With the interchange of variable, all design processes are similar. The only exception is in the determination of the resonant frequency when the passband edge frequency is used. The highpass relationship is:

$$\omega_o = \sqrt[n]{\varepsilon}\,\omega_c. \tag{9.35}$$

Example 9.5

A high-pass Butterworth filter is to be designed to meet the following design criteria:

Passband

nominal gain, $A_{Vo} = 1$

passband edge, $f_c = 3\,\text{kHz}$ $\qquad \gamma_{\max} = 0.5\,\text{dB}$

Stopband

$$f_s = 1\,\text{kHz} \qquad\qquad \gamma_{\min} = 50\,\text{dB minimum.}$$

Determine the Butterworth design parameters.

Solution:

A 0.5 dB variation in gain in the passband sets the value of ε (Equation (9.32)):

$$\sqrt{1+\varepsilon^2} = 10^{\frac{0.5}{20}} \qquad \Rightarrow \qquad \varepsilon = 0.3493.$$

The order of the filter can now be obtained by solving Equation (9.34) modified to allow for $\varepsilon \neq 1$:

$$|B_n(\omega)| = \sqrt{1+\varepsilon^2\left(\frac{\omega_c}{\omega}\right)^{2n}} \qquad \Rightarrow \qquad 10^{\frac{50}{20}} = \sqrt{1+0.3493^2\left(\frac{2\pi\, f_c}{2\pi\, f_s}\right)^{2n}}.$$

This has a solution $n = 6.197$: a seventh-order filter is necessary.

The resonant frequency of the filter is given by Equation (9.35):

$$\omega_o = \sqrt[n]{\varepsilon} \qquad \omega_c = \sqrt[7]{0.3493}\,(2\pi\,(3000)) = 16.220 \times 10^3\,\text{rad/s} \qquad f_o = 2.581\,\text{kHz}.$$

The design goals of this filter can be met by a seventh-order Butterworth filter with resonant frequency 2.581 kHz. The seventh-order Butterworth polynomial has one real pole and three pairs of complex conjugate poles with damping coefficients 0.2225, 0.6235 and 0.9010.

9.4 OPAMP REALIZATIONS OF BUTTERWORTH FILTERS

One of the major problems in designing passive high-order filters is the interaction of cascaded filter stages. Each passive stage presents a load to preceding and following stages that can vary the design parameters of the filter. While this is not an insurmountable problem, elimination of stage interaction can make the design process significantly more simple. While limited to the maximum range of frequencies at which they can operate, OpAmp circuits provide the required isolation of stages in many electronic applications.

Individual OpAmp circuits can be placed in cascade without interaction of the individual stages: each stage does not typically present a gain-changing load to either preceding or following stages. Thus, the voltage transfer function of a cascade connection of several OpAmp stages is the product of the individual transfer functions. Mathematically one can represent the total voltage transfer function, $A_{VT}(\omega)$, of a series of N individual stages in terms of the gain of the individual stages:

$$A_{VT}(\omega) = \prod_{i=1}^{N} A_{Vi}(\omega). \tag{9.36}$$

The voltage transfer relationship represented by Equation (9.36) is particularly useful when using OpAmp circuits to realize the transfer function of a filter. As with the Butterworth polynomials, filter transfer functions are specified as a product of first and second order polynomials in $(j\omega)$. If simple OpAmp circuits are constructed to have the transfer characteristic of these first and second order polynomials, then a high-order filter can be realized with a cascade of the simple OpAmp circuits. The OpAmp circuits must meet the following design criteria:

- The resonant frequency, ω_o, must be variable in both first and second order stages.
- The damping coefficient, ζ, of second order stages must be variable.

In the case of Butterworth low-pass and high-pass filters, ω_o is the 3 dB frequency and ζ is the damping coefficient (tabulated in Table 9.2). Fortunately circuits that meet these design criteria are readily available to provide all types of frequency selective filters. The specifics of each type are sufficiently different so that discussion of low-pass, high-pass, band-pass, and band-stop filters must be separated.

9.4.1 LOW-PASS OPAMP FILTERS:

Figure 9.15 presents the schematic representation of two stages with appropriate first and second order low-pass voltage transfer relationships.

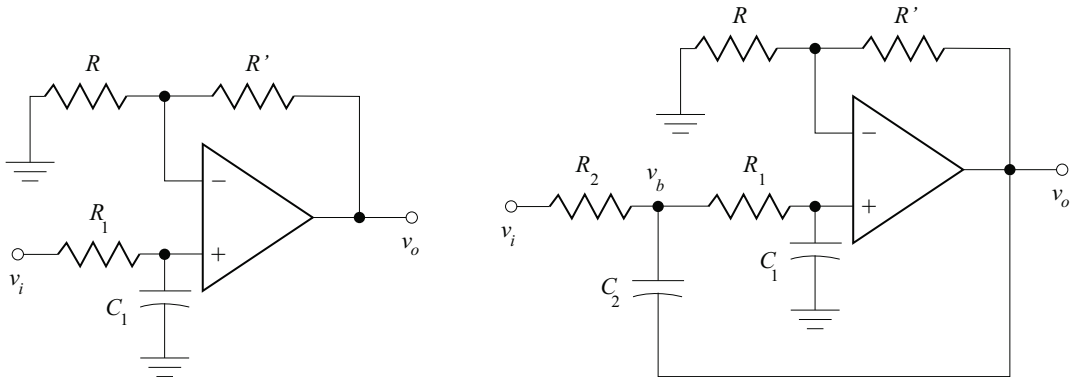

(a) First order low-pass (b) Second order low-pass

Figure 9.15: Low-pass section realizations.

First order low-pass stage

The response of the first order OpAmp filter stage (Figure 9.15a) is obtained by noting that the circuit is a non-inverting amplifier in series with a low-pass passive RC filter. The transfer char-

acteristic is therefore given by:

$$\frac{v_o}{v_i} = \frac{1 + R'/R}{1 + j\omega R_1 C_1}. \tag{9.37}$$

This circuit meets the design goal of adjustable resonant frequency. The resonant frequency, ω_o, of this circuit is determined by the input RC time constant:

$$\omega_o = \frac{1}{R_1 C_1}. \tag{9.38}$$

In addition the low-frequency gain of the circuit is adjustable through the elements R' and R:

$$A_{Vo} = 1 + \frac{R'}{R}. \tag{9.39}$$

Second order low-pass stage

The second order stage (Figure 9.15b) was developed by R. P. Sallen and E. L. Key and is therefore known as the Sallen and Key circuit. It includes, as its core element, a first order stage whose transfer characteristic has been derived to be:

$$\frac{v_o}{v_b} = \frac{1 + R'/R}{1 + j\omega R_1 C_1}. \tag{9.40}$$

The additional elements present necessitate an additional relationship so that the total transfer characteristic can be determined. If the currents are summed at the node identified with v_b the resultant equation is:

$$\frac{v_i - v_b}{R_2} + (v_0 - v_b)(j\omega C_2) - \frac{v_b}{R_1 + 1/j\omega C_1} = 0. \tag{9.41}$$

Equations 9.40 and 9.41 are combined to determine the transfer characteristic:

$$\frac{v_o}{v_i} = \frac{1 + R'/R}{1 + j\omega\left[(R_1 + R_2)C_1 - (R'/R)R_2C_2\right] + (j\omega)^2(R_1R_2C_1C_2)}. \tag{9.42}$$

This relationship is immediately recognizable as a second order low-pass characteristic with the following parameters:

$$A_{Vo} = 1 + R'/R, \tag{9.43}$$

$$\omega_o = \frac{1}{\sqrt{R_1R_2C_1C_2}}. \tag{9.44}$$

$$\frac{2\zeta}{\omega_o} = (R_1 + R_2)C_1 - \left(R'/R\right)R_2C_2. \tag{9.45}$$

This is the best of all possible worlds: there are only three constraints on the design and five quantities to vary. While an infinite variety of possible solutions for any specific design exists, there are two specific cases that are of particular interest and which commonly occur in electronic design. These cases are characterized by (a) a need for unity gain in the passband or (b) uniform time constants in the filter section.

Unity gain designs:

Often it is important that a filter have unity gain in the passband. This restriction leads to the following constraints:

$$A_{Vo} = 1 \qquad \Rightarrow \qquad R'/R = 0. \tag{9.46}$$

In order to achieve the gain requirements, a short circuit is connected between the output and the inverting input of the OpAmp and resistor R is omitted ($R = \infty$). The transfer relationship reduces to:

$$\frac{v_o}{v_i} = \frac{1}{1 + j\omega\left[\left(R_1 + R_2\right)C_1\right] + \left(j\omega\right)^2\left(R_1 R_2 C_1 C_2\right)}. \tag{9.47}$$

The pertinent design parameters are then:

$$\omega_o = \frac{1}{\sqrt{R_1 R_2 C_1 C_2}}, \tag{9.48}$$

and

$$\frac{2\zeta}{\omega_o} = \left(R_1 + R_2\right)C_1. \tag{9.49}$$

Example 9.6

Design a fourth-order Butterworth low-pass filter with unity gain in the passband that has a 3 dB frequency at 1 kHz.

Solution:

A fourth order filter is constructed from two second-order stages. Each stage will have its resonant frequency at:

$$\omega_o = 2\pi f_{3\,\mathrm{dB}} = 6.2832\,\mathrm{krad/s}.$$

The damping coefficients of the two Butterworth stages are obtained from the fourth-order row of Table 9.2:

$$\zeta_1 = 0.3827 \qquad \zeta_2 = 0.9239.$$

While there appears to only be two constraints on the values chosen for the elements, realistic solutions are of vital importance. Resistance values must be large with respect to the output resistance of the OpAmp and small with respect to OpAmp input resistance. Limited commercial capacitor availability suggests that they be chosen first. A directed approach usually produces appropriate results, but iteration may be necessary.

For the stage with $\zeta_1 = 0.3827$

In working with the constraints of Equations (9.48) and (9.49), a good to start is the balance between C_1 and the sum of R_1 and R_2:

Choose $C_1 = 0.010\,\mu\text{F}$

The two constraint equations become;

$$R_1 + R_2 = 12.182\,\text{k}\Omega \quad \text{and} \quad R_1 R_2 C_2 = 2.5330.$$

Here the resultant sum of resistor values is such that the resistors will probably fall into the acceptable range. Attention must now be placed on C_2. Whenever the sum and the product of two variables are known, real, non-zero solutions exist only if:

$$R_1 R_2 < \frac{(R_1 + R_2)^2}{4}.$$

C_2 is chosen so that criterion is met reasonably.
Choose $C_2 = 0.082\,\mu\text{F} \quad \Rightarrow \quad R_1 R_2 = 30.89 \times 10^6$.
This choice leads to the resistor values:[8]

$$R_1 = 8.5824\,\text{k} \approx 8.56\,\text{k}\Omega \qquad R_2 = 3.5993\,\text{k} \approx 3.61\,\text{k}\Omega.$$

For the stage with $\zeta_1 = 0.9239$, the same process is followed. In order to reduce complexity, it is convenient to try the same capacitor values:

Choose $C_1 = 0.010\,\mu\text{F} \quad \Rightarrow \quad R_1 + R_2 = 29.409\,\text{k}\Omega \quad \text{and} \quad R_1 R_2 C_2 = 2.5330.$

Choose $C_2 = 0.082\,\mu\text{F} \quad \Rightarrow \quad R_1 R_2 = 30.89 \times 10^6$.

Those value choices lead to the resistor values:

$$R_1 = 1.091\,\text{k} \approx 1.09\,\text{k}\Omega \qquad R_2 = 28.318\,\text{k} \approx 28.4\,\text{k}\Omega.$$

The completed design takes the final form shown below. While it is necessary to place these stages in cascade, the order of the stages is not significant.

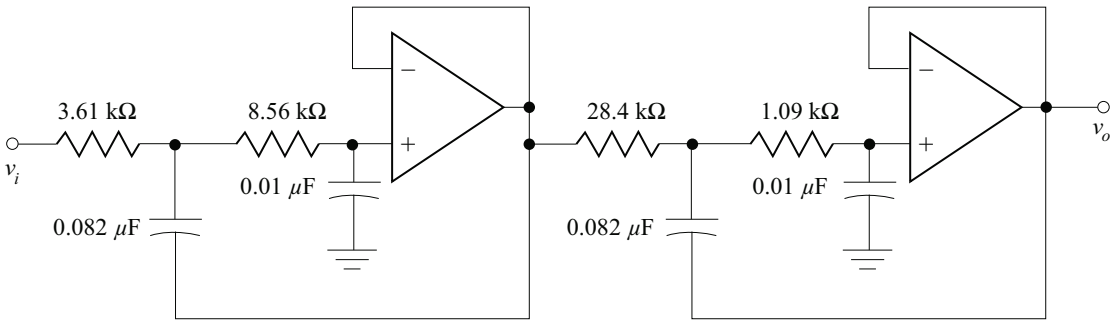

[8] Resistor values are rounded to standard values.

Uniform time constant designs:

Another interesting special case in when the value of the low-frequency gain is not significant. It that case, it is convenient to set the capacitors and associated resistors to specific values:

$$C_1 = C_2 = C_c \qquad R_1 = R_2 = R_c. \tag{9.50}$$

The pertinent filter parameters are then reduced to:

$$\omega_o = \frac{1}{R_c C_c} \tag{9.51}$$

and

$$2\zeta = 2 - R'/R. \tag{9.52}$$

This specific choice of resistor and capacitor values separates the two main parameters of the filter stage. The resonant frequency, ω_o, is controlled only by R_c and C_c: the damping coefficient is controlled only by the gain of the individual stage.

Example 9.7

Design a fifth-order Butterworth low-pass filter with a 3 dB frequency at 1 kHz.

Solution:

A fifth-order filter is comprised of a single first-order stage and two second-order stages. The lack of a requirement on the passband gain suggests a uniform time constant filter would be appropriate. Table 9.2 yields the two damping coefficients necessary for a fifth-order filter:

$$\zeta_1 = 0.3090 \qquad \zeta_2 = 0.8090.$$

The filter resonant frequency is set to the 3 dB frequency:

$$\omega_o = 2\pi f_{3\,\mathrm{dB}} = 6.2832\,\mathrm{krad/s}.$$

Any reasonable pair of resistor and capacitor values that satisfy Equation (9.51) are appropriate. One pair that utilizes standard value components is:

$$R_c = 5.9\,\mathrm{k\Omega} \qquad C_c = 0.027\,\mu\mathrm{F}.$$

The gain, as established by the ratio of resistors R and R', of each second-order stage is obtained from Equation (9.52):

$$R'/R = 2 - 2\zeta = 1.382 \quad \text{and} \quad 0.382.$$

If R is set to 10 kΩ in each stage, the two values for R' are (standard values):

$$R' \approx 13.8\,\mathrm{k\Omega} \quad \text{and} \quad 3.83\,\mathrm{k\Omega}.$$

The gain of the first-order stage is not significant to the performance of the filter as specified. A gain of two allows the use of identical resistors for R and R'. The final design of the specified low-pass filter is shown in schematic form below:

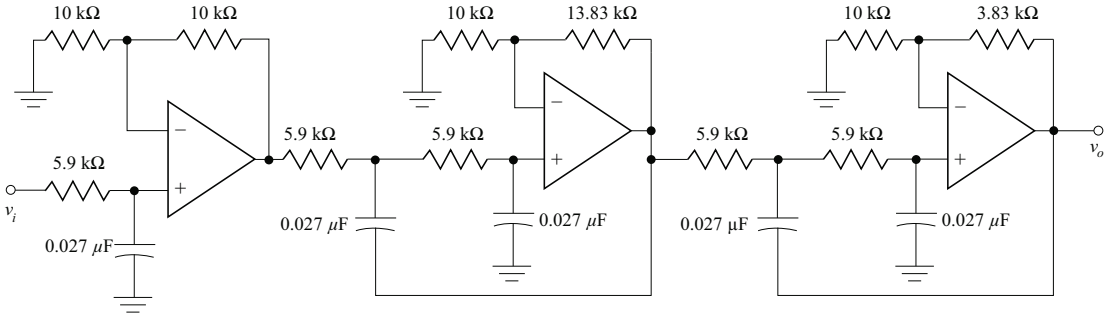

9.4.2 HIGH-PASS OPAMP FILTERS:

The two low-pass circuits of Figure 9.15 can be converted into high-pass filter sections simply by interchanging the position of the numbered capacitors with the numbered resistors. Interchanging these elements retains the same number of transfer function poles and adds zero-frequency zeroes. Figure 9.16 presents the schematic representation of these two high-pass stages.

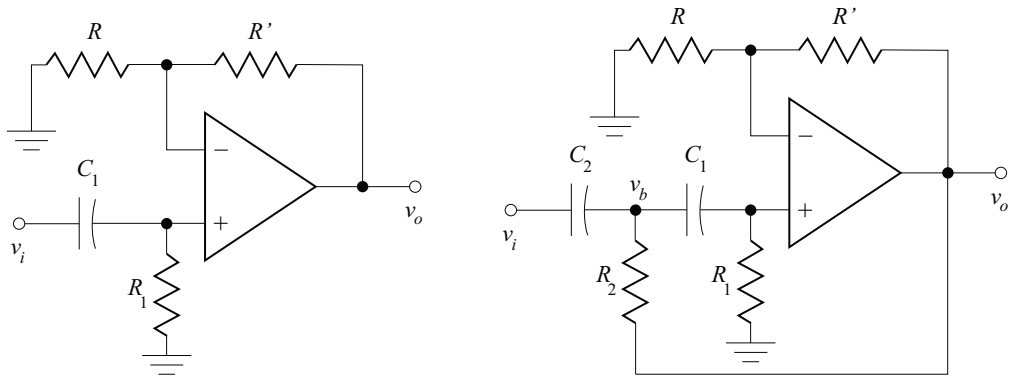

(a) First order high-pass

(b) Second order high-pass

Figure 9.16: High-pass section realizations.

First order high-pass stage

The first order OpAmp filter stage (Figure 9.16a) is a non-inverting amplifier in series with a high-pass passive RC filter. The transfer characteristic is therefore given by:

$$\frac{v_o}{v_i} = \frac{(j\omega R_1 C_1)\,(1 + R'/R)}{1 + j\omega R_1 C_1}. \tag{9.53}$$

This circuit meets the design goal of adjustable resonant frequency. The resonant frequency, ω_o, of this circuit is determined by the input RC time constant:

$$\omega_o = \frac{1}{R_1 C_1}. \tag{9.54}$$

In addition the high-frequency gain of the circuit is adjustable through the elements R' and R:

$$A_{Vo} = 1 + R'/R. \tag{9.55}$$

Second order high-pass stage

The second order high-pass stage (Figure 9.16b) transfer function is obtained in much the same fashion as the low-pass stage. The transfer characteristic is:

$$\frac{v_o}{v_i} = \frac{(j\omega)^2 (R_1 R_2 C_1 C_2)(1 + R'/R)}{1 + j\omega [R_2 (C_1 + C_2) - (R'/R) R_1 C_1] + (j\omega)^2 (R_1 R_2 C_1 C_2)}. \tag{9.56}$$

This form is immediately recognizable as a second order high-pass characteristic with the following parameters:

$$A_{Vo} = 1 + R'/R, \tag{9.57}$$

$$\omega_0 = \frac{1}{\sqrt{R_1 R_2 C_1 C_2}}, \tag{9.58}$$

$$\frac{2\zeta}{\omega_0} = R_2 (C_1 + C_2) - (R'/R) R_1 C_1. \tag{9.59}$$

The passband gain and the resonant frequency are the same as for the low-pass case. The *damping coefficient expression is different*. The same two specific design cases are of particular interest: (a) unity gain in the passband and (b) uniform time constants in the filter section.

Unity gain designs:

Often it is important that a filter have unity gain in the passband. This restriction leads to the following constraints:

$$A_{Vo} = 1 \qquad \Rightarrow \qquad R'/R = 0. \tag{9.60}$$

In order to achieve the gain requirements, a short circuit is connected between the output and the inverting input of the OpAmp and resistor R is omitted ($R = \infty$). The transfer relationship reduces to:

$$\frac{v_o}{v_i} = \frac{(j\omega)^2 (R_1 R_2 C_1 C_2)}{1 + j\omega [R_2 (C_1 + C_2)] + (j\omega)^2 (R_1 R_2 C_1 C_2)}. \tag{9.61}$$

The pertinent parameters are then:

$$\omega_o = \frac{1}{\sqrt{R_1 R_2 C_1 C_2}} \tag{9.62}$$

and

$$\frac{2\zeta}{\omega_o} = R_2 \left(C_1 + C_2\right). \tag{9.63}$$

Uniform time constant designs:

Another interesting special case in when the value of the high-frequency gain is not significant. It that case, it is convenient to set the capacitors and associated resistors to specific values:

$$C_1 = C_2 = C_c \qquad R_1 = R_2 = R_c.$$

The pertinent filter parameters are then reduced to:

$$\omega_o = \frac{1}{R_c C_c}, \tag{9.64}$$

and

$$2\zeta = 2 - R'/R. \tag{9.65}$$

Notice that these parameters are unchanged from the low-pass case. This specific choice of resistor and capacitor values separates the two main parameters of the filter stage. The resonant frequency, ω_o, is controlled only by R_c and C_c: the damping coefficient is controlled only by the gain of the individual stage.

Example 9.8

Design a 3rd order Butterworth high-pass filter with unity gain in the passband and a 3 dB frequency of 2 kHz.

Solution:

Third order filters are comprised of a first-order stage followed by a second-order stage with damping coefficient $\zeta = 0.5$. The resonant frequency is given by:

$$\omega_o = 2\pi f_{3\text{dB}} = 12.5664 \times 10^3.$$

The first order stage can be realized with element values (rounded to standard values):

$$R_{1(first)} = 7.96\,\text{k}\Omega \, C_{1(first)} = 0.01\,\mu\text{F}.$$

The second order stage requires a bit more effort. For simplicity, identical capacitors with the same value as the first-order stage capacitor will be utilized:

$$C_{1(second)} = C_{2(second)} = 0.01\,\mu\text{F}.$$

Equation (9.63) then reduces to:

$$R_{2(second)} = 3.97\,\text{k}\Omega.$$

Equation (9.62) yields the other resistor value:

$$R_{1(second)}R_{2(second)} = 63.326 \times 10^6 \quad \Rightarrow \quad R_{2(second)} = 16.0\,\text{k}\Omega.$$

The final design is shown below:

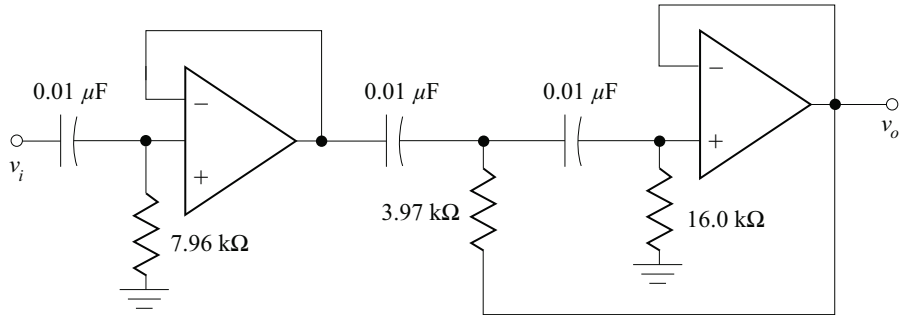

9.4.3 BAND-PASS AND BAND-STOP OPAMP FILTERS

In many cases band-pass and band-stop filters can be achieved with the series or parallel connection of high-pass and low-pass filters. These filters are particularly useful if the passband or stopband is relatively large.

The series connection of a low-pass filter with a high-pass filter will produce a band-pass filter if there exists a region of common passband. The band-pass filter will extend from the low edge of the high-pass filter passband to the high edge of the low-pass filter passband. This concept is depicted in Figure 9.17.

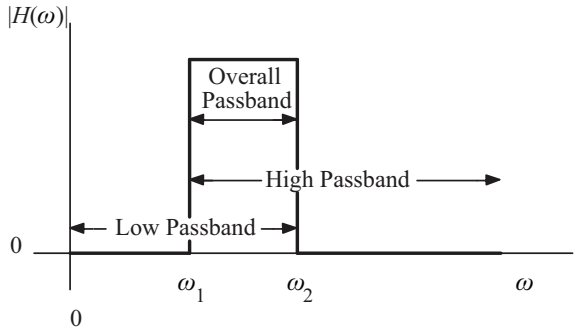

Figure 9.17: Cascaded band-pass filter characteristic.

Similarly, the parallel connection of a low-pass filter and a high-pass filter will produce a band-stop filter if there is a region of common stopband. The stopband will extend from the

low edge of the low-pass filter stopband to the high edge of the high-pass filter stopband. This concept is depicted in Figure 9.18

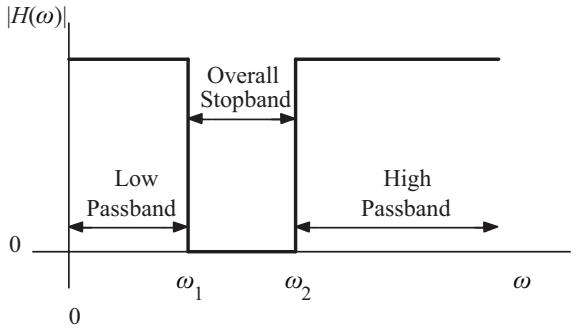

Figure 9.18: Parallel band-stop filter characteristic.

Example 9.9

Design a Butterworth band-pass filter using a minimum number of OpAmps to meet the following design goals:

Midband Region

low 3 dB frequency — 500 Hz
high 3 dB frequency — 2.35 kHz
voltage gain — any value (A_{Vo})

Stopband Region

$f \leq 150\,\text{Hz}$—$|A_V|_{\text{dB}} \leq |A_{Vo}|_{\text{dB}} - 50\,\text{dB}$
$f \geq 10\,\text{kHz}$—$|A_V|_{\text{dB}} \leq |A_{Vo}|_{\text{dB}} - 50\,\text{dB}$

Verify if the design meets the design goals using SPICE.

Solution:

This filter can be constructed with the series connection of a low-pass filter and a high-pass filter. Minimum number of OpAmps implies that the order of the filter should be kept as small as possible while still meeting specifications. The absence of a midband gain requirement suggests (but does not require) uniform time constant designs.

low-pass section:

The significant radian frequencies of interest are the 3 dB frequency and the edge of the stopband frequency:

$$\omega_{olp} = 2\pi(2350) = 14.77 \times 10^3 \qquad \omega_s = 2\pi(10{,}000) = 62.83 \times 10^3$$

50 dB attenuation translates into the magnitude of the Butterworth polynomial at the edge of the stopband

$$|B_n(\omega)| = 10^{(50/20)} = 316.23.$$

The order of this filter is found by solving Equation (9.26):

$$|B_n(\omega)| = \sqrt{1 + \left(\frac{\omega_s}{\omega_o}\right)^{2n}} \qquad \Rightarrow \qquad 316.2 = \sqrt{1 + (4.255)^{2n}}$$

$$n = \frac{\log\left(316.2^2 - 1\right)}{2\log(4.255)} = 3.975.$$

A fourth order low-pass filter is necessary. The necessary damping coefficients are found in Table 9.2:

$$\zeta_1 = 0.3827 \qquad \zeta_2 = 0.9239.$$

Uniform time constant design controls the damping coefficient with the amplifier gain:

$$R'/R = 2 - 2\zeta = 1.2346, \quad 0.1522.$$

If R is chosen arbitrarily as 10 kΩ then the two feedback resistors are:

$$R'_{lp1} = 12.3\,\text{k}\Omega \qquad R'_{lp2} = 1.52\,\text{k}\Omega.$$

The resonant frequency of the filter is chosen so that

$$\omega_o = \frac{1}{R_{c(lp)}C_{c(lp)}}.$$

Two standard value components that will satisfy this relationship are:

$$R_{c(lp)} = 1.74\,\text{k}\Omega \qquad C_{c(lp)} = 0.039\,\mu\text{F}.$$

high-pass section:
The significant frequencies of interest are:

$$\omega_{ohp} = 2\pi(500) = 3.142 \times 10^3 \qquad \omega_s = 2\pi(150) = 942.5.$$

It is found that a fifth order high-pass filter is needed:

$$n = \frac{\log\left(316.2^2 - 1\right)}{2\log(3.333)} = 4.781.$$

The damping coefficients are:

$$\zeta_1 = 0.3090 \qquad \zeta_2 = 0.8090.$$

Which lead to resistor values:

$$R = 10\,\text{k}\Omega \qquad R'_{hp1} = 13.8\,\text{k}\Omega \qquad R'_{hp2} = 3.82\,\text{k}\Omega\,.$$

The other components are chosen to have the proper 3 dB frequency:

$$R_{c(hp)} = 8.16\,\text{k}\Omega \qquad C_{c(hp)} = 0.039\,\mu\text{F}.$$

The final design is a series connection of the two sections as shown below:

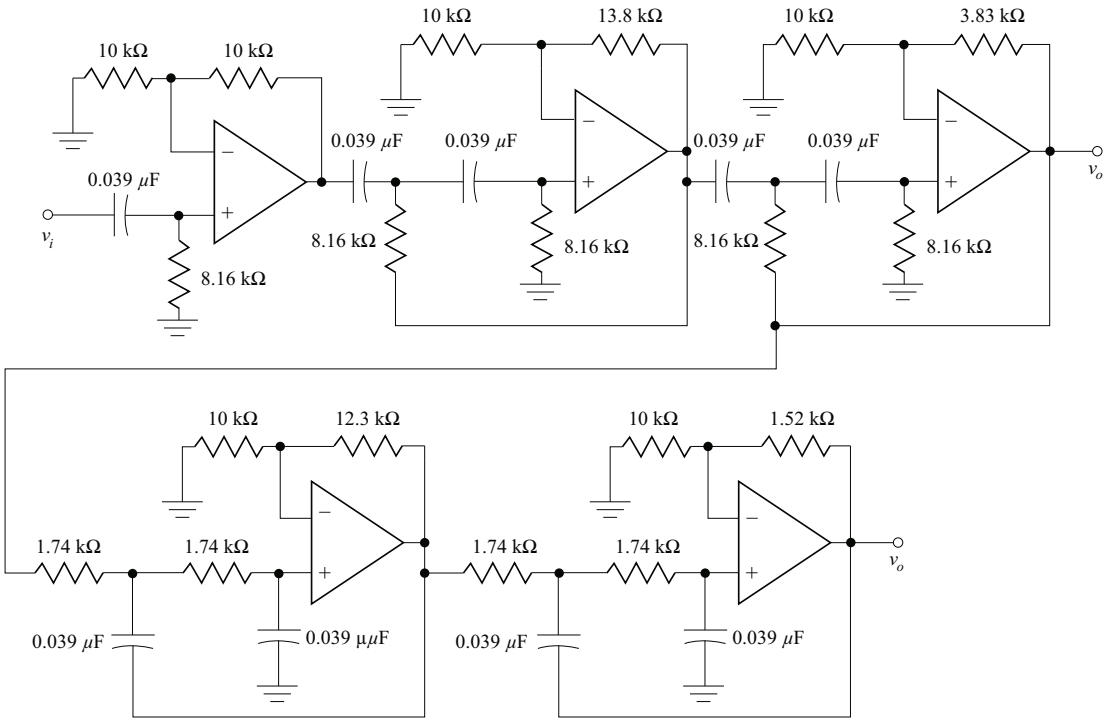

The magnitude response plot is shown below. Notice each of the predicted design goals are very close to theory. The midband gain is approximately the product of the passband gains of each stage:

$$A_{Vo} = 20\log\{(2)(2.38)(1.383)(2.23)(1.152)\} = 20\log 16.91 = 24.56\,\text{dB}.$$

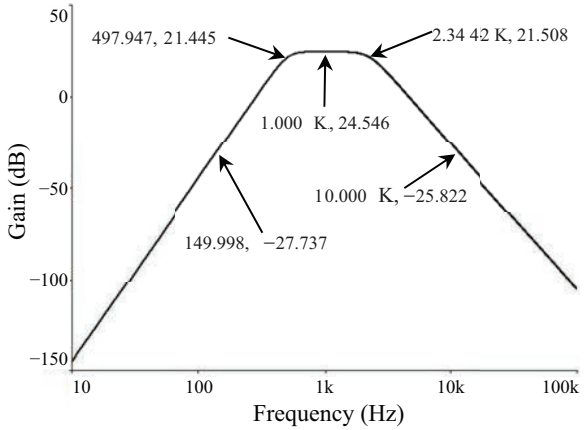

Each 3 dB frequency is exact to within a fraction of a Hz and the stopbands begin at the correct frequencies. Notice the asymmetry of the response plot due to the different order filters in high-pass and low-pass sections.

9.5 RESONANT BAND-PASS FILTERS

If the passband of a filter is relatively narrow compared to the center frequency, the series connection of high-pass and low-pass stages, as described in the last section, can become prohibitive in terms of number of components and overall cost. An alternative configuration for narrow band-pass filters utilizes the characteristics of an underdamped pole-pair in a system transfer characteristic. When such a pole pair is coupled with a zero at the origin, the transfer characteristic is:

$$H(\omega) = \frac{A_o \dfrac{j\omega_o}{\omega_o}}{1 + 2\zeta \dfrac{j\omega_o}{\omega_o} + \left(\dfrac{j\omega_o}{\omega_o}\right)^2}. \tag{9.66}$$

The Bode magnitude plot of the transfer characteristic takes the form shown in Figure 9.19: a band-pass characteristic that is centered at ω_o and that has a passband bandwidth dependent on the complex pole pair damping coefficient, ζ . Since the characteristic of interest occurs at the resonant frequency of the complex conjugate pole pair, the filter characteristic is considered a resonant filter.

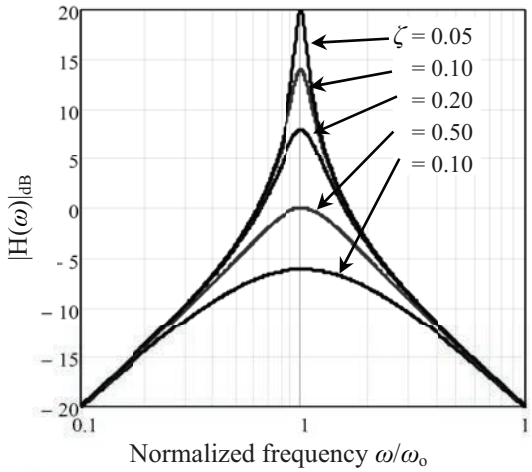

Figure 9.19: Resonant bandpass magnitude characteristics.

The gain at the resonant frequency of the filter is a function of the damping coefficient and is given by:

$$|H(\omega_o)| = \left| \frac{A_o \frac{j\omega_o}{\omega_o}}{1 + 2\zeta \frac{j\omega_o}{\omega_o} + \left(\frac{j\omega_o}{\omega_o}\right)^2} \right| = \frac{A_o}{2\zeta}. \tag{9.67}$$

The two half-power frequencies, ω_H and ω_L are easily calculated:

$$\omega_H = \omega_o \left(\zeta + \sqrt{1+\zeta^2}\right) \quad \text{and} \quad \omega_L = \frac{\omega_o}{\zeta + \sqrt{1+\zeta^2}}. \tag{9.68}$$

Subtracting the half-power frequencies yields the bandwidth of the filter passband:

$$BW = \omega_H - \omega_L = 2\zeta\omega_o. \tag{9.69}$$

Typically, filter designers define the *quality factor*, Q, of the circuit as the resonant frequency of the filter divided by the bandwidth:

$$Q = \frac{\omega_o}{BW} = \frac{\omega_o}{2\,\zeta\,\omega_o} = \frac{1}{2\,\zeta}. \tag{9.70}$$

High Q band-pass filters are easily constructed using circuits with low damping coefficient, ζ. In the regions more than about one decade from the resonance, the slope of the filter response is ± 20 dB/decade. Should greater slope be necessary in these regions, additional resonant filter stages can be cascaded to achieve that requirement.

9.5.1 *RLC* REALIZATION

There exist a large number of possible circuit topology realizations for the resonant band-pass filter characteristic of Equation (9.66). One such circuit topology is shown in Figure 9.20. This circuit uses a series connection of an inductor, capacitor and resistor.

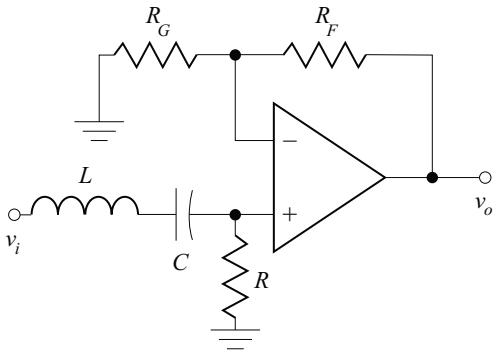

Figure 9.20: An active resonant band-pass filter.

The transfer characteristic is obtained through voltage division and the response of a non-inverting amplifier:

$$\begin{aligned} H(j\omega) &= \frac{R}{R + j\omega L + 1/j\omega C}\,(1 + R_F/R_G) \\ &= \frac{j\omega RC}{1 + j\omega RC + (j\omega)^2 LC}\,(1 + R_F/R_G)\,. \end{aligned} \tag{9.71}$$

A comparison of terms to Equation (9.66) leads to expressions for the resonant frequency:

$$\omega_o = \frac{1}{\sqrt{LC}} \tag{9.72}$$

and the damping coefficient

$$\zeta = \frac{R}{2}\sqrt{\frac{C}{L}}. \tag{9.73}$$

Another useful expression is that for the bandwidth:

$$BW = 2\zeta\omega_o = \frac{R}{L}. \tag{9.74}$$

Unfortunately, in many cases, narrow band RLC realizations may require unreasonably large inductor values.

Example 9.10

Design a RLC resonant bandpass filter with the following design goals:

$$\begin{aligned} &\text{Center frequency,} && f_o = 10\,\text{kHz} \\ &\text{3 dB bandwidth,} && B = 400\,\text{Hz}. \end{aligned}$$

Solution:

Choose $L = 0.01$ H. The bandwidth specification leads to:

$$R = L \times BW = 0.01(2\pi \times 400) = 25.1\,\Omega.$$

The resonant frequency specification leads to:

$$C = \frac{1}{L\omega_o^2} = \frac{1}{0.01(2\pi \times 10,000)^2} = 25.3\text{ nF}.$$

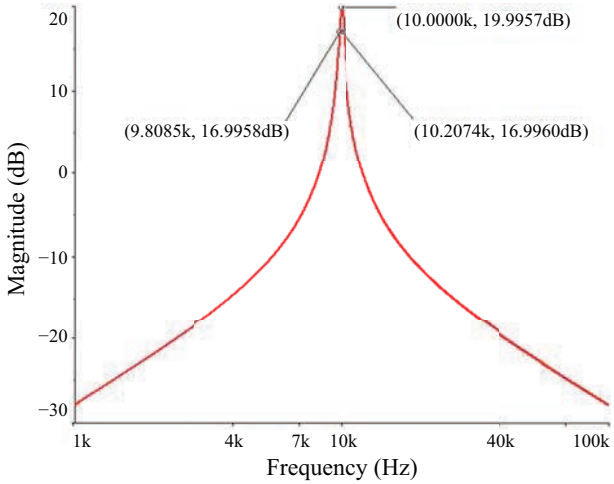

While not specified in the design goals, the gain of the filter at resonance is simply that of the non-inverting amplifier. The output to a simulation of the filter response is shown above where the midband gain was chosen to be 10 (20 dB). The filter correctly peaks at 10 kHz with a bandwidth of 400 Hz.

9.5.2 *RC* REALIZATION

It is also possible to implement the transfer characteristic of Equation (9.66) in a OpAmp circuit containing only resistors and capacitors (Figure 9.21).

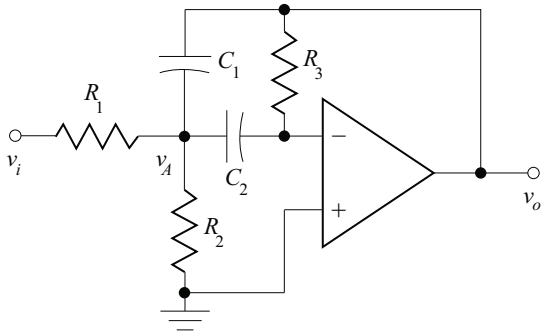

Figure 9.21: An active resonant band-pass filter without an inductance.

The transfer characteristic of this circuit topology can be obtained through Kirchhoff's current law applied at the negative input terminal of the OpAmp and at the node identified by v_A:

At the negative input terminal of the OpAmp:

$$\frac{v_o}{R_3} + j\omega C_2 v_A = 0 \qquad \Rightarrow \qquad v_A = \frac{v_o}{j\omega R_3 C_2} \tag{9.75}$$

and at node v_A

$$\frac{v_i - v_A}{R_1} - \frac{v_A}{R_2} + j\omega C_1 (v_o - v_A) + \frac{v_o}{R_3} = 0. \tag{9.76}$$

Combining Equations (9.75) and (9.76) yields the filter transfer characteristic:

$$H(j\omega) = \frac{v_o}{v_i} = \frac{-j\omega \dfrac{R_P R_3 C_2}{R_1}}{1 + j\omega R_P (C_1 + C_2) + (j\omega)^2 R_P R_3 C_1 C_2}. \tag{9.77}$$

Where $R_P = R_1 // R_2$. From the form of $H(j\omega)$, one can then deduce:

$$\omega_o = \frac{1}{\sqrt{R_p R_3 C_1 C_2}} \qquad \frac{2\zeta}{\omega_o} = R_P (C_1 + C_2) \quad \text{and} \quad \frac{A_o}{\omega_o} = \frac{R_P R_3 C_2}{R_1}. \tag{9.78}$$

The filter designer is in the enviable position of having five circuit variables and only three constraints: the filter gain, resonant frequency, and bandwidth. Since capacitor values are more constrained than resistor values, filter designers typically choose the two capacitor values and calculate the three resistor values. If one further assumes the capacitors have equal value ($C_1 = C_2 = C$), the resistor values can be determined to be:

$$R_3 = \frac{1}{C\zeta\omega_o} \qquad R_1 = \frac{R_3}{2\,|\,H(\omega_o)\,|} \quad \text{and} \quad R_2 = \left(\frac{C\omega_o}{\zeta} - \frac{1}{R_1}\right)^{-1}. \tag{9.79}$$

Example 9.11

Design an RC resonant band-pass filter with the following design goals:

Midband voltage gain = 33 dB
Center frequency = 200 Hz
3 dB bandwidth = 20 Hz

Solution:

A necessary parameter that must be determined is the damping coefficient:

$$\zeta = \frac{BW}{2\omega_o} = \frac{B}{2f_o} = \frac{20}{2 \times 200} = 0.05.$$

Arbitrarily choose $C = 0.1\,\mu$F. Calculate the resistor values:

$$R_3 = \frac{1}{C\zeta\omega_o} = \frac{1}{0.1 \times 10^{-6}\,(0.05)\,(2\pi \times 200)} = 159\ \text{k}\Omega$$

$$R_1 = \frac{R_3}{2\,|H\,(\omega_o)|} = \frac{159,000}{2 \times 10^{33/20}} = 1.78\ \text{k}\Omega$$

$$R_2 = \left(\frac{C\omega_o}{\zeta} - \frac{1}{R_1}\right)^{-1} = \left(\frac{0.1 \times 10^{-6} \times 2\pi \times 200}{0.05} - \frac{1}{1780}\right) = 512\ \Omega.$$

The output to a simulation of the filter response is shown below. The filter appropriately peaks at 200 Hz with a gain of 33 dB and a bandwidth of 20 Hz.

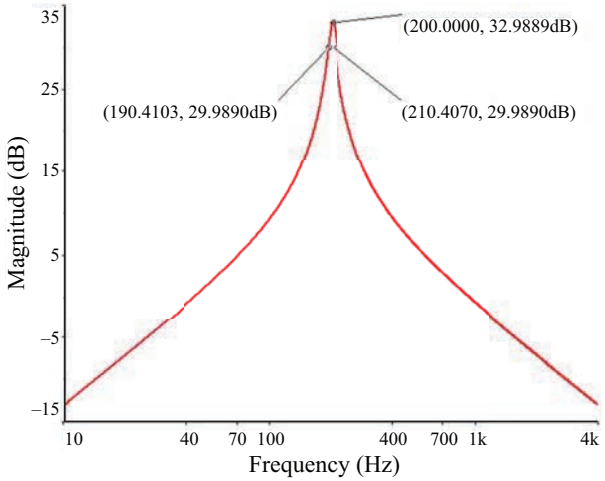

9.5.3 RESONANT BANDSTOP FILTERS

The filter designer is often faced with the task of eliminating a narrow band of frequencies while retaining the remainder of the frequency spectrum. Designing a band-stop filter as the parallel connection of a high-pass and a low-pass filter as described in Section 9.4.3 can similarly become prohibitive in terms of number of components and overall cost when the required stop band is narrow. While a number of OpAmp realizations for narrow band-stop (often called a "notch") filters exist, the circuit shown in Figure 9.22 is one that uses resonance characteristics.

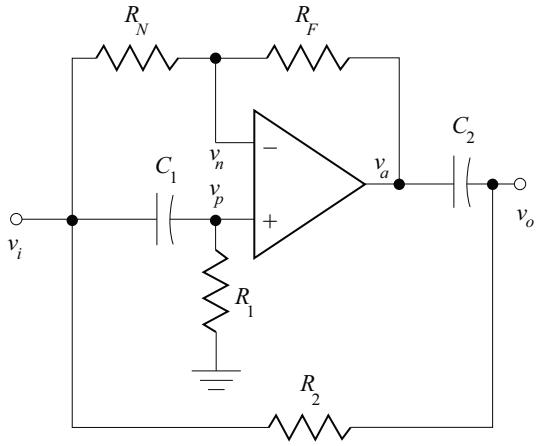

Figure 9.22: An active resonant band-stop filter.

The filter transfer relationship can be determined by solving the set of simultaneous equations obtained by applying Kirchhoff's current law at the nodes identified with voltages v_p, v_n and v_o (note that $v_n = v_p$):

$$\begin{aligned} (v_i - v_p)\, j\omega C_1 + \frac{0 - v_p}{R_1} &= 0 \\ \frac{v_i - v_n}{R_N} + \frac{v_a - v_n}{R_A} &= 0 \\ (v_a - v_o)\, j\omega C_2 + \frac{v_i - v_o}{R_2} &= 0. \end{aligned} \tag{9.80}$$

The filter transfer relationship is determined to be:

$$H(\omega) = \frac{1 + \left(C_1 R_1 - C_2 R_2 \dfrac{R_F}{R_N}\right) j\omega + (C_1 R_1 C_2 R_2)\,(j\omega)^2}{1 + (C_1 R_1 + C_2 R_2)\, j\omega + (C_1 R_1 C_2 R_2)\,(j\omega)^2}. \tag{9.81}$$

Both the numerator and denominator of $H(\omega)$ are resonant at:

$$\omega_o = \frac{1}{\sqrt{R_1 C_1 R_2 C_2}}. \tag{9.82}$$

However, the damping coefficients of the numerator, ζ_N, and the denominator, ζ_D, are different:

$$\zeta_N = \frac{C_1 R_1 - C_2 R_2 \dfrac{R_F}{R_N}}{2\sqrt{R_1 C_1 R_2 C_2}} \quad \text{and} \quad \zeta_D = \frac{C_1 R_1 + C_2 R_2}{2\sqrt{R_1 C_1 R_2 C_2}}. \tag{9.83}$$

$H(\omega)$ has the characteristics that at frequencies much less than the resonant frequency and much larger than the resonant frequency, $|H(\omega)| = 1$ and at the resonant frequency

$$|H(\omega_o)| = \frac{C_1 R_1 - C_2 R_2 \dfrac{R_F}{R_N}}{C_1 R_1 + C_2 R_2} = \frac{\zeta_N}{\zeta_D}. \tag{9.84}$$

In theory, the notch in the filter can be made arbitrarily deep: in practice it is possible to obtain as much as 60 dB of attenuation at the resonant frequency.

One typical design choice for this filter configuration sets $R_1 = R_2 = R$ and $C_1 = C_2 = C$, so that:

$$\omega_o = \frac{1}{RC}, \quad \zeta_N = 1 - \frac{R_F}{R_N}, \quad \text{and} \quad \zeta_D = 1. \tag{9.85}$$

Example 9.12

Design a resonant band-stop filter with the following design goals:

Center frequency $= 60\,\text{Hz}$

Notch depth $> 40\,\text{dB}$.

Solution:

Arbitrarily choose $C_1 = C_2 = 0.1\,\mu\text{F}$ and $R_1 = R_2 = R$.

Then

$$R = \frac{1}{\omega_o C} = \frac{1}{2\pi\,(60)\left(0.1 \times 10^{-6}\right)} = 26.5\ \text{k}\Omega$$

$$|H(\omega_o)| = 10^{\frac{-40}{20}} = \frac{\zeta_N}{\zeta_D} \qquad \Rightarrow \qquad \zeta_N = 0.01$$

and

$$\frac{R_F}{R_N} = 1 - \zeta = 0.99.$$

Choose $R_N = 10\,\text{k}\Omega$ and $R_F = 9.88\,\text{k}\Omega$ (closest standard value).

The resultant SPICE simulation plot is shown below. All design goals are met.

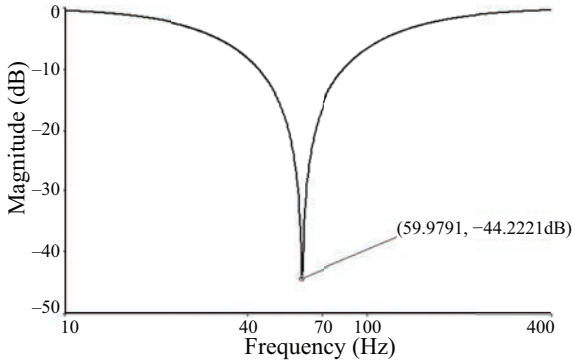

This resonant band-stop filter configuration has limitations that need to be noted. In particular, it is necessary that it be driven by a low-impedance source and that it drives a high-impedance load. As such, buffer circuitry may be necessary in some circumstances to insure proper operation.

In addition, the width of the band for which attenuation is more than 3 dB, of this particular band-stop filter is not adjustable and is fixed:

$$BW_{>3\text{dB}} \approx 2\omega_o \quad (\approx 3/4 \text{ decade}). \tag{9.86}$$

Performance similar to that obtained in Example 9.12, if obtained with a high-pass and a low-pass filter connected in parallel while maintaining this same attenuation band, would require two sixth-order filters. The savings in terms of number of components and overall cost is considerable.

The high-pass cutoff frequency, ω_{hp}, and the low-pass cutoff frequency ω_{lp} are approximately given by:

$$\omega_{hp} \approx \left(1 + \sqrt{2}\right)\omega_o \quad \text{and} \quad \omega_{lp} \approx \frac{\omega_o}{1 + \sqrt{2}}. \tag{9.87}$$

More complex circuit configurations can avoid these limitations, but are beyond the scope of this discussion.

9.6 CHEBYSHEV FILTERS

When filter design specifications allow for a small amount of ripple in either the passband or the stopband, an all-pole filter called the Chebyshev filter can be used. Two types of Chebyshev filters can be specified as shown in Figure 9.23: one containing ripple in the passband, classified as type 1, and the other with the ripple in the stopband called type 2. The disadvantage of the ripple in the filter response is counteracted by a steeper transition band for a given filter order. That is, for a low-pass filter of a given order, the Chebyshev filter has a lower stopband frequency than the Butterworth filter.

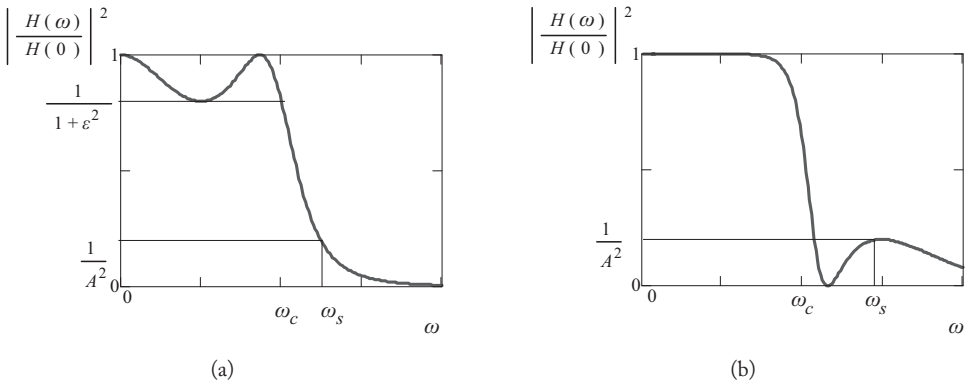

Figure 9.23: (a) Chebyshev type 1 low-pass filter response; (b) Chebyshev type 2 low-pass filter response.

In most electronic applications, the Chebyshev type 1 response, with ripple in the passband, is the more common of the two types. The Chebyshev type 1 filter transfer function is,[9]

$$\left|\frac{H(\omega)}{H_o}\right|^2 = \frac{1}{1+\varepsilon^2 C_n^2\left(\frac{\omega}{\omega_c}\right)}, \tag{9.88}$$

where $\left|\frac{H(\omega)}{H_o}\right|$, and $C_n\left(\frac{\omega}{\omega_c}\right)$ are the normalized magnitude o f the filter transfer function and the Chebyshev polynomials defined from a recursive formula given in Table 9.3, respectively. The parameter is related to the ripple defined in Equation (9.32):

$$\gamma_{\max} = \sqrt{1+\varepsilon^2}.$$

Table 9.3 is a tabulation of the first nine Chebyshev polynominals. It is evident that for $x = 0$, the Chebyshev polynomial $C_n(0)$ is 1 when n is even, and zero when n is odd. The resulting response is,

$$\left|\frac{H(0)}{H_o}\right|^2 = \begin{cases} \frac{1}{1+\varepsilon^2}, & n \text{ even} \\ 1, & n \text{ odd} \end{cases}. \tag{9.89}$$

The two general shapes of the Chebyshev type 1 low-pass filter for n odd and even are shown in Figure 9.24. The squared magnitude frequency response oscillates between 1 and $(1+\varepsilon)^{-1}$ within the passband and has a value of $(1+\varepsilon)^{-1}$ at the cutoff frequency ω_c. The response is monotonic outside the passband. The stopband edge is defined by ω_s corresponding to a magnitude of A^{-2} .

[9]The Chebyshev type 2 filter transfer function is: $\left|\frac{H(\omega)}{H_o}\right|^2 = \frac{\varepsilon^2 C_n^2\left(\frac{\omega_c}{\omega}\right)}{1+\varepsilon^2 C_n^2\left(\frac{\omega_c}{\omega}\right)}$.

Table 9.3: First nine Chebyshev polynomials

n	$C_n(x)$, where $x = \frac{\omega}{\omega_c}$
0	1
1	x
2	$2x^2 - 1$
3	$4x^3 - 3x$
4	$8x^4 - 8x^2 + 1$
5	$16x^5 - 20x^3 + 5x$
6	$32x^6 - 48x^4 + 18x^2 - 1$
7	$64x^7 - 112x^5 + 56x^3 - 7x$
8	$128x^8 - 256x^6 + 160x^4 - 32x^2 + 1$
9	$256x^9 - 1280x^7 + 432x^5 - 120x^3 + 9x$

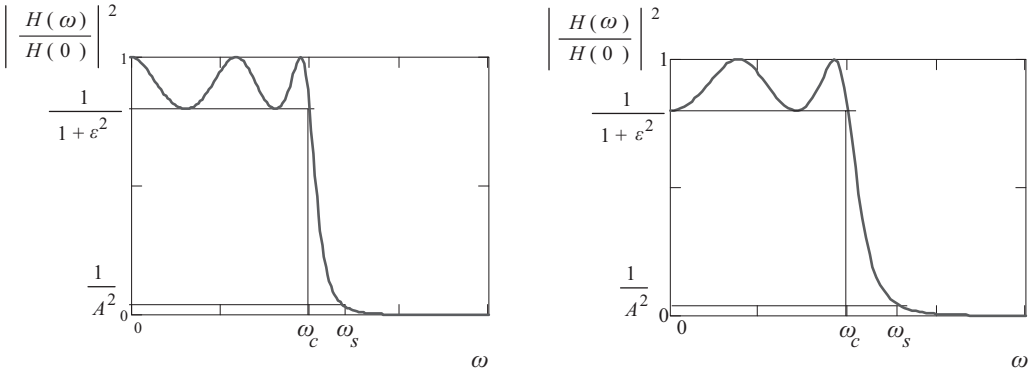

Figure 9.24: (a) Frequency Response of odd order Chebyshev type 1 filter; (b) Frequency Response of even order Chebyshev type 1 filter.

The roots of $1 + \varepsilon^2 C_n^2\left(\frac{\omega}{\omega_c}\right)$ in the denominator of the Chebyshev type 1 transfer function (the poles) lie on an ellipse on the complex plane as shown in Figure 9.25. For simplicity, let $\omega_r = \omega/\omega_c$. The amount of ripple in the response is related to the eccentricity of the ellipse.

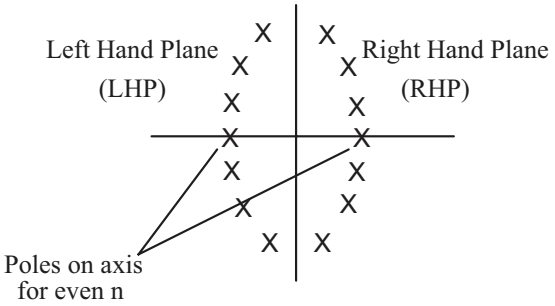

Figure 9.25: Poles of a low-pass Chebyshev type 1 filter.

Using the LHP poles only, the transfer function can be written as,

$$\frac{H(\omega_r)}{H_o} = \frac{K}{\prod_{k=1}^{n}[(j\omega_r - s_k)]} = \frac{K}{V_n(j\omega_r)}, \tag{9.90}$$

where s_k are the pole locations,

$$V_n(j\omega_r) = (j\omega_r)^n + b_{n-1}(j\omega_r)^{n-1} + \ldots + b_1(j\omega_r) + b_0.$$

Here K is a normalizing constant that makes

$$\frac{H(0)}{H_o} = \begin{cases} \dfrac{1}{\sqrt{1+\varepsilon^2}}, & n \text{ even} \\ 1, & n \text{ odd} \end{cases}.$$

The normalizing constant is therefore,

$$K = V_n(0) = b_0, \qquad n \text{ odd}$$
$$K = \frac{V_n(0)}{\sqrt{1+\varepsilon^2}}, \qquad n \text{ even}.$$

Table 9.4 provides the normalized polynomials for Chebyshev type 1 filters for orders $n = 1$ to 9 and ε corresponding to 0.5, 1, 2, and 3 dB ripples in the passband.

The required order of a Chebyshev type 1 low-pass filter depends on the following factors:

- Cutoff frequency
- Stopband frequency
- Stopband attenuation

- Passband ripple

Design specifications usually provide the required minimum attenuation desired at a certain stopband frequency instead of an exact attenuation. The required order of the filter, n, is found by applying Equation (9.91):

$$n = \frac{\log\left[g + \sqrt{g^2 - 1}\right]}{\log\left[\omega_r + \sqrt{\omega_r{}^2 - 1}\right]}, \tag{9.91}$$

where

$$A = \left|\frac{H_o}{H(\omega_r)}\right|, \tag{9.92}$$

and

$$g = \sqrt{\frac{A^2 - 1}{\varepsilon^2}}. \tag{9.93}$$

Example 9.13
Find the transfer function for a low-pass filter with the following specifications:

1. Cutoff frequency $f_c = 1000\,\text{Hz}$.
2. Acceptable passband ripple of 2 dB.
3. Stopband attenuation of $\geq 20\,\text{dB}$ beyond 1300 Hz.

Solution:

The specifications imply the following relationships:

$$20\log\left|\frac{H(2\pi \times 1\text{k})}{H_o}\right| = 20\log\left[\frac{1}{\sqrt{1+\varepsilon^2}}\right] = -2\,\text{dB}$$

and

$$20\log\left|\frac{H(2\pi \times 1.3\text{k})}{H_o}\right| = 20\log\left[\frac{1}{\sqrt{A^2}}\right] = -20\,\text{dB}.$$

The solutions to the two relationships above are: $\varepsilon = 0.7648$ and $A = 10$. The relative stopband frequency is $1.3\,\text{k}/1\,\text{k} = 1.3$.

The required order of the Chebyshev type 1 low-pass filter is found by using Equations (9.91)–(9.93),

$$g = \sqrt{\frac{A^2 - 1}{\varepsilon^2}} = 13.01,$$

and

$$n = \left\lceil \frac{\log\left[13.01 + \sqrt{13.01^2 - 1}\right]}{\log\left[1.3 + \sqrt{1.3 - 1}\right]} \right\rceil = \lceil 4.3 \rceil = 5.$$

Table 9.4: Normalized Chebyshev polynomials *(Continues.)*

n	0.5 dB ripple ($\varepsilon = 0.3493$)
1	$j\omega + 2.863$
2	$(j\omega)^2 + 1.426(j\omega) + 1.516$
3	$[(j\omega)+0.626]\{[(j\omega)+0.313]^2+1.022^2\}$
4	$\{[(j\omega)+0.175]^2+1.016^2\}\{[(j\omega)+0.423]^2+0.421^2\}$
5	$[(j\omega)+0.362]\{[(j\omega)+0.112]^2+1.012^2\}\{[(j\omega)+0.293]^2+0.625^2\}$
6	$\{[(j\omega)+0.078]^2+1.009^2\}\{[(j\omega)+0.212]^2+0.738^2\}\{[(j\omega)+0.290]^2+0.270^2\}$
7	$[(j\omega)+0.256]\{[(j\omega)+0.057]^2+1.006^2\}\{[(j\omega)+0.160]^2+0.807^2\}\{[(j\omega)+0.231]^2+0.448^2\}$
8	$\{[(j\omega)+0.044]^2+1.005^2\}\{[(j\omega)+0.124]^2+0.852^2\}\{[(j\omega)+0.186]^2+0.569^2\}\{[(j\omega)+0.219]^2+0.200^2\}$
9	$[(j\omega)+0.198]\{[(j\omega)+0.034]^2+1.004^2\}\{[(j\omega)+0.099]^2+0.883^2\}\{[(j\omega)+0.152]^2+0.655^2\}\{[(j\omega)+0.186]^2+0.349^2\}$

n	1.0 dB ripple ($\varepsilon = 0.5089$)
1	$j\omega + 1.962$
2	$(j\omega)^2 + 1.098(j\omega) + 1.103$
3	$[(j\omega)+0.494]\{[(j\omega)+0.247]^2+0.966^2\}$
4	$\{[(j\omega)+0.140]^2+0.983^2\}\{[(j\omega)+0.337]^2+0.407^2\}$
5	$[(j\omega)+0.289]\{[(j\omega)+0.090]^2+0.990^2\}\{[(j\omega)+0.234]^2+0.612^2\}$
6	$\{[(j\omega)+0.062]^2+0.993^2\}\{[(j\omega)+0.170]^2+0.727^2\}\{[(j\omega)+0.232]^2+0.266^2\}$
7	$[(j\omega)+0.205]\{[(j\omega)+0.046]^2+0.995^2\}\{[(j\omega)+0.128]^2+0.798^2\}\{[(j\omega)+0.185]^2+0.443^2\}$
8	$\{[(j\omega)+0.035]^2+0.997^2\}\{[(j\omega)+0.100]^2+0.845^2\}\{[(j\omega)+0.149]^2+0.564^2\}\{[(j\omega)+0.176]^2+0.198^2\}$
9	$[(j\omega)+0.159]\{[(j\omega)+0.028]^2+0.997^2\}\{[(j\omega)+0.080]^2+0.877^2\}\{[(j\omega)+0.122]^2+0.651^2\}\{[(j\omega)+0.150]^2+0.346^2\}$

Table 9.5: *(Continued.)* Normalized Chebyshev polynomials

n	2.0 dB ripple ($\varepsilon = 0.7648$)
1	$j\omega + 1.308$
2	$(j\omega)^2 + 0.804(j\omega) + 0.637$
3	$[(j\omega)+0.369]\{[(j\omega)+0.184]^2+0.923^2\}$
4	$\{[(j\omega)+0.105]^2+0.958^2\}\{[(j\omega)+0.253]^2+0.397^2\}$
5	$[(j\omega)+0.218]\{[(j\omega)+0.068]^2+0.974^2\}\{[(j\omega)+0.177]^2+0.602^2\}$
6	$\{[(j\omega)+0.047]^2+0.982^2\}\{[(j\omega)+0.128]^2+0.719^2\}\{[(j\omega)+0.175]^2+0.263^2\}$
7	$[(j\omega)+0.155]\{[(j\omega)+0.035]^2+0.987^2\}\{[(j\omega)+0.097]^2+0.791^2\}\{[(j\omega)+0.140]^2+0.440^2\}$
8	$\{[(j\omega)+0.027]^2+0.990^2\}\{[(j\omega)+0.075]^2+0.839^2\}\{[(j\omega)+0.113]^2+0.561^2\}\{[(j\omega)+0.133]^2+0.197^2\}$
9	$[(j\omega)+0.121]\{[(j\omega)+0.021]^2+0.992^2\}\{[(j\omega)+0.060]^2+0.872^2\}\{[(j\omega)+0.092]^2+0.647^2\}\{[(j\omega)+0.113]^2+0.345^2\}$

n	3.0 dB ripple ($\varepsilon = 0.9953$)
1	$j\omega + 1.002$
2	$(j\omega)^2 + 0.645(j\omega) + 0.708$
3	$[(j\omega)+0.299]\{[(j\omega)+0.149]^2+0.904^2\}$
4	$\{[(j\omega)+0.085]^2+0.947^2\}\{[(j\omega)+0.206]^2+0.392^2\}$
5	$[(j\omega)+0.178]\{[(j\omega)+0.055]^2+0.966^2\}\{[(j\omega)+0.144]^2+0.597^2\}$
6	$\{[(j\omega)+0.038]^2+0.976^2\}\{[(j\omega)+0.104]^2+0.715^2\}\{[(j\omega)+0.143]^2+0.262^2\}$
7	$[(j\omega)+0.127]\{[(j\omega)+0.028]^2+0.983^2\}\{[(j\omega)+0.079]^2+0.788^2\}\{[(j\omega)+0.114]^2+0.437^2\}$
8	$\{[(j\omega)+0.022]^2+0.987^2\}\{[(j\omega)+0.062]^2+0.837^2\}\{[(j\omega)+0.092]^2+0.559^2\}\{[(j\omega)+0.109]^2+0.196^2\}$
9	$[(j\omega)+0.098]\{[(j\omega)+0.017]^2+0.990^2\}\{[(j\omega)+0.049]^2+0.870^2\}\{[(j\omega)+0.075]^2+0.646^2\}\{[(j\omega)+0.092]^2+0.344^2\}$

The partial bracket, $\lceil\ \rceil$, is a symbol for the operation to round up to the next integer. Using Table 9.4 for $n = 5$ and 2 dB ripple, the transfer function is,

$$\frac{H\left(\frac{\omega}{\omega_c}\right)}{H_o} = \frac{1}{\left[\left(j\frac{\omega}{\omega_c}\right)+0.218\right]\left\{\left[\left(j\frac{\omega}{\omega_c}\right)+0.068\right]^2+0.974^2\right\}\left\{\left[\left(j\frac{\omega}{\omega_c}\right)+0.177\right]^2+0.602^2\right\}}$$

$$= \frac{1}{\left[\frac{j\omega}{0.218\omega_c}+1\right]\left[\frac{(j\omega)^2}{0.953\omega_c^2}+\frac{0.136\,(j\omega)}{0.953\omega_c}+1\right]\left[\frac{(j\omega)^2}{0.394\omega_c^2}+\frac{0.354\,(j\omega)}{0.394\omega_c}+1\right]}.$$

The response of the fifth order low-pass filter transfer function in this example is shown below.

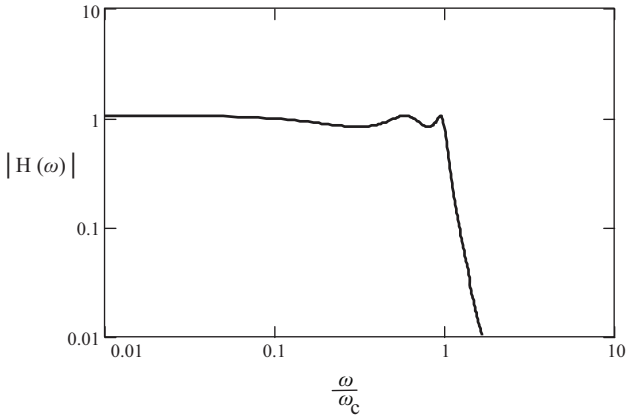

High-Pass Characterization:

High-pass Chebyshev filters are characterized by using the analog-to-analog transformation. The Chebyshev low-pass to high-pass transformation, like the Butterworth low-pass to high-pass analog-to-analog transformation, has the effect of adding two zero-frequency zeroes to the transfer function. The generic procedure for the analog-to-analog transformation from low to high-pass shown in Figure 9.26 is not restricted to Chebyshev filters, but may be used for other filter types.

The general procedure to find the transfer function of a high-pass filter is as follows:

1. Perform a backward transformation using the high-pass filter specifications for the cutoff frequency, ω_c, and the stopband frequency, ω_s, which is associated with some level of attenuation. The backward transformation of frequencies yields the normalized low-pass ratio of stopband to cutoff frequency, ω_r.
2. Use the normalized low-pass ratio of stopband to cutoff frequency, ω_r, to find the order of the filter.
3. Use Table 9.4 to find the transfer function of the normalized low-pass filter.
4. Perform a forward transformation on the transfer function by replacing all $(j\omega)$ with $\frac{\omega_c}{j\omega}$.

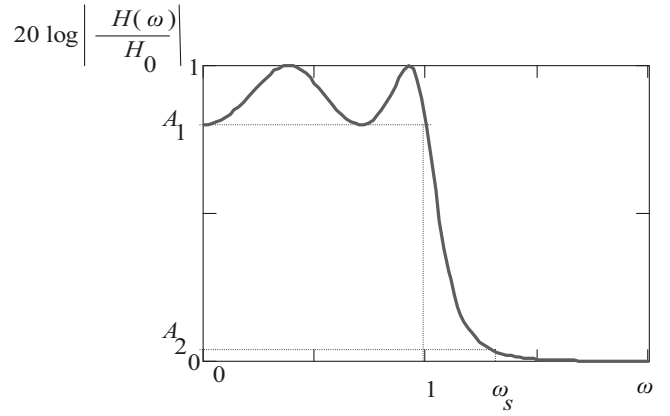

(a)

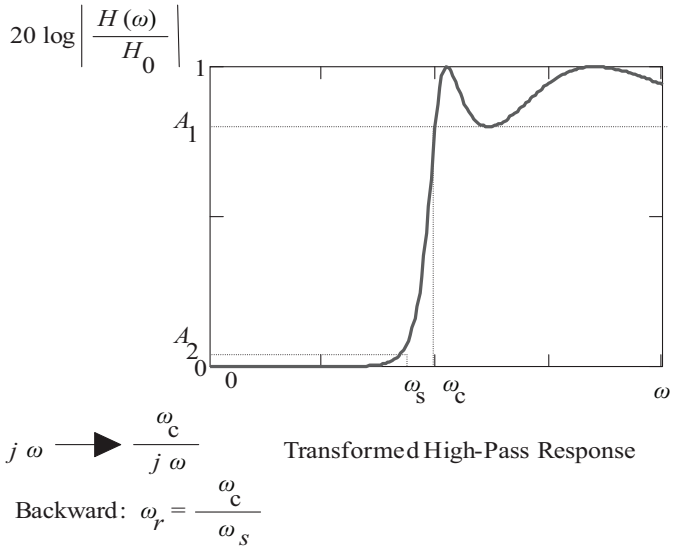

(b)

Figure 9.26: Analog-to-analog transformation: low-pass to high-pass.

Example 9.14
Find the transfer function for a high-pass filter with the following specifications:

1. Cutoff frequency $f_c = 1000\,\text{Hz}$.
2. Acceptable passband ripple of 2 dB.
3. Stopband attenuation of $\geq 20\,\text{dB}$ below 500 Hz.

Solution:

The high-pass to low-pass transformation procedure yields,

$$\omega_r = \frac{\omega_c}{\omega_s} = \frac{2\pi\,(1000)}{2\pi\,(500)} = 2.$$

The specifications imply the following relationships:

$$20\log\left|\frac{H\,(2\pi\times 1\text{k})}{H_o}\right| = 20\log\left[\frac{1}{\sqrt{1+\varepsilon^2}}\right] = -2\,\text{dB},$$

and

$$20\log\left|\frac{H\,(2\pi\times 500)}{H_o}\right| = 20\log\left[\frac{1}{\sqrt{A^2}}\right] = -20\,\text{dB}.$$

The solutions to the two relationships above are: $\varepsilon = 0.7648$ and $A = 10$.

The required order of the Chebyshev type 1 low-pass filter is found by using Equations (9.91)–(9.93),

$$g = \sqrt{\frac{A^2-1}{\varepsilon^2}} = \sqrt{\frac{10^2-1}{0.7648^2}} = 13.01,$$

and

$$n = \left\lceil \frac{\log\left[13.01+\sqrt{13.01^2-1}\right]}{\log\left[2+\sqrt{2-1}\right]} \right\rceil = \lceil 2.96 \rceil = 3.$$

Using Table 9.4 for $n = 3$ and 2 dB ripple, the transfer function is,

$$\frac{H\left(\frac{\omega}{\omega_c}\right)}{H_o} = \frac{1}{\left[\left(j\frac{\omega}{\omega_c}\right)+0.299\right]\left\{\left[\left(j\frac{\omega}{\omega_c}\right)+0.149\right]^2+0.904^2\right\}}$$

$$= \frac{1}{\left[\left(j\frac{\omega}{\omega_c}\right)+0.299\right]\left[\left(j\frac{\omega}{\omega_c}\right)^2+0.298\left(j\frac{\omega}{\omega_c}\right)+0.839\right]}.$$

Perform a forward transformation to yield the high-pass filter transfer function:

$$\left.\frac{H(\omega)}{H_o}\right|_{j\omega\rightarrow\frac{\omega_c}{j\omega}} = \frac{1}{\left[\left(\frac{\omega_c}{j\omega}\right)+0.299\right]\left[\left(\frac{\omega_c}{j\omega}\right)^2+0.298\left(\frac{\omega_c}{j\omega}\right)+0.839\right]}.$$

The normalized high-pass filter function is:

$$\left.\frac{H\left(\frac{\omega}{\omega_c}\right)}{H_o}\right|_{j\omega\rightarrow\frac{\omega_c}{j\omega}} = \frac{\left(\frac{j\omega}{\omega_c}\right)^3}{\left[1+0.299\left(\frac{j\omega}{\omega_c}\right)\right]\left[1+0.298\left(\frac{j\omega}{\omega_c}\right)+0.839\left(\frac{j\omega}{\omega_c}\right)^2\right]}.$$

The response of the third order high-pass filter transfer function in this example is shown below.

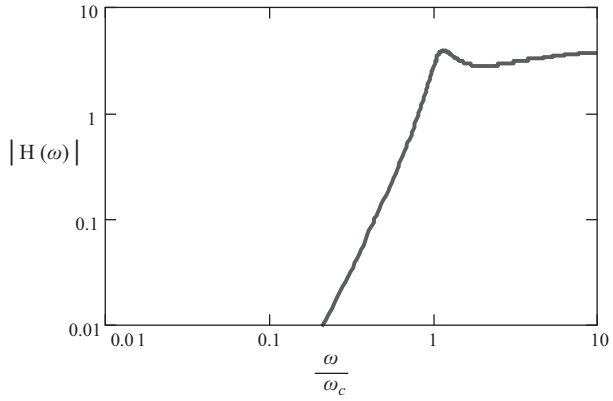

9.6.1 OPAMP REALIZATION OF CHEBYSHEV FILTERS

Since the Chebyshev type 1 low-pass filter is an all-pole filter, the OpAmp circuit implementation is identical to the Butterworth filter circuit configurations. Both the unity gain and Sallen and Key configurations can be used to implement Chebyshev type 1 filters.

Low-Pass OpAmp Filters

Although the OpAmp circuit configurations for the Chebyshev Type 1 and the Butterworth low-pass filters are identical, the calculations for the components of the circuit components differ. The calculations for the first order low-pass stages of Chebyshev Type 1 and Butterworth filters is identical. However, the calculation of the component values for the Chebyshev Type 1 transfer function of second order low-pass stages requires some modification from the Butterworth calculations.

These modifications for calculating second order stages of Chebyshev Type 1 low-pass filters are as follows. If

$$H\left(\frac{\omega}{\omega_c}\right) = \prod_{i=1}^{n} \frac{1}{\left[\frac{(j\omega)^2}{a_i\omega_c^2} + \frac{b_i\,(j\omega)}{a_i\omega_c} + 1\right]}, \tag{9.94}$$

then the "relative" resonant frequency for the two second order stages are:

$$\omega_{oi} = \sqrt{a_i}\omega_c. \tag{9.95}$$

The damping coefficient is,

$$(2\zeta_i) = \frac{b_i}{\sqrt{a_i}}. \tag{9.96}$$

Then Equation 9.44 is replaced by,

$$\omega_{oi} = \frac{1}{\sqrt{R_1R_2C_1C_2}}. \tag{9.97}$$

Using the uniform time constant form of the Sallen and Key second-order stage where $R_1 = R_2$ and $C_1 = C_2$, the gain can be expressed as,

$$A_{Vi} = 3 - (2\zeta_i)\,. \tag{9.98}$$

Example 9.15
Design a low-pass filter with the following specifications:

1. Cutoff frequency $f_c = 1000$ Hz.
2. Acceptable passband ripple of 3 dB.
3. Stopband attenuation of ≥ 20 dB above 1400 Hz.

Implement the filter transfer function with the Sallen and Key configuration.

Solution:
The specifications imply the following relationships:

$$20\log\left|\frac{H\,(2\pi \times 1\text{k})}{H_o}\right| = 20\log\left[\frac{1}{\sqrt{1+\varepsilon^2}}\right] = -3\text{ dB}$$

and

$$20\log\left|\frac{H\,(2\pi \times 1400)}{H_o}\right| = 20\log\left[\frac{1}{\sqrt{A^2}}\right] = -20\text{ dB}.$$

The solutions to the two relationships above are: $\varepsilon = 1$ and $A = 10$.

The required order of the Chebyshev type 1 low-pass filter is found by using Equations (9.91)–(9.93),

$$g = \sqrt{\frac{A^2 - 1}{\varepsilon^2}} = \sqrt{\frac{10^2 - 1}{1^2}} = 9.95,$$

and

$$n = \left\lceil \frac{\log\left[9.95 + \sqrt{9.95^2 - 1}\right]}{\log\left[1.4 + \sqrt{1.4^2 - 1}\right]} \right\rceil = \lceil 3.45 \rceil = 4.$$

Using Table 9.4 for $n = 4$ and 3 dB ripple, the transfer function is,

$$\begin{aligned}
\frac{H\left(\frac{\omega}{\omega_c}\right)}{H_o} &= \frac{1}{\left\{\left[\left(j\frac{\omega}{\omega_c}\right) + 0.085\right]^2 + 0.947^2\right\}\left\{\left[\left(j\frac{\omega}{\omega_c}\right) + 0.206\right]^2 + 0.392^2\right\}} \\
&= \frac{1}{\left[\left(j\frac{\omega}{\omega_c}\right)^2 + 0.170\left(j\frac{\omega}{\omega_c}\right) + 0.904\right]\left[\left(j\frac{\omega}{\omega_c}\right)^2 + 0.412\left(j\frac{\omega}{\omega_c}\right) + 0.196\right]} \\
&= \frac{5.644}{\left[\frac{(j\omega)^2}{0.904\omega_c^2} + \frac{0.170j\omega}{0.904\omega_c} + 1\right]\left[\frac{(j\omega)^2}{0.196\omega_c^2} + \frac{0.412j\omega}{0.196\omega_c} + 1\right]}
\end{aligned}$$

The "relative" resonant frequencies for the two second order stages are:

$$\omega_{o1} = \sqrt{0.904}\omega_c = (0.951)\,(2\pi)\,(1\text{k}) = 5.98 \text{ krad/s},$$

and

$$\omega_{o2} = \sqrt{0.196}\omega_c = (0.443)\,(2\pi)\,(1\text{k}) = 2.78 \text{ krad/s}.$$

The damping coefficients are:

$$2\zeta_1 = \frac{0.170}{\sqrt{0.904}} = 0.179$$

and

$$2\zeta_2 = \frac{0.412}{\sqrt{0.196}} = 0.931.$$

Let the capacitors be equal and $C = 0.1\,\mu$F. Let the frequency controlling resistances within each stage be identical. Then, the frequency controlling resistors for the two stages are:

$$R_1 = \frac{1}{\omega_{01} C} = \frac{1}{5.98\text{k}\,(0.1\mu)} = 3.6\ \text{k}\Omega,$$

and

$$R_2 = \frac{1}{\omega_{02} C} = \frac{1}{2.78\,\text{k}\,(0.1\mu)} \approx 1.6\ \text{k}\Omega \quad \text{(standard value)}.$$

The gain for the two stages are:

$$A_{v1} = 3 - (2\xi_1) = 2.82, \quad \text{and} \quad A_{v2} = 3 - (2\xi_1) = 2.07.$$

If $R'_{gain1} = R'_{gain2} = 10\,\text{k}\Omega$, then $R_{gain1} \approx 18\,\text{k}\Omega$ and $R_{gain2} \approx 10\,\text{k}\Omega$.

The completed fourth-order Chebyshev filter design is shown below.

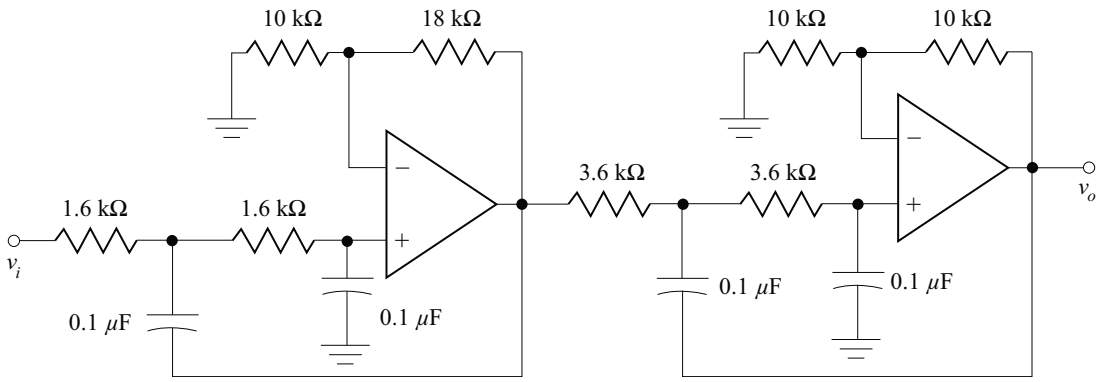

High-Pass OpAmp Filters

Unlike Butterworth filters, the Chebyshev high-pass OpAmp filter is not arrived at by simple interchanges of the frequency controlling resistances and capacitances. As shown in Section 9.6.1, the transfer function of the Chebyshev high-pass filter is found by performing analog-to-analog transformations. The high-pass transfer function is then implemented by a circuit using the same techniques outlined for the Chebyshev low-pass filter.

Example 9.16

Design a high-pass filter with the following specifications:

1. Cutoff frequency $f_c = 1000\,\text{Hz}$.
2. Acceptable passband ripple of 3 dB.

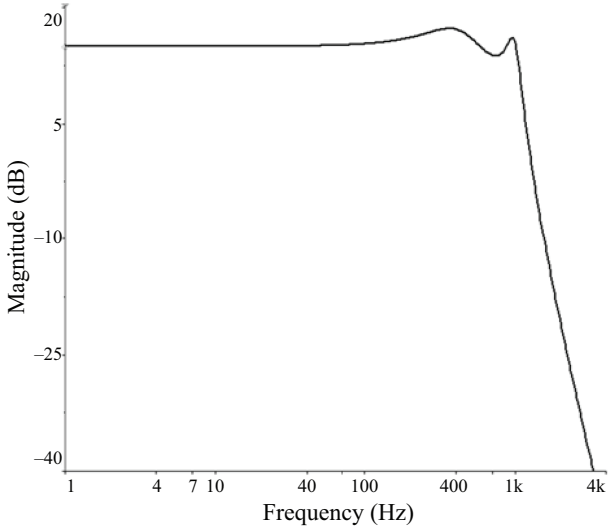

Figure 9.27: SPICE frequency response for Example 9.15.

3. Stopband attenuation of ≥ 20 dB below 600 Hz.

Implement the filter transfer function with the Sallen and Key configuration.

Solution:

The specifications imply the following relationships:

$$20\log\left|\frac{H\,(2\pi\times 1\text{k})}{H_o}\right| = 20\log\left[\frac{1}{\sqrt{1+\varepsilon^2}}\right] = -3\,\text{dB}$$

and

$$20\log\left|\frac{H\,(2\pi\times 600)}{H_o}\right| = 20\log\left[\frac{1}{\sqrt{A^2}}\right] = -20\,\text{dB}.$$

The solutions to the two relationships above are: $\varepsilon = 1$ and $A = 10$.

An analog-to-analog transformation is performed to determine the transformed normalized LOW-PASS characteristics. The backward transformation from high to low-pass yields,

$$\omega_r = \frac{\omega_c}{\omega_s} = \frac{2\pi\,(1000)}{2\pi\,(600)} = 1.67.$$

The required order of the normalized Chebyshev type 1 low-pass filter is found by using Equations (9.91)–(9.93),

$$g = \sqrt{\frac{A^2 - 1}{\varepsilon^2}} = \sqrt{\frac{10^2 - 1}{1^2}} = 9.95,$$

and

$$n = \left\lceil \frac{\log\left[9.95 + \sqrt{9.95^2 - 1}\right]}{\log\left[1.67 + \sqrt{1.67 - 1}\right]} \right\rceil = \lceil 3.27 \rceil = 4.$$

Using Table 9.4 for $n = 4$ and 3 dB ripple, the transfer function is,

$$\begin{aligned}\frac{H(\omega)}{H_o} &= \frac{1}{\left\{[(j\omega) + 0.085]^2 + 0.947^2\right\}\left\{[(j\omega) + 0.206]^2 + 0.392^2\right\}} \\ &= \frac{1}{\left[(j\omega)^2 + 0.170(j\omega) + 0.904\right]\left[(j\omega)^2 + 0.412(j\omega) + 0.196\right]}.\end{aligned}$$

Another analog-to-analog transformation is performed to yield the normalized HIGH-PASS transfer function by replacing $j\omega$ with $\frac{\omega_c}{j\omega}$.

$$\begin{aligned}\frac{H(\omega)}{H_o} &= \frac{1}{\left[\left(\frac{\omega_c}{j\omega}\right)^2 + 0.170\left(\frac{\omega_c}{j\omega}\right) + 0.904\right]\left[\left(\frac{\omega_c}{j\omega}\right)^2 + 0.412\left(\frac{\omega_c}{j\omega}\right) + 0.196\right]} \\ &= \frac{\left(\frac{j\omega}{\omega_c}\right)^2}{\left[1 + 0.170\left(\frac{j\omega}{\omega_c}\right) + 0.904\left(\frac{j\omega}{\omega_c}\right)^2\right]\left[1 + 0.412\left(\frac{j\omega}{\omega_c}\right) + 0.196\left(\frac{j\omega}{\omega_c}\right)^2\right]} \\ &= \frac{\left(\frac{j\omega}{\omega_c}\right)^2}{\left[1 + \frac{0.188}{1}\left(\frac{j\omega}{\omega_c}\right) + \frac{1}{1}\left(\frac{j\omega}{\omega_c}\right)^2\right]\left[1 + \frac{2.112}{1}\left(\frac{j\omega}{\omega_c}\right) + \frac{1}{1}\left(\frac{j\omega}{\omega_c}\right)^2\right]}.\end{aligned}$$

The "relative" resonant frequencies for the two second order stages are:

$$\omega_{o1} = \sqrt{\frac{1}{0.904}} \qquad \omega_c = (1.052)(2\pi)(1\text{k}) = 6.61 \text{ krad/s}$$

and

$$\omega_{o2} = \sqrt{\frac{1}{0.196}} \qquad \omega_c = (2.259)\,(2\pi)\,(1\text{k}) = 14.18 \text{ krad/s}.$$

The damping coefficients are:

$$2\zeta_1 = \frac{0.188}{\sqrt{\frac{1}{0.904}}} = 0.179 \quad \text{and} \quad \zeta_2 = \frac{2.112}{\sqrt{\frac{1}{0.196}}} = 0.935.$$

Note that the damping coefficients are identical (except for round-off error) to that of the fourth order low-pass example in Example 9.15

Let the capacitors be equal and $C = 0.1\,\mu$F. Let the frequency controlling resistances within each stage be identical. Then, the frequency controlling resistors for the two stages are:

$$R_1 = \frac{1}{\omega_{01} C} = \frac{1}{6.61\,\text{k}\,(0.1\mu)} \approx 1.5\ \text{k}\Omega,$$

and

$$R_2 = \frac{1}{\omega_{02} C} = \frac{1}{14.18\,\text{k}\,(0.1\mu)} \approx 680\ \Omega \quad \text{(standard value)}.$$

The gain for the two stages are:

$$A_{v1} = 3 - (2\xi_1) = 2.82 \quad \text{and} \quad A_{v2} = 3 - (2\xi_1) = 2.07.$$

If $R'_{gain1} = R'_{gain2} = 10\,\text{k}\Omega$, then $R_{gain1} \approx 18\,\text{k}\Omega$ and $R_{gain2} \approx 10\,\text{k}\Omega$: the gain resistors are identical to the fourth order low-pass example in Example 9.15.

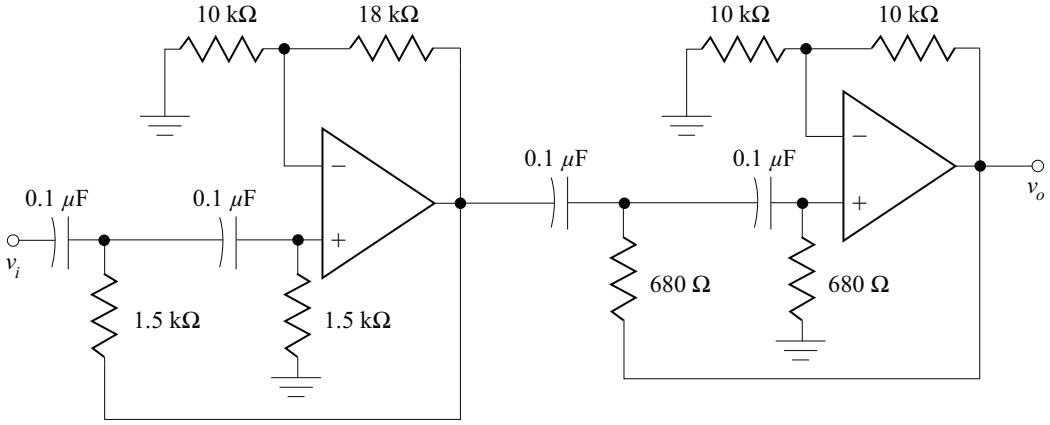

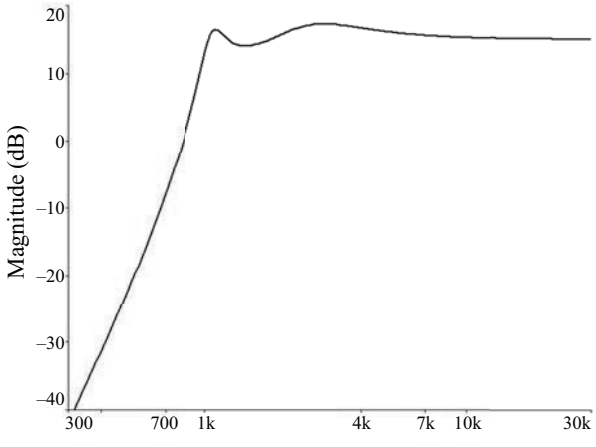

Figure 9.28: High-pass Chebyshev filter of Example 9.16.

9.7 COMPARISON OF FILTER TYPES

The Butterworth and Chebyshev filter types have been discussed in the previous section. The three filter types offer different performance characteristics that may be used to fulfill design specifications. To simplify the choice of filter used to fulfill a certain specification, several key characteristics are compared:

1. Cut-off frequency

   The Butterworth filter passband is typically defined by the cut-off frequency which is the half power point in the frequency response. However, in Chebyshev filters the passband, and therefore, the so-called cut-off frequency, is defined by the frequency that identifies the end of the ripple. These two frequencies are different unless $\varepsilon = 1$. Therefore, it is important to keep separate the definitions of cut-off frequency and half-power points for different filter types.

2. Ripple

   The Butterworth filter has a maximally flat response which results in a ripple-free passband and stopband. Chebyshev filters exhibit ripple in either the passband or the stopband for Chebyshev type 1 or type 2 filters; that is, passband ripple corresponds to type 1 filters and stopband ripple corresponds to type 2 filters. In the Chebyshev response, the ripple is dependent on the factor ε.

3. DC response for a low-pass filter

In the Butterworth filter, the response is peaked at DC. However, in the Chebyshev designs, the DC filter response may be either peaked or at the power level of the response at the cut-off frequency: that is, the DC response is peaked for odd order filters, and corresponds to the cut-off frequency power level for even order filters.

4. Transition band

   One of the most important filter specifications is the steepness of the transition band. Steeper transitions from the passband to stopband requires the use of higher order filters: higher order filters require more electronic components to implement. Fortunately, the three filter types discussed in the previous section have varying transition band steepness given an identical filter order. The Butterworth filter is the least steep in the transition band.

For example, for a $n = 5$ filter (with $\varepsilon = 1$), the Chebyshev response has 24 dB greater attenuation than the Butterworth response.

9.8 SWITCHED-CAPACITOR FILTERS

Using MOSFETS as switches, switched-capacitor (SC) filters can be designed in precision monolithic integrated circuits, and is widely used in digital signal procession applications. The advantage of using MOSFET SC filters is derived from the simple fact that it is difficult to manufacture precision resistors in integrated circuits. OpAmps and capacitors are more easily fabricated. Although accurate values of capacitances may be difficult to achieve, precise ratios of capacitances can easily be achieved in integrated circuits.

The key features of SC filters are:

- The filter can be fabricated in a precision monolithic integrated circuit.
- Since MOS technology allows high component density in integrated circuits, a single chip can be fabricated to fulfill both analog and digital signal processing.
- MOS devices have very low power dissipation and temperature coefficients.
- Precise capacitance ratios can be fabricated. This is particularly important since active filters depend largely on RC time constants: the time constant can be controlled by capacitance ratios.
- Because resistors are eliminated, power consumption is reduced.

9.8.1 MOS SWITCH

The FET as an analog switch was discussed in Section 4.5 (Book 1). Ideal enhancement type NMOSFET switch has the following design goals:

- In the ON state ($V_{GS} > V_T$), it passes signal from the drain to source without attenuation.

- In the OFF state ($V_{GS} < V_T$), the signal is not passed from the drain to source.
- Transitions between the ON and OFF states is instantaneous.

Real NMOSFET switches have the following characteristics:

- In the ON state ($V_{GS} > V_T$), the drain-source resistance, r_D, is in the order of kilo-ohms ($< 10\,\text{k}\Omega$).[10]
- In the OFF state ($V_{GS} < V_T$), the drain-source resistance, r_D, is in the order of several hundred mega-ohms ($100\,\text{M}\Omega$–$1000\,\text{M}\Omega$).

The ratio of the resistance values between the ON and OFF states of an enhancement NMOSFET is in the order or 10^5 or 100 dB. An equivalent representation of the characteristic of enhancement NMOSFET switches is shown in Figure 9.29.

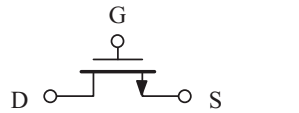

Enhancement NMOSFET Symbol

Condition	Switch State	Equivalent Resistor	Switch Model
$V_{GS} > V_T$	ON	10 kΩ	
$V_{GS} < V_T$	OFF	100MΩ	

Figure 9.29: Circuit and switch representation of enhancement NMOSFET.

A voltage signal is applied to the gate-source junction with fast rise and fall times and with a peak amplitude greater than V_T. Since the gate-source voltage is now a time varying signal, it is represented as v_{gs} or more commonly as a pulse train signal ϕ. The NMOSFET switch is open or closed depending on the value of ϕ. This type of switch is known as the single-pole single-throw (SPST) switch.

The clock signal, ϕ, which is a pulse train signal, is usually generated by an external digital system. The pulse train is periodic with a period of T_C with a clock frequency of $f = 1/T_C$. The clock signal is used to turn the NMOSFET ON or OFF.

A two phase clock is shown in Figure 9.30. The two clock signals, ϕ_1 and ϕ_2, have the same clock frequency but is out of phase; that is, when ϕ_1 is ON, ϕ_2 is OFF. The duty cycle (percentage of time ON to the period of the signal) is commonly slightly less than 50% to insure non-overlapping clocks.

[10]The comparatively large ON resistance of these switches is due to on-chip geometries that are not present in discrete FET switches as described in 4 (Book 1).

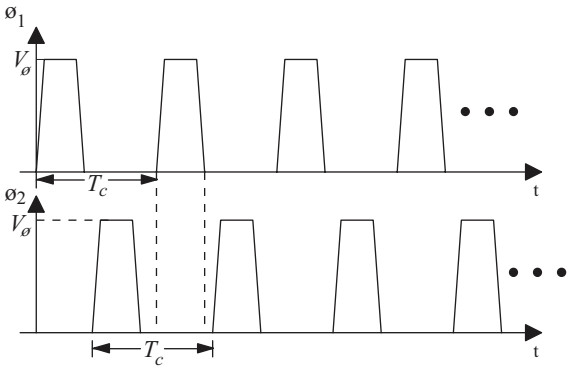

Figure 9.30: Biphase non-overlapping clocks.

For two NMOSFET switches in series in a "T" arrangement with a capacitor forms an SC circuit, shown in Figure 9.31a, with each FET with M_1 driven by ϕ_1 and M_2 by ϕ_2, one of the two FETs will always be ON. Simplified equivalent diagrams of the SC circuit are shown in Figure 9.31b and c. Figure 9.31b is derived by directly replacing the NMOSFETs with SPST switch representations, while Figure 9.31c is the functional equivalent diagram of the SC circuit. With biphase clock signal inputs ϕ_1 and ϕ_2 to FETs M_1 and M_2, respectively, it is evident that there will never be a direct connection between v_1 and v_2, as shown in Figure 9.31c. The term "switched capacitor" derives from the switching operation of the FETs on the capacitor.

For a time varying input voltage, $v_1(t)$, with switch S_1 closed and S_2 open, the equivalent circuit is that shown in Figure 9.32. If $v_1(t)$ is a constant voltage, the voltage across the capacitor, C, will increase with the time constant $\tau = R_{ON1}C$, where R_{ON1} is the ON resistance of the NMOSFET M_1. For typical capacitance of $C = 1\,\text{pF}$ and $R_{ON1} = 10\,\text{k}\Omega$, the voltage across the capacitor will reach 63% of the input voltage when $\tau = R_{ON1}C = 10\,\text{ns}$.

For the switched capacitor filter to operate properly, the time constant formed by $R_{ON1}C$ must be significantly small compared to the variations in the input voltage signal. If the switch position is changed from 1 to 2, the charge on the capacitor will discharge at the output, v_2. The charge transferred is,

$$Q = C\,(v_1 - v_2)\,, \tag{9.99}$$

over a discharge time, T_C. The average current through the capacitor during this discharging period in time is,

$$i\,(t) = \frac{dQ}{dt} = \frac{\Delta Q}{\Delta t} \approx \frac{C\,(v_1 - v_2)}{T_C}. \tag{9.100}$$

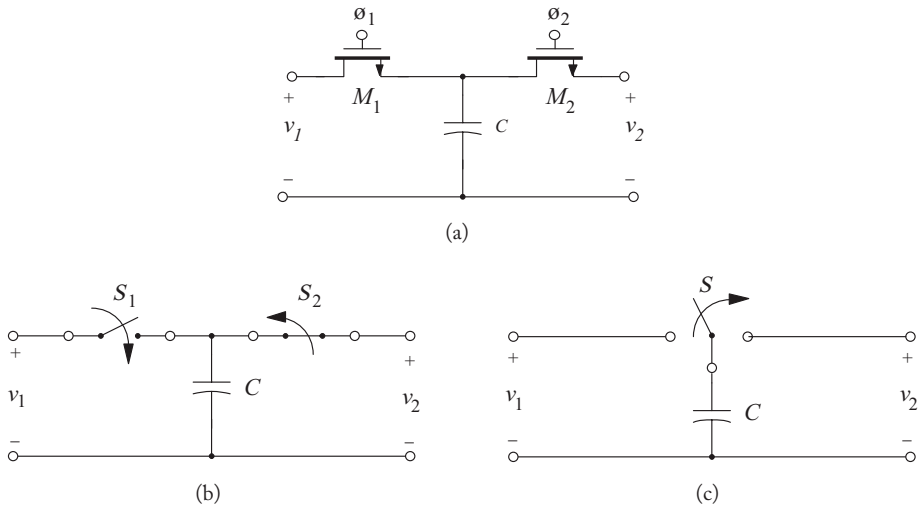

Figure 9.31: (a) NMOSFET switched capacitor, (b) FETs replaced by SPST switches, (c) simplified functional circuit representation.

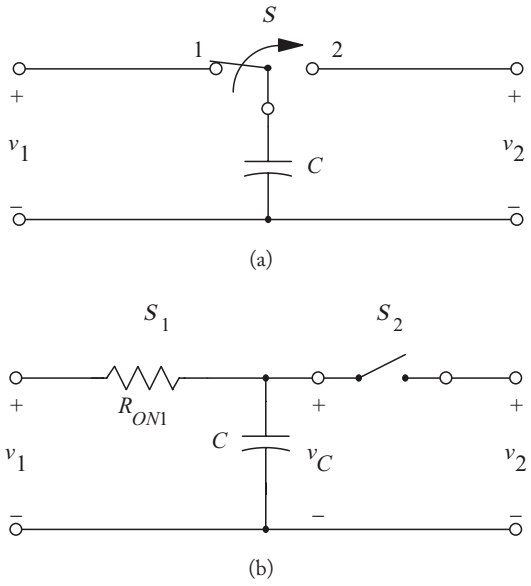

Figure 9.32: (a) Switched capacitor with node 1 closed, (b) Equivalent circuit with FET ON resistance shown.

The *equivalent resistor* formed by the switched capacitor to yield the same value of current is:

$$R_{EQ} = \frac{v_1 - v_2}{i(t)} = \frac{T_C}{C} = \frac{1}{f_c C}, \tag{9.101}$$

since $i(t) = \frac{v_1 - v_2}{R_{EQ}}$ the approximate equivalent circuit for the switched capacitor of Figure 9.31a is Figure 9.33.

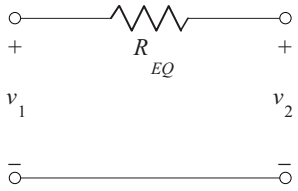

Figure 9.33: Approximate equivalent circuit for a switched capacitor.

Consider the range of values of R_{EQ}. Using $C = 1\,\text{pF}$ (requiring a silicon area on the chip of approximately $0.01\,\text{mm}^2$) and a typical switching frequency of the NMOSFETs of $f_c = 100\,\text{kHz}$, R_{EQ} is found to be $10\,\text{M}\Omega$. For the switched capacitor network to be useful, the switching frequency, f_C, must be much larger than the signal frequencies of interest in $v_1(t)$ and $v_2(t)$.

9.8.2 SIMPLE INTEGRATOR

The switched capacitor networks are used to implement active circuits for a variety of analog operations. A simple integrator shown in Figure 9.34a is described by the transfer function,

$$\frac{v_o(\omega)}{v_i(\omega)} = -\frac{1}{j\omega R C_f}. \tag{9.102}$$

The resistance in the integrator of Figure 9.34a can be replaced with a switched capacitor to obtain Figure 9.34b. The integrator transfer function can be rewritten using Equation (9.101),

$$\frac{v_o(\omega)}{v_i(\omega)} = -\frac{f_C C_1}{j\omega C_f}. \tag{9.103}$$

The transfer function of the switched capacitor implementation of the active integrator clearly shows a dependence on the clock frequency of the NMOSFET input signals and the *ratio* of the two capacitors. Since MOS integrated circuit technology can hold tight tolerances on capacitance ratios, precision integrators may be fabricated using the switched capacitor implementation.

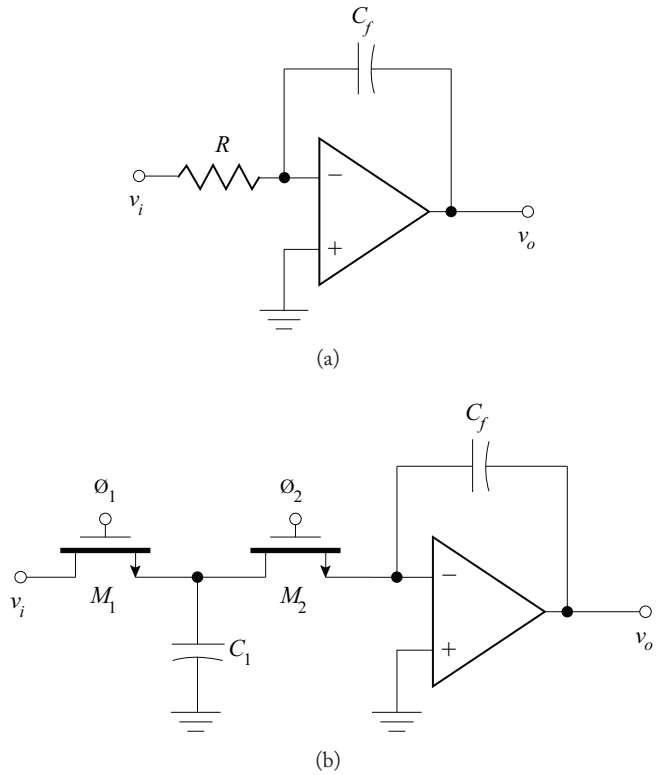

Figure 9.34: (a) Simple active RC integrator, (b) Switched capacitor implementation of (a).

9.8.3 GAIN STAGE

A switched capacitor inverting amplifier arrangement is shown in Figure 9.35a with two switched capacitor filter networks, each equivalent to a resistance. The gain of the circuit is,

$$A_V = \frac{v_o}{v_i} = -\frac{C_2}{C_1}. \tag{9.104}$$

In Figure 9.35a, the capacitor C_1 is charged to input signal level for $\phi_1 = V_\phi$ and C_2 is discharged. When $\phi_1 = 0$ then the voltage across C_1 is applied to the OpAmp and C_2 becomes the feedback path.

A direct replacement of the resistors in the inverting OpAmp amplifier configuration with switched capacitors yields the circuit shown in Figure 9.35b. This circuit is unworkable since the switches used to form the feedback resistance is never closed simultaneously. Therefore, the feedback path from the output to the input of the OpAmp is only periodically closed and the OpAmp will saturate.

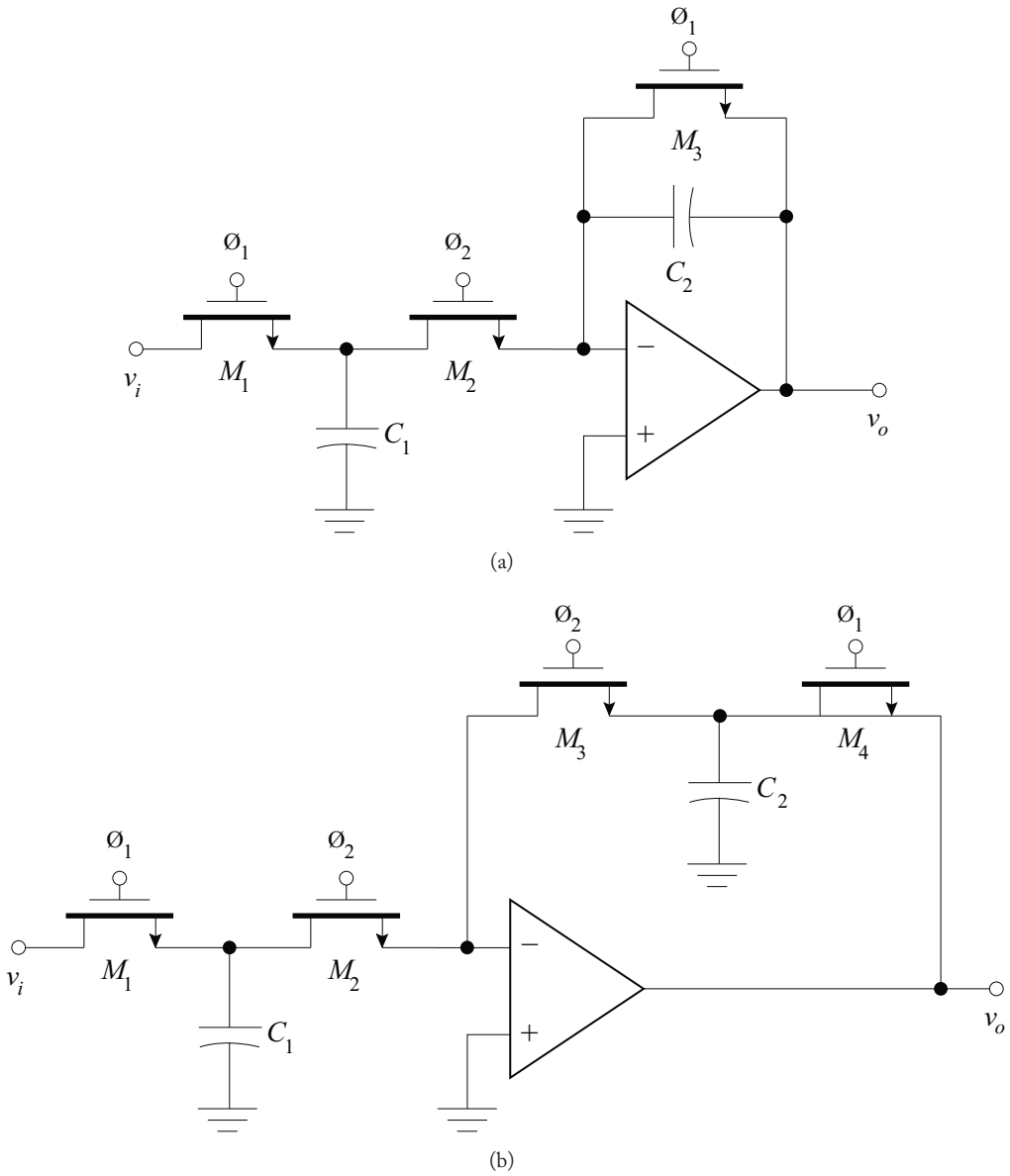

Figure 9.35: (a) Practical switched capacitor inverting amplifier, (b) Unworkable switched capacitor inverting amplifier.

9.8.4 LOW-PASS FILTERS

A switched capacitor active low-pass filter is shown in Figure 9.36. The NMOSFETs M_1 and M_2 and the capacitor C_1 form the equivalent resistance, R_{EQ}, such that the transfer function of this circuit is,

$$\frac{v_o(\omega)}{v_i(\omega)} = \frac{1}{R_{EQ}C_2}\left(\frac{1}{j\omega + \frac{1}{R_{EQ}C_2}}\right) = \frac{f_C C_1}{C_2}\left(\frac{1}{j\omega + \frac{f_C C_1}{C_2}}\right). \tag{9.105}$$

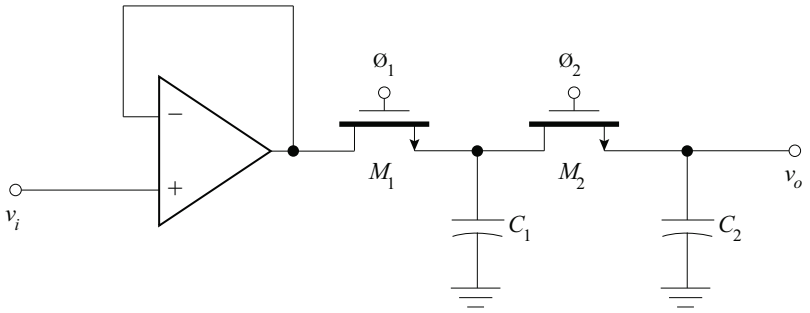

Figure 9.36: First-order low-pass filter.

Through careful switched capacitor network arrangements, second order switched capacitor filter circuit can be implemented. Figure 9.37 shows a Sallen and Key second order all-pole low-pass filter and its switched capacitor equivalent. Note that resistors R_2 and R_3 are in the feedback path and the switched capacitor implementation replaces these resistors with the alternate switched capacitor network of a NMOSFET in parallel with the switched capacitor.

9.9 OPAMP LIMITATIONS

Thus, far, designs using OpAmps have assumed that the OpAmp has very large open-loop gain ($A \geq 200\,\text{k}$) over all frequencies. Filter designs have used this assumption by ignoring potential frequency effects of OpAmps in their design. In reality, OpAmps themselves have a frequency response: the frequency response is dependent on the closed loop gain of the amplifier. Therefore, the OpAmp may itself limit the operational frequency range of the application.

When a large step input voltage is applied to an OpAmp, the output waveform rises with a finite slope called the *slew rate*. The slewing behavior of the output is due to amplifier nonlinearities. Therefore, the slew rate cannot be calculated from the frequency response of the OpAmp using linear analysis. The inability of the OpAmp output to rise in voltage as quickly as linear theory predicts will also limit the frequency range of the amplifier.

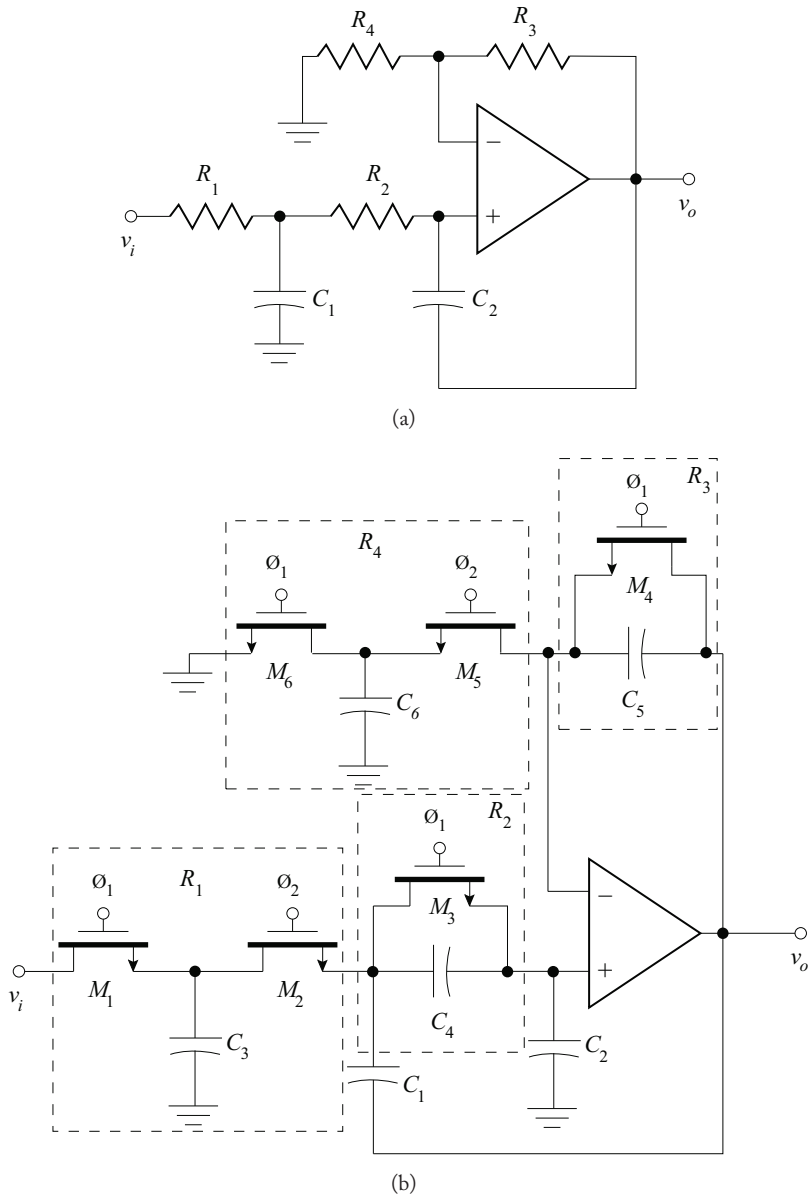

Figure 9.37: (a) Sallen and key second order low-pass filter section, (b) Switched capacitor implementation.

9.9.1 FREQUENCY RESPONSE OF OPAMPS

Returning to the definition of the OpAmp output voltage presented in Equation 1.2 (Book 1), a frequency dependent gain is used,

$$v_o = A(j\omega)[v_2 - v_1] = A(j\omega)\, v_i, \tag{9.106}$$

where

$A(j\omega)$ is the frequency dependent large signal gain
v_2 is the non-inverting input voltage
v_1 is the inverting input voltage
v_o is the output voltage, and
v_i is the voltage applied between the input terminals of the OpAmp.

For a μA741, the gain characteristics are shown in Figure 9.38. The μA741 is an internally compensated OpAmp, meaning that a capacitor is fabricated on the chip to for stability resulting in a low-frequency pole in the transfer function.

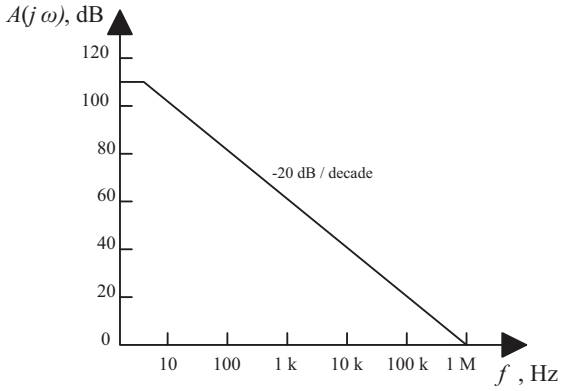

Figure 9.38: OpAmp open loop gain characteristics.

The curve shows an open loop gain of between 100 and 120 dB at DC. Then at the OpAmp corner frequency, $f_{ca} = 5$ Hz, the gain falls off at -20 dB/decade, reaching 0 dB at 1 MHz. The product of the gain with the bandwidth is constant and is defined as the *Gain Bandwidth Product (GBP)*. The GBP of the μA741 is 10^6. The open loop gain, $A(j\omega)$, of this curve is,

$$A(j\omega) = \frac{A_o}{1 + \dfrac{j\omega}{\omega_{ca}}} = \frac{A_o \omega_{ca}}{j\omega + \omega_{ca}} = \frac{GBP}{j\omega + \omega_{ca}}, \tag{9.107}$$

where A_o is the open loop gain at DC,

$$\omega_{ca} = 2\pi f_{ca}$$

and

$$GBP = A_o \omega_{ca}. \tag{9.108}$$

Referring to Figure 9.39, the GBP is confirmed as being constant, where the bandwidth is defined by the corner frequency (f_c) and the closed loop gain as A_v.

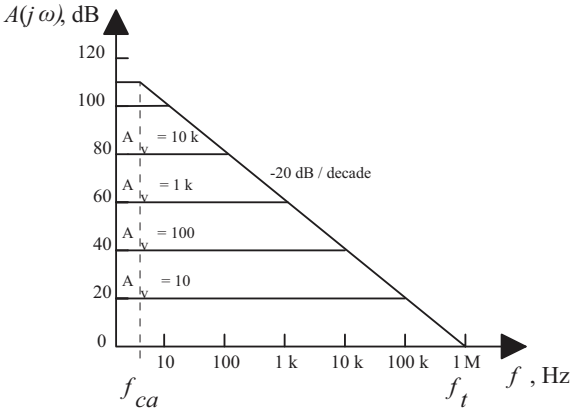

Figure 9.39: Closed loop gain characteristics.

The output voltage, v_o, of an inverting OpAmp amplifier shown in Figure 9.40 is,

$$v_o = A\,(j\omega)\, v_a, \tag{9.109}$$

where v_a is the input to the OpAmp.
The input voltage to the OpAmp is,

$$v_a = \left(\frac{v_o - v_i}{R_s + R_f}\right) R_s + v_i. \tag{9.110}$$

Combining Equations (9.109) and (9.110), and knowing that $R_f/R_s = K$, the gain of the circuit is,

$$A_V = \frac{v_o}{v_i} = -K\frac{A(j\omega)/(1+K)}{1 + A(j\omega)/(1+K)}. \tag{9.111}$$

Let $A(j\omega) = GBP/j\omega$ then the voltage gain in Equation (9.111) becomes,

$$A_V = \frac{v_o}{v_i} = -K\frac{GBP/(1+K)}{j\omega + GBP/(1+K)}. \tag{9.112}$$

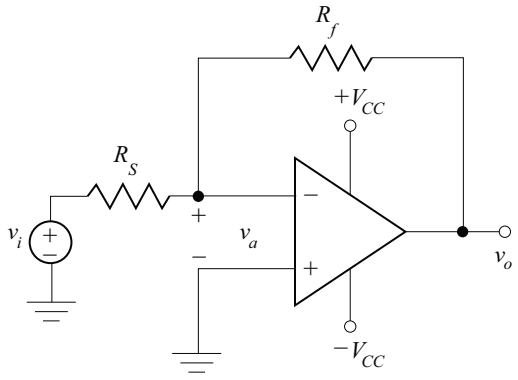

Figure 9.40: Inverting OpAmp amplifier.

Equation (9.112) is a transfer function of the inverting OpAmp amplifier taking into account the frequency response of the OpAmp. It is of the form of a single-pole transfer function with 3 dB frequency:

$$\omega_{3\,\mathrm{dB}} = \frac{GBP}{1+K}. \tag{9.113}$$

9.9.2 OPAMP SLEW RATE

Time domain responses of OpAmp circuits require a introduction to a characteristic that is important in the specification of OpAmps. The most important of these is the *slew rate*. Because OpAmps have responses that are frequency dependent, the output due to a step input is not a perfect step, causing the output to be distorted.

When a step function, shown in Figure 9.41a, is applied to a unity gain follower OpAmp circuit, the resulting output is that similar to Figure 9.41b. The output voltage is in the form of a low-pass filter,

$$A_V(\omega) = \frac{v_o(\omega)}{v_i(\omega)} = \frac{1}{1+\frac{j\omega}{\omega_t}}, \tag{9.114}$$

where

$v_o(\omega)$ is the output voltage
$v_i(\omega)$ is the input voltage
ω_t is the unity gain bandwidth.

The step response of the circuit is an exponentially rising waveform,

$$v_o(t) = V_1(1-e^{-\omega_t t}) = V_1\left(1-e^{-t/\tau}\right). \tag{9.115}$$

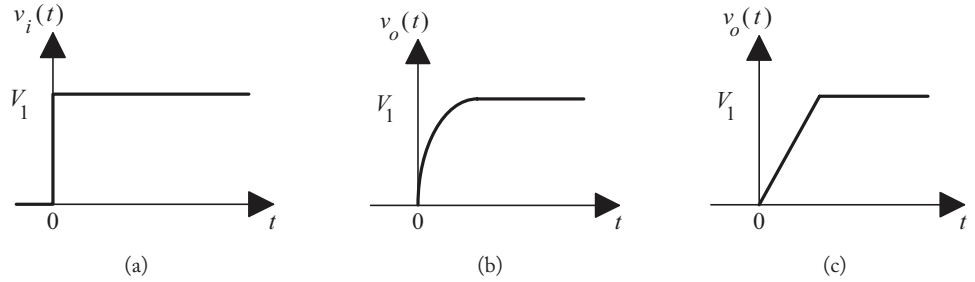

Figure 9.41: (a) Input voltage to OpAmp unity gain follower (b) Output waveform with V_1 small (Non-Saturating) (c) Input waveform with V_1 large.

For a small input voltage V_1, the output will be non-saturating, and the output waveform is shown in Figure 9.41b.

The initial slope of the output voltage is,

$$\frac{dv_o(t)}{dt} = V_1\omega_t = V_1(GBP). \tag{9.116}$$

The results above are valid for linear operation; implying that the input voltage must be sufficiently small so that the OpAmp does not saturate. For a large, saturating input voltage, the output waveform is shown in Figure 9.41c. Note that the initial slope of the output response is lower than predicted for linear theory. The inability of the OpAmp to rise as quickly as predicted by linear theory is called *slew rate limiting*. The initial slope of the output response is called the *slew rate*, SR, defined as,

$$SR = \left.\frac{dv_o(t)}{dt}\right|_{maximum}. \tag{9.117}$$

The OpAmp begins slewing when the initial slope of the output waveform is less than $V_1(GBP)$. The slew rate is specified in manufacture's specifications in volts per microsecond.

The slew rate is related to power bandwidth, f_p. The power bandwidth of the OpAmp is defined as the frequency at which a sinusoidal output begins to distort. The implication is that slew rate limits the bandwidth of OpAmp operation for amplifier and filter designs.

Given a output signal at the rated output voltage of the OpAmp,

$$v_o(t) = V_{out}\sin\left(2\pi f_p t\right), \tag{9.118}$$

the maximum slew rate is,

$$\left.\frac{dv_o(t)}{dt}\right|_{maximum} = V_{out}2\pi f_p \cos\left(2\pi f_p t\right)\Big|_{t=0} = V_{out}2\pi f_p. \tag{9.119}$$

If $V_{out} 2\pi f_p > SR$, the output waveform is distorted. The power bandwidth is therefore defined by the slew rate,

$$f_p = \frac{SR}{2\pi V_{rated}}, \tag{9.120}$$

where V_{rated} is the rated OpAmp output voltage.

Detailed SPICE models for the μA741, created from its equivalent models and including all the above discussed properties, are available in essentially every modern SPICE simulation package.

9.10 CONCLUDING REMARKS

Signal filtering concepts have been described in this chapter. It was demonstrated that bandpass filters could be designed by cascading low-pass and high-pass filters. Three types of active filters employing OpAmps were shown. Design criteria such as cutoff frequency, passband ripple, and stopband attenuation are used to determine order and type of active filter that best suits the requirements.

The three filter types and their characteristics are:

Butterworth Filter

- Maximally flat - no ripple
- All pole low-pass filter
- Can be implemented using Sallen and Key circuit

Chebyshev Type 1 Filter

- Ripple in the passband
- All pole low-pass filter
- Can be implemented using Sallen and Key circuit
- Has a steeper transition region than Butterworth for a given order filter

Switched capacitor networks were discussed as a means to implement active circuits in MOS integrated circuit using capacitance ratios instead of resistors. The design advantage lies in the elimination of resistors, which require large areas when fabricated in integrated circuits. The major drawback is the frequency limitations imposed by the switching.

The frequency response limitations of OpAmps was discussed in terms of gain bandwidth (GBP) and slew rate (SR). The response of an active circuit depends not only on the components external to the OpAmp, but on the OpAmp itself.

SUMMARY DESIGN EXAMPLE

Digital-to-Analog (D/A) conversion of electrical signals typically requires output low-pass filtering in order to remove undesirable high-frequency signal components. As an example, digital audio systems typically require this low-pass filtering at the output so that the signals passed on to the power amplification stages are faithful reproductions of the original audio input.

Audio signals are contained to the frequency band, $40\,\text{Hz} < f < 20\,\text{kHz}$. Compact disk systems sample this audio signal at 44.1 kHz prior to analog-to-digital conversion. The digital samples are then converted to 16 binary bits of information (65,536 levels) and encoded onto the compact disk. When the disk is to be replayed, the individual words of information are sampled several times (oversampled) before D/A conversion. The output of the D/A converter contains the original signal spectrum with sidebands centered at frequencies that are multiples of the product of the sampling rate and the oversampling constant. It is these sidebands that must be eliminated.

Design a filter to eliminate the sidebands of 4x oversampled compact disk D/A conversion without distorting the frequency content of the original signal by more than 0.25 dB at any frequency.

Solution:

The human ear is particularly sensitive to variations in frequency content: the designed filter should be smooth in the passband. A Butterworth filter is a good choice (Chebyshev, Type 2 might be an alternative). The sideband signals should be attenuated so that they are less than one level of digitization. Quantization into 65,536 levels implies that filter must introduce 96.33 dB attenuation at the lower frequency edge of the first sideband. The lower edge of this sideband is at:

$$f_s = 4(44.1\,\text{kHz}) - 20\,\text{kHz} = 156.4\,\text{kHz}.$$

A 0.25 dB variation at the edge of the passband sets the value of for the Butterworth filter:

$$\sqrt{1+\varepsilon^2} = 10^{0.025} \qquad \Rightarrow \qquad \varepsilon = 0.24342.$$

The order of the filter is then determined to be:

$$n = \frac{1}{2}\left\{\frac{\log\left(10^{9.633}-1\right) - \log\left(\varepsilon^2\right)}{\log\left(\dfrac{f_s}{f_c}\right)}\right\} = 6.08.$$

At least a seventh-order Butterworth filter is necessary. The three second-order damping coefficients necessary for this filter are:

$$\zeta_1 = 0.2225 \qquad \zeta_2 = 0.6235 \qquad \zeta_3 = 0.9010.$$

The resonant frequency for the Butterworth filter is given by:

$$\omega_o = \frac{\omega_c}{\sqrt[n]{\varepsilon}} = \frac{2\pi\,(20,000)}{\sqrt[7]{0.24343}} = 153.77\,\text{krad/s} \quad (24.473\,\text{kHz})\,.$$

Since gain is not a factor in the design requirements, a uniform time constant realization is chosen for simplicity and uniformity. One resistor-capacitor pair that will adequately approximate the resonant frequency (the filter resonant frequency has been chosen slightly larger [24.54 kHz] than the theoretical value) is:

$$R = 1.38\,\text{k}\Omega \qquad C = 0.0047\,\mu\text{F}.$$

One possible filter realization is shown below with the SPICE verification:

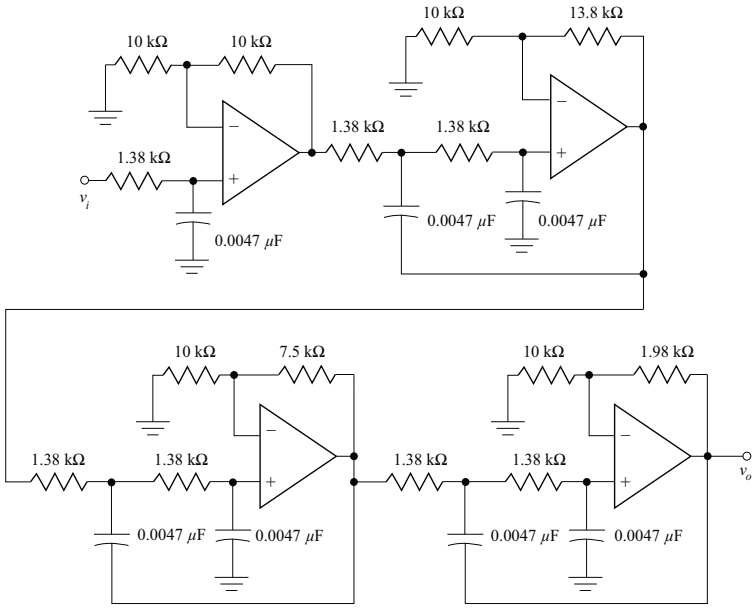

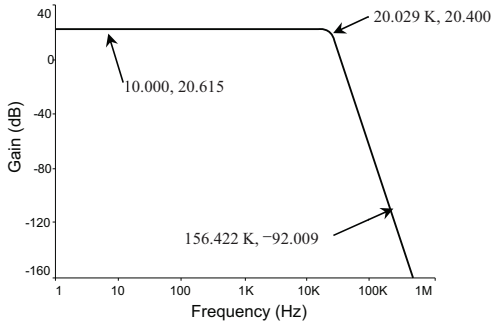

PROBLEMS

9.1. A complex-conjugate pair of poles is characterized by its resonant frequency and damping coefficient:

$$\omega_o = 1\,\text{krad/sec} \qquad \zeta = 0.6.$$

(a) Determine the maximum magnitude error of the Bode straight-line magnitude approximation.

(b) Determine the maximum magnitude phase error of the ζ-dependent Bode straight-line phase approximation.

9.2. The voltage gain of an amplifier is described by the following transfer function:

$$A_v(\omega) = \frac{(j\omega)^2}{\left(1 + 0.9\frac{j\omega}{50} + \left(\frac{j\omega}{50}\right)^2\right)\left(1 + \frac{j\omega}{10{,}000}\right)\left(1 + \frac{j\omega}{80{,}000}\right)}.$$

Plot the straight-line approximate Bode diagram. Compare results to a computer generated exact plot of the magnitude and phase.

9.3. The transconductance of an amplifier is described by the following transfer function:

$$G_M(\omega) = \frac{(j\omega)^2}{\left(1 + \frac{j\omega}{10}\right)\left(1 + \frac{j\omega}{40}\right)\left(1 + 0.7\frac{j\omega}{15{,}000} + \left(\frac{j\omega}{15{,}000}\right)^2\right)}.$$

Plot the straight-line approximate Bode diagram. Compare results to a computer generated exact plot of the magnitude and phase.

9.4. The transresistance of an amplifier is described by flat midband region of value 20 kΩ edged by low- and high-frequency poles.

The two low-frequency poles are at:

$$f_{L1} = 100\,\text{Hz} \quad \text{and} \quad f_{L2} = 30\,\text{Hz}.$$

There are three high-frequency poles: a complex-conjugate pair described by:

$$f_{Ho} = 80\,\text{kHz} \quad \text{and} \quad \zeta = 0.8,$$

and a single pole at

$$f_{H3} = 300\,\text{kHz}.$$

(a) How many zero-frequency zeros does the expression for the transresistance contain?

(b) Plot the straight-line approximate Bode diagram.

9.5. The current gain of an amplifier is described by flat midband region of value 1.8 kA/A edged by low- and high-frequency poles.

There are three low-frequency poles: a complex-conjugate pair described by:

$$f_{Lo} = 70\,\text{Hz} \quad \text{and} \quad \zeta = 0.7,$$

and a single pole at

$$f_{L3} = 20\,\text{Hz}.$$

The three high-frequency poles are at:

$$f_{H1} = 14\,\text{kHz}, \quad f_{H2} = 26\,\text{kHz}, \quad \text{and} \quad f_{H3} = 160\,\text{kHz}.$$

(a) How many zero-frequency zeros does the expression for the transresistance contain?

(b) Plot the straight-line approximate Bode diagram.

9.6. Design requirements require the use of a 14th order low-pass Butterworth Filter. Available tables only provide the damping coefficients for first through eleventh order filters. What are the damping coefficients necessary for this 14th order low-pass Butterworth filter?

9.7. Design requirements require the use of a 15th order high-pass Butterworth Filter. Available tables only provide the damping coefficients for first through eleventh order filters. What are the damping coefficients necessary for this 15th order high-pass Butterworth filter?

9.8. A low-pass Butterworth filter is to be designed to meet the following design criteria:

Passband

nominal gain, $A_{vo} = 1$

$\gamma_{\text{max}} = 0.6\,\text{dB}$ at frequency, $f_c = 150\,\text{Hz}$.

Stopband

$f_s = 900\,\text{Hz}$

$\gamma_{\text{min}} = 60\,\text{dB}$ min.

Determine the order of filter necessary to achieve the design goals and the filter transfer function.

9.9. A high-pass Butterworth filter is to be designed to meet the following design criteria:

Passband

nominal gain, $A_{vo} = 1$

$\gamma_{\max} = 0.3\,\text{dB}$ at frequency, $f_c = 150\,\text{Hz}$

Stopband

$f_s = 60\,\text{Hz}$

$\gamma_{\min} = 50\,\text{dB}$ min.

Determine the order of filter necessary to achieve the design goals and the filter transfer function.

9.10. First-order filter stages can be realized with a variety of OpAmp circuit topologies. Determine the frequency response of the transfer function of the two first-order stages shown.

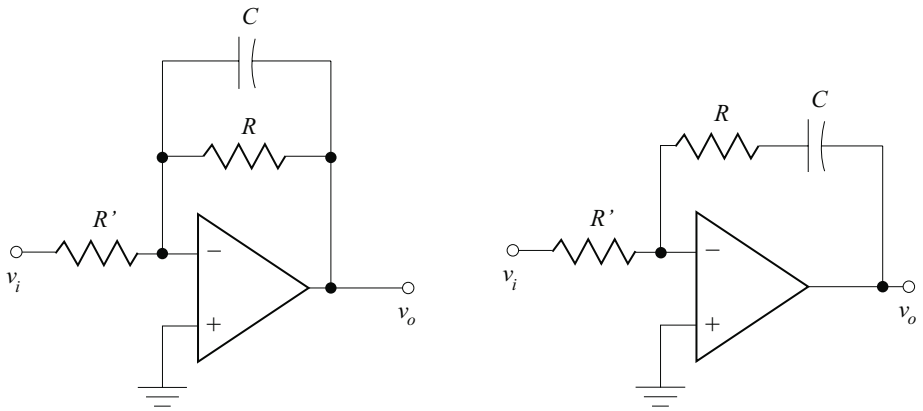

9.11. Third-order Butterworth transfer functions can be realized using a single OpAmp.

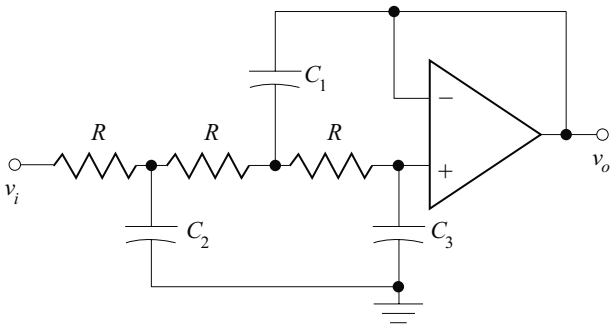

(a) Determine the transfer function of the circuit shown.

(b) Choose appropriate component values to achieve a third-order low-pass Butterworth filter with resonant frequency, $\omega_o = 2$ krad/sec.

(c) Verify the design using SPICE.

9.12. A second-order, resonant band-pass filter can be realized as shown.

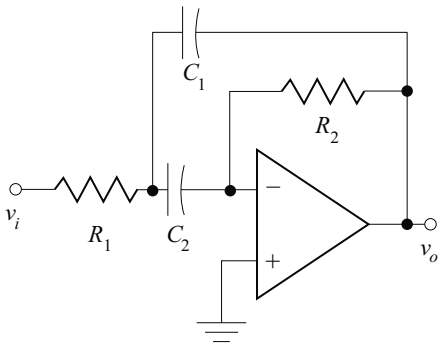

(a) Determine the transfer function of the circuit shown.

(b) Choose appropriate component values to achieve a resonant frequency of 1 kHz with a damping coefficient of 0.5.

(c) Use SPICE to simulate the circuit: determine the bandwidth between 3 dB frequencies.

9.13. Design a unity gain 7th order Butterworth low-pass filter using OpAmps, resistors, and capacitors with a 3 dB frequency of 200 Hz. Verify your design with SPICE.

9.14. Design a uniform time constant 6th order Butterworth low-pass filter using OpAmps, resistors, and capacitors with a passband edge at 400 Hz and $\gamma_{\max} = 1.5$ dB. Verify your design with SPICE.

9.15. Design a unity gain 5th order Butterworth high-pass filter using OpAmps, resistors, and capacitors with a 3 dB frequency of 200 Hz. Verify your design with SPICE.

9.16. Design a uniform time constant 8th order Butterworth high-pass filter using OpAmps, resistors, and capacitors with a passband edge at 1 kHz and $\gamma_{\max} = 2.2$ dB. Verify your design with SPICE.

9.17. A high-pass filter is to be designed to meet the following specifications.

Passband

nominal voltage gain, $A_{Vo} = 25$ dB

passband edge, $f_c = 500\,\text{Hz}$

$\gamma_{\max} = 1.5\,\text{dB}$ maximum

Stopband

$f_s = 150\,\text{Hz}$

$\gamma_{\min} = 50\,\text{dB}$ (the gain in the stopband must be less than $-25\,\text{dB}$)

(a) What is the minimum order Butterworth filter to meet these design goals?

(b) Design such a filter.

(c) Verify the design with computer simulation

9.18. A low-pass filter is to be designed to meet the following specifications.

Passband

nominal voltage gain, $A_{Vo} = 0\,\text{dB}$

passband edge, $f_c = 500\,\text{Hz}$

$\gamma_{\max} = 1.3\,\text{dB}$ maximum

Stopband

$f_s = 1.6\,\text{kHz}$

$\gamma_{\min} = 55\,\text{dB}$

(a) What is the minimum order Butterworth filter to meet these design goals?

(b) Design such a filter.

(c) Verify the design with computer simulation

9.19. A Butterworth band-pass filter is to be constructed to meet the following design goals:

Passband

nominal voltage gain, $A_{Vo} = 0\,\text{dB}$

passband edges, $f_{c1} = 600\,\text{Hz}$ and $f_{c2} = 4\,\text{kHz}$

$\gamma_{\max} = 0.4\,\text{dB}$ maximum

Stopbands

$\gamma_{\min} = 35\,\text{dB}$ (both stopbands)

cutoff frequencies, $f_{s1} = 300\,\text{Hz}$ and $f_{s2} = 8\,\text{kHz}$

Design the filter and verify the design goals using SPICE.

9.20. *Scenario:* You are a junior engineer at Alcalá Engineering (a significant, but fictitious, electronics firm). The company is in the process of designing a device that has an analog multiplier as a critical component. In the process of investigating many possible designs for this multiplier, the attached design was uncovered (reprinted from ***EDN***, October 25, 1990). Your boss, the chief engineer, stops by your desk, comments on the inferior design of the lowpass filter, asks you to fix it, and leaves.

Your task:

- Investigate the design of the current four-pole, low-pass filter.
- Prepare a design that will improve on the current design.
- Prepare a formal proposal to the chief engineer for your design. Theoretical analysis and computer simulation of designs are mandatory.

Constraints:

- Alcalá Engineering is operating in a highly competitive environment: thus the addition of a significant number of component parts is unacceptable (i.e., the filter is to remain a four-pole filter).
- The low-frequency gain of this filter is significant to the design of the analog multiplier and therefore must not be changed from that of the original design.

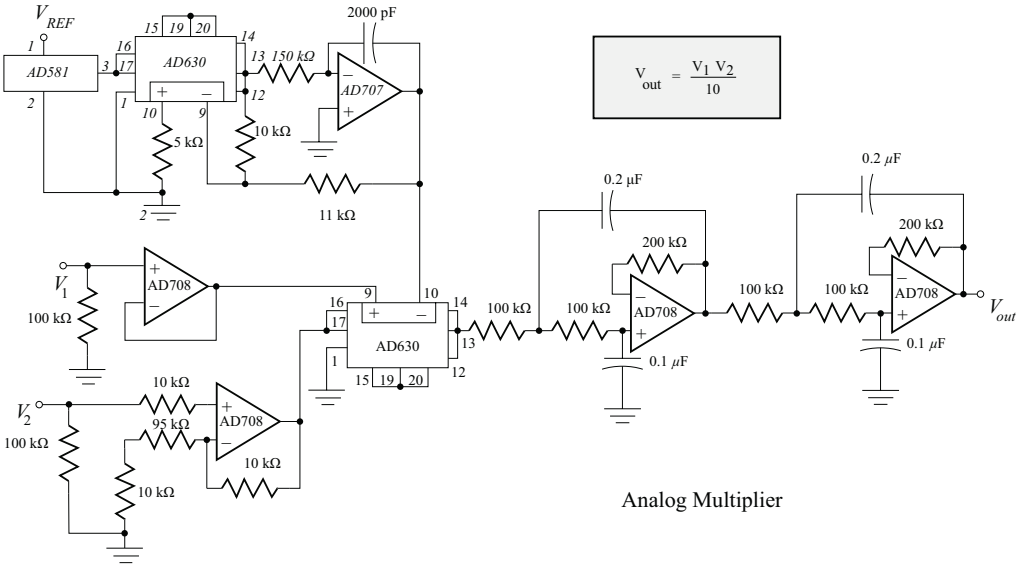

Analog Multiplier

9.21. A Butterworth band-stop filter is to be constructed from a fourth-order Butterworth low-pass filter and a fourth-order Butterworth high-pass filter. All input signals in the

frequency range 500 Hz $\leq f \leq$ 2 kHz are to be attenuated by at least 40 dB: signals in the passbands are to have unity gain and the passbands are to be as wide as possible.

Design the filter and verify the design goals using SPICE.

9.22. Design a resonant RLC band-pass filter to meet the following specifications:

Midband voltage gain = 0 dB

Center frequency = 15 kHz

3 dB bandwidth = 300 Hz

Confirm the design with SPICE.

9.23. A fifth-order low-pass Butterworth filter is under design. Its design goals include:

$$A_{vo} = 1$$
$$f_c = 1\,\text{kHz}$$
$$\gamma_{\max} = 1.5\,\text{dB}$$

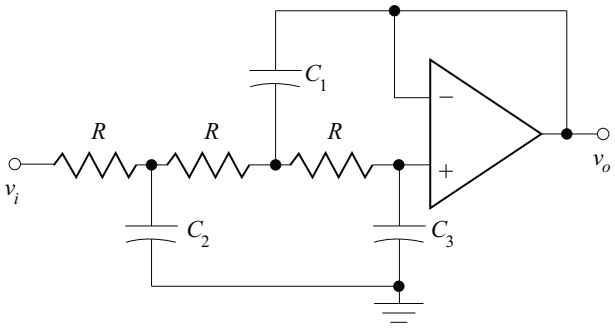

In order to reduce the number of OpAmps, it has been decided to use a unity-gain, third-order stage of the topology shown and a second-order stage.

The transfer function for this third-order stage has been determined to be:

$$v_o = \frac{v_i}{1 + j\omega R(C_2 + 3C_3) + (j\omega)^2 2R^2C_3(C_1 + C_2) + (j\omega)^3 R^3 C_1 C_2 C_3}.$$

Complete the filter design and verify compliance to the design goals using SPICE.

9.24. Design a resonant RC band-pass filter to meet the following specifications:

Midband voltage gain = 12 dB

Center frequency = 500 kHz

3 dB bandwidth = 75 Hz

Confirm the design with SPICE.

9.25. Design a resonant RC band-pass filter to meet the following specifications:

Midband voltage gain = 6 dB

Center frequency = 1 kHz

3 dB bandwidth = 50 Hz

Confirm the design with SPICE. Pass a 1 kHz square wave through the filter and determine the THD of the output.

9.26. Design a low-pass filter to meet the following specifications:

1 dB attenuation at 100 Hz

> 20 dB attenuation at 200 Hz

for the following filter types:

(a) Butterworth

(b) Chebyshev

Compare the order for each of the filters.

9.27. Design a 1 kHz Chebyshev low-pass filter with the following specifications:

Passband ripple: 2 dB

Cutoff frequency, f_c : 1 kHz

Stopband attenuation: > 20 dB at 1.8 kHz

Confirm the design with SPICE.

9.28. Plot the transfer function of a seventh order Chebyshev type I filter with a cutoff frequency of 4 kHz and 1 dB passband ripple. Determine the stopband attenuation at 6 kHz.

9.29. Contrast the attenuation provided by a fourth order low-pass Chebyshev filter to a Butterworth filter of the same order at a stopband frequency twice that of the cutoff frequency. Let the ripple of the Chebyshev filter equal 1 dB.

9.30. Find the transfer function of a low-pass filter with the following specifications:

Cutoff frequency, f_c : 200 Hz

Passband ripple: 2 dB

- Stopband attenuation > 20 dB above 400 Hz

9.31. Find the transfer function of a high-pass filter with the following specifications:

Cutoff frequency, f_c : 100 Hz

Passband ripple: 3 dB

Stopband attenuation > 20 dB below 50 Hz

9.32. Design a high-pass filter with the following specifications:

Cutoff frequency, f_c : 100 Hz

Passband ripple: 3 dB

Stopband attenuation > 20 dB below 50 kHz

Confirm the design with SPICE.

9.33. A switched-capacitor integrator, shown in the figure, is designed to have as its output the following expression:

$$v_o(t) = -10 \int v_i(t)\, dt.$$

If the switching frequency is 100 kHz, what value capacitor, C, is necessary?

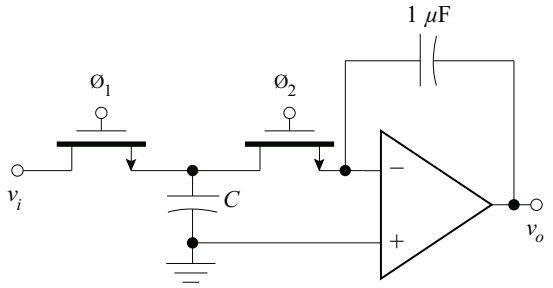

9.34. For the switched-capacitor integrator shown below, what input resistance corresponds to the 2 pF and 12 pF for C_1 with a clock frequency of 100 kHz?

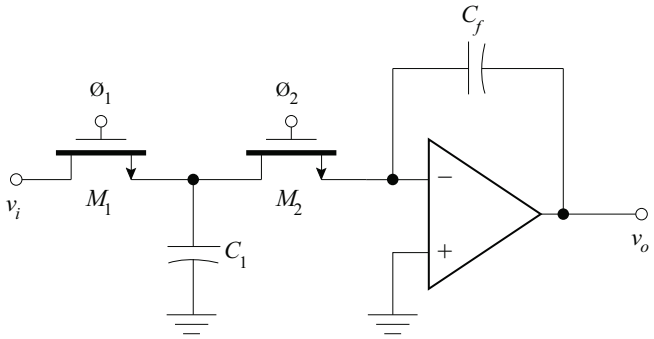

9.35. Design a switched-capacitor version of the differential integrator shown and find the transfer function.

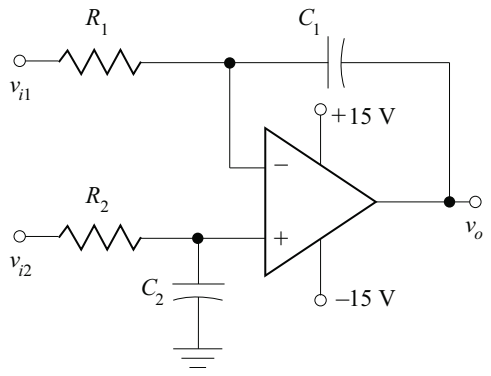

9.36. Design an inverting amplifier with a gain of -10 using the circuit shown below. Assume a clock frequency of 100 kHz and $C_1 = 5$ pF. Show the clock waveforms for ϕ_1 and ϕ_2.

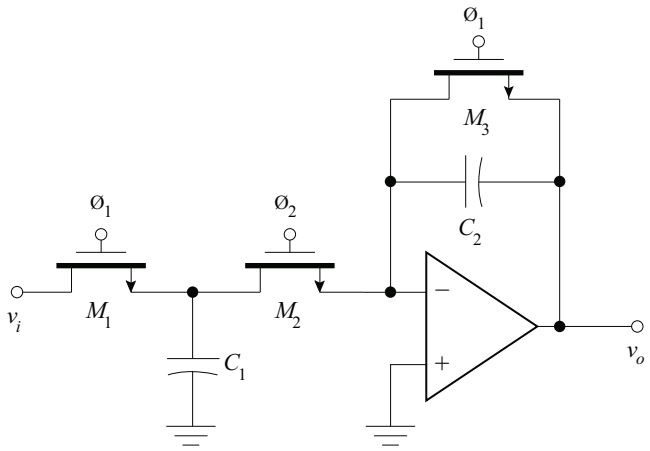

9.37. Design a first order low-pass switched-capacitor filter with a cutoff frequency of 500 Hz with a clock frequency of 100 kHz. Use a capacitor value of 8 pF for one of the fixed capacitors. Find the transfer function of the circuit.

9.38. Design a first order high-pass switched-capacitor filter with a cutoff frequency of 500 Hz with a clock frequency of 100 kHz. Use a capacitor value of 8 pF for one of the fixed capacitors. Find the transfer function of the circuit.

9.39. Design a switched-capacitor version of the difference amplifier shown and find the transfer function.

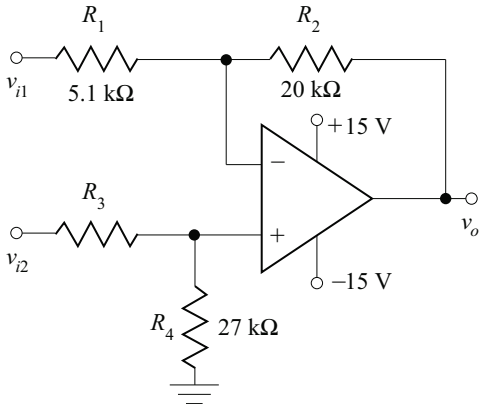

9.40. For an OpAmp with a slew rate of 7 V/μs used in the unity gain configuration, what is the shortest 0 V to 5 V pulse that can be used to ensure a full-amplitude output?

9.41. For an inverting amplifier using an OpAmp with a slew rate of 8 V/μs, determine the highest frequency input at which an 18 V peak-to-peak output sine wave can be generated.

REFERENCES

[1] Bowron, P. and Stephenson, F. W., *Active Filters for Communications and Instrumentation*, McGraw-Hill Book Company, New York, 1979.

[2] Chen, W. K., *Passive and Active Filters: Theory and Implementations*, John Wiley and Sons, Publishers, New York, 1986.

[3] Ghausi, M. S., *Electronic Devices and Circuits: Discrete and Integrated*, Holt, Rinehart and Winston, New York, 1985.

[4] Ludeman, L. C., *Fundamentals of Digital Signal Processing*, Holt, Rinehart, and Winston, Philadelphia, 1986.

[5] Millman, J. and Grabel, A., *Microelectronics*, 2nd ed., McGraw-Hill Book Company, New York, 1987.

[6] Millman, J. and Halkias, C. C., *Integrated Electronics: Analog and Digital Circuits and Systems*, McGraw-Hill Book Company, New York, 1972.

[7] Nilsson, J. W., *Electrical Circuits*, 3rd ed., Addison-Wesley, Reading, 1990.

[8] Savant, C. J., Roden, M. S., and Carpenter, G. L., *Electronics Design: Circuits and Systems*, 2nd ed., Benjamin/Cummings Publishing Company, Redwood City, 1991.

[9] Sedra, A. S. and Smith, K. C., *Microelectronic Circuits*, 3rd ed., Holt, Rinehart, and Winston, Philadelphia, 1991.

[10] Van Valkenburg, M. E., *Analog Filter Design*, Holt, Rinehart, and Winston, Philadelphia, 1982.

CHAPTER 10

Frequency Response of Transistor Amplifiers

The characterization of the performance of amplifiers as described in Book 2 of this text has suppressed all frequency-dependent effects. The amplifiers have been described in the so-called "mid-band" frequency range. This range of frequencies is characterized by two basic simplifying assumptions:

- The midband frequencies are high enough so that discrete circuit capacitors appear to have negligible impedance with respect to the resistances in the circuit, and
- The midband frequencies are low enough so that the active elements (transistors, OpAmps, etc.) appear to have frequency-invariant properties.

The magnitude of the gain of a typical amplifier is shown in Figure 10.1. At low frequencies the circuit coupling and bypass capacitors reduce the gain.[1] At high frequencies the circuit active elements degrade in performance. This degradation in performance also causes a drop in the gain magnitude. Between these two extremes, the midband region of constant gain prevails.

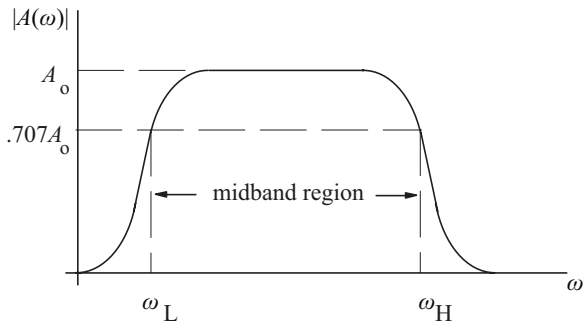

Figure 10.1: Typical amplifier gain frequency response.

In order to predict the frequency-dependent performance of amplifiers and other electronic circuitry, several options are available:

[1]Amplifiers without bypass or coupling capacitors do not experience degradation in performance characteristics at low frequencies. The midband region for such amplifiers extends to DC.

- Computer simulation
- Analytic calculations using phasor techniques and expanded transistor models on the entire circuit
- Separate high-frequency and low-frequency effects from midband performance in analytic calculations

Computer simulation alone accurately predicts circuit performance but gives the circuit designer little insight into which factors are dominant in determining the performance characteristics. Analytic calculations also give accurate performance prediction but these calculations often involve extremely difficult algebraic manipulation which must be repeated for each individual circuit. The separation of individual effects (midband, low-frequency, and high-frequency) gives the designer insight into exactly which circuit elements are dominant in each performance characteristic.

This chapter focuses on the separation of effects method as the primary analysis and design tool with computer simulation as an aid in final fine tuning of designs. The separation method follows the basic procedure:

1. The amplifier midband performance properties are determined as described in Book 2 of this text,
2. The pole locations that affect low-frequency performance are separately determined,
3. The pole locations that affect high-frequency performance are separately determined, and
4. The results of steps 1–3 are combined to form the total response characteristic.

As was seen in Chapter 9, midband gain and pole location are sufficient to determine a frequency response characteristic.

After a short reminder on frequency distortion, the chapter discusses time-domain testing of amplifiers through the step response. Since amplifier performance characteristics are usually only of interest between the 3-dB frequencies, the concept of dominant poles is explored. The effect of bias and coupling capacitors on low-frequency response is discussed for both simple BJT and FET amplifier stages. After modeling the high-frequency characteristics of diodes, BJTs, and FETs, the high-frequency response of simple amplifier stages is discussed. Multistage amplifier frequency response is determined through the cascading of the responses of the simple stages.

The frequency response of feedback amplifiers is discussed in Chapter 11.

10.1 FREQUENCY DISTORTION

In the previous chapters, transistor amplifiers were assumed to have constant gain-frequency response over the desired frequency passband. These amplifiers were described in the so-called mid-band frequency range where external reactive elements and the reactive components of the

transistor small-signal model did not affect the frequency domain properties of the amplifier. The gain of the amplifier outside the mid-band frequency range is dependent on the reactive elements, causing possible unequal gains for the frequency components of the input signal. This *frequency distortion* is reflected in the gain-frequency (Bode) and phase-frequency plots of the amplifier.

10.1.1 GAIN AND PHASE RESPONSE

In Section 9.2, a frequency response in the passband was shown to have no distortion when the circuit transfer function is constant with respect to frequency and the phase shift induced by the circuit is linear with respect to frequency. The gain of an amplifier is reduced outside of the mid-band. The gain-frequency curve is that of a band-pass filter.

Consider a single-pole high-pass function,

$$H_{HP}(\omega) = \frac{1}{1 - j\dfrac{\omega_L}{\omega}}, \tag{10.1}$$

where ω_L is the (lower) cutoff frequency for the high-pass transfer function.

The magnitude and phase of the single-pole transfer function of Equation (10.1) are,

$$|H_{HP}(\omega)| = \frac{1}{\sqrt{1 + \left(\dfrac{\omega_L}{\omega}\right)^2}}, \tag{10.2}$$

and

$$\angle H_{HP}(\omega) = \tan^{-1}\left(\frac{\omega_L}{\omega}\right). \tag{10.3}$$

The frequency response is shown on a Bode diagram in Figure 10.2.

When a single-pole system is excited with an input signal consisting of two sinusoids of frequencies $0.5\omega_L$ and $6\omega_L$ (Figure 10.3a), the output (Figure 10.3b) is distorted due to the difference in gain and phase of the two input sinusoids.

Similar analysis may be performed to show frequency distortion in systems described by single-pole low-pass transfer functions,

$$H_{LP}(\omega) = \frac{1}{1 + j\dfrac{\omega}{\omega_H}}, \tag{10.4}$$

where ω_H is the (high) cutoff frequency for the low-pass transfer function.
The magnitude and phase of the single-pole low-pass transfer function are

$$|H_{LP}(\omega)| = \frac{1}{\sqrt{1 + \left(\dfrac{\omega}{\omega_H}\right)^2}}, \tag{10.5}$$

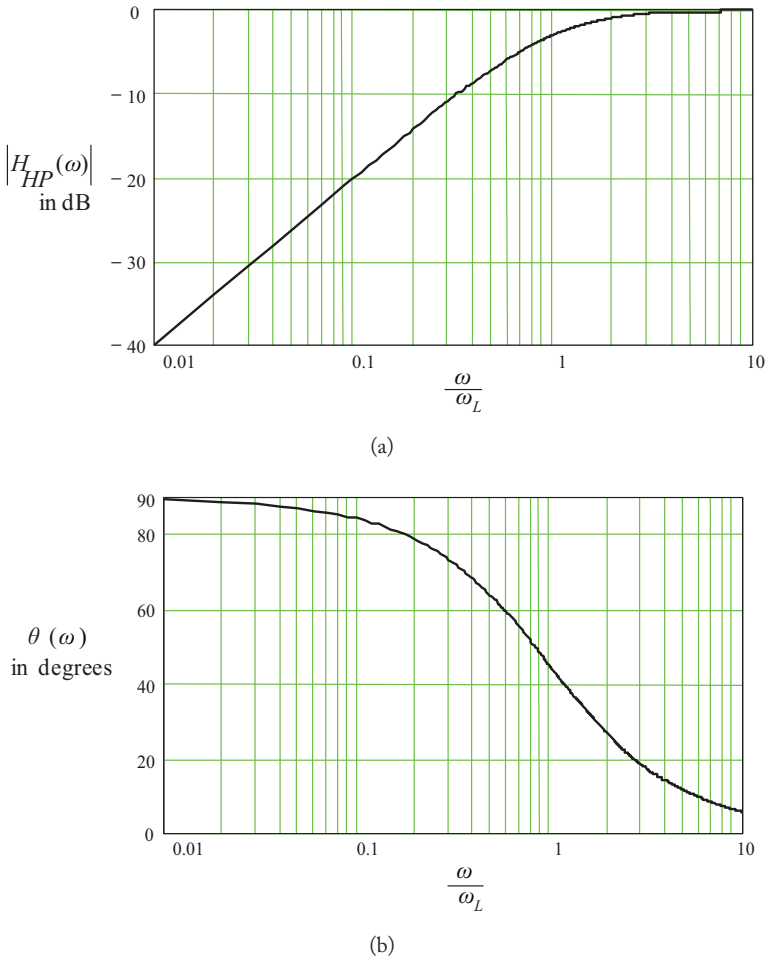

Figure 10.2: (a) Magnitude of high-pass transfer function, (b) Phase of high-pass transfer function.

and

$$\angle H_{LP}(\omega) = -\tan^{-1}\left(\frac{\omega}{\omega_H}\right). \tag{10.6}$$

Bode diagrams of Equations (10.5) and (10.6) are mirror images of Figure 10.2 with a high cutoff frequency of ω_H.

10.1.2 STEP AND PULSE RESPONSE

Signal distortion by an amplifier can be classified into three general categories:

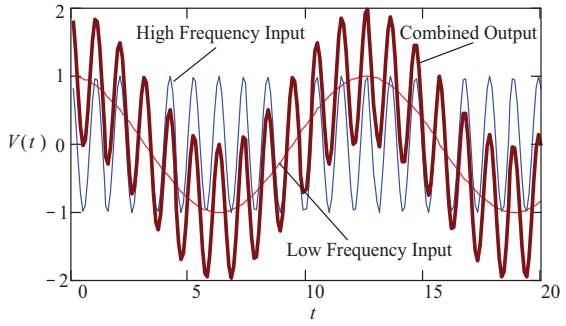

(a)

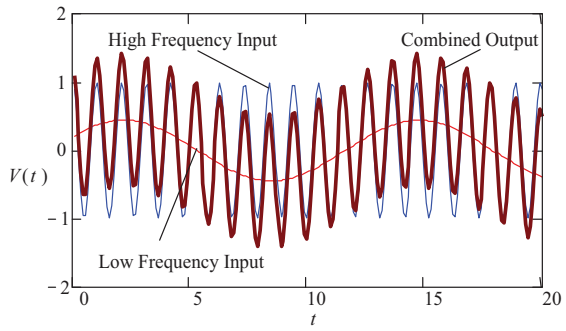

(b)

Figure 10.3: (a) Input signal of consisting of two sinusoids, (b) Resulting distorted output due to high-pass transfer function.

1. If an amplifier is linear but its amplitude response is not constant with frequency, the amplifier introduces *amplitude distortion*. The amount of amplitude distortion can be determined from the frequency response of the amplifier.

2. If an amplifier is linear but its phase shift is not a linear function of frequency, it introduces *phase*, or *delay*, *distortion*.

3. If an amplifier is non-linear, *non-linear distortion* results; e.g., superposition can no longer be used.

The step response provides information about all three types of distortion mentioned above. Therefore, the determination of the step response (pulse response testing is a subset of step response) is a powerful test of amplifier linearity.

A step voltage, shown in Figure 10.4, is a voltage signal that maintains a zero value for all time $t < 0$ and a constant value V_1 for all time $t > 0$. The transition between the two voltage levels

occurs at $t = 0$ and is ideally instantaneous. In real systems, the transition time from 0 to V_1 is accomplished in an arbitrarily small time interval that is significantly smaller than the response time of the circuit under test.

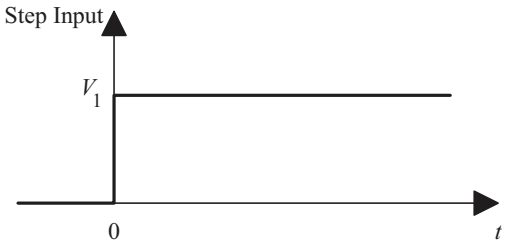

Figure 10.4: Step input voltage.

For a single-pole electronic circuit, the output voltage in the time domain is of the form,

$$v_o = B_1 + B_2 e^{-t/\tau}, \tag{10.7}$$

where

v_o is the output voltage,
B_1 and B_2 are constants, and
τ is the time constant of the electronic circuit.

The constant B_1 is the final steady-state value of the output voltage as $t \to \infty$. If the final voltage is defined as V_f, then $B_1 = V_f$. The constant B_2 is determined by the initial voltage, V_i. At $t = 0, v_o = V_i = B_1 + B_2$, or $B_2 = V_i - V_f$. Therefore, the general solution for a single-pole electronic circuit,

$$v_o = V_f + \left(V_i - V_f\right) e^{-t/\tau}. \tag{10.8}$$

Low Pass Circuit Response

For a low-pass electronic circuit, the initial voltage $V_i = 0$ and the final voltage $V_f = V_1$.[2] The output therefore is given by,[3]

$$v_o = V_1 \left(1 - e^{-t/\tau}\right), \tag{10.9}$$

where

$$\tau = \frac{1}{\omega_H}. \tag{10.9a}$$

[2]In this discussion, only the time varying portion of the signal is considered: in order to obtain the total output signal, the quiescent condition must be included.
[3]The relationship between Equation (10.4) and (10.9) is obtained through Laplace techniques.

The low-pass circuit step response is shown in Figure 10.5. The rise time, t_r, is defined as the time it takes the voltage to rise from 0.1 to 0.9 of its final value. The time required for v_o to rise to $0.1V_1$ is approximately 0.1τ and the time to reach $0.9V_1$ is approximately 2.3τ. The difference between these two time values is the rise time of the circuit, and is given by

$$t_r = (2.3 - 0.1)\tau = 2.2\tau. \tag{10.10}$$

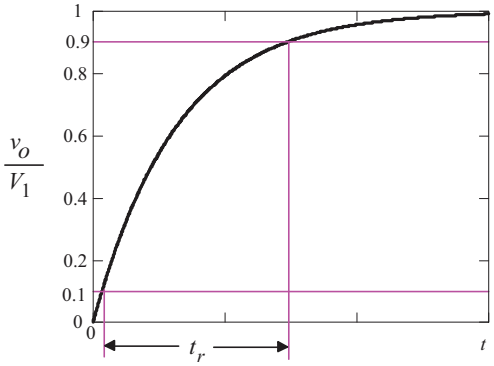

Figure 10.5: Low-pass circuit step response.

Since the time constant, τ, of a circuit is equal to the inverse of the low-pass cutoff frequency in radians, ω_H, Equation (10.10) can be related to the cutoff frequency,

$$t_r = 2.2\tau = \frac{2.2}{\omega_H} = \frac{2.2}{2\pi f_H} \approx \frac{0.35}{f_H}. \tag{10.11}$$

Thus, the rise time is proportional to the time constant of the circuit and inversely proportional to the cutoff frequency.

A variant of the step input voltage is the pulse input shown in Figure 10.6. The low-pass circuit response to a pulse is identical to that of the step response given in Equation (10.12) for $t < t_p$. At the end of the pulse ($t = t_p$), the output voltage is at a peak of V_p and must decrease to zero with a time constant τ for $t > t_p$, as indicated in Figure 10.7. The output waveform is distorted when compared to the input pulse waveform. In particular, the output waveform extends well beyond the pulse width.

To minimize pulse distortion, the rise time must be small compared to the pulse width. If the cutoff frequency, f_H, is chosen to be $1/\tau_p$, then the rise time is $t_r = 0.35t_p$. The output voltage for this case is shown in Figure 10.8. A rule of thumb that may be used with regards to pulse response is: *a pulse shape will be preserved if the cutoff frequency is greater than the reciprocal of the pulse width.*

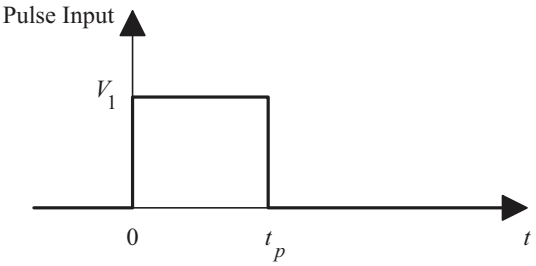

Figure 10.6: Pulse input voltage.

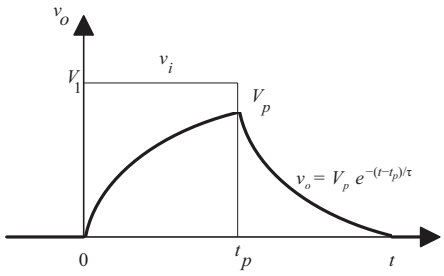

Figure 10.7: Low-pass circuit pulse response.

High-Pass Circuit Response

From Equation (10.8), the time domain response of the high-pass circuit has an initial voltage $V_i = V_1$ and a final voltage $V_f = 0$. Therefore, the output voltage of the high-pass circuit is that of a decaying exponential,

$$v_o = V_1 e^{-t/\tau}, \tag{10.12}$$

where, in this case τ is related to the lower cutoff frequency:

$$\tau = \frac{1}{\omega_L}. \tag{10.12a}$$

The input and output voltages are shown in Figure 10.9. The output voltage is 0.61 of its initial value at 0.5τ, 0.37 at 1.0τ, and 0.14 at 2.0τ. The output is nearly decayed to 5% of the peak voltage after 3.0τ, and less than 1% if $t > 5.0\tau$.

For a pulse with t_p small compared to the time constant τ, the output response is shown in Figure 10.10. The output at $t = t_p$ is $v_o = V_1 e^{-t_p/\tau} = V_p$. Since V_p is less than V_1, the voltage becomes negative and decays exponentially to zero. For $t > t_p$, the output voltage is,

$$v_o = V_1 \left(e^{-t_p/\tau} - 1\right) e^{-(t-t_p)/\tau}. \tag{10.13}$$

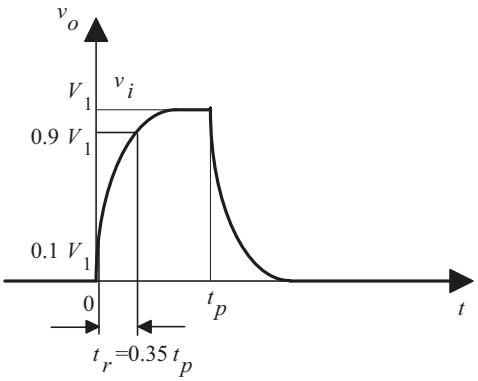

Figure 10.8: Low-pass pulse response with short time constant for $f_H = \frac{1}{\tau_p}$.

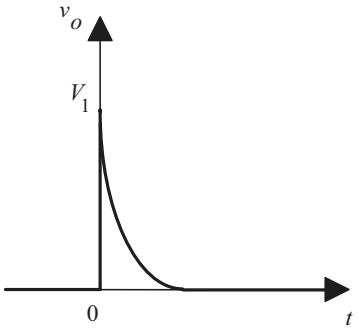

Figure 10.9: High-pass circuit step response.

Note that the distortion in the pulse caused by the high-pass circuit has resulted in a tilt to the top of the pulse and an undershoot at the end of the pulse. The percent *tilt* or *sag* in time t_p is approximately

$$v_o \approx V_1 \left(1 - \frac{t}{\tau}\right). \tag{10.14}$$

If Figure 10.9 is re-drawn for $t_p \ll \tau$, shown in Figure 10.11, the tilt in the output voltage is clear. The percent *tilt* or *sag* in time t_1 is,

$$sag = \frac{V_1 - V_p}{V_1} \times 100 = \frac{t_p}{\tau} \times 100\%. \tag{10.15}$$

Equation (10.15) is valid for the tilt of each half cycle of a symmetrical square wave with peak-to-peak voltage of V_1 and a period $T = 2t_p$. If $f_{sq} = 1/T_{sq}$ is the frequency of the square wave,

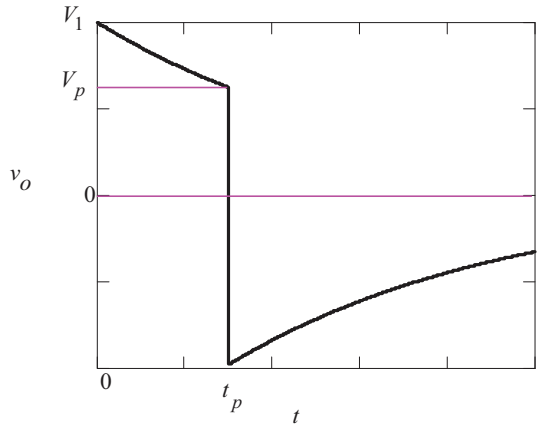

Figure 10.10: High-pass circuit pulse response.

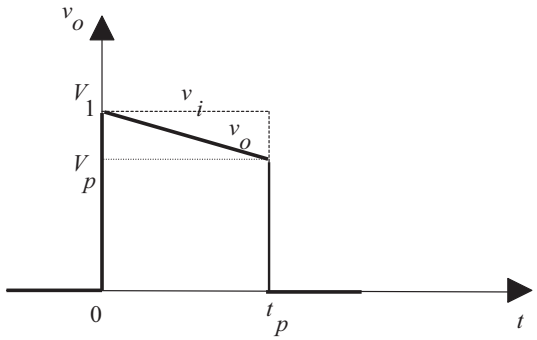

Figure 10.11: Tilt in step or pulse response due to high-pass circuit.

the *sag* may be expressed as,

$$sag = \frac{T_{sq}}{2\tau} \times 100 = \frac{1}{2 f_{sq} \tau} \times 100 = \frac{\pi f_L}{f} \times 100\%. \tag{10.16}$$

The tilt is then directly proportional to the cutoff frequency, f_L.

Example 10.1
Find the single-pole unity gain frequency response required for 10% *sag* at 1 kHz.

Solution:

Using Equation (10.16), the cutoff frequency of the high-pass transfer function is determined:

$$f_L = \frac{sag}{100}\left(\frac{f}{\pi}\right) = \frac{10(1000)}{100\,\pi} = 31.85\,\text{Hz}.$$

The cutoff frequency must not exceed 31.85 Hz for the desired *sag*. Therefore, the transfer function from Equation (10.1) is,

$$H_{HP}(\omega) = \frac{1}{1 - j\dfrac{\omega_L}{\omega}} = \frac{1}{1 - j\dfrac{2\pi(31.85)}{\omega}} = \frac{1}{1 - j\dfrac{200}{\omega}}.$$

10.2 DOMINANT POLES

The location of the high or low cutoff frequency for electronic circuits with more than one pole (and zero) becomes increasingly difficult to find analytically as the number of poles increases. Computer software packages with an equation solver, such as MathCAD, or advanced engineering and scientific calculators with the equation solver capabilities may be required to find the cutoff frequency. However, it may be desirable to use simple formulas and approximations that yield the cutoff frequencies when initially designing a circuit.

The dominant pole approximation simply ignores second-order effects of poles (and zeros) that are far removed from the pole that dominates in the calculation for the cutoff frequency of the electronic circuit. The low cutoff frequency of a high-pass response is dominated by the largest pole in the transfer function; whereas the high cutoff frequency of a low-pass response is dominated by the smallest pole. When circuits are designed with dominant poles, the analysis of the cutoff frequencies becomes considerably simpler. Non-dominant poles and zeros must be carefully analyzed in some instances that may affect circuit stability, such as in feedback amplifiers and oscillators. Stability issues in feedback amplifiers are discussed in Chapter 11.

10.2.1 LOW CUTOFF FREQUENCY (HIGH PASS)

The general form of the transfer function of a low-frequency response is,

$$H_{HP}(\omega) = \frac{(j\omega + \omega_{z1})(j\omega + \omega_{z2})\ldots(j\omega + \omega_{zn})}{(j\omega + \omega_{p1})(j\omega + \omega_{p2})\ldots(j\omega + \omega_{pn})}, \tag{10.17}$$

where $\omega_{z1}, \ldots, \omega_{zn}$ the frequencies for the low-frequency zeros of the response,
and $\omega_{p1}, \ldots, \omega_{pn}$ the frequencies for the low-frequency poles of the response.
If a midband region exists, the number of poles must equal the number of zeros. The highest pole frequency is ω_{p1} and subsequent poles are ordered such that $\omega_{p1} \geq \omega_{p2} \geq \omega_{p3} \geq \ldots \geq \omega_{pn}$. As ω approaches midband frequencies, $H_{HP}(\omega)$ approaches unity.

In designing a circuit, the zeros are placed at very low frequencies so that they do not contribute appreciably to the determination of the low cutoff frequency. A dominant pole, say ω_{p1}, has a much higher frequency than the others. In this case, the transfer function in Equation (10.17) can be approximated as a first-order high-pass response,

$$H_{HP}(\omega) \approx \frac{j\omega}{(j\omega + \omega_{p1})}. \tag{10.18}$$

The approximate transfer function implies that the amplifier low cutoff frequency is dominated by a pole at $j\omega = -\omega_{p1}$, and that the low cutoff frequency is approximately

$$\omega_1 \approx \omega_{p1}. \tag{10.19}$$

As a rule of thumb, the dominant pole approximation can be made if the highest frequency pole is separated from the nearest pole or zero by a factor of four.

If a dominant pole does not exist, a complete Bode plot may have to be constructed to determine the low cutoff frequency. Alternately, approximate formulas may be used to determine the location of the low cutoff frequency. For instance, a frequency response with two poles and two zeros has a transfer function of the form,

$$H_{HP}(\omega) = \frac{(j\omega + \omega_{z1})(j\omega + \omega_{z2})}{(j\omega + \omega_{p1})(j\omega + \omega_{p2})}. \tag{10.20}$$

The squared magnitude of the transfer function is,

$$|H_{HP}(\omega)|^2 = \frac{(\omega^2 + \omega_{z1}^2)(\omega^2 + \omega_{z2}^2)}{(\omega^2 + \omega_{p1}^2)(\omega^2 + \omega_{p2}^2)}. \tag{10.21}$$

The low cutoff frequency is defined by $|H_{HP}(\omega_l)|^2 = 1/2$. Therefore, Equation (10.21) becomes,

$$\begin{aligned} \frac{1}{2} &= \frac{(\omega_l^2 + \omega_{z1}^2)(\omega_l^2 + \omega_{z2}^2)}{(\omega_l^2 + \omega_{p1}^2)(\omega_l^2 + \omega_{p2}^2)} \\ &= \frac{1 + \left(\frac{1}{\omega_l^2}\right)(\omega_{z1}^2 + \omega_{z2}^2) + \left(\frac{1}{\omega_l^4}\right)(\omega_{z1}^2\omega_{z2}^2)}{1 + \left(\frac{1}{\omega_l^2}\right)(\omega_{p1}^2 + \omega_{p2}^2) + \left(\frac{1}{\omega_l^4}\right)(\omega_{p1}^2\omega_{p2}^2)}. \end{aligned} \tag{10.22}$$

Equation (10.22) is simplified by assuming that the zeros are significantly smaller than the low cutoff frequency,

$$\frac{1}{2} \approx \frac{1}{1 + \left(\frac{1}{\omega_l^2}\right)(\omega_{p1}^2 + \omega_{p2}^2) + \left(\frac{1}{\omega_l^4}\right)(\omega_{p1}^2\omega_{p2}^2)}. \tag{10.23}$$

Solving for ω_l using the quadratic equation yields,

$$\omega_l = \frac{\omega_{p1}}{\sqrt{\dfrac{-(1+k^2)+\sqrt{(1+k^2)^2+4k^2}}{2}}}, \tag{10.24}$$

where $\omega_{p1} = k\omega_{p2}$.

A plot of Equation (10.24) is shown in Figure 10.12, clearly showing that for $k > 4$, the dominant pole frequency is within 5.4% of the low cutoff frequency.

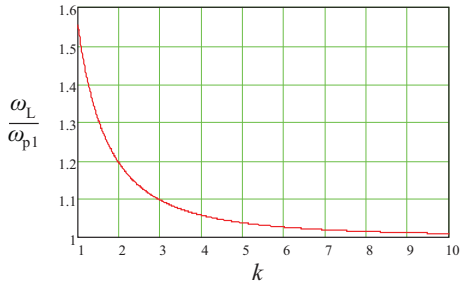

Figure 10.12: Low cutoff frequency as a function of the ratio of pole locations.

If the zeros cannot be ignored, Equation (10.22) can be solved by using the approximation that ω_L is greater than all of the poles and zeros. By neglecting the terms containing $1/\omega_L^4$, the low cutoff frequency is approximately,

$$\omega_L \approx \sqrt{\omega_{p1}^2 + \omega_{p2}^2 - 2\omega_{z1}^2 - 2\omega_{z2}^2}. \tag{10.25}$$

Equation (10.25) can be extended to any number of poles and zeros; that is,

$$\omega_L \approx \sqrt{\omega_{p1}^2 + \omega_{p2}^2 + \cdots + \omega_{pn}^2 - 2\omega_{z1}^2 - 2\omega_{z2}^2 - \cdots - 2\omega_{zn}^2}. \tag{10.26}$$

If a dominant pole exists, Equations (10.25) and (10.26) reduce to Equation (10.19).

10.2.2 LOW-PASS RESPONSE

The general form of the transfer function of a high-frequency response is,

$$H_{LP}(\omega) = \frac{\left(1+\dfrac{j\omega}{\omega_{z1}}\right)\left(1+\dfrac{j\omega}{\omega_{z2}}\right)\cdots\left(1+\dfrac{j\omega}{\omega_{zn}}\right)}{\left(1+\dfrac{j\omega}{\omega_{p1}}\right)\left(1+\dfrac{j\omega}{\omega_{p2}}\right)\cdots\left(1+\dfrac{j\omega}{\omega_{pn}}\right)}, \tag{10.27}$$

where $\omega_{z1}, \ldots, \omega_{zn}$ the frequencies for the high-frequency zeros of the response, and $\omega_{p1}, \ldots, \omega_{pn}$ the frequencies for the high-frequency poles of the response.

If a midband region exists, the number of poles must be greater than or equal to the number of zeros. The lowest pole frequency is ω_{p1} and subsequent poles are ordered such that $\omega_{p1} \leq \omega_{p2} \leq \omega_{p3} \leq \cdots \leq \omega_{pn}$. As ω approaches midband frequencies, $H_{LP}(\omega)$ approaches unity.

In designing a circuit, the zeros are placed at very high frequencies so that they do not contribute appreciably to the determination of the high cutoff frequency. A dominant pole, say ω_{p1}, has a much low-frequency than the others. In this case, the transfer function in Equation (10.17) can be approximated as a first order high-pass response,

$$H_{LP}(\omega) \approx \frac{1}{\left(1 + \dfrac{j\omega}{\omega_{p1}}\right)}. \tag{10.28}$$

The approximate transfer function implies that the amplifier high cutoff frequency is dominated by a pole at $j\omega = -\omega_{p1}$, and that the high cutoff frequency is approximately

$$\omega_H \approx \omega_{p1}. \tag{10.29}$$

As a rule of thumb, the dominant pole approximation can be made if the lowest frequency pole is separated from the nearest pole or zero by a factor of four.

If a dominant pole does not exist, approximate formulas may be used to determine the location of the high cutoff frequency. For instance, a frequency response with two poles and two zeros has a transfer function of the form,

$$H_{LP}(\omega) = \frac{\left(1 + \dfrac{j\omega}{\omega_{z1}}\right)\left(1 + \dfrac{j\omega}{\omega_{z2}}\right)}{\left(1 + \dfrac{j\omega}{\omega_{p1}}\right)\left(1 + \dfrac{j\omega}{\omega_{p2}}\right)}. \tag{10.30}$$

An approximate formula for the high cutoff frequency can be derived in a manner similar to that used above to determine the low cutoff frequency. The high cutoff frequency is,

$$\omega_H = \omega_{p1}\sqrt{\frac{-(1+k^2) + \sqrt{(1+k^2)^2 + 4k^2}}{2}}, \tag{10.31}$$

where

$$\omega_{p1} = \omega_{p2}/k.$$

Figure 10.12 can be used to show that for $k \geq 4$, the dominant pole frequency, ω_{p1}, is within 5.4% of the high cutoff frequency.

If the zeros cannot be ignored, ω_H is approximately,

$$\omega_H \approx \frac{1}{\sqrt{\frac{1}{\omega_{p1}^2}+\frac{1}{\omega_{p2}^2}-\frac{2}{\omega_{z1}^2}-\frac{2}{\omega_{z2}^2}}}. \tag{10.32}$$

Equation (10.32) can be extended to any number of poles and zeros; that is,

$$\omega_H \approx \frac{1}{\sqrt{\frac{1}{\omega_{p1}^2}+\frac{1}{\omega_{p2}^2}+\cdots+\frac{1}{\omega_{pn}^2}-\frac{2}{\omega_{z1}^2}-\frac{2}{\omega_{z2}^2}-\cdots-\frac{2}{\omega_{zn}^2}}}. \tag{10.33}$$

If a dominant pole exists, Equations (10.32) and (10.29) reduce to Equation (10.29).

10.3 EFFECT OF BIAS AND COUPLING CAPACITORS ON LOW-FREQUENCY RESPONSE

As mentioned in the preface to this chapter, the low-frequency response is separately determined by analyzing the effects of bias and coupling capacitors on the circuit. In this section, the methods for determining BJT and FET amplifier low cutoff frequency are shown.

10.3.1 BJT LOW-FREQUENCY RESPONSE

Common-emitter Amplifier

A single stage common-emitter amplifier with input and output coupling capacitors is shown in Figure 10.13a. The small-signal equivalent model of the circuit is shown in Figure 10.13b.

In performing the analysis, it is convenient to assume that h_{oe}^{-1} is very large. With this assumption, the small-signal circuit shows that there is little interaction between the coupling capacitors. The poles can be found by determining the output voltage and input current of the amplifier.

The input impedance is of the small-signal equivalent of Figure 10.13b is,

$$Z_i = R_{in} + R_S + \frac{1}{j\omega C_1} = \left[R_B // \left(h_{ie} + \left(1 + h_{fe}\right) R_E\right)\right] + R_S + \frac{1}{j\omega C_1}. \tag{10.34}$$

The input current to the circuit is the ratio for the input voltage to the input impedance,

$$i_i = \frac{v_i}{R_{in} + R_S + \frac{1}{j\omega C_1}}, \tag{10.35}$$

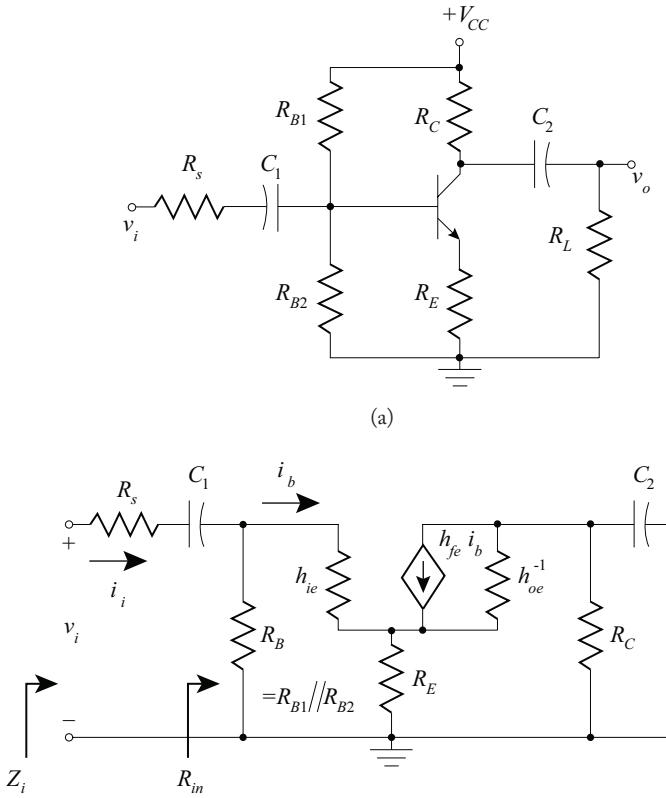

Figure 10.13: (a) Common-emitter amplifier with input and output coupling capacitors, (b) Small-signal equivalent circuit.

and the base current is,

$$\begin{aligned} i_i &= \frac{v_i R_B}{R_B + h_{ie} + (1 + h_{fe}) R_E} \frac{j\omega C_1}{1 + j\omega C_1 (R_{in} + R_S)} \\ &= \frac{v_i}{h_{ie} + (1 + h_{fe}) R_E} \frac{j\omega R_{in} C_1}{j\omega C_1 (R_{in} + R_S) + 1} \\ &= \frac{v_i R_{in} C_1}{[h_{ie} + (1 + h_{fe}) R_E] \omega_{p1}} \left(\frac{j\omega}{j\omega + \omega_{p1}} \right), \end{aligned} \tag{10.36}$$

where the one of the pole locations is,

$$\omega_{p1} = \frac{1}{C_1 \left\{R_S + \left[R_B // \left[h_{ie} + \left(1 + h_{fe}\right) R_E\right]\right]\right\}}. \tag{10.37}$$

The output voltage of the amplifier is,

$$v_o = -\frac{h_{fe} i_b R_C R_L}{R_C + R_L + \frac{1}{j\omega C_2}} = -h_{fe} i_b R_O \frac{j\omega}{j\omega + \omega_{p2}}, \tag{10.38}$$

where the other pole is at,

$$\omega_{p2} = \frac{1}{C_2 \left(R_C + R_L\right)}. \tag{10.39}$$

Inspection of the pole frequencies shows that the poles are determined by the capacitor multiplied by the resistive discharge path. This is merely the time constant of the circuit.

That is, the discharge path for C_1 is through the resistance $R_S + \{R_B//[h_{ie} + (1 + h_{fe})R_E]\}$ and discharge path for C_2 is through the resistance $R_C + R_L$. Therefore, the poles can be found by simply determining the time constant of that portion of the amplifier circuit being analyzed. From the bias conditions and selection of the two capacitor values, the dominant pole can be established by one of the capacitors.

Common-Emitter Amplifiers with Emitter-Bypass Capacitors

The simple analysis described above cannot be accurately used for a common-emitter amplifier with emitter-bypass capacitor shown in Figure 10.14a due to the interaction of the capacitors C_1 and C_E. By studying the small-signal equivalent in Figure 10.14b, it becomes obvious that there is some interaction between the input coupling capacitor and the emitter-bypass capacitor.

In performing the analysis, it is again convenient to assume that h_{oe}^{-1} is very large. To find the pole locations, nodal analysis is carried out using frequency domain equivalent impedances. The current gain $A_i(\omega)$, is found by nodal analysis:

$$I_S = \frac{v_i}{R_S} = \frac{v_1}{R_S} + j\omega C_1 \left(v_1 - v_2\right) \tag{10.40a}$$

$$j\omega C_1 \left(v_1 - v_2\right) = \frac{v_2}{R_B} + \frac{\left(v_2 - v_3\right)}{h_{ie}} \tag{10.40b}$$

$$\frac{\left(v_2 - v_3\right)}{h_{ie}} + h_{fe} i_b = v_3 \left(j\omega C_E + \frac{1}{R_E}\right) \tag{10.40c}$$

$$0 = h_{fe} i_b + \frac{v_4}{R_C} + v_4 \frac{j\omega C_2}{R_L C_2 + 1}. \tag{10.40d}$$

The small-signal base current is,

$$i_b = \frac{\left(v_2 - v_3\right)}{h_{ie}}. \tag{10.41}$$

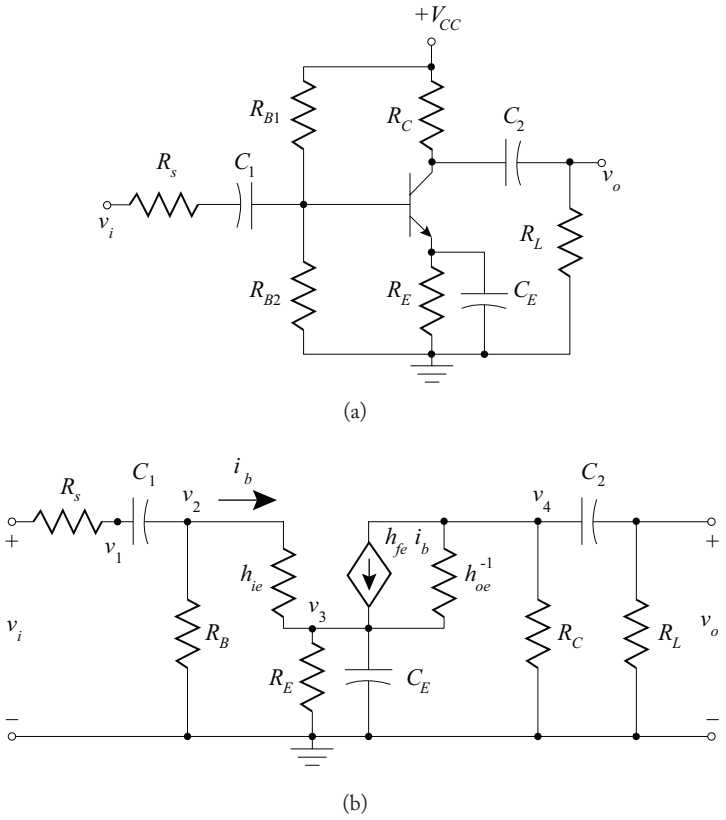

Figure 10.14: (a) Common-emitter amplifier with emitter-bypass capacitor, (b) Small-signal equivalent circuit.

The output current is,

$$i_o = \frac{j\omega C_2 v_4}{j\omega R_L C_2 + 1}. \tag{10.42}$$

The solution to the nodal equations in Equation (10.40) for the current gain is,

$$A_i(\omega) = \frac{i_o}{i_S} = \frac{-A_{im}(j\omega)^2\left(j\omega + \dfrac{1}{R_E C_E}\right)}{\left[j\omega + \dfrac{1}{(R_L + R_C)C_2}\right][(j\omega)^2 + j\omega a_2 + a_1]}, \tag{10.43}$$

where

$$a_2 = \frac{\dfrac{R_B + h_{ie}}{C_1} + \dfrac{(R_B + R_S)\left[h_{ie} + \left(1 + h_{fe}\right) R_E\right] + R_S R_B}{R_E C_E}}{R_B R_S + h_{ie}\left(R_B + R_S\right)} \tag{10.44a}$$

$$\approx \frac{1}{C_1\left(R_S + h_{ie}\right)} + \frac{h_{fe}}{C_E\left(R_S + h_{ie}\right)}, \quad R_B \gg R_S, h_{ie}$$

$$a_1 = \frac{R_B + h_{ie} + \left(1 + h_{fe}\right) R_E}{R_E C_E C_1\left[R_B R_1 + h_{ie}\left(R_B + R_S\right)\right]} \tag{10.44b}$$

$$\approx \frac{R_B + \left(1 + h_{fe}\right) R_E}{R_B R_E\left(R_S + h_{ie}\right) C_1 C_E}, \quad R_B \gg R_S, h_{ie},$$

and A_{im} is the midband current gain with all capacitors shorted,

$$A_{im} = \frac{h_{fe}\left(R_S // R_B\right)\left(R_C\right)}{\left[\left(R_S // R_B\right) + h_{ie}\right]\left(R_C + R_L\right)} \approx \frac{h_{fe} R_S}{R_S + h_{ie}}\left(\frac{R_C}{R_C + R_L}\right), \tag{10.44c}$$

for $R_B \gg R_s$.

As expected, the order of the numerator and denominator are the same: three zeros and three poles. It is evident from the above equations that, as expected, the output coupling capacitor, C_2, does not interact with the emitter-bypass capacitor, C_E, and the input coupling capacitor, C_1, since C_2 does not appear in Equation (10.44) and contributes a pole in Equation (10.43). From Equation (10.44a) and (10.44b), a strong interaction between C_1 and C_E is evident.

The three capacitor values can be manipulated to design a circuit with a specific low cutoff frequency, ω_l. Since C_2 contributes its own pole and does not interact with the other capacitors, the difficulty in determining the pole locations does not rest with this capacitor value. The pole location due to C_2 can be designed to be significantly lower than the chosen dominant pole. The other two poles are a complex interaction of C_1 and C_E. The zero location due to $1/R_E C_E$ must be significantly smaller than the low cutoff frequency. The two remaining pole locations are found by making the following approximations:

$$\begin{aligned}(j\omega)^2 + j\omega a_2 + a_1 &= \left(j\omega + \omega_{p1}\right)\left(j\omega + \omega_{p2}\right), \quad \text{where } \omega_{p1} \gg \omega_{p2} \\ &\approx \left(j\omega + a_2\right)\left(j\omega + \frac{a_1}{a_2}\right), \quad \text{where } a_2 \gg \frac{a_1}{a_2}.\end{aligned} \tag{10.45}$$

The pole locations due to the interacting C_1 and C_E are found from Equations (10.43) and (10.45),

$$\omega_{p1} \approx a_2 \approx \frac{1}{\left(R_S + h_{ie}\right)}\left(\frac{1}{C_1} + \frac{\left(1 + h_{fe}\right)}{C_E}\right) \tag{10.46}$$

and

$$\omega_{p2} \approx \frac{a_1}{a_2} \approx \frac{R_B + \left(1 + h_{fe}\right) R_E}{R_B R_E \left[C_E + \left(1 + h_{fe}\right) C_1\right]}. \tag{10.47}$$

In designing a circuit with a specific low cutoff frequency, it is suggested that the cutoff frequency equal $\omega_l \approx \omega_{p1} \approx a_2$, and select the values for C_1 and C_E. The value for C_2 can be designed to be significantly lower than the dominant pole. Since one end of the emitter-bypass capacitor, C_E is ground, a large value chemical capacitor (electrolytic or tantalum) can be used. In doing so, a suggested value of C_E is,

$$C_E \geq (h_{fe} + 1)C_1, \tag{10.48}$$

which allows for the solution for C_1 using Equation (10.46) and $\omega_l \approx \omega_{p1} \approx a_2$,

$$C_1 \approx \frac{2}{\omega_l \left(R_S + h_{ie}\right)}. \tag{10.49}$$

With the C_1 and C_E established, the ω_{p2} can be found,

$$\omega_{p2} = \frac{R_B + \left(1 + h_{fe}\right) R_E}{2h_{FE} R_B R_E C_1}. \tag{10.50}$$

The pole location due to C_2 is fixed at $\omega_{p3} \ll \omega_l$,

$$\omega_{p3} = \frac{1}{\left(R_C + R_L\right) C_2} \leq \frac{\omega_l}{10}. \tag{10.51}$$

Therefore, the output-coupling capacitor value is:

$$C_2 \geq \frac{10}{\omega_l \left(R_C + R_L\right)}. \tag{10.52}$$

Example 10.2

Complete the design for the common-emitter amplifier shown below for a low cutoff frequency of 40 Hz. Find the midband gain. From the quiescent point, the following parameters were determined: $h_{fe} = 200, h_{ie} = 34.7\,\text{k}\Omega$.

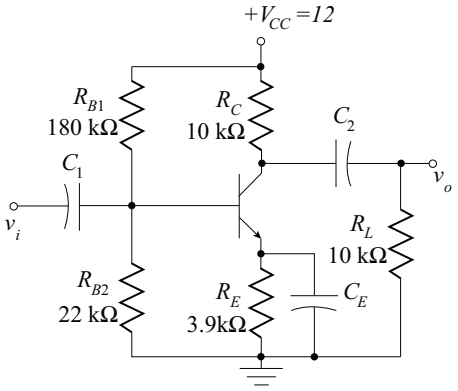

Solution:

The midband gain is easily found from the midband small-signal model,

$$A_{vm} = \frac{-h_{fe}\,(R_C\,//\,R_L)}{h_{ie}} = \frac{-200(5000)}{34.7\,\text{k}} = -28.8.$$

Equation (10.49) yields the value for C_1,

$$C_1 \approx \frac{2}{\omega_l\,(h_{ie})} = \frac{2}{2\pi\,(40)\,(34.7\,\text{k})} \approx 0.22\,\mu\text{F}.$$

Using Equation (10.48), the value of the emitter-bypass capacitor is,

$$C_E \geq h_{fe}C_1 = 200(0.22\,\mu) = 44\,\mu\text{F} \Rightarrow 47\,\mu\text{F}\,(\text{standard value}).$$

Lastly, Equation (10.52) yields,

$$C_2 \geq \frac{10}{\omega_l\,(R_C + R_L)} = \frac{10}{2\pi(40)(20\,\text{k})} \approx 2\,\mu\text{F} \Rightarrow 2.2\,\mu\text{F}(\text{standard value}).$$

The values of the capacitors are consistent with a dominant pole response.

Although the exact analysis above will yield accurate results, it may be preferable in design to use approximate relationships using a simplified approach. The simplified approach consists of assuming that the capacitances do not interact. The pole corresponding to each capacitor is determined with the other capacitors shorted: that is, The pole location corresponding to each capacitor is determined by finding the resistance in its discharge path.

For the common-emitter amplifier with coupling and bypass capacitors, the poles corresponding to C_1 and C_2 have been solved above in the analysis for the common-emitter amplifier with input and output capacitors (Equations (10.37) and (10.39)). The voltage gain of the circuit

with C_1 and C_2 shorted yields the frequency dependent effects of the emitter-bypass capacitor. The base current is then,

$$i_b = \frac{v_i}{h_{ie} + (h_{fe} + 1)\left(R_E // \frac{1}{j\omega C_E}\right)}, \tag{10.53}$$

where $\frac{1}{j\omega C_E}$ is the impedance of the emitter-bypass capacitor. The output voltage is,

$$v_o = -h_{fe} i_b \left(R_C // R_L\right). \tag{10.54}$$

Substituting Equation (10.53) into (10.54) yields the voltage gain,

$$A_v(\omega) = \frac{v_o}{v_i} = \frac{-h_{fe}(R_C // R_L)\left(1 + \frac{1}{j\omega R_E C_E}\right)}{h_{ie}\left(1 + \frac{1}{j\omega R_E C_E}\right) + \frac{(1 + h_{fe})}{j\omega C_E}}. \tag{10.55}$$

With the capacitor shorted, the midband gain is found,

$$A_v = \frac{v_o}{v_i} = \frac{-h_{fe}\left(R_C // R_L\right)}{h_{ie}}. \tag{10.56}$$

The gain is therefore,

$$A_v(\omega) = \frac{A_{vm}\left(j\omega + \frac{1}{R_E C_E}\right)}{j\omega + \left(\frac{1}{R_E} + \frac{h_{fe} + 1}{h_{ie}}\right)\frac{1}{C_E}}. \tag{10.57}$$

The pole due to C_E is therefore,

$$\omega_{P3} = \left(\frac{1}{R_E} + \frac{h_{fe} + 1}{h_{ie}}\right)\frac{1}{C_E}. \tag{10.58}$$

The pole in Equation (10.58) is then designed to be significantly smaller than ω_{p1} and ω_{p2} in Equations (10.37) and (10.39) to complete the simplified design approach: that is, C_E is chosen so that $\omega_{p3} \leq \omega_{p1}, \omega_{p2}$.

In integrated circuit design, it is undesirable to have large coupling and bypass capacitors since they require large chip area. Since most integrated circuit amplifiers use constant current source biasing schemes and are commonly DC coupled in a differential amplifier configuration, a low cutoff frequency does not exist. This implies that DC signals are amplified by these circuits.

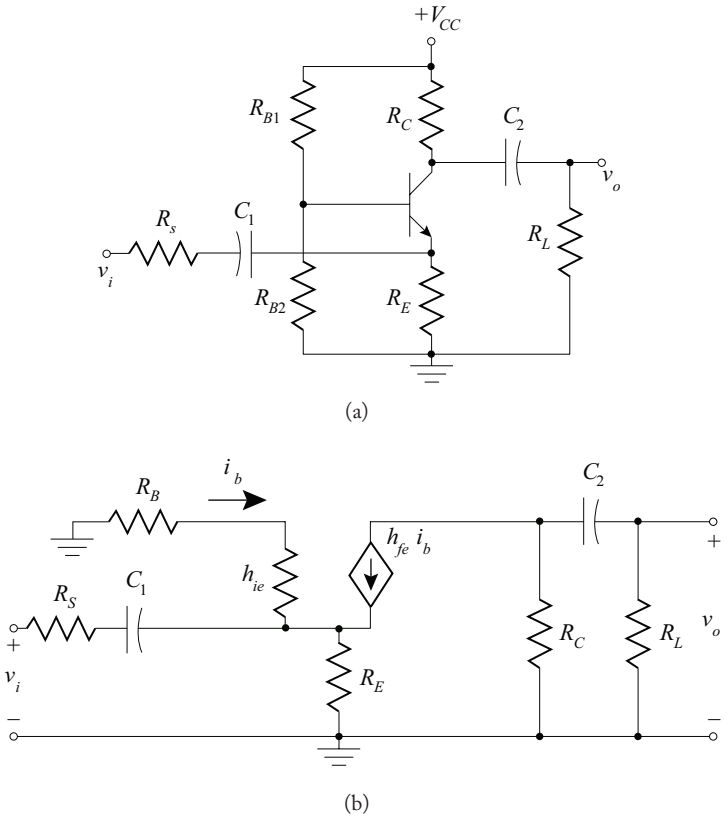

Figure 10.15: (a) Common-base amplifier with input and output coupling capacitors, (b) Small-signal equivalent circuit.

Common-Base Amplifier

Figure 10.15 shows a common-base amplifier and its small-signal equivalent. The analysis and design procedure follows that of the common-emitter amplifier.

In performing the analysis, it is again convenient to assume that h_{oe}^{-1} is very large. With this assumption, the small-signal circuit shows that there is little interaction between the coupling capacitors. Therefore, the pole locations due to each capacitor can be independently calculated. The discharge path for C_1 is through the resistance

$$R_S + \left[\left(1 + h_{fe}\right) R_E // \left[h_{ie} + R_B\right]\right].$$

Therefore, the pole due to C_1 is,

$$\omega_{p1} = \frac{1}{C_1 \left\{R_S + \left[\left(1 + h_{fe}\right) R_E // \left[h_{ie} + R_B\right]\right]\right\}}. \tag{10.59}$$

The discharge path for C_2 is through the resistance $R_C + R_L$. Therefore, the pole due to C_2 is,

$$\omega_{p2} = \frac{1}{C_2 (R_C + R_L)}. \tag{10.60}$$

From the bias conditions and selection of the two capacitor values, the dominant pole can be established by one of the capacitors.

The simple analysis described above cannot be accurately used for a common-base amplifier with base-bypass capacitor, C_B from the base to ground, due to the interaction of the capacitors C_1 and C_B. For this circuit, the analysis is similar to that performed for the common-emitter amplifier with emitter bypass capacitor is required. However, if an exact solution to the poles is not required, a simplified approach similar to that shown for the common-emitter amplifier with emitter-bypass capacitor may be used, where the pole determined by C_B is significantly smaller than the other two poles found in Equations (10.59) and (10.60). That is, the pole due to C_B may be ignored since $\omega R_B C_B \gg 1$.

10.3.2 FET LOW-FREQUENCY RESPONSE

A single stage common source enhancement NMOSFET amplifier with input and output coupling capacitors and source-bypass capacitor is shown in Figure 10.16a. The small-signal equivalent model of the circuit is shown in Figure 10.16b.

In performing the analysis, it is convenient to assume that r_d is large compared to the output load and that the impedance of the dependent current source is also very large. With these assumptions, the small-signal circuit shows that there is little interaction between the coupling and bypass capacitors due to the large input resistance inherent in FETs. Therefore, the pole locations due to each capacitor can be independently calculated.

The discharge path for C_1 is through the resistance, $R_G + R_i$. Therefore, the pole due to C_1 is,

$$\omega_{p1} = \frac{1}{C_1 (R_G + R_i)}. \tag{10.61}$$

When C_2 and C_S are shorted, the transfer function of the amplifier due to C_1 is,

$$A_{v1}(\omega) = \frac{A_{vm}(j\omega)}{j\omega + \dfrac{1}{C_1 (R_G + R_i)}}, \tag{10.62}$$

where A_{vm} is the midband gain of the amplifier. The midband gain of the amplifier is found by analyzing the circuit with all capacitors shorted. The midband gain is,

$$A_{vm} = -\frac{g_m R_G (R_D + R_L + r_d)}{R_i + R_G}. \tag{10.63}$$

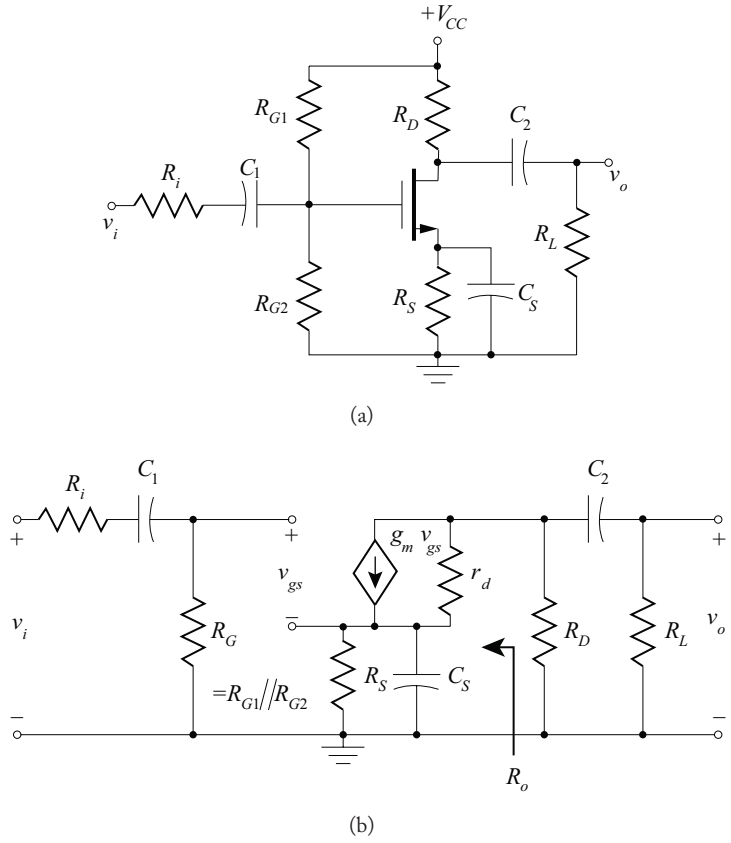

Figure 10.16: (a) Common source amplifier, (b) Small-signal equivalent circuit.

The discharge path for C_2 is through the resistance R_L and the parallel combination of R_D and the R_o. Therefore, the pole due to C_2 is,

$$\omega_{p2} = \frac{1}{C_2\left[R_L + [R_D // R_o]\right]} = \frac{1}{C_2\left[R_L + [R_D // (r_d + (1 + g_m r_d) R_S)]\right]}. \tag{10.64}$$

When C_1 and C_S are shorted, the transfer function of the amplifier due to C_2 is,

$$A_{v2}(\omega) = \frac{A_{vm}(j\omega)}{j\omega + \dfrac{1}{C_2\left[R_L + [R_D // (r_d + (1 + g_m r_d) R_S)]\right]}}, \tag{10.65}$$

When C_1 and C_2 are shorted, the transfer function of the amplifier due to C_S is,

$$A_{v3}(\omega) = \frac{A_{vm}\left(\dfrac{1}{R_S C_S}\right)}{j\omega + \dfrac{r_d + (R_D//R_L) + (1 + g_m r_d)\, R_S}{R_S C_S\,[r_d + (R_D//R_L)]}}. \tag{10.66}$$

Therefore, the pole location due to C_S is,

$$\omega_{pS} = \frac{r_d + (R_D//R_L) + (1 + g_m r_d)\, R_S}{R_S C_S\,[r_d + (R_D//R_L)]}. \tag{10.67}$$

It is typical to let C_1 or C_2 establish the dominant pole. The value for C_S can be designed so that ω_{pS} is significantly lower than the dominant pole frequency. Since one end of the emitter-bypass capacitor, C_S is ground, a large value chemical capacitor (electrolytic or tantalum) can be used.

Because of the inherently large input resistance of the FET, the common gate and common drain amplifier analysis and design procedures follow that of the common source amplifier: in all cases, each pole location is determined by calculating the pole location for each capacitor while the others are shorted since the capacitors do not interact to establish the poles.

10.4 HIGH-FREQUENCY MODELS OF THE BJT

Analysis of the response of BJT circuits at high frequencies is based on accurate modeling of the frequency dependent performance of transistors. The dominant model used for small-signal analysis of a BJT in the forward-active region, the *h*-parameter model as presented in 3 (Book 1) does not contain frequency sensitive elements and is therefore invariant with respect to changes in frequency. It is therefore necessary to introduce a new BJT model or to reinterpret an old model to include frequency-dependent terms. Once again, the Ebers-Moll model provides an excellent basis for creation of a simpler model in the forward-active region. In this modeling process, it is necessary to begin with a slight variation of the Ebers-Moll model that was presented in 3 (Book 1). As is shown in Figure 10.17, this presentation has added an additional base resistance of small value, r_b, to model the parasitic bulk resistance between the physical base terminal contact and the active base region[4] and a large output resistance, r_o, to model reduced output resistance due to early voltage (V_A) effects.

In the forward-active region and at low frequencies the Ebers-Moll Model of Figure 10.17 can be replaced by the linear two-port model shown in Figure 10.18. This model is known as the hybrid-π model. It is similar to the *h*-parameter model used previously in this text, but has particular utility when frequency-dependent terms are included. Also of particular interest is the direct correlation between the individual hybrid-π impedances and the corresponding circuit elements in the Ebers-Moll model.

[4]Many models also include parasitic bulk resistances in series with the emitter and collector terminals. These two resistances typically have a much smaller effect on amplifier performance than rb and therefor will be ignored (assumed to be zero) in the presentation provided here.

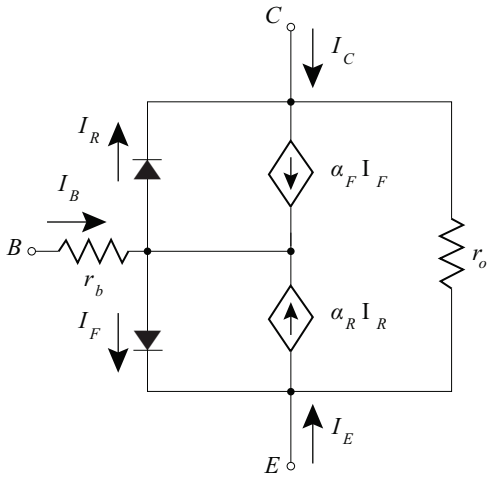

Figure 10.17: The Ebers-Moll model of a BJT.

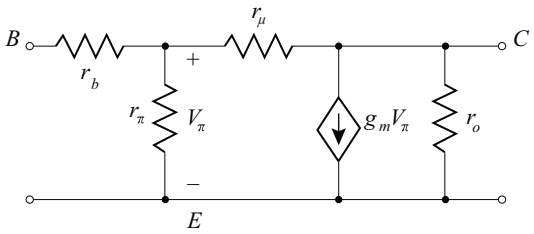

Figure 10.18: Low-frequency Hybrid-BJT model.

The resistances r_b and r_o are directly carried from one model to the other, while r_π and r_μ are the forward resistance of the base-emitter junction and the reverse resistance of the base-collector junction respectively.

The relationships between h-parameter and hybrid-π models can be obtained by application of the two-port parameter tests as was performed (albeit on the Ebers-Moll model) in Section 5.2 (Book 2).

The base-collector junction reverse resistance is extremely large ($r_\mu > 20\,M\Omega$) and is typically ignored (left as an open circuit) the model. The simplified hybrid-π parameters are related to the h-parameter model parameters by:

$$g_m = \frac{h_{fe}}{r_\pi} = \frac{|I_c|}{\eta V_t} \qquad r_\pi = \beta_F \frac{\eta V_t}{|I_c|} = \frac{\beta_F}{g_m},$$
$$r_o \approx \frac{1}{h_{oe}} = \frac{|V_A|}{|I_c|} \qquad r_b = h_{ie} - r_\pi. \tag{10.68}$$

As will be seen in Section 10.7, the hybrid-π model is also useful in modeling FETs.

In addition to the modeling these purely resistive, second-order, low-frequency effects, the diodes of the Ebers-Moll model are replaced by more complex, frequency-dependent models. The frequency-dependent component of transistor behavior is based on the capacitive component of p-n junction impedance. Once the capacitive nature of a p-n junction is known, a frequency dependent model for a BJT can be obtained.

10.4.1 MODELING A *P-N* JUNCTION DIODE AT HIGH FREQUENCIES

In the semiconductor region near a p-n junction under a voltage bias, there is a significant buildup of electrical charge on each side of the junction. Since this charge buildup is dependent on the voltage applied across the junction, there is a capacitance associated with the junction. This capacitance is strongly dependent on the doping densities of the two semiconductor regions and the geometry of the junction. It is modeled as a capacitor shunting the dynamic resistance of the junction (Figure 10.19).

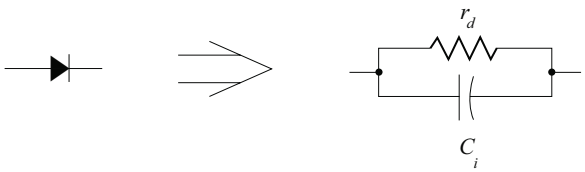

Figure 10.19: High-frequency model of a p-n junction.

In most electronic applications the p-n junction capacitance is dominated by the diffusion of carriers in the depletion regions. A good analytic approximation of this depletion capacitance, C_j, is given by:

$$C_j \approx \frac{C_{jo}}{\left(1 - \dfrac{V_d}{\psi_o}\right)^m}, \tag{10.69}$$

where,

C_{jo} = small-signal junction capacitance at zero voltage bias,
ψ_o = junction built-in potential, and
m = junction grading coefficient ($0.2 < m \leq 0.5$).

While theoretical derivations are possible for each of the capacitance parameters, it is more common in practice to determine these parameters empirically. A plot the junction capacitance as described by Equation (10.69) is shown in Figure 10.20. This expression is very accurate for reverse biased junctions and for forward biased junctions where the junction current is small. In most electronic applications, it provides an adequate level of modeling.[5]

Notice that the junction capacitance under reverse-biased conditions exhibits small variation while under forward-biased conditions it increases dramatically with bias voltage.

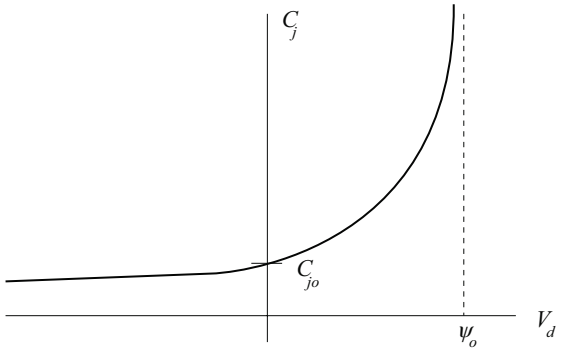

Figure 10.20: p-n junction depletion capacitance.

Example 10.3

If the zero-bias capacitance of a p-n junction is 5 pF and the built-in potential, ψ_o, is 640 mV, determine the junction capacitance at junction voltages

$$V_d = -20\,\text{V},\ \ -10\,\text{V},\ \ -5\,\text{V},\ \ -1\,\text{V},\ \ 0.3\,\text{V},\ \ 0.6\,\text{V}.$$

Assume the junction grading coefficient has value, $m = 0.40$.

Solution

Equation (10.69) yields:

$$C_j \approx \frac{5\ \text{pF}}{\left(1 - \dfrac{V_d}{0.64}\right)^{0.40}}.$$

The tabulated results are:

[5]High forward current modeling requires two modifications. Equation (10.69) indicates infinite capacitance at the built-in potential: in actuality, the depletion capacitance decreases slightly for voltages above the built-in potential. An additional capacitance term, the carrier diffusion capacitance, must also be included. This term is directly proportional to diode current.

$V_d =$	$-20\,\text{V}$	$C_j =$	$1.25\,\text{pF}$
	$-10\,\text{V}$		$1.62\,\text{pF}$
	$-5\,\text{V}$		$2.09\,\text{pF}$
	$-1\,\text{V}$		$3.43\,\text{pF}$
	$0.3\,\text{V}$		$6.44\,\text{pF}$
	$0.6\,\text{V}$		$15.2\,\text{pF}$

The small variation in the junction capacitance for a wide range of negative bias is evident.

10.4.2 MODELING THE BJT AT HIGH FREQUENCIES IN THE FORWARD-ACTIVE REGION

In order to model the BJT at high frequencies, the hybrid-π model of Figure 10.18 is altered by shunting each p-n junction dynamic resistance with an appropriate junction capacitance. This alteration is shown in Figure 10.21. Here, the base-emitter junction has been modeled by a capacitor, C_π, in parallel with the junction forward resistance, r_π. Similarly, the base-collector junction has been modeled by a capacitor, $C_\mu (r_\mu \approx \infty)$.

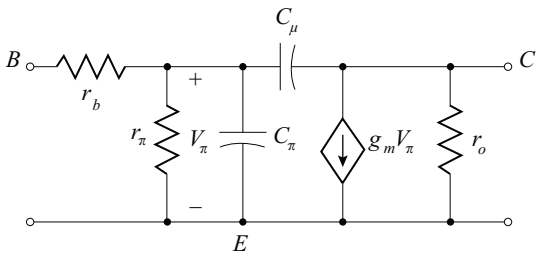

Figure 10.21: The high-frequency hybrid-π model of a BJT.

Determination of the values of the two junction capacitances for a particular transistor is necessary in order to complete the modeling process. While it is possible to analytically determine these capacitances from the physical dimensions and properties of and individual transistor, it is quite common to determine the values experimentally. The base-collector junction is reverse biased when the BJT is in the forward-active region, hence the junction capacitance, C_μ, is *relatively* independent of quiescent conditions. Typical manufacturer data sheets provide a value for C_μ at a given reverse bias (typically, $V_{CB} = 5$ or $10\,\text{V}$): further discussions of C_μ in this text will consider it to be constant at the manufacturer's supplied value.[6] The forward-biased base-emitter junction

[6] C_μ exhibits the same variation with junction bias as is given in Equation (10.69). If data is available to determine the built-in potential, ψ_o, and the junction grading coefficient, m, the values should be used to determine a better approximation for C_μ.

exhibits greater variation with bias conditions: its junction capacitance, C_π, must therefore be determined with greater caution.

The value of the base-emitter junction capacitance, C_π, for a BJT is usually determined through a measurement of the variation with frequency of the BJT short-circuit current gain. The transistor is placed in a test fixture as shown in Figure 10.22. The term "short-circuit" applies to the collector-emitter port of the BJT which appears, *in an ac sense*, to be a short circuit. A plot of the current gain frequency response is then determined experimentally.

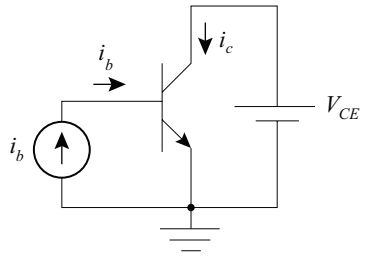

Figure 10.22: Measurement of the short-circuit current gain.

In order to correlate these measurements with the hybrid-π parameters, an ac equivalent circuit of the test circuit must be created (Figure 10.23).

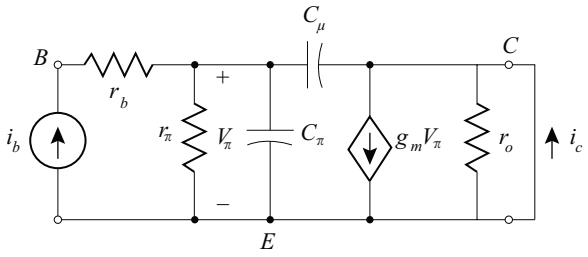

Figure 10.23: Short-circuit current gain AC equivalent circuit.

The current gain is found to be:

$$A_I(\omega) = \frac{i_c(\omega)}{i_b(\omega)} = \left(\frac{i_c}{V_\pi}\right)\left(\frac{V_\pi}{i_b}\right), \tag{10.70}$$

or:

$$A_I(\omega) = (g_m)\left(\frac{r_\pi}{1 + j\omega r_\pi \left(C_\pi + C_\mu\right)}\right) = \frac{h_{fe}}{1 + j\omega r_\pi \left(C_\pi + C_\mu\right)}. \tag{10.71}$$

This current gain expression is in the form of a single-pole low-pass frequency response. The transistor short-circuit current gain has a low-frequency value of h_{fe} and a 3-dB frequency of:

$$\omega_{3dB} = \frac{1}{r_\pi \left(C_\pi + C_\mu\right)}. \tag{10.72}$$

A more common description of the results of Equation (10.71) depends on at the frequency at which the current gain is unity, ω_T,

$$\omega_T = \frac{h_{fe} - 1}{r_\pi \left(C_\pi + C_\mu\right)} \approx \frac{g_m}{C_\pi + C_\mu}. \tag{10.73}$$

This unity-gain frequency, ω_T, is often referred to as the gain-bandwidth product: the product of short-circuit current gain at a particular frequency and that frequency has constant value for all frequencies greater than $\omega_{3\text{dB}}$. Manufacturer's data sheets will either provide a value for ω_T or provide the gain at some other high frequency. The gain-bandwidth is given by:

$$\omega_T = A_m \omega_m, \tag{10.74}$$

where ω_m is the frequency at which the manufacturer made the gain measurement and A_m is the gain at that frequency.

Example 10.4
Given a Silicon *npn* BJT with parameters:

$\beta_F = 150,$
$V_A = 350,$
$r_b = 30\,\Omega,$
$C_\mu = 3\,\text{pF},$
$f_T = 250\,\text{MHz}.$

Determine an appropriate small-signal hybrid-π model for the transistor.

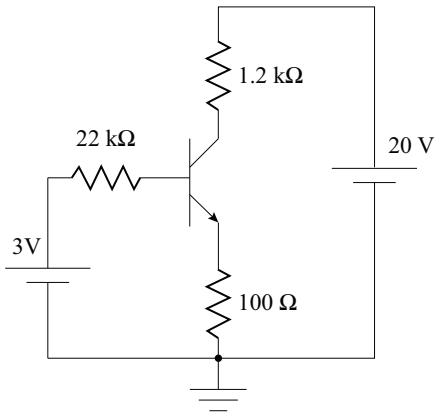

Solution:

The first step in modeling any BJT is to determine the quiescent conditions. Since this is the same transistor and circuit as Example 5.6 (Book 2), the quiescent conditions have already been determined to be:

$$I_C = 9.3\,\text{mA} \quad \text{and} \quad V_{CE} = 7.90\,\text{V}.$$

The BJT is in the forward-active region and the hybrid-π model parameters can be determined from Equations (10.68) and (10.73). Equation (10.68) yields the low-frequency parameters:

$$g_m = \frac{|I_c|}{V_t} = \frac{9.30\,\text{m}}{26\,\text{m}} = 358\,\text{mS} \qquad r_\pi = \frac{\beta_F}{g_m} = \frac{150}{0.358} = 419.4\,\Omega,$$
$$r_o = \frac{|V_A|}{|I_c|} = \frac{350}{9.30\,\text{m}} = 37.6\,\text{k}\Omega \qquad r_b = 30\,\Omega.$$

Equation (10.73) yields the capacitor values:

$$C_\mu = 3\,\text{pF}$$
$$C_\pi = \frac{g_m}{\omega_T} - C_\mu = \frac{0.358}{2\pi(250\,M)} - 3\,\text{pF} = 225\,\text{pF}.$$

10.5 MILLER'S THEOREM

The process of determining the high-frequency poles for transistor amplifiers is not always a simple process. In particular, the introduction of an impedance that connects amplifier input and output ports adds a great deal of complexity in the analysis process. One technique that often helps reduce the complexity in some circuits is the use of Miller's theorem. Miller's theorem addresses the problem introduced by the interconnection of input and output ports.

Miller's theorem applies to the process of creating equivalent circuits. This general circuit theorem is particularly useful in the high-frequency analysis of certain transistor amplifiers at high frequencies. It is based on the principle that two circuits appear equivalent if they have identical voltage-current relationships at the ports where they interconnect with any adjoining circuitry.

Miller's Theorem generally states:

> *Given any general linear network having a common terminal and two terminals whose voltage ratio, with respect to the common terminal, is given by:*
>
> $$V_2 = AV_1. \tag{10.75}$$
>
> *If the two terminals of the network are then interconnected by an impedance, Z, an equivalent circuit can be formed. This equivalent circuit consists of the same general linear network*

and two impedances; each of which shunt a network terminal to common terminal. These two impedances have value (Figure 10.24):

$$Z_1 = \frac{Z}{1-A} \qquad Z_2 = \frac{AZ}{A-1} \tag{10.76}$$

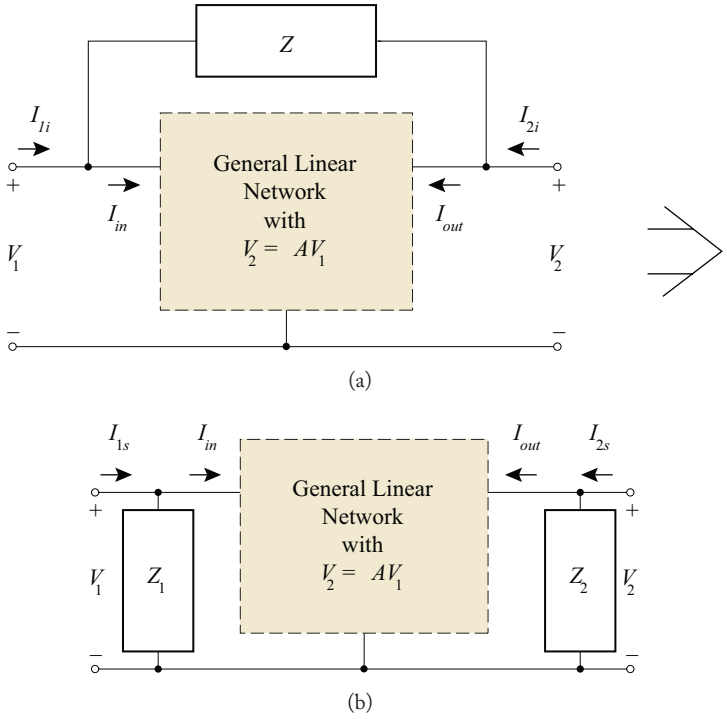

Figure 10.24: Miller equivalent circuits: (a) Interconnecting impedance, (b) Port-shunting impedances.

Miller's Theorem can be verified by showing that the voltage-current relationships at each port of the two circuits are identical. Notice that the voltage at each port of the linear network is applied in the same manner so that the port currents, I_{in} and I_{out}, are unchanged by the attached impedances. At the left port of Figure 10.24a, the input current, I_{1i}, is given by:

$$I_{1i} = I_{in} + \frac{V_1 - V_2}{Z} = I_{in} + \frac{V_1 - AV_1}{Z}. \tag{10.77}$$

The input current of the equivalent circuit (Figure 10.24b is given by:

$$I_{1s} = I_{in} + \frac{V_1}{Z_1}. \tag{10.78}$$

Using the relationship given in Equation (10.76), the input current expression becomes:

$$I_{1s} = I_{in} + \frac{\frac{V_1}{Z}}{1 - A} = I_{in} + \frac{V_1(1 - A)}{Z} = I_{1i}. \tag{10.79}$$

Similarly, at the right port of Figure 10.24a, the output current, I_{2s}, is given by:

$$I_{2i} = I_{out} + \frac{V_2 - V_1}{Z} = I_{in} + \frac{V_2 - 1/A\, V_2}{Z}. \tag{10.80}$$

The output current of the equivalent circuit (Figure 10.24b) is given by:

$$I_{2s} = I_{out} + \frac{V_2}{Z_2}. \tag{10.81}$$

Using the relationship given in Equation (10.76), the output current expression becomes:

$$I_{2s} = I_{out} + V_2\left(\frac{A - 1}{AZ}\right) = I_{out} + \frac{V_2 - 1/A\, V_2}{Z} = I_{2i}. \tag{10.82}$$

For these two Miller equivalent circuits, the individual port voltage-current relationships are identical and the two circuits appear identical to any other circuitry that may be connected at these two ports.

Replacement of the input-output interconnection is particularly useful in the analysis of common-emitter and common source amplifiers. In these amplifiers, the voltage gain necessary to invoke Miller's theorem is easily attainable and the substitution produces significant reduction in analysis complexity.

Example 10.5

The circuit shown consists of an OpAmp inverting amplifier bridged by a capacitor.

Determine the Miller equivalent circuit if the inverting amplifier is considered to be the general linear network.

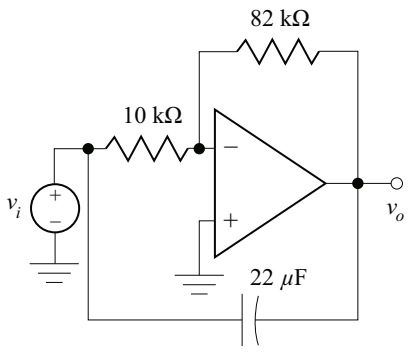

Solution:

The gain of the OpAmp inverter is given by:

$$A = \frac{v_o}{v_i} = -\frac{82\,\text{k}\Omega}{10\,\text{k}\Omega} = -8.2.$$

The two Miller impedances are given by:

$$Z_1 = \frac{Z}{1-A} = \frac{\dfrac{1}{j\omega(22\times 10^{-6})}}{1-(-8.2)} = \frac{1}{j\omega(202.4\times 10^{-6})}$$

and

$$Z_2 = \frac{AZ}{A-1} = \frac{-8.2\left(\dfrac{1}{j\omega(22\times 10^{-6})}\right)}{-8.2-1} = \frac{1}{j\omega(24.68\times 10^{-6})}.$$

Z_1 appears to be a 202.4 μF capacitor and Z_2 a 24.68 μF capacitor.

The Miller equivalent circuit is given by:

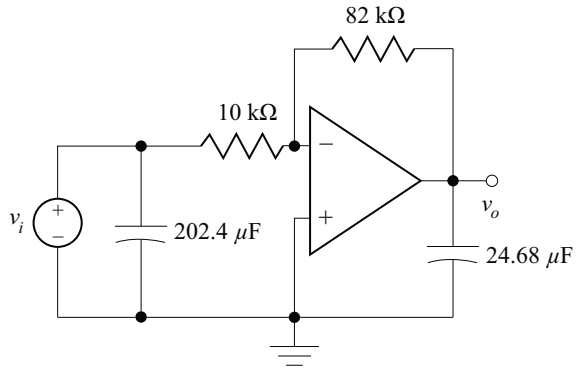

10.6 HIGH-FREQUENCY RESPONSE OF SIMPLE BJT AMPLIFIERS

At high frequencies, amplifier response is characterized by the midband gain and the high-frequency poles. Each poles effects the frequency response curves by introducing a 20 dB/decade attenuation which begins at the pole frequency. Once the midband gain of an amplifier has been determined in the usual fashion, it is only important to determine the pole locations in order to completely determine the amplifier high-frequency response.

In this section, the four single-transistor BJT amplifier types are analyzed in order to determine their high-frequency pole locations. Miller's theorem is first applied to the common-emitter configuration using the traditional approximation for the Miller gain. A more accurate, frequency-dependent application of Miller's theorem to the common-emitter and common-collector configurations follows. The common-base configuration is analyzed using the techniques developed in Chapter 5 (Book 2), and symbolic solutions to simultaneous equations are used for the most complex case: the common-emitter amplifier with emitter degeneration ($CE + Re$) case. As in all small-signal analysis, transistor quiescent conditions must be first calculated so that the transistor parameters can be accurately determined. In order to focus discussion on pole frequency determination, it is assumed that the quiescent analysis has been previously performed and that the transistor parameters are well-known.

While the emphasis of this section is on analysis, the information gained in that analysis is significant in the practice of design. Only with a secure knowledge of the effects of circuit element values and transistor parameters on amplifier response can the designer make appropriate adjustments to meet or exceed specifications.

10.6.1 COMMON-EMITTER AMPLIFIER HIGH-FREQUENCY CHARACTERISTICS

The midband AC model of a typical common-emitter amplifier and its high-frequency equivalent, which uses the hybrid-π BJT model, are shown in Figure 10.25.

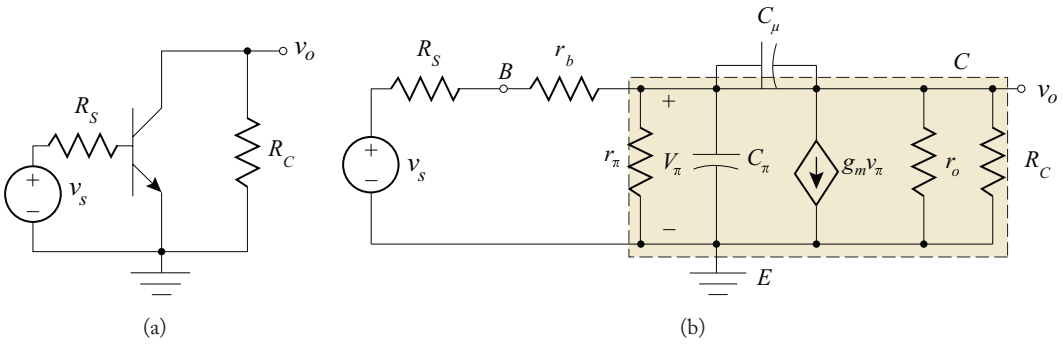

Figure 10.25: Common-emitter equivalent circuits: (a) Midband AC equivalent, (b) High-frequency equivalent.

The use of the analysis techniques previously developed in this text for this circuit is made difficult by the presence of the capacitor C_μ, which interconnects the input and output sections of the amplifier. Miller's Theorem is particularly useful in reducing the analysis complexity for this case. In Figure 10.25b, the shaded two-port network has two terminals for which the voltage gain is

well-known:

$$A = \frac{v_o}{v_\pi} = -g_m(r_o//R_c) = -g_m R'_c, \tag{10.83}$$

where R'_c is the equivalent load resistance including the output impedance of the BJT:

$$R'_c = r_o//R_c. \tag{10.84}$$

The Miller gain as expressed in Equation (10.83) is a first-order approximation: it is the product of the transconductance, g_m, and the collector *resistance* rather than the collector *impedance*. This approximate application of Miller's produces first-order approximations to the two pole frequencies. As such, it estimates the lower-frequency, often dominant, pole accurately, but seriously underestimates the higher-frequency pole. Still, much insight into amplifier frequency response is gained through this Miller approach. An exact, frequency-dependent application of Miller's theorem is presented in the next Section 10.6.2.

The capacitor, C_μ, bridges the two terminals of the shaded two port network. Miller's theorem replaces this bridging capacitor with equivalent capacitances that shunt the ports of the network (Figure 10.26).

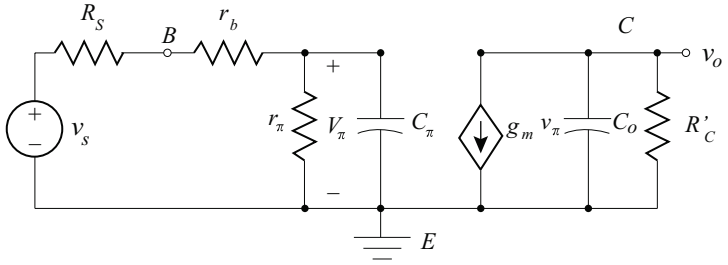

Figure 10.26: Miller's theorem applied to a common-emitter amplifier.

The input capacitance, C_i, is the parallel combination of C_π and the Miller input capacitance, C_1:

$$C_i = C_\pi + (1 + g_m R'_c)C_\mu, \tag{10.85}$$

and the output capacitance, C_o, is the Millers output capacitance, C_2:

$$C_o = C_\mu \left(\frac{1 + g_m R'_c}{g_m R'_c} \right). \tag{10.86}$$

The voltage gain of the circuit is easily determined through typical phasor techniques. In this case, the gain is the product of a voltage division at the input and a current source-impedance product

at the output:

$$A_V = \frac{v_o}{v_s} = \left(\frac{v_o}{v_\pi}\right)\left(\frac{v_\pi}{v_s}\right) = \left(\frac{-g_m R_c'}{1 + j\omega C_o R_c'}\right)\left(\frac{\dfrac{r_\pi}{1 + j\omega C_i r_\pi}}{\dfrac{r_\pi}{1 + j\omega C_i r_\pi} + R_s + r_b}\right). \tag{10.87}$$

Algebraic manipulation yields the desired result:

$$A_V = -g_m R_c'\left(\frac{r_\pi}{r_\pi + R_s + r_b}\right)\left(\frac{1}{1 + j\omega C_o R_c'}\right)\left(\frac{1}{1 + j\omega C_i \{r_\pi // (R_s + r_b)\}}\right). \tag{10.88}$$

This gain has two simple poles at frequencies

$$\omega_{p1} = \left(\frac{1}{C_i \{r_\pi // (R_s + r_b)\}}\right) = \left(\frac{1}{\{C_\pi + C_\mu (1 + g_m R_c')\}\{r_\pi // (R_s + r_b)\}}\right) \tag{10.89}$$

and

$$\omega_{p2} = \left(\frac{1}{C_o R_c'}\right) = \frac{1}{C_\mu\left(\dfrac{1 + g_m R_c'}{g_m R_c'}\right) R_c'} = \frac{1}{C_\mu (1/g_m + R_c')}. \tag{10.90}$$

Typical circuit element values imply that $\omega_{p1} < \omega_{p2}$, but small signal-source resistance, R_s, may reverse that relationship: both pole locations should always be checked. Typically, the high-frequency response of a common-emitter amplifier is limited by C_i through the multiplicative alteration of C_μ using Miller's theorem. This increase in the input circuit capacitance and the resulting decrease in pole frequency magnitude is called the Miller effect. The two pole locations, with the midband gain, determine the total high-frequency response of a common-emitter amplifier.

Example 10.6

Determine the high 3-dB frequency for the common-emitter circuit shown. Assume a Silicon *npn* BJT with parameters:

$\beta_F = 150,$
$V_A = 350,$
$r_b = 30\,\Omega,$
$C_\mu = 3\,\text{pF},$
$f_T = 100\,\text{MHz}.$

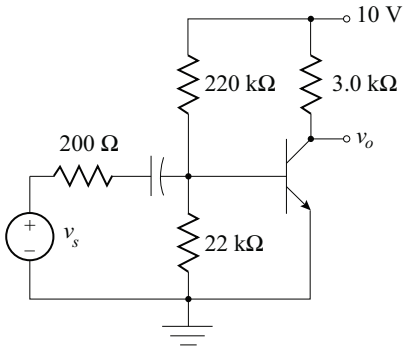

Solution:

The coupling capacitor is replaced by an open circuit to determine the BJT quiescent—they are found to be:

$$I_B = 10.45\,\mu\text{A} \qquad I_C = 1.568\,\text{mA} \qquad V_{CE} = 5.30\,\text{V}.$$

The hybrid-π parameters are then determined from these quiescent conditions:

$$\begin{aligned} g_m &= 60.31\,\text{mS}, \quad r_\pi = 2.487\,\text{k}\Omega, \quad C_\mu = 3.0\,\text{pF}, \\ r_o &= 223.2\,\text{k}\Omega, \quad r_b = 30\,\Omega, \quad C_\pi = 93.0\,\text{pF}. \end{aligned}$$

The source resistance, R_s, is the 200 Ω resistor in parallel with the two biasing resistors; thus the two pole frequencies are determined from Equations (10.89) and (10.90):

$$\omega_{p1} = \frac{1}{\{C_\pi + C_\mu\,(1 + g_m R_c')\}\,\{r_\pi // (R_s + r_b)\}} = 7.957\,\text{Mrad/s} \;\; (1.27\,\text{MHz})$$

$$\omega_{p2} = \frac{1}{C_\mu\left(\dfrac{1}{g_m} + R_c'\right)} = \frac{1}{3p\left\{\dfrac{1}{60.31\,\text{m}} + 2.96\,\text{k}\right\}} = 112.0\,\text{Mrad/s}\,(17.8\,\text{MHz})\,.$$

Clearly ω_{p1} is a dominant pole and the high 3-dB frequency is:

$$f_H \approx 1.27\,\text{MHz}.$$

10.6.2 EXACT COMMON-EMITTER HIGH-FREQUENCY CHARACTERISTICS

It has been found that Equations (10.89) and (10.90) accurately estimate the lower-frequency pole, whichever it may be, but underestimate the higher-frequency pole.[7] A frequency dependent

[7]T. F. Schubert, Jr., and E. M., Kim, "A Short Study on the Validity of Miller's Theorem Applied to Transistor Amplifier High-Frequency Performance," *IEEE Transactions on Education,* vol. 52, no. 1, pp. 92–98, Feb. 2009.

application of Miller's Theorem removes the approximations inherent in the traditional application of Miller's Theorem to transistor amplifiers. As such, the Miller equivalent circuit derived by this frequency-dependent application is an exact performance equivalent and any performance parameters derived apply exactly to the original the hybrid-π model of the circuit. Both poles and the zero of the amplifier gain and input impedance are calculated exactly.

The Miller voltage gain, $A_M(\omega)$, is given by the product of the output of the voltage-controlled dependent current source, $-g_m$, and the parallel combination of the Miller output capacitance, C_o, and the effective load resistance, $R'_c = r_o//R_c$. As stated above, the Miller gain is given in phasor domain as:

$$A_M(\omega) = \frac{-g_m R'_c}{1 + j\omega R'_c C_o}. \tag{10.91}$$

However, the Miller output capacitance, C_o, has also been shown to be a function of the Miller gain:

$$C_o = \frac{1 - A_M(\omega)}{A_M(\omega)} C_\mu. \tag{10.92}$$

Solving the above equation pair for the Miller gain, $A_M(\omega)$, yields:

$$A_M(\omega) = \frac{-g_m R'_c \left(1 - j\omega \dfrac{C_\mu}{g_m}\right)}{1 + j\omega R'_c C_\mu}. \tag{10.93}$$

The Miller voltage gain experiences a pole at $-(R'_c C_o)^{-1}$ and a negative-phase zero (*np*-zero) at $g_m C_\mu^{-1}$. An *np*-zero has the same magnitude response as a typical zero, but the phase is inverted: some sources in the literature associate an *np*-zero with negative-value components. In this case, the *np*-zero is due to the Miller gain changing from a large negative, real quantity to positive unity as frequency increases: there must be a total of 180° of phase shift in the Miller gain at very high frequencies.

The amplifier input capacitance, C_i, now takes on a frequency dependent characteristic:

$$C_i(\omega) = C_\pi + \left[1 + \frac{g_m R'_c \left(1 - j\omega \dfrac{C_\mu}{g_m}\right)}{1 + j\omega R'_c C_\mu}\right] C_\mu; \tag{10.94}$$

and the input gain can be written as:

$$A_i(\omega) = \frac{\left[\dfrac{r_\pi}{R_s + r_b + r_\pi}\right](1 + j\omega R'_c C_\mu)}{1 + j\omega\left\{R_i C_\pi + \left(1 + g_m R'_c\right) R_i C_\mu + R'_c C_\mu\right\} + (j\omega)^2\left\{R_i R'_c C_\pi C_\mu\right\}} \tag{10.95}$$

where

$$R_i = r_\pi//(R_s + r_b).$$

Notice that the zero of the input gain, $A_i(\omega)$, is at exactly same frequency as the pole of the Miller gain, $A_M(\omega)$. Thus, pole-zero cancellation occurs and any poles in the Miller gain become irrelevant in the total gain expression (the *np*-zero, however, remains). This pole-zero cancellation is not coincidental: it is the direct result of Miller gain poles appearing in the denominator of the input gain, thusly becoming zeroes. The total voltage gain of the amplifier can now be expressed as:

$$A_V = \frac{\left[\dfrac{r_\pi}{R_s + r_b + r_\pi}\right](-g_m R_c')\left[1 - j\omega\dfrac{C_\mu}{g_m}\right]}{1 + j\omega\left\{R_i C_\pi + \left(1 + g_m R_c'\right) R_i C_\mu + R_c' C_\mu\right\} + (j\omega)^2\left\{R_i R_c' C_\pi C_\mu\right\}}. \tag{10.96}$$

Comparison of the expression for the Miller-derived gain and numerical solutions resulting from node-voltage analysis yields exactly (to with the accuracy of the computation package) the same results. The total gain expression retains the *np*-zero of the Miller gain at $g_m C_\mu^{-1}$ and has two poles.

Use of the quadratic formula leads to exact values of the pole frequencies:

$$\omega_{p1} = \frac{-b + \sqrt{b^2 - 4a}}{2a} \quad \text{and} \quad \omega_{p2} = \frac{-b - \sqrt{b^2 - 4a}}{2a};$$

where

$$b = R_i C_\pi + \left(1 + g_m R_c'\right) R_i C_\mu + R_c' C_\mu \quad \text{and} \quad a = R_i R_c' C_\pi C_\mu. \tag{10.97}$$

The complexity of these expressions can be reduced by noting that in essentially all practical common-emitter and common-source amplifiers $4a \ll b^2$, and a good approximation of the square root terms can be made:

$$\sqrt{1 - \varepsilon} \approx 1 - \frac{\varepsilon}{2} \quad \Rightarrow \quad \sqrt{b^2 - 4a} \approx b - \frac{2a}{b}. \tag{10.98}$$

The resultant approximate pole frequencies are:

$$\omega_{p1A} \approx \frac{-1}{b} = \frac{-1}{\left\{C_\pi + \left(1 + g_m R_c'\right) C_\mu\right\} R_i + R_c' C_\mu},$$

and

$$\omega_{p2A} \approx \frac{-b}{a} + \frac{1}{b} = \frac{1}{\omega_{p1A} R_i R_c' C_\pi C_\mu} - \omega_{p1A}. \tag{10.99}$$

The Miller effect (multiplication of C_μ by the quantity $(1 + g_m R_c')$ is still strongly apparent in the expression for ω_{p1A}, however, the expression for ω_{p2A} takes a completely different form than what is typically presented in the literature.

The input impedance for common-emitter amplifiers can be directly derived from the input gain $A_i(\omega)$, replacing the term R_i by r_π:

$$Z_{in} = r_b + \frac{r_\pi\left(1 + j\omega R_c' C_\mu\right)}{1 + j\omega\left\{r_\pi C_\pi + \left(1 + g_m R_c'\right) r_\pi C_\mu + R_c' C_\mu\right\} + (j\omega)^2\left\{r_\pi R_c' C_\pi C_\mu\right\}}. \tag{10.100}$$

As a result, there is a true zero at $-(R'_c C_\mu)^{-1}$ and the approximate poles are somewhat shifted from those of the voltage gain:

$$\omega_{p1in} \approx \frac{-1}{r_\pi C_\pi + (1 + g_m R'_c) r_\pi C_\mu + R'_c C_\mu},$$

and

$$\omega_{p2in} \approx \frac{1}{\omega_{p1in} r_\pi R'_c C_\pi C_\mu} - \omega_{p1in}. \tag{10.101}$$

While the frequency-independent application of Miller's Theorem does not lead to productive results concerning output impedance, the frequency-dependent approach leads to an exact representation. The representation of the output impedance is somewhat difficult to obtain by direct inspection; however, the Thévenin Theorem leads to an appropriate expression:

$$Z_{out} = \frac{\text{Open circuit voltage}}{\text{Short circuit current}} = \frac{A_V(\omega)}{\lim\limits_{R_L \to 0} \left\{ \dfrac{A_V(\omega)}{R_L} \right\}},$$

or

$$Z_{out} = \frac{R'_c \{1 + j\omega R_i (C_\pi + C_\mu)\}}{1 + j\omega \{R_i C_\pi + (1 + g_m R'_c) R_i C_\mu + R'_c C_\mu\} + (j\omega)^2 \{R_i R'_c C_\pi C_\mu\}}. \tag{10.102}$$

The output impedance also has a zero and two poles. Since the denominator of the output impedance is the same expression as the voltage gain, the *expressions* for the pole frequencies of the output impedance match those for the voltage gain. However, the output impedance pole frequencies will depend on exactly where that impedance is measured. Particular attention must be paid to the quantity $R'_c = r_o // R_c$ which depends on where the output impedance measurement is taken (that is, what resistances make up R_c) and may not be the same value as is used for voltage gain.

Example 10.7

Determine the high-frequency poles for the common-emitter circuit of Example 10.6.

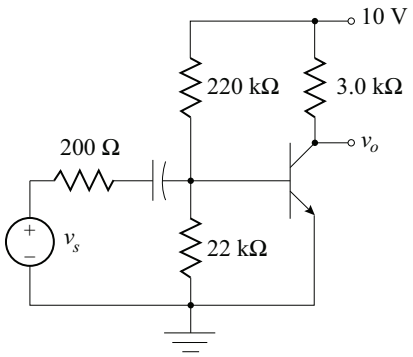

Solution:

The hybrid-π parameters were determined from the quiescent conditions in Example 10.6:

$$g_m = 60.31\,\text{mS}, \quad r_\pi = 2.487\,\text{k}\Omega,$$
$$r_o = 223.2\,\text{k}\Omega, \quad r_b = 30\,\Omega,$$
$$C_\pi = 93.0\,\text{pF}, \quad C_\mu = 3.0\,\text{pF}.$$

Also determined in Example 10.6 were the circuit parameters:

$$R_s = 200//220\,\text{k}//22\,\text{k} = 198\,\Omega$$
$$R_i = r_\pi//(R_s + r_b) = 208.8\,\Omega \qquad R'_c = r_o//3\,\text{k} = 2.96\,\text{k}\Omega.$$

The poles can then be calculated to be:

$$\omega_{p1A} = 7.428\,\text{Mrad/s} \quad (1.18\,\text{MHz}) \qquad \omega_{p2A} = 811.3\,\text{Mrad/s} \quad (129\,\text{MHz}).$$

There is definitely a dominant pole and the high 3-dB frequency consequently at that pole frequency: 1.18 MHz. Notice that this result compares nicely with the estimated 3-dB frequency of Example 10.6 (1.27 MHz). However, the estimated second pole as determined in Example 10.6 is drastically too low (0.86 decades low). If the location of the second pole is important, the poles determined by the frequency-dependent Miller approach must be used.

10.6.3 COMMON-COLLECTOR AMPLIFIER HIGH-FREQUENCY CHARACTERISTICS

Miller's Theorem is a valid and useful technique when applied to common-collector amplifiers. The simplified model of a common-collector amplifier and its high-frequency equivalent, using the hybrid-π BJT model, are shown in Figure 10.27. The capacitor, C_π, and the resistor, r_π, bridge the input and output terminals of the amplifier. Miller's theorem replaces these bridging impedances with equivalent impedances shunting the input and output ports of the network (Figure 10.28). For simplicity of notation, the substitution $R'_e = r_o//R_e$ has been made.
For this circuit, the Miller voltage gain is defined as:

$$A_M(\omega) = \frac{v_o}{v_B}. \tag{10.103}$$

The Miller gain can be directly determined to be:

$$A_M(\omega) = \frac{R'_e}{R'_e + R_\pi} \frac{1 + j\omega R_\pi C_\pi}{1 + j\omega(R_\pi//R'_e)C_\pi}, \tag{10.104}$$

where

$$R_\pi = r_\pi//(1/g_m) = \frac{r_\pi}{1 + g_m r_\pi}. \tag{10.105}$$

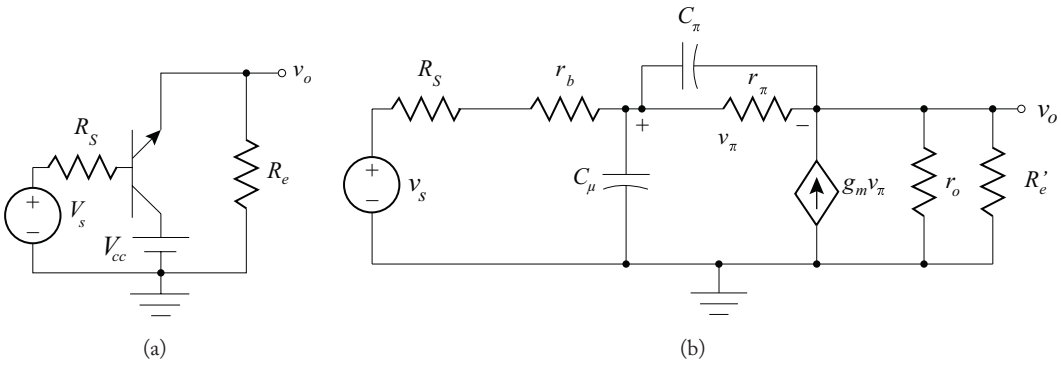

Figure 10.27: Common-collector circuits: (a) Simplified equivalent, (b) High-Frequency equivalent.

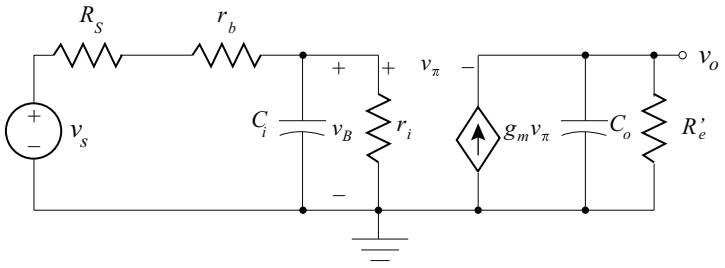

Figure 10.28: Miller's theorem applied to a common-collector amplifier high-frequency model.

The total amplifier voltage gain can then be written as the product of the input gain and the Miller gain:

$$A_V(\omega) = \frac{v_o}{v_s} = \left(\frac{v_B}{v_s}\right)\left(\frac{v_o}{v_B}\right) = A_i(\omega)A_M(\omega), \tag{10.106}$$

where

$$A_i(\omega) = \frac{v_B}{v_s} = \frac{Z_i}{Z_i + R_S + r_b}. \tag{10.107}$$

Under the Miller transformations, the input impedance, Z_i, becomes the parallel combination of C_μ and the Miller input impedance:

$$Z_i = \frac{1}{j\omega C_\mu} // \left[\frac{r_\pi}{1 + j\omega r_\pi C_\pi}\frac{1}{1 - A_M}\right]. \tag{10.108}$$

After much manipulation and the standard substitution for the current gain, $\beta = g_m r_\pi$; the total common-collector gain can be expressed as:

$$A_V = \left[\frac{\left\{ \frac{R'_e}{R'_e + \frac{R_S + r_b + r_\pi}{1+\beta}} \right\} \left(1 + j\omega \frac{r_\pi C_\pi}{1+\beta} \right)}{1 + j\omega \left(\frac{r_\pi (R'_e + R_s + r_b) C_\pi + (R_s + r_b)\left[R'_e (1+\beta) + r_\pi \right] C_\mu}{R_s + r_b + r_\pi + R'_e (1+\beta)} \right) + (j\omega)^2 \left(\frac{(R_s + r_b) R'_e r_\pi C_\pi C_\mu}{R_s + r_b + r_\pi + R'_e (1+\beta)} \right)} \right].$$

This gain has a single zero at:

$$\omega_z = -\frac{1+\beta}{r_\pi C_\pi}, \tag{10.109}$$

and, using the same quadratic approximations as for the common-emitter case, poles at:

$$\omega_{p1A} \approx \frac{-1}{b} = -\frac{R_s + r_b + r_\pi + (1+\beta) R'_e}{\left(R_s + r_b + R'_e \right) r_\pi C_\pi + (R_s + r_b)\left[r_\pi + (1+\beta) R'_e \right] C_\mu},$$

and

$$\omega_{p2A} \approx -\frac{(R_s + r_b + R'_e) r_\pi C_\pi + (R_s + r_b)\left[r_\pi + (1+\beta) R'_e \right] C_\mu}{(R_s + r_b) r_\pi R'_e C_\pi C_\mu} - \omega_{p1A}. \tag{10.110}$$

Since the zero lies, in frequency, between the two poles, it is typical to model a common-collector amplifier as a single-pole amplifier using ω_{p1A} as the pole frequency:

$$\omega_{3-\text{dB}} \approx \omega_{p1A} \approx -\frac{R_s + r_b + r_\pi + (1+\beta) R'_e}{\left(R_s + r_b + R'_e \right) r_\pi C_\pi + (R_s + r_b)\left[r_\pi + (1+\beta) R'_e \right] C_\mu}. \tag{10.111}$$

The input impedance can be directly obtained from the series combination of the BJT base resistance, r_b, and the Miller input gain:

$$\begin{aligned} Z_{in} &= r_b + Z_i \\ &= r_b + \frac{\left[r_\pi + (1+\beta) R'_e \right] \left[1 + \frac{r_\pi R'_e C_\pi}{r_\pi + (1+\beta) R'_e} j\omega \right]}{1 + \left[r_\pi \left(C_\pi + C_\mu \right) + (1+\beta) R'_e C_\mu \right] j\omega + \left(r_\pi R'_e C_\pi C_\mu \right) (j\omega)^2}. \end{aligned} \tag{10.112}$$

The poles are again somewhat shifted from those of the voltage gain:

$$\omega_{p1in} \approx \frac{-1}{r_\pi C_\pi + \left(1 + g_m R'_c \right) r_\pi C_\mu + R'_c C_\mu},$$

and

$$\omega_{p2in} \approx \frac{1}{\omega_{p1in} r_\pi R'_c C_\pi C_\mu} - \omega_{p1in}. \tag{10.113}$$

The output impedance also has a zero and two poles. Since the denominator of the output impedance is the same expression as the voltage gain, the *expressions* for the pole frequencies of the output impedance match those for the voltage gain. However, the output impedance pole frequencies will depend on exactly where that impedance is measured. Particular attention must be paid to the quantity $R_c' = r_o // R_c$ which depends on where the output impedance measurement is taken (that is, what resistances make up R_c) and may not be the same value as is used for voltage gain.

10.6.4 COMMON-BASE AMPLIFIER HIGH-FREQUENCY CHARACTERISTICS

The midband AC model of typical common-base amplifier and its high-frequency equivalent are shown in Figure 10.29. Notice that there is no element bridging the input and output terminals. It is not necessary to invoke Miller's Theorem in order to find the pole frequencies. The capacitance-increasing Miller effect is not present in common-base amplifiers: the pole magnitudes are consequently at very high frequencies.

In order to simplify the analysis of this complex circuit, notice that the voltage across the resistor, r_b, is very small: both r_b and the BJT base current are relatively small quantities. It is therefore reasonable to assume the voltage at B' is essentially AC ground and the voltage at the emitter is given by:

$$v_e \approx -v_\pi. \tag{10.114}$$

The output voltage is given by the product of the current source value and the impedance between the collector and common:

$$v_o = -g_m v_\pi \left(\frac{1}{1 + j\omega C_\mu R_c} \right). \tag{10.115}$$

In order to find the relationship between v_π and v_s, the currents are summed at the emitter terminal of the BJT:

$$\frac{v_s + v_\pi}{R_s} + g_m v_\pi + j\omega C_\pi v_\pi + \frac{v_\pi}{r_\pi} = 0. \tag{10.116}$$

This expression can be solved for v_π:

$$v_\pi = \frac{-\frac{v_s}{R_s}\left(R_s + g_m + \frac{1}{r_\pi} \right)}{1 + j\omega C_\pi \left(\frac{1}{R_s} + g_m + \frac{1}{r_\pi} \right)}. \tag{10.117}$$

Equations (10.105) and (10.107) are combined to form the total gain expression:

$$v_o = -g_m \left(\frac{-\frac{v_s}{R_s}\left(\frac{1}{R_s} + g_m + \frac{1}{r_\pi} \right)}{1 + j\omega C_\pi \left(\frac{1}{R_s} + g_m + \frac{1}{r_\pi} \right)} \right) \left(\frac{1}{1 + j\omega C_\mu R_c} \right). \tag{10.118}$$

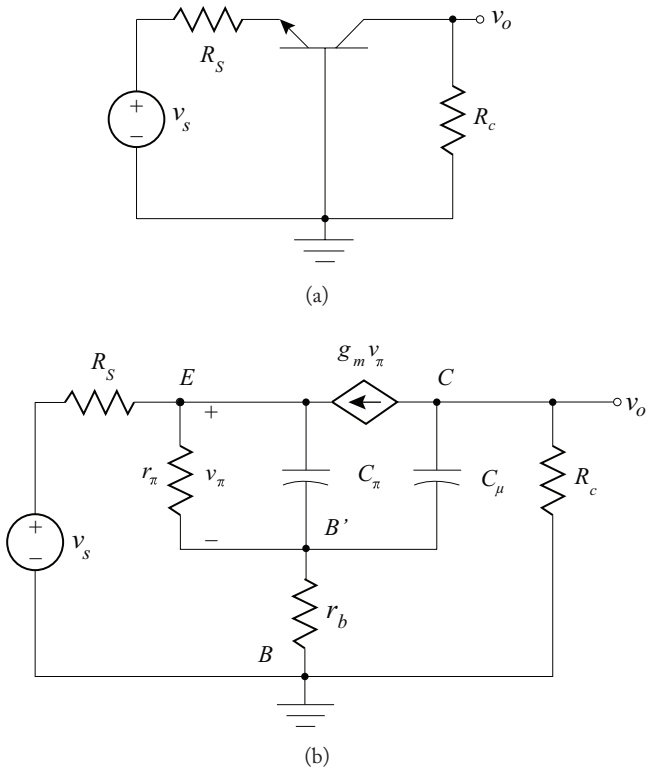

Figure 10.29: Common-base equivalent circuits: (a) Midband AC equivalent, (b) High-frequency equivalent.

There are two simple poles. The input pole is at frequency:

$$\omega_{p1} = \frac{r_\pi + g_m r_\pi R_s + R_s}{C_\pi r_\pi R_s} = \frac{r_\pi + (1 + g_m r_\pi) R_s}{C_\pi r_\pi R_s}. \tag{10.119}$$

Since $g_m r_\pi = \beta_F$, the expression can be further simplified:

$$\omega_1 = \frac{r_\pi + (1 + \beta_F)\, R_s}{C_\pi r_\pi R_s} \approx \frac{\beta_F}{C_\pi r_\pi} = \omega_T. \tag{10.120}$$

The output pole is at frequency:

$$\omega_{p2} = \frac{1}{C_\mu R_c}. \tag{10.121}$$

Both poles are at very high frequencies: Common-base amplifier stages are not usually the frequency limiting elements in a multistage amplifier.

10.6.5 COMMON-EMITTER WITH EMITTER DEGENERATION ($CE + R_e$) CHARACTERISTICS

A typical common emitter amplifier with emitter degeneration is shown in Figure 10.30a. Here the transistor is biased by Thévenin sources and resistances: they represent the total linear circuits connected to the terminals of the transistor. Figure 10.30b is a small-signal ac equivalent of that amplifier with the transistor replaced by its high-frequency hybrid-π model. While the BJT hybrid-π model includes an output resistance, r_o, that resistance, in typical common-emitter applications, is large compared to $R_C + R_E$ and will be ignored in this analysis.

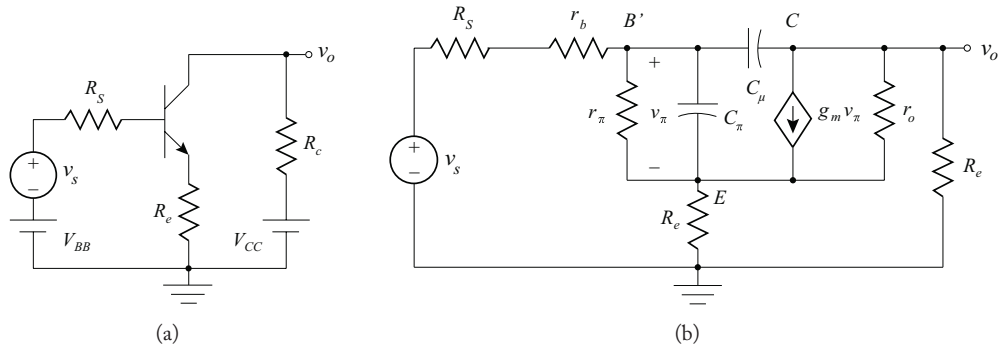

Figure 10.30: Common emitter equivalent circuits: (a) Driven by Thévenin sources, (b) High-frequency equivalent.

The application of Kirchhoff's current law at the nodes B', E, and C respectively, produces the following set of equations that can be solved simultaneously in order to determine the frequency response:

$$\begin{aligned}
&\frac{v_s - v_b}{R_s + r_b} + \frac{v_e - v_b}{r_\pi} + (v_e - v_b)\, sC_\pi + (v_o - v_b)\, sC_\mu = 0 \\
&(v_b - v_e)\, sC_\pi + \frac{v_b - v_e}{r_\pi} + g_m\,(v_b - v_e) - \frac{v_e}{R_e} = 0 \\
&(v_b - v_o)\, sC_\mu - g_m\,(v_b - v_e) - \frac{v_o}{R_c} = 0.
\end{aligned} \tag{10.122}$$

Here frequency is represented by $s = j\omega$. Exact symbolic solutions for the voltage gain $A_V = v_o/v_s$ take the form of the quotient of two second-order polynomials in s:

$$A_V = \frac{v_o}{v_s} = \frac{a_z s^2 + b_z s + c_z}{a_p s^2 + b_p s + c_p}, \tag{10.123}$$

with denominator polynomial constants (note $R'_s = R_s + r_b$):

$$\begin{aligned} a_p &= \left(R'_s R_c + R'_s R_e + R_c R_e\right) r_\pi C_\pi C_\mu, \\ b_p &= \left[\begin{array}{l} (1 + g_m r_\pi)\left(R'_s R_c + R'_s R_e + R_c R_e\right) + \\ +r_\pi \left(R'_s + R_c\right) \end{array} \right] C_\mu + r_\pi \left(R'_s + R_e\right) C_\pi \\ c_p &= R'_s + r_\pi + (1 + g_m r_\pi) R_e, \end{aligned} \tag{10.124}$$

and numerator polynomial constants:

$$b_z = \left[(1 + g_m r_\pi) R_c R_e + r_\pi R_c\right] C_\mu \quad \text{and} \quad c_z = -g_m r_\pi R_c. \tag{10.125}$$

The roots of the denominator polynomial lead to the poles of the gain and the roots of the numerator lead to the zeros. Use of the quadratic formula on the polynomials gives exact values of the pole and zero frequencies:

$$\omega_1 = \frac{-b + \sqrt{b^2 - 4ac}}{2a} \quad \text{and} \quad \omega_2 = \frac{-b - \sqrt{b^2 - 4ac}}{2a}. \tag{10.126}$$

For all practical amplifiers of this topology, the first pole is usually considered dominant in determining the cutoff frequency of the amplifier and common-emitter amplifiers with emitter degeneration are typically modeled for this purpose by only a single-pole. Single-pole modeling typically results in a slight underestimation of the 3-dB frequency response due to the first zero being relatively near the dominant pole. When the emitter resistor is small, the second pole and the first zero exchange order and single-pole modeling can slightly overestimate the 3-dB frequency response due to the first zero being relatively near the dominant pole. When the emitter resistor is small, the second pole and the first zero exchange order and single-pole modeling can slightly overestimate the 3-dB frequency.

The complexity of the pole frequency expressions can be reduced by noting that in essentially all practical common-emitter and common-source amplifiers, the pole polynomial constants are such that $b^2 \gg |4ac|$, and a good approximation of the square root terms can be made:

$$\sqrt{1 - \varepsilon} \approx 1 - \frac{\varepsilon}{2} \quad \Rightarrow \quad \sqrt{b^2 - 4ac} \approx b\left(1 - \frac{2ac}{b^2}\right) = b - \frac{2ac}{b}. \tag{10.127}$$

The pole frequencies can then be approximated by reasonable algebraic expressions

$$\omega_{p1A} \approx \frac{-c_p}{b_p} = \frac{-\left[R'_s + r_\pi + (1 + g_m r_\pi) R_e\right]}{\left[(1 + g_m r_\pi)\left(R'_s R_c + R'_s R_e + R_c R_e\right) + r_\pi \left(R'_s + R_c\right)\right] C_\mu + r_\pi \left(R'_s + R_e\right) C_\pi}$$

and

$$\begin{aligned} \omega_{p2A} &\approx \frac{-b_p}{a_p} + \frac{c_p}{b_p} \\ &= \frac{-\left[(1 + g_m r_\pi)\left(R'_s R_c + R'_s R_e + R_c R_e\right) + r_\pi \left(R'_s + R_c\right)\right] C_\mu + r_\pi \left(R'_s + R_e\right) C_\pi}{\left[R'_s R_c + R'_s R_e + R_c R_e\right] r_\pi C_\pi C_\mu} - \omega_{p1A}. \end{aligned} \tag{10.128}$$

The approximate 3-dB frequency can be cast in more familiar terms by noting that $g_m r_\pi = \beta_F$:

$$\omega_{3\text{dB}} \approx \frac{-\left[R'_s + r_\pi + (1+\beta_F)\,R_e\right]}{\left[(1+\beta_F)\left(R'_s R_c + R'_s R_e + R_c R_e\right) + r_\pi\left(R'_s + R_c\right)\right] C_\mu + r_\pi\left(R'_s + R_e\right) C_\pi}. \tag{10.129}$$

Here the Miller effect is evident in the multiplication of C_μ as is the widening of the amplifier bandwidth with feedback (by increasing R_E). These approximations increase the underestimation of the 3-dB frequency somewhat over the exact single-pole estimation.

A comparison of bandwidth calculations for the typical small-signal amplifier of Figure 10.31a is shown in Table 10.1. In this example circuit, the quotient of polynomials representation of gain as derived by the frequency-dependent form of Miller's Theorem is essentially identical to the SPICE simulation with only −2% (1/100 decade) variation in the 3-dB frequency and no more than 0.1 dB variation over the entire range of frequencies (Figure 10.31b). Single-pole approximations to common-emitter with emitter degeneration amplifiers are common and accurately estimate the high 3-dB frequency. In this case, the exact single pole estimate underestimated the 3-dB frequency by only ∼6.3% (∼1/28 decade) while the approximate, single-pole expression underestimates the 3-dB frequency, as compared to SPICE simulation, by only ∼14% (∼1/15 decade). A summary of the various high 3-dB calculations is given in Table 10.2, and the one-pole frequency response plots are also shown in Figure 10.31.

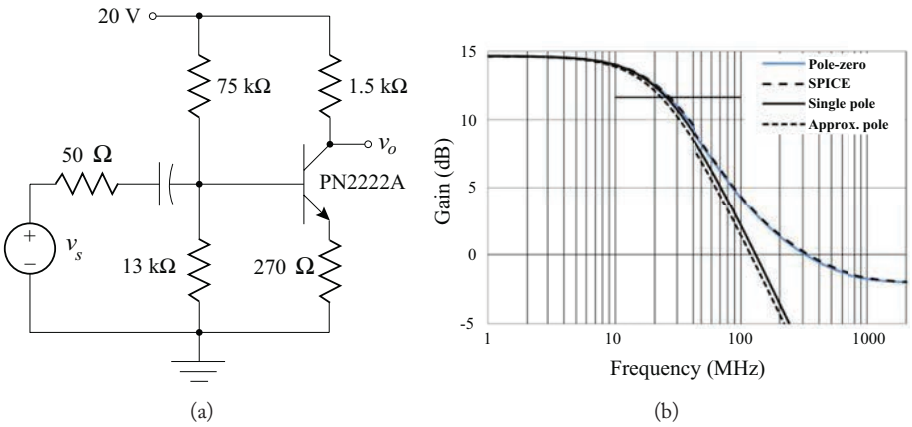

Figure 10.31: (a) Typical common-emitter amplifier, (b) Frequency responses characterizations.

Table 10.1: Comparison of 3-dB frequencies for the common-emitter amplifier of Figure 10.31

3-dB frequency			
SPICE	two poles + two zeros	single pole (ω_{p1})	approx. pole (ω_{p1a})
26.2 MHz	25.6 MHz	24.6 MHz	22.5 MHz
variation	- 2.4% 1/100 decade	- 6.3% 1/28 decade	- 14% 1/15 decade

Table 10.2: Summary of BJT amplifier high-frequency pole locations

Amplifier Type	*Pole Locations (rad/s.)*
Common-emitter (single pole) (use the smaller)	$\dfrac{1}{\{r_\pi // R'_s\}\{C_\pi + (1+g_m R'_c)C_\mu\}}$ *or* $\dfrac{1}{\left(\dfrac{1}{g_m} + R'_c\right)C_\mu}$
Common-emitter (two poles)	$\omega_1 = \dfrac{1}{R_i\{C_\pi + (1+g_m R'_c)C_\mu\} + R'_c C_\mu}$, $\dfrac{1}{\omega_{p1A} R_i R'_c C_\pi C_\mu} - \omega_{p1A}$
Common-emitter with emitter degeneration	$\dfrac{[R'_s + r_\pi + (1+\beta_F)R_e]}{[(1+\beta_F)(R'_s R_c + R'_s R_c + R_c R_e) + r\ (R'_s + R_c)]C_\mu + r_\pi(R'_s + R_e)C_\pi}$
Common-collector	$\dfrac{R'_s + r_\pi + (1+\beta)R'_e}{(R'_s + R'_e)r_\pi C_\pi + R'_s[r_\pi + (1+\beta)R'_e]C_\mu}$
Common-base	ω_T , $\dfrac{1}{R_c C_\mu}$

Note: $R'_c = R_c // r_o$, $R'_s = R_s + r_b$, $R_i = r_\pi // R'_s$, and $R'_e = R_e // r_o$

10.7 HIGH-FREQUENCY MODELS OF THE FET

Analysis of the response of JFET and MOSFET circuits at high frequencies is based on accurate modeling of the frequency dependent performance of the transistors. The FET models used for signal analysis in the low to midband frequencies in the saturation region, as presented in Chapter 4 (Book 1), do not contain frequency sensitive elements and are therefore invariant with respect to changes in frequency. It is therefore necessary to introduce the high-frequency variant of the model to include the frequency-dependent terms.

10.7.1 DYNAMIC MODELS FOR THE FET

The current-voltage relationships of the JFET in Chapter 4 (Book 1) and the small-signal models of Chapter 5 (Book 2) were derived only for voltages assumed to change slowly with time. For high-frequency analysis, the relationships must be modified to include the following two effects:

1. The JFET structure acts as a parallel plate capacitor when viewed from the gate and source terminals, with the gate and channel forming the two plates. The plate capacitor separation is the width of the gate-to-channel junction depletion region. A capacitive current will flow when there is a change in the gate-to-source voltage.

2. The majority carriers require a finite transition time to cross the source to gate channel. If the gate voltage changes significantly during the time when the majority carriers are traversing the channel, the static expression of the drain current becomes invalid.

There is also a small capacitance in the region between the drain and source formed by the channel and the two terminal regions.[8] There is an additional large gate-to-drain resistance, r_{gd}, that for all practical purposes is an open circuit. The frequency-dependent components are: C_{gs}—gate-to-source capacitance, C_{gd}—gate-to-drain capacitance (sometimes called the overlap capacitance), and C_{ds}—drain-to-source capacitance. Since $C_{gs} \gg C_{ds}$, C_{ds} can usually be ignored.

The frequency dependent effects due to charge storage in JFETs occurs mainly in the two gate junctions. The drain-source capacitance, C_{ds}, is small and therefore does not appreciably affect the high-frequency response of the FET. The two remaining capacitances can be modeled as voltage dependent capacitors with values determined by the following expressions:

$$C_{gs} = \frac{C_{gso}}{\left(1 + \dfrac{|V_{GS}|}{\psi_o}\right)^m} \tag{10.130}$$

$$C_{gd} = \frac{C_{gdo}}{\left(1 + \dfrac{|V_{GD}|}{\psi_o}\right)^m} \tag{10.131}$$

[8] A detailed discussion of the capacitances for the JFET and MOSFET high frequency small signal model is beyond the scope of this book. For more detailed descriptions, the reader is referred to the books (listed as references at the end of this chapter) by M. S. Tyagi, P. R. Gray and R. G. Meyer, and P. Antognetti and G. Massobrio.

where

C_{gso}, C_{gdo}	are the zero-bias gate-source and gate-drain junction capacitances, respectively, in Farads;
V_{GS}, V_{DS}	are the quiescent gate-source and drain-source voltages, respectively;
m	is the gate p-n grading coefficient (SPICE default = 0.5);
ψ_o	is the gate junction (barrier) potential, typically 0.6 V (SPICE default = 1 V).

The frequency dependent elements for the MOSFET can be obtained in the same manner as the JFET. The gate-to-source capacitance C_{gs} is a function of the rate of change of gate charge with respect to the instantaneous gate voltage. The effect of the electrostatic coupling between the gate and the drain can be represented by the incremental gate-to-drain capacitance, C_{gd}. Since both of these capacitances are effected by the gate voltage, the intrinsic capacitance formed by the between the gate, oxide layer, and the channel is of critical interest. The capacitance formed by the oxide layer at the gate is defined as

$$C_{ox} = \frac{\varepsilon_{ox} WL}{t_{ox}} = C'_{ox} WL, \tag{10.132}$$

where

C_{ox}	is the oxide capacitance formed by the gate and channel.
C'_{ox}	is the oxide capacitance per unit area.
ε_{ox}	is the permittivity of the oxide layer (silicon oxide— SiO_2: $3.9\varepsilon_o$).
t_{ox}	is the thickness of the oxide layer (separation between the gate and channel).
W, L	are the width and the length of the channel under the gate, respectively.

The permittivity of vacuum is, $\varepsilon_o = 8.851 \times 10^{-12}$ F/m. The oxide capacitance per unit area can be calculated from physical parameters:

$$C'_{ox} = \frac{1}{\mu}\left(\frac{2I_{DSS}}{V_{PO}^2}\right), \quad \text{for depletion MOSFETs} \tag{10.133a}$$

$$C'_{ox} = \frac{1}{\mu}(2K), \quad \text{for enhancement MOSFETs,} \tag{10.133b}$$

where μ is the charge mobility (typically 600 cm^2/V-s for n-channel, 200 cm^2/V-s for p-channel.

For a MOSFET operating in saturation, the relevant capacitances for the small-signal high-frequency model are,

$$C_{gs} = \frac{2}{3}C_{ox} + C_{gso} W, \tag{10.134}$$

and

$$C_{gd} = C_{gdo} W, \tag{10.135}$$

where C_{gso}, C_{gdo} are the zero bias gate-source and gate drain capacitances, respectively, (typically $C_{gso} = C_{gdo} = 3 \times 10^{-12}$ F/m), and are related to C'_{ox}.

The capacitances in the high-frequency small-signal model of the MOSFET are relatively constant over the frequency range. *Note also that the MOSFET zero bias capacitance has dimensions of F/m and in the JFET, it has units of F.*

Although the values of the components are different, the JFET and MOSFET share the same small-signal model arrangement shown in Figure 10.32.

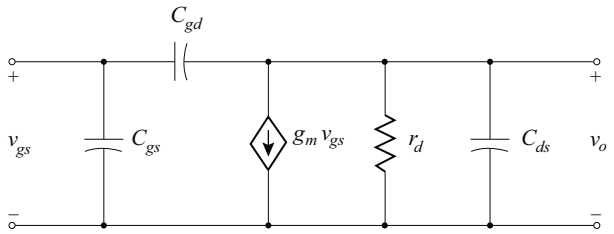

Figure 10.32: Accurate FET high-frequency model.

Since C_{ds} is small compared to C_{gs}, the drain-source capacitance may be ignored in most analysis and design situations, and the simplified model shown in Figure 10.33 may be used.

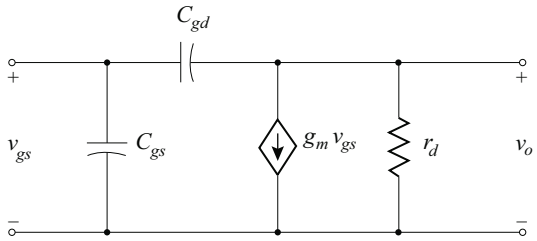

Figure 10.33: Simplified FET High-frequency model.

Circuit parameters, at specific bias conditions, can be obtained from the manufacturers' data sheets. The data is usually provided in terms of *y*-parameters. More specifically, the common-source short-circuit input capacitance C_{iss}, reverse transfer capacitance C_{rss}, and output capacitance, C_{oss} are provided. These manufacturer-specified capacitances are related to the high-frequency small-signal model parameters by the following relationships:

$$C_{gd} \approx C_{rss} \tag{10.136}$$

$$C_{gs} \approx C_{iss} - C_{rss} \tag{10.137}$$

$$C_{ds} \approx C_{oss} - C_{rss}. \tag{10.138}$$

The maximum operating frequency, ω_T, is the frequency at which the FET no longer amplifies the input signal: that is, the dependent current source $g_m v_{gs}$ is equal to the input current.[9] Using an analysis similar to that found in 10.4 to find the BJT maximum operating frequency,

$$\omega_T = \frac{g_m}{(C_{gs} + C_{ds})}. \tag{10.139}$$

In general, BJTs have higher maximum operating frequencies than FETs. Two factors are responsible for the lower frequency performance of FETs compared to BJTs:

- For a given area and operating current, the g_m of silicon FETs is less than half of silicon BJTs.
- In MOSFET structures, considerable capacitance is observed at the input due to the oxide layer. In JFETs, semiconductor properties and physical dimensions of the device result long channel lengths that reduce high-frequency performance.

Example 10.8

Given an enhancement NMOSFET with parameters:

$K = 2.96\,\text{mA/V}^2$, $V_A = 150\,\text{V}$, $V_T = 2\,\text{V}$,
$C_{iss} = 60\,\text{pF}$ at $V_{GS} = 0\,\text{V}$, $C_{oss} = 25\,\text{pF}$ at $V_{GS} = 0\,\text{V}$, $C_{rss} = 5\,\text{pF}$ at $V_{GS} = 0\,\text{V}$,
$W = 30\,\mu\text{m}$, $L = 10\,\mu\text{m}$,
$\mu = 600\,\text{cm}^2/\text{V} - \text{s} = 0.6\,\text{m}^2/\text{V} - \text{s}$.

operating at $I_D = 5\,\text{mA}$.

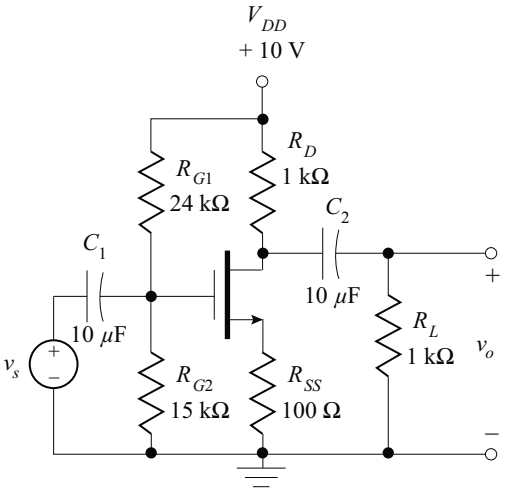

Determine an appropriate small-signal model for the transistor and the ac equivalent of the circuit shown.

[9] The overlap resistance, r_{gd}, and the capacitances, C_{gs} and C_{gd}, allow for the existence of a significant input current at high frequencies.

Solution:

The first step to modeling any FET (or any transistor circuit) is to determine the quiescent conditions. Since this is the same transistor and circuit as Example 5.12 (Book 2), the quiescent conditions have already been determined to be,

$$V_{GS} = 3.3\,\text{V} \quad \text{and} \quad I_D = 5\,\text{mA},$$

operating in the saturation region.

The transconductance is,

$$g_m = 2\sqrt{I_D K} = 2\sqrt{\left(5 \times 10^{-3}\right)\left(2.96 \times 10^{-3}\right)} = 7.7\,\text{mS}.$$

The drain-source resistance of the FET is,

$$r_d = \frac{V_A}{I_D} = \frac{150}{5 \times 10^{-3}} = 30\,\text{k}\Omega.$$

The MOSFET capacitances provided are for zero bias conditions. Therefore, the following zero bias small-signal capacitors can be found:

$$C_{gdo} = C_{rss}/W = 5/W\ \text{pF/m}$$
$$C_{gso} = (C_{iss} - C_{rss})/W = 55/W\ \text{pF/m}.$$

In saturation, the small-signal capacitances are,

$$C_{gs} = \frac{2}{3}\left(\frac{2KWL}{\mu}\right) + C_{gso}W = 1.97 \times 10^{-12} + 55 \times 10^{-12} \approx 57\,\text{pF}$$
$$C_{gd} = C_{gdo}W = 5\,\text{pF}.$$

The complete small-signal model of the circuit is shown below:

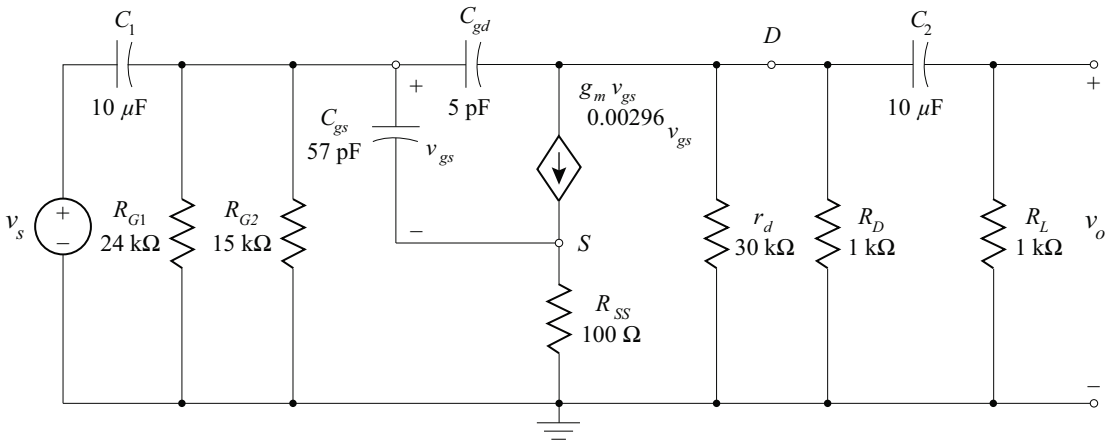

10.8 HIGH-FREQUENCY RESPONSE OF SIMPLE FET AMPLIFIERS

The high-frequency response of simple FET amplifiers is, as with BJT amplifiers, characterized by the amplifier high-frequency pole locations. This section parallels the derivations for BJT amplifier topologies (Section 10.6): the analyses are similar, differing only in the transistor parameter names and typical values. As in all small-signal analysis, transistor quiescent conditions must be first calculated so that the transistor parameters can be accurately determined. In order to focus discussion on pole frequency determination, it is assumed that the quiescent analysis has been previously performed and that the transistor parameters are well-known.

10.8.1 COMMON-SOURCE AMPLIFIER HIGH-FREQUENCY CHARACTERISTICS

A typical common-source amplifier and its high-frequency equivalent, which uses the hybrid-π FET model, are shown in Figure 10.34.

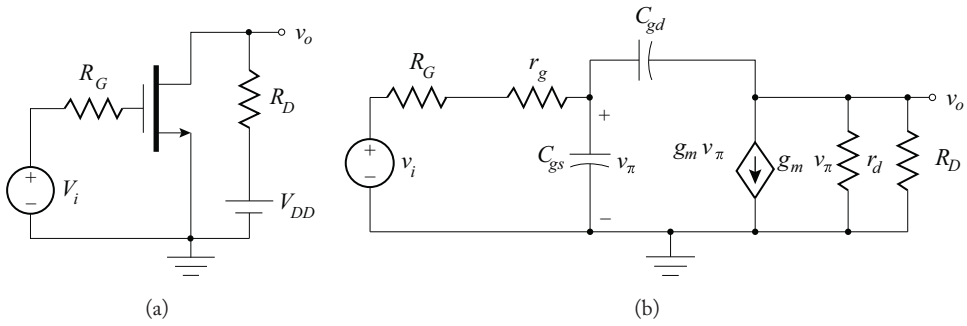

Figure 10.34: Common-source equivalent circuits: (a) Simplified equivalent, (b) High-frequency AC equivalent.

The traditional application of Miller's Theorem to this circuit again reduces the complexity of the analysis. The Miller gain can be approximated as:

$$A = \frac{v_o}{v_\pi} = -g_m\,(r_d // R_D) = -g_m R'_D, \tag{10.140}$$

where R'_D is the equivalent load resistance including the output impedance of the FET:

$$R'_D = r_d // R_D. \tag{10.141}$$

The Miller gain as expressed in Equation (10.140) is a first-order approximation: it is the product of the transconductance, g_m, and the collector *resistance* rather than the collector *impedance*.

This approximate application of Miller's produces first-order approximations to the two pole frequencies. As such, it estimates the lower-frequency, often dominant, pole accurately, but seriously underestimates the higher-frequency pole. An exact, frequency-dependent application of Miller's theorem is presented in the next Section 10.8.3.

Miller's theorem replaces the bridging capacitor, C_{gd}, with equivalent capacitances that shunt the ports of the network (Figure 10.35).

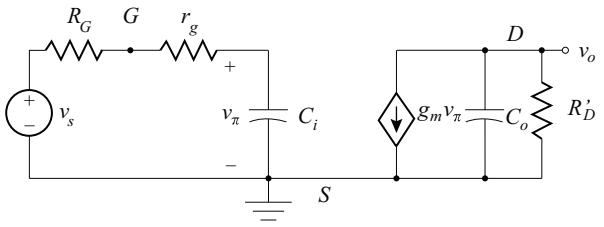

Figure 10.35: Miller's theorem applied to a common-source amplifier.

The input capacitance, C_i, is the parallel combination of C_{gs} and the Miller input capacitance, C_1:

$$C_i = C_{gs} + (1 + g_m R'_D) C_{gd} \tag{10.142}$$

and the output capacitance, C_o, is the Millers output capacitance, C_2:

$$C_o = C_{gd} \left(\frac{1 + g_m R'_D}{g_m R'_D} \right). \tag{10.143}$$

The voltage gain of the circuit is easily determined through typical phasor techniques. In this case, the gain is the product of a voltage division at the input and a current source-impedance product at the output:

$$A_V = \frac{v_o}{v_s} = \left(\frac{v_o}{v_\pi} \right) \left(\frac{v_\pi}{v_s} \right) = \left(\frac{-g_m R'_D}{1 + j\omega C_o R'_D} \right) \left(\frac{1}{1 + j\omega C_i \left(R_G + r_g \right)} \right). \tag{10.144}$$

This gain has two simple poles which, after making the substitution $R'_G = R_G + r_g$, can be shown to be:

$$\omega_{p1} = \frac{1}{C_i \left(R'_G \right)} = \frac{1}{\left[C_{gs} + (1 + g_m R'_D) C_{gd} \right] R'_G} \tag{10.145}$$

and

$$\omega_{p2} = \frac{1}{C_o R'_D} = \frac{1}{C_{gd} \left(\frac{1 + g_m R'_D}{g_m R'_D} \right) R'_D} = \frac{1}{C_{gd} \left(1/g_m + R'_D \right)}. \tag{10.146}$$

Typical circuit element values imply that $\omega_{p1} < \omega_{p2}$, but small signal-source resistance, R_G, may reverse that relationship: both pole locations should always be checked.

10.8.2 EXACT COMMON-SOURCE HIGH-FREQUENCY CHARACTERISTICS

As is the case for the common-emitter amplifier, it has been found that Equations (10.145) and (10.146) accurately estimate the lower-frequency pole, whichever it may be, but underestimate the higher-frequency pole. The frequency dependent application of Miller's Theorem removes the approximations inherent in the traditional application of Miller's Theorem to transistor amplifiers and determines both poles and the zero of the amplifier gain and input impedance exactly.

The Miller voltage gain, $A_M(\omega)$, is given by the product of the output of the voltage-controlled dependent current source, $-g_m$, and the parallel combination of the Miller output capacitance, C_o, and the effective load resistance, $R'_D = r_d // R_D$. As stated above, the Miller gain is given in phasor domain as:

$$A_M(\omega) = \frac{-g_m R'_D}{1 + j\omega R'_D C_o}. \tag{10.147}$$

However, the Miller output capacitance, C_o, is a function of the Miller gain:

$$C_o = \frac{1 - A_M(\omega)}{A_M(\omega)} C_{gd}. \tag{10.148}$$

Solving the above equation pair for the Miller gain, $A_M(\omega)$, yields:

$$A_M(\omega) = \frac{-g_m R'_D \left(1 - j\omega \dfrac{C_{gd}}{g_m}\right)}{1 + j\omega R'_D C_{gd}}. \tag{10.149}$$

The amplifier input capacitance, C_i, now takes on a frequency dependent characteristic:

$$C_i(\omega) = C_{gs} + \left[1 + \frac{g_m R'_D \left(1 - j\omega \dfrac{C_{gd}}{g_m}\right)}{1 + j\omega R'_D C_{gd}}\right] C_{gd}; \tag{10.150}$$

and the input gain can be written as:

$$A_i(\omega) = \frac{\left(1 + j\omega R'_D C_{gd}\right)}{1 + j\omega\left\{R'_G C_{gs} + \left(1 + g_m R'_D\right) R'_G C_{gd} + R'_D C_{gd}\right\} + (j\omega)^2\left\{R'_G R'_D C_{gs} C_{gd}\right\}}. \tag{10.151}$$

When determining the total voltage gain, there is again pole-zero cancellation resulting in:

$$A_V = \frac{(-g_m R'_D)\left[1 - j\omega \dfrac{C_{gd}}{g_m}\right]}{1 + j\omega\left\{R'_G C_{gs} + (1 + g_m R'_D) R'_G C_{gd} + R'_D C_{gd}\right\} + (j\omega)^2\left\{R'_G R'_D C_{gs} C_{gd}\right\}}. \tag{10.152}$$

With resultant approximate pole frequencies:

$$\omega_{p1A} \approx \frac{-1}{R'_G C_{gs} + (1 + g_m R'_D) R'_G C_{gd} + R'_D C_{gd}}, \tag{10.153}$$

and

$$\omega_{p2A} \approx \frac{1}{\omega_{p1A} R'_G R'_D C_{gs} C_{gd}} - \omega_{p1A}.$$

10.8.3 COMMON-DRAIN HIGH-FREQUENCY CHARACTERISTICS

Miller's Theorem can also be applied to common-drain amplifiers. The simplified model of a common-source amplifier and its high-frequency equivalent, using the hybrid-π FET model, are shown in Figure 10.27. The capacitor, C_{gs}, bridges the input and output terminals of the amplifier. Miller's theorem replaces this bridging capacitance with equivalent capacitancess shunting the input and output ports of the network (Figure 10.37). For simplicity of notation, the substitution $R'_S = r_d // R_S$ has been made.

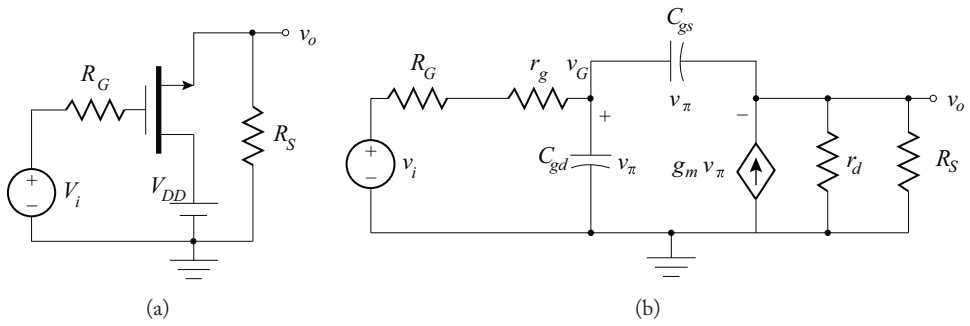

Figure 10.36: Common-drain equivalent circuits: (a) Simplified equivalent, (b) High-frequency AC equivalent.

For this circuit, the Miller voltage gain is defined as:

$$A_M(\omega) = \frac{v_o}{v_G}. \tag{10.154}$$

The Miller gain can be directly determined to be:

$$A_M(\omega) = \frac{R'_S}{R'_S + R_m} \frac{1 + j\omega R_m C_{gs}}{1 + j\omega (R_m // R'_S) C_{gs}}, \tag{10.155}$$

where

$$R_m = 1/g_m \quad \text{and} \quad R'_G = R_G + r_g.$$

The total amplifier voltage gain can then be written as the product of the input gain and the Miller gain:

$$A_V(\omega) = \frac{v_o}{v_i} = \left(\frac{v_B}{v_i}\right)\left(\frac{v_o}{v_B}\right) = A_i(\omega) A_M(\omega). \tag{10.156}$$

The derivation of $A_V(\omega)$ follows that of Section 10.6.3 and results in a voltage gain with a zero at

$$\omega_{zF} = \frac{-g_m}{C_\pi}, \tag{10.157}$$

and poles at

$$\omega_{p1F} = \frac{-(1 + g_m R'_S)}{(R'_G + R'_S) C_{gs} + R'_G [1 + g_m R'_S] C_{gd}},$$

and (10.158)

$$\omega_{p2F} \approx \frac{-b}{a} + \frac{1}{b} = -\frac{(R'_G + R'_S) C_{gs} + R'_G [1_\pi + g_m R'_S] C_{gd}}{R'_G R'_S C_\pi C_\mu} - \omega_{p1F}.$$

As is the case for common-collector amplifiers, the zero for common-drain amplifiers lies, in frequency, between the two poles, it is therefore typical to model a common-drain amplifier as a single-pole amplifier using ω_{p1A} as the pole frequency:

10.8.4 COMMON-GATE HIGH-FREQUENCY CHARACTERISTICS

The midband AC model of typical common gate amplifier and its high-frequency equivalent are shown in Figure 10.37.

Common gate amplifiers are similar to common-base amplifiers in that they do not suffer from performance reducing Miller effects. The bridging resistance, r_d, does present problems in the analysis of the circuit. One method of analysis that brings results fairly quickly for the common-base circuit is the node-voltage method. At the drain node of the FET, Kirchhoff's current law is applied:

$$v_o G_d + v_o(j\omega C_{gd}) + g_m v_{gs} + (v_o + v_{gs}) g_d = 0. \tag{10.159}$$

The shorthand notation of replacing inverse resistance with conductance (signified by the letter "g" with the appropriate subscript) has been used to simplify analytic representation. At the source

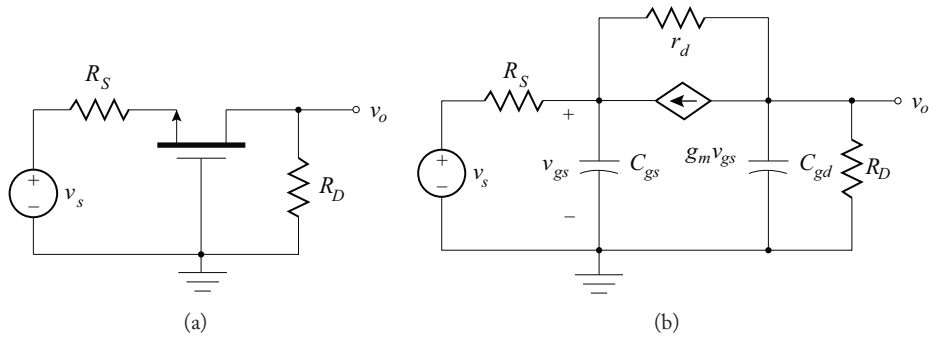

Figure 10.37: Common gate equivalent circuits: (a) Midband AC equivalent, (b) High frequency equivalent.

node of the FET a similar operation is performed:

$$(v_s + v_{gs})G_s + v_{gs}(j\omega C_{gs}) + g_m v_{gs} + (v_o + v_{gs})g_d = 0. \tag{10.160}$$

These two nodal equations are combined (eliminating v_{gs}) to form the gain expression for the common gate amplifier:

$$A_V = \frac{v_o}{v_s} = \frac{G_s}{\left(\dfrac{G_d + g_d + j\omega C_{gd}}{g_m + g_d}\right)(G_s + g_m + j\omega C_{gs}) - g_d}. \tag{10.161}$$

In this gain expression, it should be noted that the output resistance of the FET, r_d, is typically much larger than the circuit resistors R_s and R_d (as well as the inverse of g_m). It is therefore reasonable to approximate the gain expression of Equation (10.157) by ignoring the small negative term in the denominator:

$$A_V \approx \frac{G_s\,(g_m + g_d)}{(G_d + g_d + j\omega C_{gd})(G_s + g_m + j\omega C_{gs})}. \tag{10.162}$$

This approximate gain expression for the common gate amplifier has poles at:

$$\omega_{p1} = \frac{R_s}{C_{gs}\,(1 + g_m R_s)}, \quad \text{and} \quad \omega_{p2} = \frac{1}{C_{gd}\,(r_d \,//\, R_d)}. \tag{10.163}$$

These two poles are at very high frequencies: as with the common-base amplifier, the common gate amplifier is not usually the frequency limiting element in a multistage amplifier.

10.8.5 COMMON-SOURCE WITH SOURCE DEGENERATION ($CS + Rs$) CHARACTERISTICS

Common-source amplifiers with source degeneration are analyzed in the same fashion as common-emitter amplifiers with the exception that a different hybrid-π model is used for the field effect transistor. An amplifier of this topology driven by Thévenin sources is shown in Figure 10.38a and its high-frequency ac equivalent is shown in Figure 10.38b. While a depletion-mode n-channel FET is shown, the analysis is the same for all types of FET.

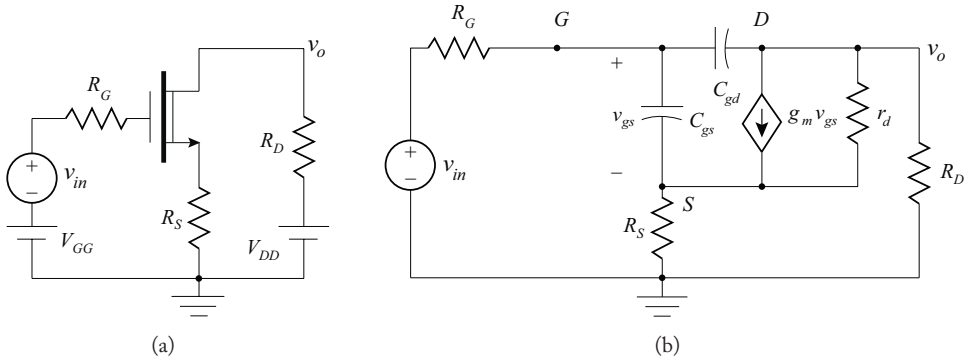

Figure 10.38: Common source equivalent circuits. (a) Driven by Thévenin souces (b) High-frequency equivalent.

The application of Kirchhoff's current law at the nodes G, S, and D respectively, produces the following set of equations that can be solved simultaneously in order to determine the frequency response:

$$\begin{aligned}
&\frac{v_{in} - v_g}{R_G} + (v_s - v_g)\, s\, C_{gs} + (v_o - v_g)\, s\, C_{gd} = 0 \\
&(v_g - v_s)\, s\, C_{gs} + g_m (v_g - v_s) + \frac{v_o - v_s}{r_d} - \frac{v_s}{R_S} = 0 \\
&(v_g - v_o)\, s\, C_{gd} - g_m (v_g - v_s) + \frac{v_s - v_o}{r_d} - \frac{v_o}{R_D} = 0.
\end{aligned} \tag{10.164}$$

The exact symbolic solution for the voltage gain, $A_V = v_o/v_s$, to this set of simultaneous equations take the form of the quotient of two second-order polynomials in s:

$$A_V = \frac{v_o}{v_s} = \frac{a_z s^2 + b_z s + c_z}{a_p s^2 + b_p s + c_p}, \tag{10.165}$$

where the denominator polynomial constants are:

$$\begin{aligned} a_p &= (R_G R_D + R_G R_S + R_D R_S)\, r_d C_{gs} C_{gd} \\ b_p &= [(1 + g_m r_d)(R_G R_D + R_G R_S + R_D R_S) + r_d (R_D + R_G)]\, C_{gd} \\ &\quad + [R_G R_D + R_G R_S + R_D R_S + r_d (R_G + R_S)]\, C_{gs} \\ c_p &= R_D + r_d + (1 + g_m r_d) R_S, \end{aligned} \tag{10.166}$$

and the numerator polynomial constants are:

$$\begin{aligned} a_z &= r_d R_D R_S C_{gs} C_{gd} \\ b_z &= [(1 + g_m r_d) R_D R_S + r_d R_D]\, C_{gd} + R_D R_S C_{gs} \\ c_z &= -g_m r_d R_D. \end{aligned} \tag{10.167}$$

Exact pole and zero expressions can be found through the quadratic formula. As is the case with common-emitter amplifiers, common-source amplifiers with source degeneration are typically modeled by a single-pole. The complexity of the first pole expression can be similarly simplified so that the approximate 3-dB frequency is given by:

$$\omega_{3\text{dB}} \approx \frac{[R_D + r_d + (1 + g_m r_d) R_S]}{[(1 + g_m r_d)(R_G R_D + R_G R_S + R_D R_S)]\, C_{gd} + [R_G R_D + R_G R_S + R_D R_S + r_d (R_G + R_S)]\, C_{gs}}. \tag{10.168}$$

In this new expression for high 3-dB frequency, the Miller effect is again evident in the multiplication of C_{gd} as is the widening of the amplifier bandwidth with feedback (by increasing R_S).

A summary of all derived FET amplifier high-frequency poles is given in Table 10.3.

Table 10.3: Summary of FET amplifier high-frequency pole locations

Amplifier Type	*Pole Locations (rad/s.)*
Common-source (single pole) (use the smaller)	$\dfrac{1}{\left[C_{gs}+\left(1+g_m R'_{\mathrm{D}}\right)C_{gd}\right]R'_{\mathrm{G}}}$ *or* $\dfrac{1}{\left\{1/g_m + R'_{\mathrm{D}}\right\}C_{gd}}$
Common-source (two poles)	$\omega_{\mathrm{p1A}} = \dfrac{-1}{R'_{\mathrm{G}}C_{gs}+\left(1+g_m R'_{\mathrm{D}}\right)R'_{\mathrm{G}}C_{gd}+R'_{\mathrm{D}}C_{gd}}$, $\dfrac{1}{\omega_{\mathrm{p1A}}R'_{\mathrm{G}}R'_{\mathrm{D}}C_{gs}C_{gd}} - \omega_{\mathrm{p1A}}$
Common-source with source degeneration	$\dfrac{\left[R_{\mathrm{D}} + r_d + \left(1 + g_m r_d\right)R_{\mathrm{S}}\right]}{\left[\left(1+g_m r_d\right)\left(R_3 R\right)\right]C_{gd} + \left[R_3 R + r_d\left(R_{\mathrm{G}} + R_{\mathrm{S}}\right)\right]C_{gs}}$ where $R_3 R = R_{\mathrm{G}}R_{\mathrm{D}} + R_{\mathrm{G}}R_{\mathrm{S}} + R_{\mathrm{D}}R_{\mathrm{S}}$
Common-drain	$\dfrac{\left(1+g_m R'_{\mathrm{S}}\right)}{\left(R'_{\mathrm{G}}+R'_{\mathrm{S}}\right)C_{gs}+R'_{\mathrm{G}}\left[1+g_m R'_{\mathrm{S}}\right]C_{gd}}$
Common-gate	$\dfrac{R_{\mathrm{S}}}{C_{gs}\left(1+g_m R_{\mathrm{S}}\right)}$, $\dfrac{1}{C_{gd}R'_{\mathrm{D}}}$

Note: $R'_{\mathrm{G}} = R_{\mathrm{G}} + r_g$, $R'_{\mathrm{D}} = r_d // R_{\mathrm{D}}$, and $R'_{\mathrm{S}} = r_d // R_{\mathrm{S}}$

Example 10.9

Determine the high frequency poles for the amplifier shown.

The JFET parameters are:

$I_{DSS} = 6\,\mathrm{mA}$, $V_{PO} = -4.7\,\mathrm{V}$,
$V_A = 100\,\mathrm{V}$,
$C_{iss} = 4.5\,\mathrm{pF}$ at $V_{GS} = 0$,
$C_{rss} = 1.5\,\mathrm{pF}$ at $V_{GS} = 0$.

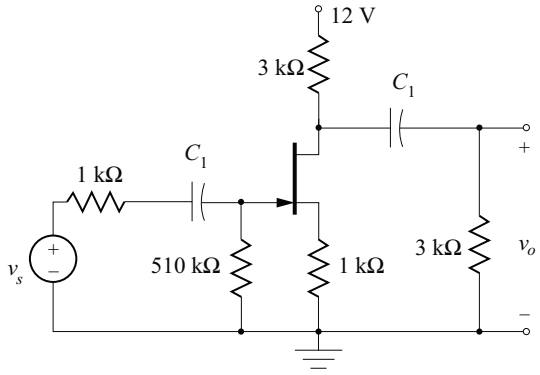

Solution:

Find the quiescent conditions to determine if the JFET is in the saturation region: that is, the bias condition must fulfill the following criteria:

$$V_{DS} \geq V_{GS} - V_{PO}.$$

Solve for V_{GS} by finding the voltage across R_S. The drain current, I_D, is

$$I_D = I_{DSS}\left(1 - \frac{V_{GS}}{V_{PO}}\right)^2 = I_{DSS}\left(1 - \frac{(V_G - V_S)}{V_{PO}}\right).$$

Substituting $V_G = 0$ and $V_S = I_D R_S$ in to the equation for the drain current above,

$$I_D = I_{DSS}\left(1 + \frac{I_D R_S}{V_{PO}}\right)^2.$$

Solving for I_D in the second order equation above yields $I_D = 2\,\text{mA}$. Therefore,

$$V_{GS} = V_G - V_S = 0 - I_D R_S = -0.002(1000) = -2\,\text{V}.$$

The condition for operation in the saturation is confirmed:

$$V_{DS} \geq V_{GS} - V_{PO} \quad \text{or} \quad 4 \geq -2 - (-4.7) = 2.7.$$

The small-signal parameters for the JFET are:

$$g_m = \frac{-2I_D}{(V_{PO} - V_{GS})} = \frac{-0.002}{(-4.7 - (-2))} = 1.48\,\text{mS},$$

and

$$r_d = \frac{V_A}{I_D} = \frac{100}{0.002} = 50\,\text{k}\Omega.$$

The zero bias small-signal capacitors are:

$$C_{gso} \approx C_{iss} - C_{rss} = 4.5\,\text{pF} - 1.5\,\text{pF} = 3\,\text{pF}$$
$$C_{gdo} \approx C_{rss} = 1.5\,\text{pF}.$$

The small-signal capacitors at the quiescent point are:

$$C_{gs} = \frac{C_{gso}}{\sqrt{1 + \dfrac{|V_{GS}|}{\psi_o}}} = \frac{3 \times 10^{-12}}{\sqrt{1 + \dfrac{2}{0.6}}} = 1.44\ \text{pF}$$
$$C_{gd} = \frac{C_{gdo}}{\sqrt{1 + \dfrac{|V_{GD}|}{\psi_o}}} = \frac{1.5 \times 10^{-12}}{\sqrt{1 + \dfrac{6}{0.6}}} = 0.452\,\text{pF}.$$

Substituting values in to the previously derived mathematical expressions for the poles of a common source with source degeneration amplifier yields:

$$\omega_{3\text{dB}} \approx \frac{[R_D + r_d + (1 + g_m r_d)\, R_S]}{[(1 + g_m r_d)\,(R_G R_D + R_G R_S + R_D R_S)]\, C_{gd} + [R_G R_D + R_G R_S + R_D R_S + r_d\,(R_G + R_S)]\, C_{gs}}$$
$$= 443.8\,\text{Mrad/sec}(70.6\text{MHz}).$$

10.9 MULTISTAGE AMPLIFIERS

Multistage amplifier frequency domain analysis is a combination of techniques shown in the previous sections of this chapter and the analysis and design techniques shown in Chapter 6 (Book 2). The important concepts from Chapter 6 (Book 2) and the previous sections of this chapter that will be used for multistage amplifier analysis are:

- The total voltage gain of a cascade-connected amplifier can be expressed as a product of gains of the individual stages and simple voltage divisions.
- Each stage presents a load to the previous stage: its input resistance is part of the total load that is apparent to the previous stage.
- The total input resistance or total output resistance may be modified by the interaction of individual stages.

The analysis procedure used for designing multistage amplifiers is:

- Perform midband gain analysis of the total circuit and of each stage taking into account the load presented by the input resistance of the next stage.
- Perform low-frequency analysis of the circuit. In most cases, careful application of the time constant approach will yield a good approximation of the low cutoff frequency.
- Perform high-frequency analysis using the high-frequency model of the circuit. When appropriate, use Miller's theorem to create a Miller's equivalent circuit of the amplifier. In most cases, the high-frequency output capacitance of the Miller's equivalent model may be ignored since the pole associated with the output capacitance is significantly higher than the pole for the Miller's equivalent input capacitance. This greatly simplifies analysis and design without sacrificing a great deal of accuracy.

The analysis of multistage amplifier high-frequency response is greatly simplified by assuming non-interacting capacitances in the high-frequency model. This assumption is particularly important when determining the gain of an amplifier stage loaded by the input impedance of a following stage: often a complex impedance. That impedance is evaluated at midband frequencies, thus eliminating the reactive component from the analysis. Using this assumption, the input impedance of the amplifier stage at the output of the stage under consideration presents a purely resistive load.

10.9.1 CAPACITOR COUPLING BETWEEN STAGES

A common method found in multistage amplifier design makes use of coupling capacitors between stages. This method has the advantage that the bias condition of each stage is unaffected by the others. The disadvantage is the potential degradation in amplifier low-frequency response: that is, the low cutoff frequency may increase without careful selection of capacitor values. Additionally, the use of coupling capacitors between stages does not lend itself to integrated circuit implementations of the circuit since large capacitors require large areas, or "real estate,"[10] on the chip.

Figure 10.39 depicts a two stage common-emitter cascaded amplifier.
The AC model of the circuit is shown in Figure 10.40. Note that parallel resistors are replaced by their equivalent: $R_{B1} = R_{B11}//R_{B21}$ and $R_{B2} = R_{B21}//R_{B22}$.

The midband gain of the circuit has been previously determined in Example 6.1 (Book 2). While it is possible to recast the gain expressions using hybrid-π parameters, using h-parameter expressions is equivalently valid. The midband gain has been determined to be:

$$A_{Vm} = \left(\frac{v_o}{v_s}\right) = \left(\frac{v_{b1}}{v_s}\right)\left(\frac{v_{b2}}{v_{b1}}\right)\left(\frac{v_o}{v_{b2}}\right), \tag{10.169}$$

[10]Area on integrated circuits are sometimes referred to as "real estate" since a chip may be designed with a near capacity of number of components, and space may not be available.

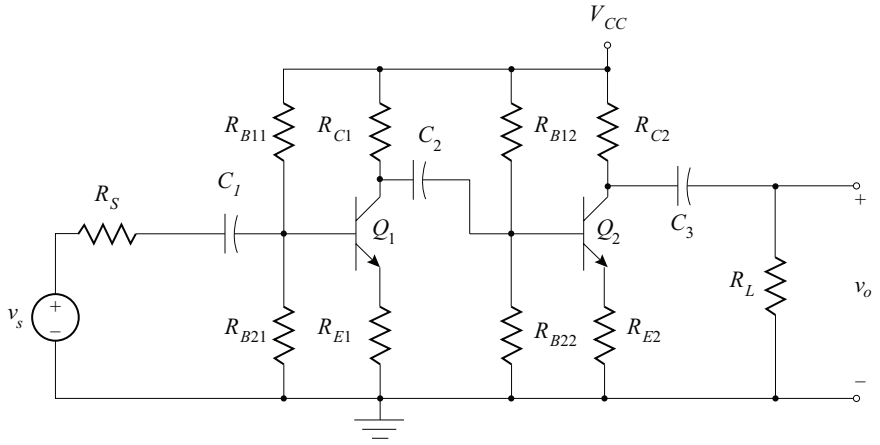

Figure 10.39: Two-stage common-emitter cascaded amplifier.

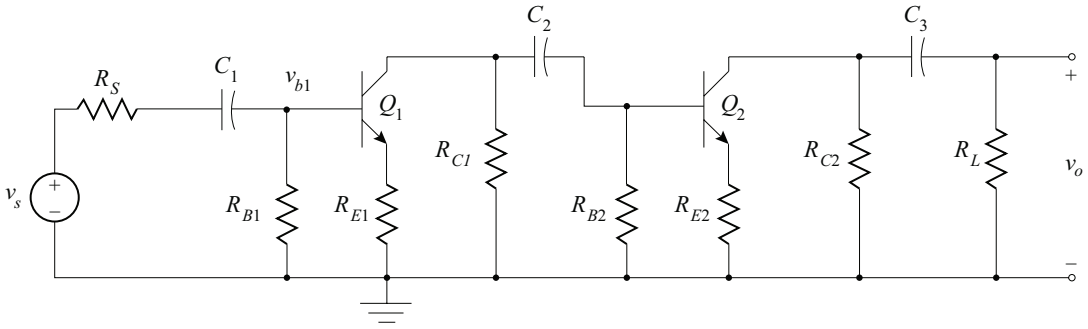

Figure 10.40: AC model of Figure 10.39.

where

$$\frac{v_{i1}}{v_s} = \frac{R_{i1}}{R_{i1} + R_S}, \tag{10.170}$$

$$\frac{v_{o1}}{v_{i1}} = -\frac{h_{fe1}\left[(R_{C1} // R_{B2}) // R_{i2}\right]}{h_{ie1} + \left(1 + h_{fe1}\right) R_{E1}}, \tag{10.171}$$

$$\frac{v_o}{v_{o1}} = -\frac{h_{fe}\left(R_{C2} // R_L\right)}{R_{i2}}, \tag{10.172}$$

where

$$R_{i1} = h_{ie1} + \left(1 + h_{fe1}\right) R_{E1} \quad \text{and} \quad R_{i2} = h_{ie2} + \left(1 + h_{fe2}\right) R_{E2}.$$

The low cutoff frequency is found by using the equations derived in Section 10.6 setting all high-frequency transistor capacitors as open circuits and following the time constant analysis of Section 10.3. The low-frequency poles of the amplifier in Figure 10.39 are:

$$\omega_{L1} = \frac{1}{C_1 \left\{R_S + \left[R_{B1} \,//\, \left(h_{ie1} + \left(1 + h_{fe1}\right) R_{E1}\right)\right]\right\}}, \tag{10.173}$$

$$\omega_{L2} = \frac{1}{C_2 \left[R_{C1} + \left(R_{B2} \,//\, R_{i2}\right)\right]}, \tag{10.174}$$

$$\omega_{L3} = \frac{1}{C_3 \left(R_{C2} + R_L\right)}. \tag{10.175}$$

The high cutoff frequency is found using the equations summarized in Table 10.2 for each stage, using the applicable transistor parameters and circuit element values. For this particular circuit, both stages are common-emitter with emitter degeneration stages. In determining the correct values for the resistances in the expressions, total Thévenin resistances at the amplifier terminal must be used.

For the first stage, the appropriate resistances are:

$$\begin{aligned} R'_s &= r_{b_1} + R_S // R_{B1} \\ R_c &= R_{C1} // R_{B2} // R_{i2} \\ R_E &= R_{E1}. \end{aligned} \tag{10.176a}$$

For the second stage, the resistances are:

$$\begin{aligned} R'_s &= r_{b2} + R_{c1} // R_{B2} \\ R_c &= R_{C2} // R_L \\ R_e &= R_{E2}. \end{aligned} \tag{10.176b}$$

Example 10.10

The two stage cascade connected amplifier of Example 6.1 (Book 2) is shown. The two silicon BJTs have characteristic parameters:

$$h_{fe} \approx \beta_F = 150, \quad r_b = 30\,\Omega, \quad V_A = 350.$$
$$C_{\mu 1} = C_{\mu 2} = 3\,\text{pF},$$
$$\omega_{T1} = \omega_{T2} = 2\pi(400)\,\text{Mrad/s}.$$

Determine the low and high cutoff frequencies of the circuit.

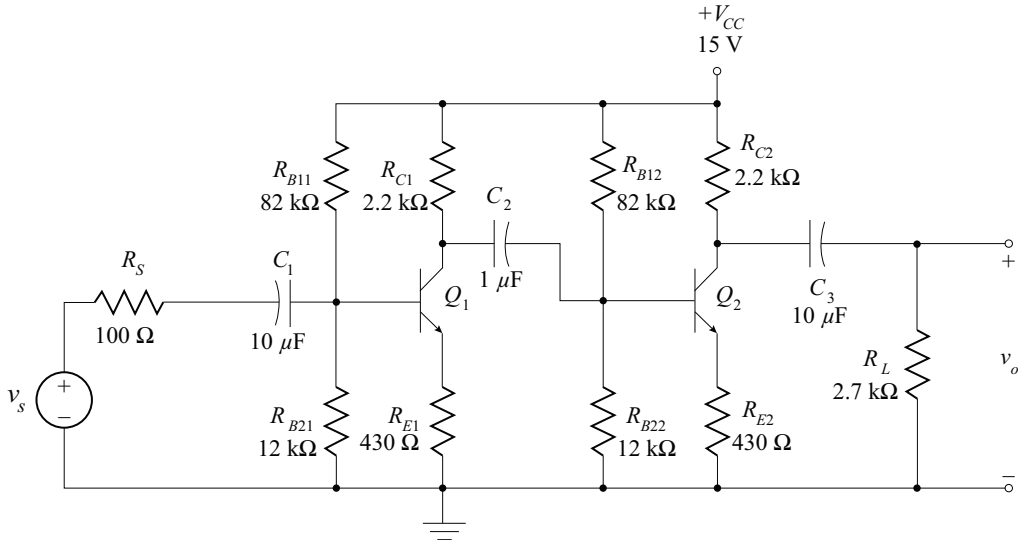

Solution:

The determination of the multistage amplifier performance follows the same basic steps that were derived in Chapter 6 (Book 2):

1. Model the transistors with the appropriate DC model.
2. Determine the circuit quiescent conditions. Verify forward-active region for BJTs or saturation region for FETs.
3. Determine transistor AC parameters from quiescent conditions.
4. Create AC equivalent circuit.
5. Determine the midband performance of each amplifier stage by:
   (a) replacing the transistors by their respective AC models, or
   (b) using previously derived results for the circuit topology.
6. Combine stage performance quantities to obtain total midband gain.
7. Perform low-frequency analysis to determine the low cutoff frequency using the small signal AC model with all internal (high-frequency) capacitors open circuited.
8. Perform high-frequency analysis to determine the high cutoff frequency using the small signal AC model including the internal (high-frequency) capacitors and short circuiting all external (coupling and bypass) capacitors.

9. Combine results of DC, midband, low-frequency and high-frequency analysis to obtain total circuit performance.

The DC analysis was performed in Example 6.1 (Book 2) and the result for both collector currents and collector-emitter voltages are:

$$I_C = 2.427\,\text{mA} \quad \text{and} \quad V_{CE} = 8.64\,\text{V}.$$

The quiescent conditions lead to $h_{ie} = 1.624\,\text{k}\Omega$.

The hybrid-π small signal parameters are:

$$r_{\pi 1} = r_{\pi 2} = h_{ie} - r_b = 1.624\,\text{k} - 30 = 1.594\,\text{k}\Omega$$
$$g_{m1} = g_{m2} = g_m = \frac{\beta_F}{r_\pi} = \frac{150}{1594} = 94.1\,\text{mS}$$
$$C_{\pi 1} = C_{\pi 2} = \frac{g_m}{\omega_T} - C_\mu = \frac{0.0941}{2\pi\left(400 \times 10^3\right)} - 3 \times 10^{-12} = 34.4\,\text{pF}.$$

The AC model of the circuit is shown below:

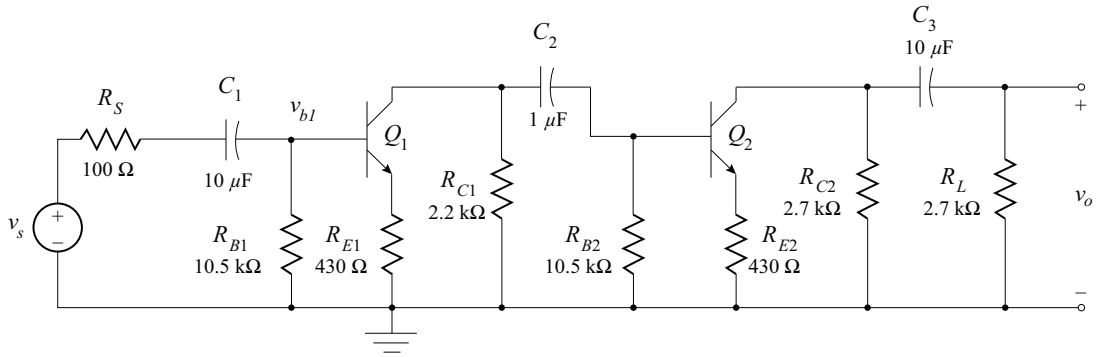

Where $R_{B1} = R_{B11} // R_{B21}$ and $R_{B2} = R_{B12} // R_{B22}$. Since V_A is very large, the output resistance, h_{oe}^{-1}, is very large and can be approximated as an infinite resistance.

The low-frequency poles are:

$$\omega_{L1} = \frac{1}{C_1\left\{R_S + \left[R_{B1} // \left(h_{ie1} + \left(1 + h_{fe1}\right) R_{E1}\right)\right]\right\}} \Rightarrow 10.9\,\text{rad/s} = 1.74\,\text{Hz}$$
$$\omega_{L2} = \frac{1}{C_2\left[R_{C1} + \left(R_{B2} // R_{i2}\right)\right]} = 88.9\,\text{rad/s} \Rightarrow 14.2\,\text{Hz}$$
$$\omega_{L3} = \frac{1}{C_3\left(R_{C2} + R_L\right)} = 20.4\,\text{rad/s} \Rightarrow 3.25\,\text{Hz}.$$

The high-frequency poles for the common-emitter with emitter degeneration stages are found using Table 10.2 with applicable circuit element values.

For the first stage, those resistances are:

$$R'_s = r_{b1} + R_S//R_{B1} = 30 + 100//10.5\,\text{k} = 226\,\Omega$$
$$R_c = R_{C1}//R_{B2}//R_{i2} = 2.2\,\text{k}//10.5\,\text{k}//(1.62\,\text{k} + 151 \times 430) = 1.77\,\text{k}\Omega$$
$$R_e = R_{E1} = 430\,\Omega.$$

For the second stage, the resistances are:

$$R'_s = r_{b1} + R_{c1}//R_{B2} = 1.889\,\text{k}\Omega$$
$$R_c = R_{C2}//R_L = 1.212\,\text{k}\Omega$$
$$R_e = R_{E2} = 430\,\Omega.$$

The single high-frequency pole approximations for each stage are then calculated as:

$$\omega_{H1} = 108\,\text{Mrad/s} \quad \Rightarrow \quad 17.3\,\text{MHz}$$
$$\omega_{H2} = 39.1\,\text{Mrad/s} \quad \Rightarrow \quad 6.22\,\text{MHz},$$

ω_{L2} is the dominant low-frequency pole. The lower 3-dB frequency is 14.2 Hz.

The high frequency poles are separated by a factor of $k = 2.78$ thus the high 3-dB frequency is computed as described in Section 10.2.2:

$$f_H = 6.22\,\text{MHz}\sqrt{\frac{-(1+k^2) + \sqrt{(1+k^2)^2 + 4k^2}}{2}} = 5.59\,\text{MHz}$$

10.9.2 DC (DIRECT) COUPLING BETWEEN STAGES

In Example 10.10, the coupling capacitor between the two stages established the dominant low-frequency pole, and therefore the low cutoff frequency. The effect of coupling capacitors between amplifier stages on the low-frequency response can be eliminated by DC coupling the stages. The midband analysis of a DC (or direct) coupled two-stage common source—common-collector amplifier (Figure 10.42) was shown in Example 6.2 (Book 2).

The analysis of the midband gain, low cutoff frequency, and high cutoff frequency are found in the manner as the capacitor-coupled amplifiers. Following the analysis of the capacitor coupled multistage amplifier, and the results in Sections 10.6 and 10.8, the midband gain of the direct coupled common source—common-collector amplifier is,

$$A_{Vm} = \frac{v_o}{v_s} = -\left(\frac{R_{G1}}{R_{G1} + R_{OS}}\right)\frac{g_{m1}r_d\,(R_{D1}//R_{i2})}{[r_d + (R_{D1}//R_{i2}) + (1+\mu)\,R_{S1}]}\left[\frac{R_{i2} - (h_{ie})}{R_{i2}}\right] \quad (10.177)$$

where

$$R_{i2} = h_{ie} + (1 + h_{fe})\,(R_{E2}//R_L).$$

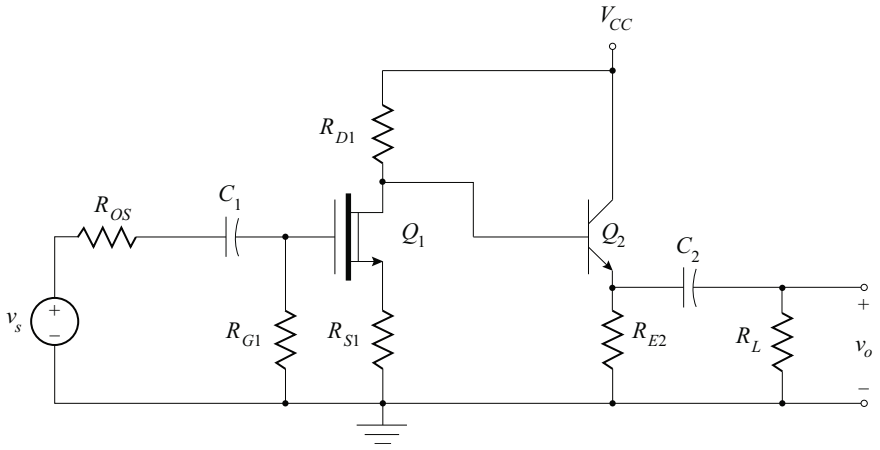

Figure 10.41: DC (Direct) coupled two-stage amplifier.

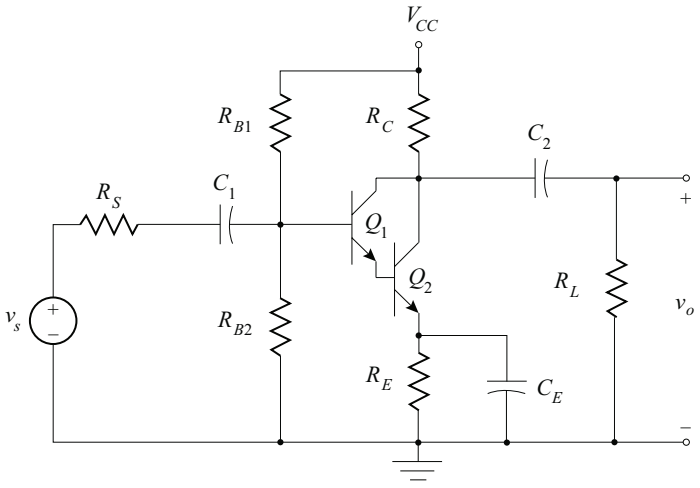

Figure 10.42: Common-emitter amplifier using Darlington pair.

The low-frequency poles are calculated from the product of the resistive discharge paths, calculated using Thévenin equivalent resistances, and the external capacitors:

$$\omega_{l1} = \frac{1}{C_1 \left(R_{OS} + R_G\right)} \tag{10.178}$$

$$\omega_{l2} = \frac{1}{C_2 \left\{R_L + \left[R_{E2} \,//\, \frac{h_{ie} + r_d + \left(1 + g_{m1} r_d\right) R_{S1}}{1 + h_{fe}}\right]\right\}}. \tag{10.179}$$

The high-frequency poles are found by applying Equation from Table 10.3 for the common source stage and Table 10.1 for the common-collector stage. The appropriate circuit element calculations for this circuit are:

Common source with source degeneration stage:

$$\begin{aligned} R_D &= R_{D1}//R_{i2} \\ R_S &= R_{S1} \\ R_G &= R_{OS}//R_{G1}. \end{aligned} \tag{10.180}$$

Common collector stage

$$\begin{aligned} R'_s &= r_b + R_{D1}//Ro1 \\ R'_e &\approx R_{E2}//R_L. \end{aligned} \tag{10.181}$$

Each stage will, in this case, provide a single pole. The total amplifier high 3-dB frequency is determined by appropriately combining those two poles.

10.9.3 DARLINGTON PAIR

The frequency response of amplifiers using the Darlington pairs can be found using the techniques developed thus far in this chapter. Figure 10.42 is a common-emitter amplifier using the dual common-collector composite transistor.

The complete hybrid-π small signal equivalent is shown in Figure 10.43. The analysis of this amplifier follow techniques developed in this chapter. The midband gain is found by treating all external (bypass and coupling) capacitors as short circuits and all high-frequency capacitors as open circuits. The gain expression is a little different than those that have been derived thus far. The midband gain has additive terms because the two dependent current sources, $g_{m1}v_{\pi 1}$ and $g_{m2}v_{\pi 2}$, add to yield the amplifier output current. The midband gain of the amplifier is,

$$A_{Vm} = -\left(\frac{v_{i1}}{v_s}\right)(g_{m1}v_{\pi 1} + g_{m2}v_{\pi 2})\,R_O, \tag{10.182}$$

where

$$\begin{aligned} R_O &= R_C//R_L \quad \text{for midband and high-frequency analysis,} \\ R_B &= R_{B1}//R_{B2}, \end{aligned}$$

and

$$\frac{v_{i1}}{v_s} = \frac{R_B}{R_B + R_S}.$$

The controlling voltages for the dependent current sources are,

$$v_{\pi 1} = \frac{v_{i1}r_{\pi 1}}{r_{b1} + (1 + g_{m1}r_{\pi 1})\,(r_{b2} + r_{\pi 2})}, \tag{10.183}$$

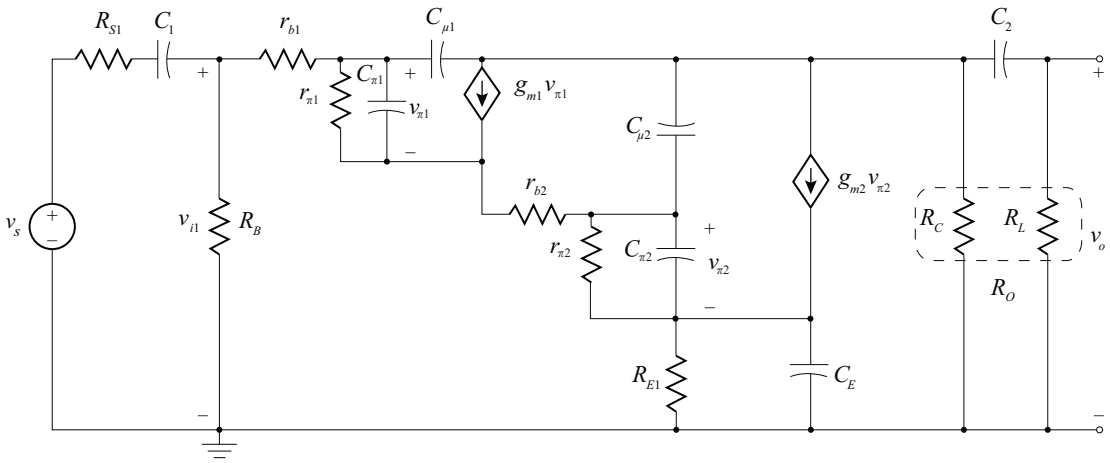

Figure 10.43: All-frequency hybrid-π small signal model of Figure 10.42.

and

$$v_{\pi 2} = \frac{v_{i1} r_{\pi 2} (1 + g_{m1} r_{\pi 1})}{r_{b1} + r_{\pi 1} + (1 + g_{m1} r_{\pi 1}) (r_{b2} + r_{\pi 2})}. \tag{10.184}$$

The complete expression for the midband gain is found by substituting Equations (10.183) and (10.184) into (10.182),

$$A_{vm} = -\frac{R_B R_O}{R_B + R_S} \left(\frac{g_{m1} r_{\pi 1}}{r_{b1} + (1 + g_{m1} r_{\pi 1}) (r_{b2} + r_{\pi 2})} + \frac{g_{m2} r_{\pi 2} (1 + g_{m1} r_{\pi 1})}{r_{b1} + r_{\pi 1} + (1 + g_{m1} r_{\pi 1}) (r_{b2} + r_{\pi 2})} \right). \tag{10.185}$$

The high-frequency model is simplified using Miller's theorem to yield the high-frequency Miller's equivalent small signal model shown in Figure 10.44. The high-frequency Miller's equivalent output capacitances since the poles associated with these capacitances are not dominant. The pole locations are found by determining the input impedance, Z_i in Figure 10.44,

$$\begin{aligned} Z_i &= r_{b1} + \left(r_{\pi 1} \parallel \frac{1}{j\omega C_{i1}} \right) + (1 + g_{m1}) \left[r_{b2} + \left(r_{\pi 2} \parallel \frac{1}{j\omega C_{i2}} \right) \right] \\ &= \frac{\left[r_{b1} \left(\frac{1}{r_{\pi 1} C_{i1}} + j\omega \right) + \frac{r_{\pi 1}}{r_{\pi 1} C_{i1}} \right] \left(\frac{1}{r_{\pi 2} C_{i2}} + j\omega \right) + (1 + g_{m1} r_{\pi 1}) \left[r_{b2} \left(\frac{1}{r_{\pi 2} C_{i2}} + j\omega \right) + \frac{r_{\pi 2}}{r_{\pi 2} C_{i2}} \right] \left(\frac{1}{r_{\pi 1} C_{i1}} + j\omega \right)}{\left(\frac{1}{r_{\pi 2} C_{i2}} + j\omega \right) \left(\frac{1}{r_{\pi 1} C_{i1}} + j\omega \right)}. \end{aligned} \tag{10.186}$$

From Equation (10.186), the pole locations of the Darlington circuit in Figure 10.42 are,

$$\frac{1}{r_{\pi 1} C_{i1}} \quad \text{and} \quad \frac{1}{r_{\pi 2} C_{i2}}. \tag{10.187}$$

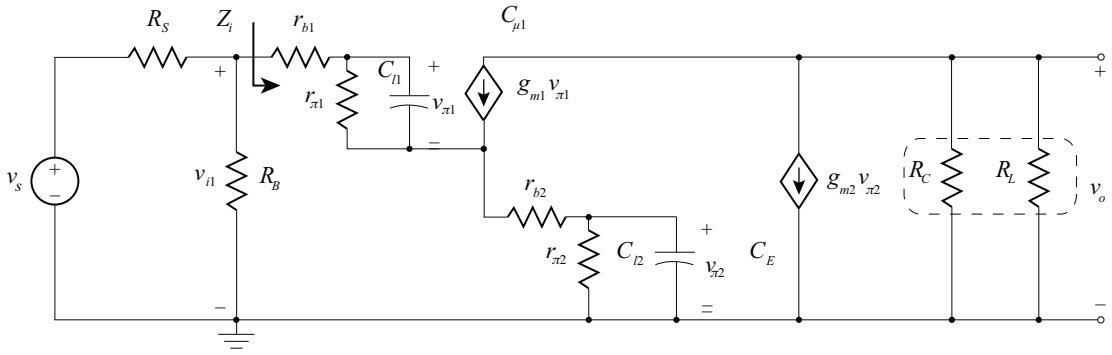

Figure 10.44: High-frequency Miller's equivalent circuit of Figure 10.43.

10.9.4 CASCODE AMPLIFIER

A cascode amplifier and its AC equivalent circuit are shown in Figure 10.45a and 10.45b where Q_1 forms the common-emitter stage and Q_2 forms the common-base stage. The analysis of the cascode amplifier is simplified because, as shown in Section 10.6.4, the common-base amplifier high-frequency cutoff is very high. Therefore, the common-base stage does not limit the high-frequency operation of the cascode amplifier.

The analysis and design for the low cutoff frequency follows the technique demonstrated in the previous sections of this chapter. Since the common-base stage does not affect the high-frequency response of the cascode amplifier, the simplified high-frequency small signal model shown in Figure 10.46 is used to find the dominant high-frequency pole.

The equivalent load resistance, R_O, of the common-emitter stage is the Thévenin input resistance of the common-base stage,

$$R_O = \frac{r_{\pi 2} + r_{b2}}{1 + g_{m2} r_{\pi 2}}. \tag{10.188}$$

The midband gain of the amplifier is,

$$A_{Vm} = -g_{m1} R_O = -g_{m1} \left(\frac{r_{\pi 2} + r_{b2}}{1 + g_{m2} r_{\pi 2}} \right). \tag{10.189}$$

The Miller's equivalent high-frequency input capacitor is,

$$C_{i1} = C_{\pi 1} + C_{\mu 1} \left(1 + g_{m1} R_O\right). \tag{10.190}$$

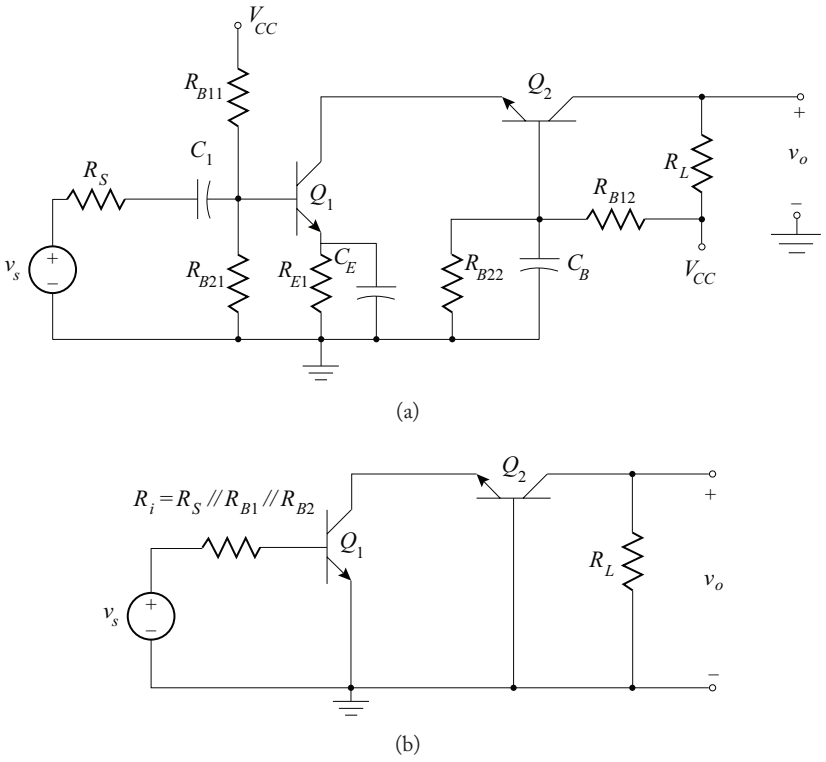

Figure 10.45: (a) Cascode amplifier, (b) AC model of the cascode amplifier.

The dominant high-frequency pole is determined from the following transfer function of the input portion of the high-frequency small signal model of Figure 10.46,

$$\frac{v_{\pi 1}}{v_s} = \frac{r_{\pi 1} // \dfrac{1}{j\omega C_{i1}}}{R_i + r_{b1} + \left(r_{\pi 1} // \dfrac{1}{j\omega C_{i1}} \right)} = \frac{1}{C_1 (R_i + r_{b1})} \left(\frac{1}{j\omega + \dfrac{r_{\pi 1} + R_i + r_{b1}}{C_1 r_{\pi 1} (R_i + r_{b1})}} \right). \quad (10.191)$$

Therefore, the high cutoff frequency is,

$$\omega_H = \frac{r_{\pi 1} + R_i + r_{b1}}{C_1 r_{\pi 1} (R_i + r_{b1})}. \quad (10.192)$$

The other high-frequency poles are significantly higher in frequency than Equation (10.192) due to the small value of the Miller's equivalent output capacitance of Q_1 and the very high cutoff frequency of the common-base stage.

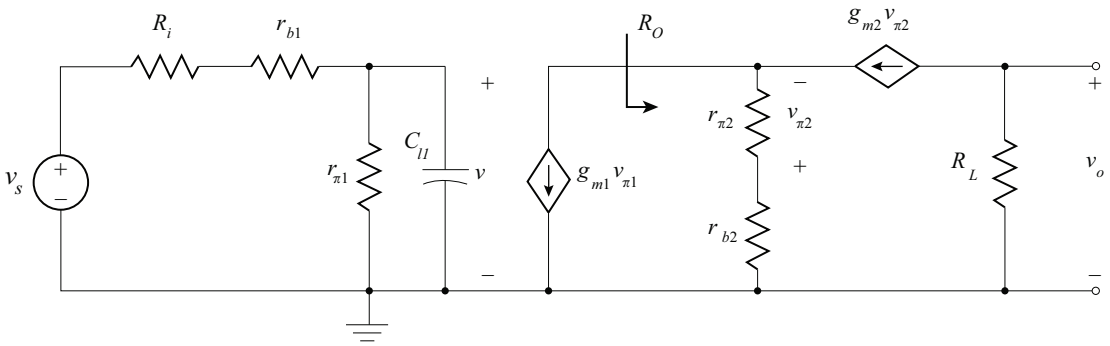

Figure 10.46: Simplified high-frequency model of the cascode amplifier.

10.10 CONCLUDING REMARKS

Frequency response of amplifiers has been discussed in this chapter. The distortion caused by frequency limitations was explored in the time domain. A demonstration of the effect of the amplifier transfer function (gain and phase response) on the input signal confirmed that frequency distortion can dramatically alter the output signal shape when compared to its input. Low and high pass responses to a pulse input were explored and the concept of sag was introduced.

For multi-pole electronic systems, the difficulty in analytically finding the low and high cutoff frequencies was resolved through simple formulas and approximations of the cutoff frequencies. This technique utilized the dominant pole of electronic systems to readily determine the cutoff frequency. Dominant poles were defined as those poles that are at least a factor of four from the next nearest pole frequency.

The low-frequency response of an electronic amplifier was shown to be a function of the external coupling and bypass capacitors of an amplifier. Although in some instances, the capacitors interacted with each other in the circuit, a method was developed for approximating the low-frequency poles by analyzing the poles associated with individual capacitors. This technique relied on the dominant pole concept.

High-frequency hybrid-π models were developed for the BJT and the FET. The high-frequency models included capacitances that determine the high-frequency operation of the devices. Miller's theorem was developed to simplify the analysis of the high-frequency models.

Single and multistage amplifiers were analyzed using the techniques developed in this chapter. The analysis and design of amplifiers followed the following procedure:

1. Model the transistors with the appropriate DC model.

2. Determine the circuit quiescent conditions. Verify forward-active region for BJTs or saturation region for FETs.

3. Determine transistor AC (hybrid-π or h-) parameters from quiescent conditions.
4. Create AC equivalent circuit.
5. Determine the midband performance of each amplifier stage by:
   (a) replacing the transistors by their respective AC models, or
   (b) using previously derived results for the circuit topology.
6. Combine stage performance quantities to obtain total midband gain.
7. Perform low-frequency analysis to determine the low cutoff frequency using the low-frequency, small-signal AC model.
8. Perform high-frequency analysis to determine the high cutoff frequency using:
   (a) The small-signal hybrid-π model including the internal (high-frequency) capacitors and short circuiting all external (coupling and bypass) capacitors. Use Miller's theorem to simplify the small-signal model of the amplifier where appropriate.
   (b) Previously derived expressions for the pole locations taking into account appropriate loading conditions.
9. Combine results of DC, midband, low-frequency and high-frequency analysis to obtain total circuit performance.

As an aid to the designer faced with a variety of sources for transistor data, Tables 10.4 (BJT), 10.5 (JFET), and 10.6 (MOSFET) have been included. These tables provide formulas for transistor parameter conversion between the various models. The three parameter sets included in the tables are: manufacturer's data book parameters, hybrid-π model parameters, and SPICE model parameters.

Table 10.4: Conversion of BJT high-frequency modeling parameters

Source of Parameters	Conversion to Hybrid-π Model Parameters[1]	Conversion to SPICE Parameters[2]
Manufacturer's Data Books f_T @ I_{CT} – gain bandwidth product C_{obo} @ V_{CB} – output capacitance C_{ibo} @ V_{EB} – input capacitance	$C_\mu = C_{obo}$ $C_\pi = \frac{g_m}{2\pi f_T} - C_\mu$	$CJC = C_{obo}\left(1+\frac{V_{CB}}{\psi}\right)^m$ $CJE = C_{ibo}\left(1+\frac{V_{EB}}{\psi}\right)^m$ $TF = \frac{1}{2\pi f_T} - \frac{\eta V_t}{\lvert I_{CT}\rvert}\left(\left[\frac{\psi+V_{EB}}{\psi-0.7}\right]^m C_{ibo} + C_{obo}\right)$
SPICE Models CJE – zero-bias base-emitter capacitance CJC – zero-bias base-collector capacitance TF – forward transit time	$C_\mu = \frac{CJC}{\left(1+\frac{V_{CB}}{\psi}\right)^m}$ $C_\pi \approx g_m TF + 1.617 \times CJE$	$VJE \approx VJC \approx \psi \approx 0.75$ $MJE \approx MJC \approx m \approx 0.33$
IC Design Models C_{ieo} – zero-bias base-emitter capacitance $C_{\mu o}$ – zero-bias base-collector capacitance τ_F – forward transit time	$C_\mu = \frac{C_{\mu o}}{\left(1+\frac{V_{CB}}{\psi}\right)^m}$ $C_\pi \approx g_m \tau_F + 1.617 \times C_{ieo}$	$CJE = C_{ieo}$ $CJC = C_{\mu o}$ $TF = \tau_F$

NOTES: (1) Use the quiescent value of V_{CB} in the equations in this column.
(2) Use the data book values for V_{CB} and V_{EB} in the equations in this column.
(3) f_T is assumed to be approximately constant in this text: It has a non-linear dependence on I_C
(4) The values for ψ and m are device dependent. The indicated values are the SPICE default values.
(5) The subscripted junction voltages are for *npn* BJTs. The equations for *pnp* BJTs are identical with these subscripts reversed.
(6) C_π is dependent on device parameters as shown below: the approximation given uses SPICE default values

$$C_\pi = g_m TF + \frac{CJE}{(1-FC)^{MJE+1}}\left[1-FC(1+MJE)+MJE\frac{V_{BE}}{VJE}\right] \approx g_m TF + 1.617 \times CJE$$

Table 10.5: Conversion of JFET high-frequency modeling parameters

Source of Parameters	Conversion to Hybrid- π Model Parameters (1)	Conversion to SPICE Parameters
Manufacturer's Data Books C_{iss} @ $V_{GS} = 0$ – input short-circuit capacitance C_{rss} @ $V_{GS} = 0$ – reverse transfer capacitance	$C_{gd} = \frac{C_{rss}}{\left(1+\frac{\lvert V_{GD}\rvert}{\psi}\right)^m}$ $C_{gs} = \frac{C_{iss}-C_{rss}}{\left(1+\frac{\lvert V_{GS}\rvert}{\psi}\right)^m}$	CGD = C_{rss} CGS = C_{iss} - C_{rss}
SPICE Models CGD – zero-bias gate-drain capacitance CGS – zero-bias gate-source capacitance	$C_{gd} = \frac{\text{CGD}}{\left(1+\frac{\lvert V_{GD}\rvert}{\psi}\right)^m}$ $C_{gs} = \frac{\text{CGS}}{\left(1+\frac{\lvert V_{GS}\rvert}{\psi}\right)^m}$	PB = $\psi \approx 0.6$ M = $m \approx 0.5$
IC Design Models C_{gdo} – zero-bias gate-drain capacitance C_{gso} – zero-bias gate-source capacitance	$C_{gd} = \frac{C_{gdo}}{\left(1+\frac{\lvert V_{GD}\rvert}{\psi}\right)^m}$ $C_{gs} = \frac{C_{gso}}{\left(1+\frac{\lvert V_{GS}\rvert}{\psi}\right)^m}$	CGD = C_{gdo} CGS = C_{gso}

NOTES: (1) Use quiescent values for V_{GD} and V_{GS} in the equations in this column.
(2)The values for ψ and m are device dependent. Typical values are as $\psi = 0.6$ and $m = 0.5$. SPICE default values are $\psi = 1.0$ and $m = 0.5$
(3) The subscripted junction voltages are for n-channel JFETs. The equations for p-channel JFETs are identical with these subscripts reversed.

Table 10.6: Conversion of MOSFET high-frequency modeling parameters

Source of Parameters	Conversion to Hybrid-π Model Parameters (1)	Conversion to SPICE Parameters
Manufacturer's Data Books C_{iss} @ V_{GS} – input capacitance C_{rss} @ V_{GS} – reverse transfer capacitance C_{oss} @ V_{GS} – output capacitance	$C_{gs} \approx C_{iss} - C_{rss}$ $C_{gd} \approx C_{rss}$ $C_{ds} \approx C_{oss} - C_{rss}$	$\text{TOX} = \frac{2}{3}\left(\frac{\varepsilon_{OX}\text{WL}}{C_{iss} - C_{rss}}\right)$ $\text{CGDO} = \frac{2C_{rss}}{\text{W}}$
SPICE Models CGDO – zero-bias gate-drain capacitance CGSO – zero-bias gate-source capacitance VTO – threshold voltage KP – transconductance coefficient	$C_{gd} = \text{CGDO}\times\text{W}$ $C_{gs} = \frac{2}{3}\left(\frac{\varepsilon_{OX}\text{WL}}{\text{TOX}}\right)$ $C_{ds} = 0$ $V_T = \text{VTO}$ $\text{K} = \frac{\text{KP}}{2}\left(\frac{\text{W}}{\text{L}}\right)$	$\varepsilon_{OX} = 3.9\,\varepsilon_o$ $= 3.9(8.51)$ pF/m for SiO_2
IC Design Models Levels 2, 3, and 4 PSpice Models	Levels 2, 3, and 4 PSpice Parameters	Levels 2, 3, and 4 PSpice Parameters

NOTES: (1) Default geometry parameters in PSpice are L = W = 100 μm. In SPICE2, the default geometry parameters are L = W = 1m. Setting L = W = 100µm or less in the MOSFET model statement is recommended. Failure to make L = W affects the constants used to determine the DC operating point.

(2) The value for ε_{OX} is dependent on the gate insulation material. The value of 3.9 ε_O is for SiO_2 insulated gates only.

(3) Integrated circuit parameters require the most accurate representation of the physical realization of the device. Detailed device geometry information is required. More complex models of the MOSFET are used in specifying parameters for IC design. These models are beyond the scope of this text: the simple model presented in this text does not have sufficient detail to be used for IC designs.

SUMMARY DESIGN EXAMPLE: PREAMPLIFIER FOR A LORAN C NAVIGATIONAL SYSTEM RECEIVER

The Loran C is a standard navigational system using pulsed information in the very low frequency (VLF) range. Loran C is a form of hyperbolic navigational system that uses time differentials between signals from a pair of widely separated transmitting sites to locate the coordinates of the receiving station. The required operational frequency range is 10 Hz to 1500 kHz. The output of a "whip" antenna, with an output resistance of 2200 Ω, must be amplified by a factor of +2 to +3 by a preamplifier. This preamplified signal is applied to the 50 Ω input of the Loran C navigational receiver which will process the incoming information. The output impedance of the preamplifier must match the input impedance of the Loran C receiver to eliminate potential signal reflections which will corrupt the signal to the Loran C receiver. It is critical that the preamplifier is a non-inverting amplifier which will preserve the duty cycle of the pulsed information detected by the whip.

Design an inexpensive Loran C preamplifier to meet the stated requirements. A +9 V automotive/marine battery is used as the power source.

Solution:

The antenna signal is applied to a common-source *n*-JFET amplifier which will provide moderate gain and high input resistance. However, since a common-source *n*-JFET amplifier inverts the input signal, a unity gain inverter is required at the output. Therefore, the output of the FET stage is applied to a unity gain common-emitter *npn* BJT amplifier. To minimize signal reflections, the output resistance of the BJT unity gain inverting amplifier must be 50 Ω. A possible topology for the amplifier is shown below:

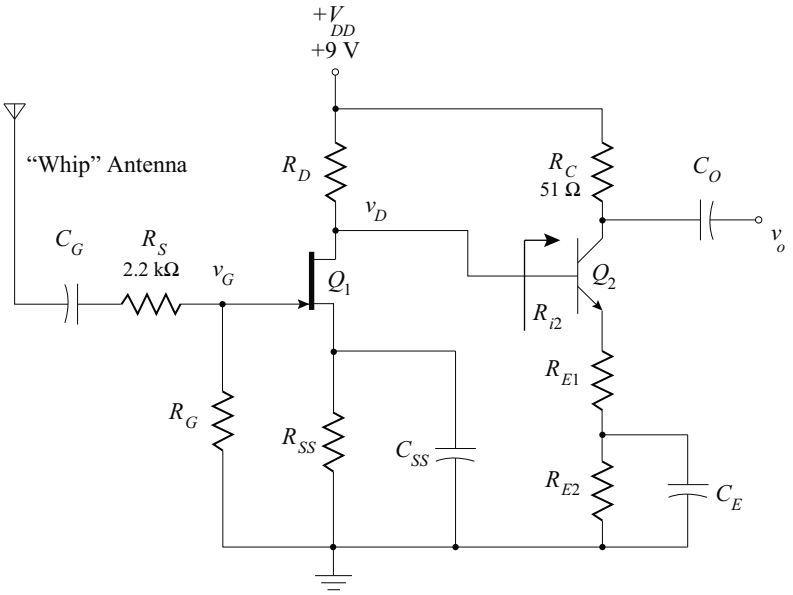

The BJT parameters are:

$$\beta_F = 200, \quad V_A = 160\,\text{V}, \quad r_b = 30\,\Omega,$$
$$C_{ibo} = 8\,\text{pF at } V_{EB} = 0.5\,\text{V}, \quad C_{obo} = 4\,\text{pF at } V_{CB} = 5\,\text{V}$$
$$f_T = 300\,\text{MHz}.$$

The JFET parameters are:

$$I_{DSS} = 6\,\text{mA}, \quad V_{PO} = -4.7\ \text{V}, \quad V_A = 100\,\text{V},$$
$$C_{iss} = 4.5\,\text{pF at } V_{GS} = 0\,\text{V}, \quad C_{rss} = 1.5\,\text{pF at } V_{GS} = 0\,\text{V}.$$

Initiate the design by selecting the DC operating point and synthesizing the circuit for operation in the midband region. The FET biasing resistor R_G is set arbitrarily large: $R_G = 510\,\text{k}\Omega$. Let $I_D = 1\,\text{mA}$. Solve for V_{GS}:

$$I_D = I_{DSS}\left(1 - \frac{V_{GS}}{V_{PO}}\right)^2,$$

or

$$V_{GS} = V_{PO}\left(1 - \sqrt{\frac{I_D}{I_{DSS}}}\right) = -4.7\left(1 - \sqrt{\frac{1}{6}}\right) = -2.8\,\text{V}.$$

Since $V_G = 0$, then $V_S = 2.8\,\text{V}$. This implies that the source resistor is,

$$R_{SS} = \frac{V_S}{I_D} = \frac{2.8}{0.001} = 2.8\,\text{k}\Omega.$$

The midland gain of the amplifier is,

$$A_v \approx \frac{v_o}{v_g} = \left(\frac{v_d}{v_g}\right)\left(\frac{v_\pi}{v_d}\right)\left(\frac{v_o}{v_\pi}\right)$$
$$= \left[-g_{m1}\left(r_d // R_D // R_{i2}\right)\right]\left[\frac{r_\pi}{r_\pi + (1 + g_{m2}r_\pi)\,R_{E1}}\right]\left[-g_{m2}R_C\right],$$

where

$$g_{m1} = \frac{-2I_D}{(V_{PO} - V_{GS})} = \frac{-2\,(0.001)}{(-4.7 - (-2.8))} = 1.05\,\text{mS}$$
$$r_\pi = (\beta_F + 1)\,\frac{\eta V_t}{|I_c|} - r_b,$$

and

$$g_{m2} = \frac{\beta_F}{r_\pi}.$$

For a gain of 2 to 3, the parallel combination of R_D and R_{i2} (assuming r_d is very large, here $r_d = 100\,\text{k}\Omega$) is in the range,

$$\frac{2}{\left[\dfrac{g_{m1}g_{m2}R_C r_\pi}{r_\pi + (1+g_{m2}r_\pi)\,R_{E1}}\right]} \leq R_D\,//R_{i2} \leq \frac{3}{\left[\dfrac{g_{m1}g_{m2}R_C r_\pi}{r_\pi + (1+g_{m2}r_\pi)\,R_{E1}}\right]}.$$

Since the second stage will be designed to have an inverting gain magnitude of approximately unity, the gain of the first stage can be designed to have a gain of -2.5.

The second stage will be designed for a collector current of 1 mA. Therefore,

$$r_\pi = 5.2\,\text{k}\Omega \quad \text{and} \quad g_{m2} = 0.038\,\text{S}.$$

For an inverting unity gain second stage,

$$A_{v2} = \frac{v_o}{v_d} = \left(\frac{v_\pi}{v_d}\right)\left(\frac{v_o}{v_\pi}\right) \approx \left(\frac{r_\pi}{r_\pi + (1+g_{m2}r_\pi)\,R_{E1}}\right)(-g_{m2}R_C)\,.$$

But $g_{m2}R_C = (0.038)\,(51) = 1.96$. Therefore, the expression $\frac{r_\pi}{r_\pi+(1+g_{m2}r_\pi)R_{E1}} \approx 0.5$ for $A_{v2} = -1$. This implies that $(1+g_{m2}r_\pi)\,R_{E1} \approx 5.2\,\text{k}\Omega$, or, $R_{E1} = 26 \approx 27\,\Omega$.
The input resistance of the second stage is then,

$$R_{i2} = r_b + r_\pi + (1+g_{m2}r_\pi)\,R_{E1} = 30 + 5200 + 5200 = 10.43\,\text{k}\Omega.$$

For an overall gain of -2.5 the R_D is,

$$R_D = 3.17\,\text{k}\Omega \approx 3.3\,\text{k}\Omega.$$

Checking the DC conditions of the first stages, the drain-source voltage of the JFET is,

$$V_{DS} = V_{DD} - I_D\,(R_D + R_{SS}) = 9 - 0.001\,(3300 + 2800) = 2.9\,\text{V}.$$

To check that the FET is in the saturation region of operation,

$$V_{DS} \geq V_{GS} - V_{PO} = -2.8 - (-4.7) = 1.9\,\text{V},$$

and since $V_{DS} = 2.9\,\text{V} > 1.9\,\text{V}$, the FET is operating in the saturation region. The DC voltage at the drain is $V_D = 9 - 0.001(3300) = 5.7\,\text{V}$.

Now solve for R_{E2} to bias the BJT at $I_C = 1\,\text{mA}$,

$$R_{E2} = \frac{\beta_F}{I_C\,(\beta_F+1)}\left(V_D - V_{\gamma 2}\right) - R_{E1} = \frac{200}{0.001\,(201)}\,(5.7 - 0.7) - 27 = 4.9\,\text{k} \approx 4.99\,\text{k}\Omega.$$

This indicates that $V_{CE} \approx 4\,\text{V}$.

To confirm that the frequency response of the circuit is sufficient to receive the Loran C signal, the device capacitances must first be found. For the FET,

$$C_{gs} = \frac{C_{gso}}{\sqrt{1+\dfrac{|V_{GS}|}{\psi_o}}} = \frac{C_{iss}-C_{rss}}{\sqrt{1+\dfrac{|V_{GS}|}{\psi_o}}} = 1.3\,\text{pF},$$

$$C_{gd} = \frac{C_{gdo}}{\sqrt{1+\dfrac{|V_{GS}|}{\psi_o}}} = \frac{C_{rss}}{\sqrt{1+\dfrac{|V_{GS}|}{\psi_o}}} = 0.463\,\text{pF}.$$

For the BJT,

$$CJC = C_{obo}\left(1+\frac{V_{CB}}{0.75}\right)^{0.33} = 7.83\,\text{pF},$$

$$CJE = C_{ibo}\left(1+\frac{V_{EB}}{0.75}\right)^{0.33} = 9.47\,\text{pF},$$

$$TF = \frac{1}{2\pi f_T} - \frac{\eta V_t}{|I_{CT}|}\left[\frac{CJE}{\left(1-\dfrac{0.7}{0.75}\right)^{0.33}} + C_{obo}\right] = 460\,\text{ps},$$

and

$$C_{\mu 2} = \frac{CJC}{\left(1+\dfrac{V_{CB}}{0.75}\right)^{0.33}} = 4.5\,\text{pF},$$

$$C_{\pi 2} = \frac{g_{m2}}{\omega_{T2}} - C_{\mu 2} = 15.9\,\text{pF}.$$

The high frequency response is found by using Tables 10.1 and 10.3. The common source amplifier has poles at:

$$\omega_{p1A} \approx \frac{-1}{R_G' C_{gs} + \left(1+g_m R_D'\right) R_G' C_{gd} + R_D' C_{gd}}$$

$$\omega_{p2A} \approx \frac{1}{\omega_{p1A} R_G' R_D' C_{gs} C_{gd}} - \omega_{p1A}.$$

While the common-emitter with emitter degeneration amplifier has a pole at:

$$\omega_{CE} = \frac{\left[R'_S + r_\pi + (1+\beta_F) R_E\right]}{\left[(1+\beta_F)\left(R'_S R_C + R'_S R_E + R_C R_E\right) + r_\pi \left(R'_S + R_C\right)\right] C_\mu + r_\pi \left(R'_S + R_E\right) C_\pi}.$$

The high-frequency poles are calculated to be:

$$\omega_{p1A} = 130\,\text{Mrad/s} \Rightarrow 20.7\,\text{MHz},$$
$$\omega_{p2A} = 2.20\,\text{Grad/s} \Rightarrow 3.5\,\text{GHz},$$
$$\omega_{CE} = 24.3\,\text{Mrad/s} \Rightarrow 3.87\,\text{MHz}.$$

There is clearly a dominant pole and the high frequency cutoff ($\approx 3.87\,\text{MHz}$) is more than double the required 1500 kHz: the high frequency cutoff meets specification.

The specifications require a low frequency cutoff of 10 Hz. Therefore, design all low frequency poles at 5 Hz or less.

$$\omega_{L1} = 10\pi = \frac{1}{C_1\,(R_S + R_G)} \Rightarrow C_1 = 3182\,\text{pF} \approx 3300\,\text{pF},$$

and let $C_E = 4700\,\mu\text{F}$.
The design is now complete.

10.11 PROBLEMS

10.1. A rectangular pulse of duration 10 μs is the input to an amplifier described by a single high-frequency pole. Plot the amplifier output for the following locations of that single pole:

(a) 10 MHz

(b) 1 MHz

(c) 100 kHz

10.2. The output voltage response of an amplifier to a input consisting of a unit voltage step is shown. Assume the high-frequency response is characterized by a single pole. Determine:

(a) The voltage gain of the amplifier.

(b) The high 3-dB frequency of the amplifier.

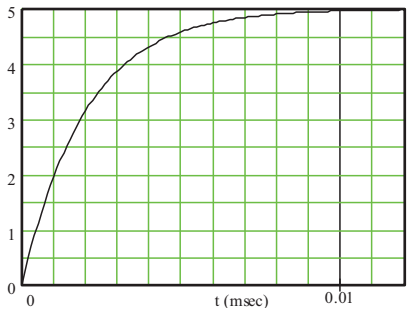

10.3. A rectangular pulse of duration 10 ms is the input to an amplifier described by a single low-frequency pole. Plot the amplifier output for the following locations of that single pole:

(a) 1 Hz

(b) 10 Hz

(c) 100 Hz

10.4. The response of a unity-gain buffer to a 100 Hz square wave with 5 V amplitude is shown. If the low-frequency response is characterized by a single pole, determine the low 3-dB frequency of the unity-gain buffer.

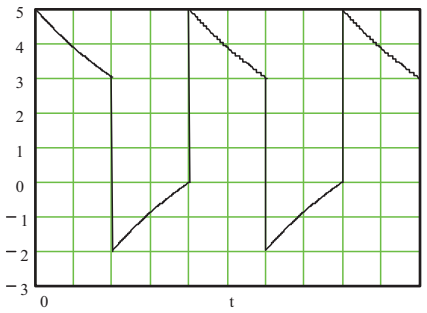

10.5. The low-frequency response of an amplifier is characterized by three poles of frequency 30 Hz, 10 Hz, and 2 Hz and three zero-frequency zeroes. Calculate the lower 3-dB frequency, f_L, using the following techniques:

(a) Dominant pole approximations.

(b) Root-sum of squares approximation (Equation (10.25)).

(c) Compare results to exact calculations.

10.6. An audio amplifier is described by a single low-frequency pole, $f_L = 100$ Hz, and a single high-frequency pole, $f_H = 20$ kHz.

(a) Sketch the response of this amplifier to square waves of frequency:

i. $f_{sq} = 250$ Hz

ii. $f_{sq} = 4$ kHz

(b) Using simple, first-order OpAmp filters to model the amplifier, use SPICE to determine the response of the amplifier to these same square waves.

(c) Compare results of parts a) and b).

10.7. A particular amplifier can be described as having a midband gain of 560, three high-frequency poles at the following frequencies:

$$f_{p1} = 25\,\text{kHz} \quad f_{p2} = 75\,\text{kHz} \quad f_{p3} = 150\,\text{kHz},$$

and a complex-conjugate pair of low-frequency poles ($\zeta = 0.6$) with resonant frequency:

$$f_o = 100\,\text{Hz}.$$

(a) Draw the idealized Bode magnitude and phase plots. On the graph label all slopes and use a small circle to indicate where the slope changes. Compare these straight-line approximate curves to exact curves (use a software package to generate the exact curves).

(b) Use dominant-pole analysis to estimate the high and low 3-dB frequencies. Compare these estimates to exact calculations.

10.8. The BJT is the given circuit is described by:

$$\beta_F = 200 \quad \text{and} \quad V_A = 150\,\text{V}.$$

(a) Determine the location of the three low-frequency poles.

(b) Which poles can be considered dominant?

(c) Determine the low 3-dB frequency of the circuit.

(d) Verify results using SPICE.

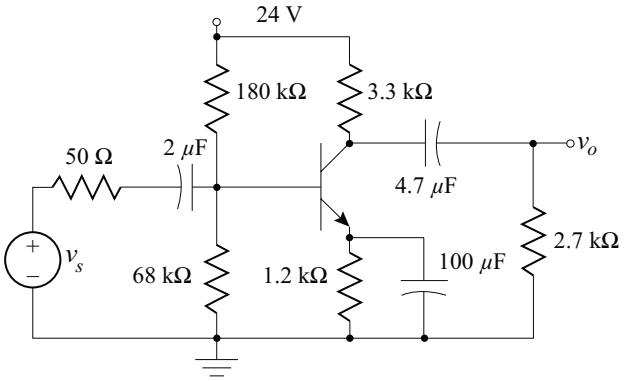

10.9. For the circuit shown, find the low 3-dB frequency and the midband voltage gain. Confirm using SPICE.

The transistor is described by:

$$\beta_F = 200,$$
$$f_T = 600\,\text{MHz}, \text{ and}$$
$$V_A = 200\,\text{V}.$$

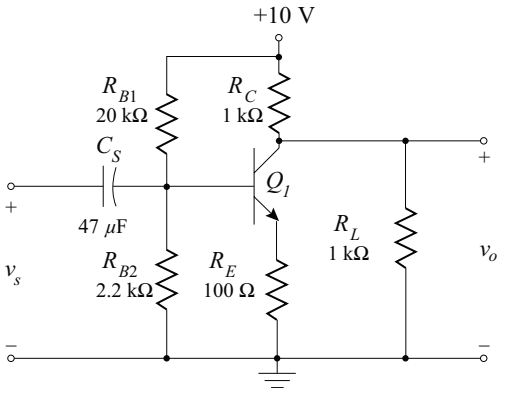

10.10. The design goals for the amplifier shown include maximum symmetrical output voltage swing and a low 3-dB frequency of 70 ± 2 Hz. The Silicon BJT is described by:

$$\beta_F = 150,$$
$$V_A = 300\,\text{V}.$$

Complete the circuit design: use SPICE to verify compliance with the design goals.

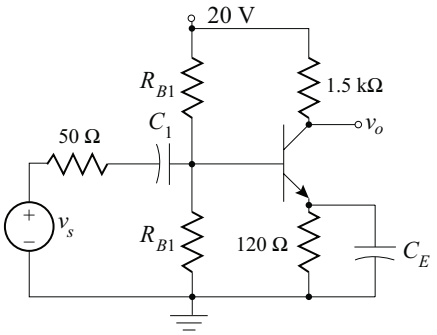

10.11. For the circuit shown below, find the midband voltage gain and low 3-dB frequency. The transistor has

$$\beta_F = 100,$$
$$f_T = 600\,\text{MHz, and}$$
$$V_A = 200\,\text{V}.$$

Let $R_{B1}//R_{B2} = 10\,\text{k}\Omega$.

Confirm results using SPICE.

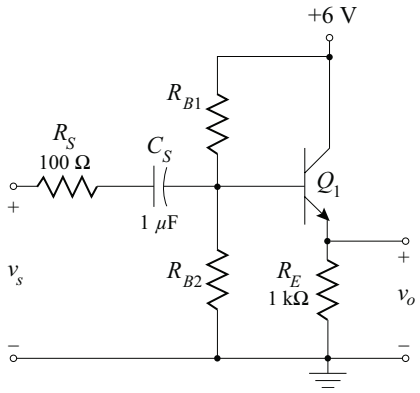

10.12. For the circuit shown, find the midband voltage gain. Complete the design to achieve a low 3-dB frequency of 40 Hz. The transistor has

$$\beta_F = 200 \text{ and}$$
$$V_A = 200\,\text{V}.$$

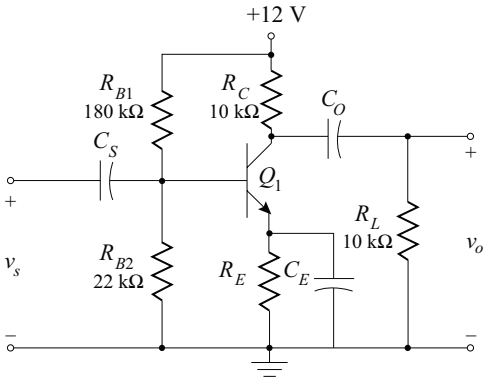

10.13. For the circuit shown below, find the low 3-dB frequency and the midband voltage gain. The transistor is described by:

$$V_{PO} = -4\,\text{V},$$
$$I_{DSS} = 8\,\text{mA}, \text{ and}$$
$$V_A = 200\,\text{V}.$$

Confirm results using SPICE.

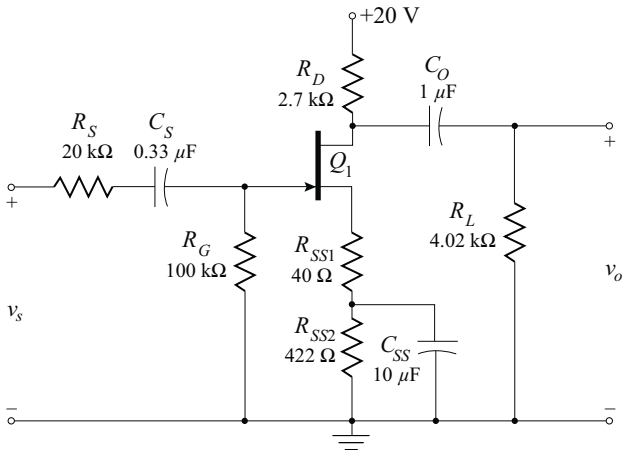

10.14. The design goals for the circuit shown include a low 3-dB frequency , f_L, at 80 Hz. The MOSFET has parameters:

$$I_{DSS} = 5\,\text{mA},$$
$$V_{PO} = -2\,\text{V},$$
$$V_A = 150\,\text{V}.$$

(a) Complete the design by specifying capacitor values that will accomplish the design goal to within ±5%.

(b) Compare the results to SPICE simulation.

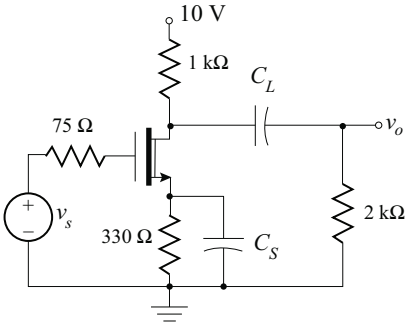

10.15. The design goals for the circuit shown include a low 3-dB frequency , f_L, at 50 Hz. The MOSFET has parameters:

$$K = 2.5\,\text{mA/V}^2,$$
$$V_T = 1.5\,\text{V},$$
$$V_A = 120\,\text{V}.$$

(a) Complete the design by specifying capacitor values that will accomplish the design goal to within ±5%.

(b) Compare the results to SPICE simulation.

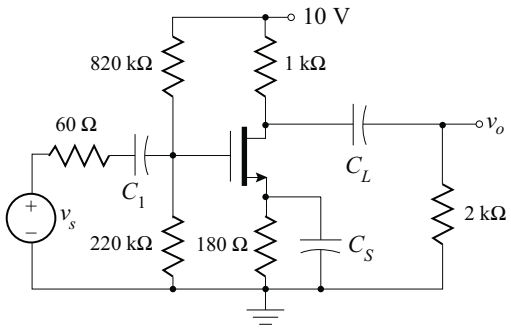

10.16. Design an *n*-JFET common-source amplifier for a low 3-dB frequency of 40 Hz with a midband voltage gain of −2. The input resistance of the amplifier is 100 kΩ. The output resistance is 10 kΩ. A power supply voltage of 12 V is available. The Q-point is defined by: $V_{DS} = 6\,\text{V}$ and $V_{GS} = -1\,\text{V}$. The transistor parameters are:

$$I_{DSS} = 5\,\text{mA}, \quad V_{PO} = -4\,\text{V}, \quad \text{and} \quad V_A = 150\,\text{V}.$$

10.17. The Silicon BJT in the circuit shown has parameters:

$$\beta_F = 120,$$
$$V_A = 200.$$

(a) Determine a realistic minimum value for the capacitor C so that a 75 Hz square wave will have will experience no more than 5% *sag*.

(b) Determine the midband gain for the circuit.

(c) Determine the low 3-dB frequency using the capacitor chosen in part a).

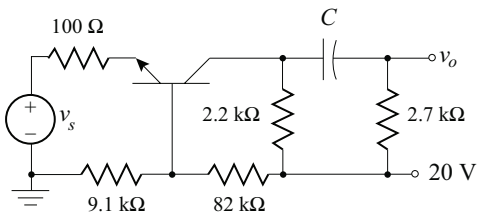

10.18. The design goals for the circuit shown include a lower 3-dB frequency, f_L, at 100 Hz. The Silicon BJT has parameters: $\beta_F = 150$ and $V_A = 350\,\text{V}$.

(a) Complete the design by specifying capacitor values that will accomplish the design goal to within ± 5%.

(b) Sketch the Bode voltage gain plot for the amplifier.

(c) Compare results to SPICE simulation.

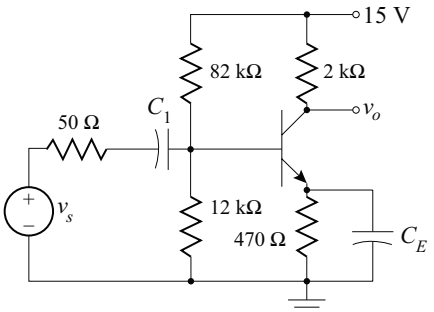

10.19. The design goals for the circuit shown include the requirement that a 100 Hz square wave will have will experience no more than 4% *sag*. The Silicon BJT has parameters: $\beta_F = 160$ and $V_A = 150$ V.

(a) Complete the design by specifying capacitor values that will accomplish the design goal to within ± 5%.

(b) Compare results to SPICE simulation.

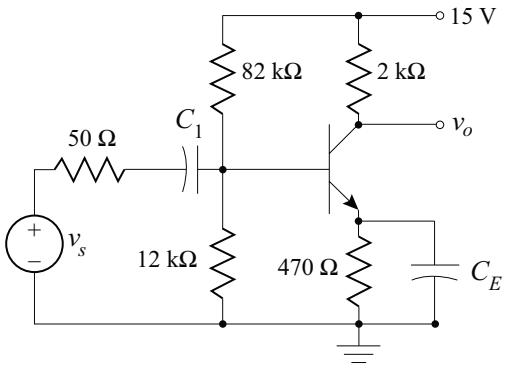

10.20. The zero-bias capacitance of a p-n junction is 2 pF and the built-in potential, ψ_o, is 780 mV, Assume the junction grading coefficient has value, $m = 0.35$.

(a) Plot the junction capacitance for the range of junction capacitances, $-10\text{ V} \leq V_d \leq 0.75\text{ V}$.

(b) If the capacitance value at $V_d = -6\,\text{V}$ is used as a reference, determine the maximum % variation in the capacitance over the range $-10\,\text{V} \leq V_d \leq -2\,\text{V}$.

10.21. A Silicon BJT is described by the following parameters:

$$\beta_F = 160, \quad V_A = 200\,\text{V}, \quad r_b = 10\,\Omega,$$
$$C_\mu = 2.5\,\text{pF}, \quad f_T = 160\,\text{MHz}.$$

Determine the high-frequency hybrid-π model for the BJT under the following bias conditions:

(a) $I_c = 2\,\text{mA}$.

(b) $I_c = 5\,\text{mA}$.

10.22. The Silicon BJT is the circuit shown is described by:

$$\beta_F = 140 V_A = 133\,\text{V}, \quad r_b = 12\,\Omega,$$
$$C_\mu = 3\,\text{pF}, \quad f_T = 120\,\text{MHz}.$$

(a) Determine the high-frequency hybrid-π model for the BJT.

(b) Determine the high 3-dB and low 3-dB frequencies for the given circuit.

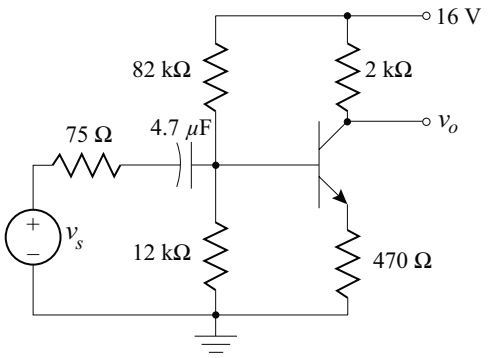

10.23. The Silicon BJT in the circuit shown is described by the following parameters:

$$\beta_F = 120, \quad V_A = 160\,\text{V},$$
$$r_b = 25\,\Omega,$$
$$C_\mu = 3.5\,\text{pF}, \quad f_T = 225\,\text{MHz}.$$

Determine the high-frequency hybrid-π model for the BJT.

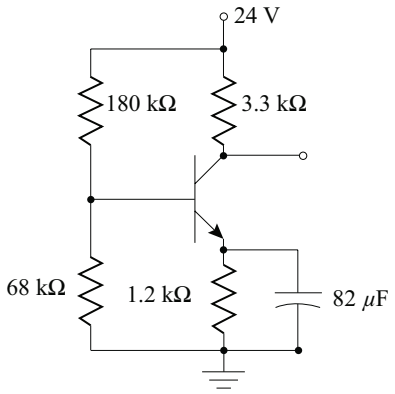

10.24. The transistors in the circuit shown are identical and have the following characteristics:

$$\beta_F = 200,\ f_T = 600\,\text{MHz},$$
$$V_A = 200\,\text{V},\ C_{obo} = 2\,\text{pF}.$$

(a) Find the midband voltage gain.

(b) Find the high 3-dB frequency.

(c) What is the largest peak-to-peak swing attainable with this circuit?

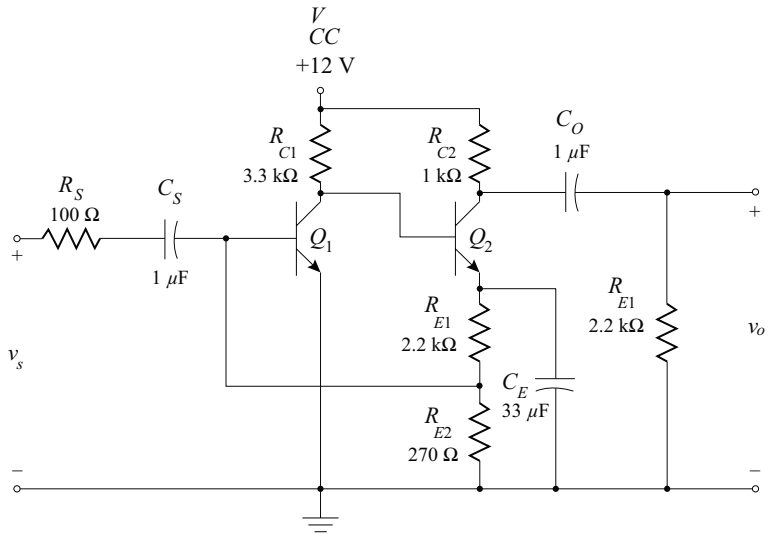

10.25. Complete the design of the circuit shown for maximum symmetrical swing in the mid-band frequency range. The transistor is described by:

$$\beta_F = 180,\ f_T = 600\,\text{MHz},\ C_{obo} = 8\,\text{pF},$$
$$V_{CE} = 2.5\,\text{V}, \quad \text{and} \quad V_A = 200\,\text{V}.$$

(a) Find the high 3-dB frequency. Confirm using SPICE.

(b) Compare a) to the SPICE frequency response for the small-signal model of the circuit.

(c) Compare b) to the SPICE frequency response found when using the Miller's equivalent model of the transistor.

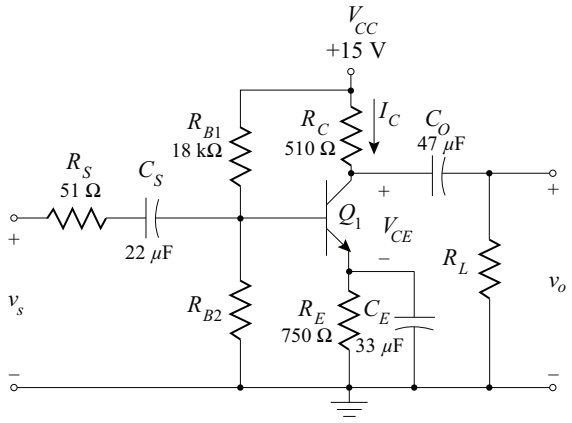

10.26. Determine the high and low 3-dB frequencies for the circuit shown. The Silicon BJT is described by:

$\beta_F = 150,$ $\quad V_A = 300\,\text{V},$
$r_b = 20\,\Omega,$ $\quad C_\mu = 3\,\text{pF},$
$f_T = 200\,\text{MHz}.$

Sketch a Bode voltage gain plot for the circuit.

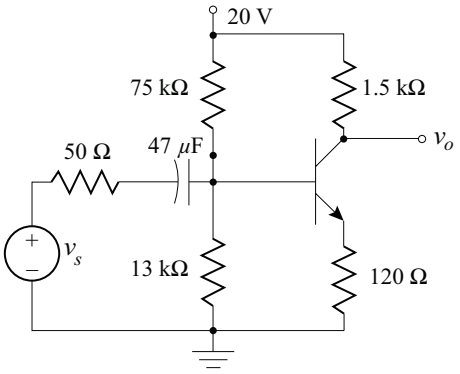

10.27. For the circuit shown, FET is described by:

$I_{DSS} = 5\,\text{mA}, \quad V_{PO} = -2\,\text{V},$
$V_A = 150\,\text{V},$
$C_{rss} = 6.5\,\text{pF}, \quad C_{iss} = 35\,\text{pF}$

(a) Determine the high 3-dB frequency for the voltage gain.

(b) Remove the capacitor shunting the resistor at the FET source (the 220 μF) and determine the high 3-dB frequency.

(c) Comment on results.

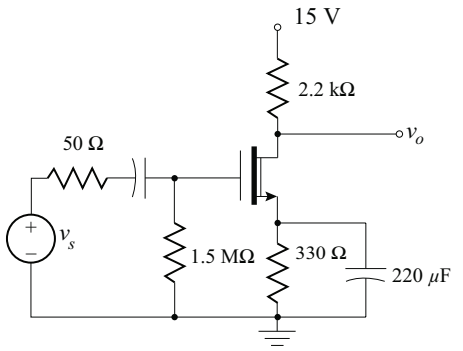

10.28. Complete the design of the amplifier shown for a Q-point defined by $V_{GS} = 5\,\text{V}$.

(a) Find the low and high 3-dB frequencies.

(b) Simulate the design using SPICE.

(c) Compare simulation in b) to a simulation of the small-signal equivalent circuit of the amplifier.

(d) In c), plot the voltage across all of the capacitors (including the device capacitances) and comment on the results.

The transistor parameters are: $K = 0.3\,\text{mA/V}^2$, $V_T = 2\,\text{V}$, $V_A = 150\,\text{V}$, $C_{iss} = 12\,\text{pF}$, and $C_{rss} = 2\,\text{pF}$.

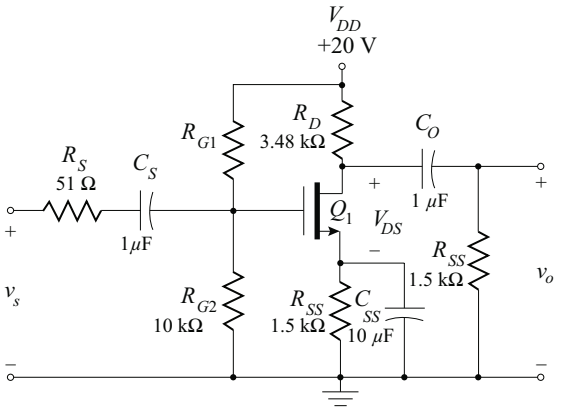

10.29. The JFET in the circuit shown is described by parameters:

$$V_{PO} = -1.8\,\text{V}, \quad I_{DSS} = 4\,\text{mA}, \quad V_A = 90\,\text{V},$$
$$C_{gso} = 3.5\,\text{pF}, \quad C_{gdo} = 1.5\,\text{pF}.$$

Determine the high-frequency model of the JFET for the following values of the gate voltage:

(a) $V_g = 0\,\text{V}$.

(b) $V_g = 1\,\text{V}$.

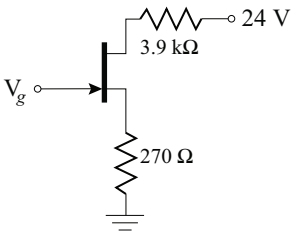

10.30. Determine the high and low 3-dB frequencies for the circuit shown. The JFET transistors have parameters,

$V_{PO} = -2\,\text{V}, \quad I_{DSS} = 5\,\text{mA},$
$V_A = 200\,\text{V},$
$C_{gso} = 3\,\text{pF}, \quad C_{gdo} = 1\,\text{pF}.$

(a) Sketch a Bode voltage gain plot for the circuit.

(b) Verify results using SPICE (note: SPICE Parameters, $CGS = C_{gso}$ and $CGD = C_{gdo}$).

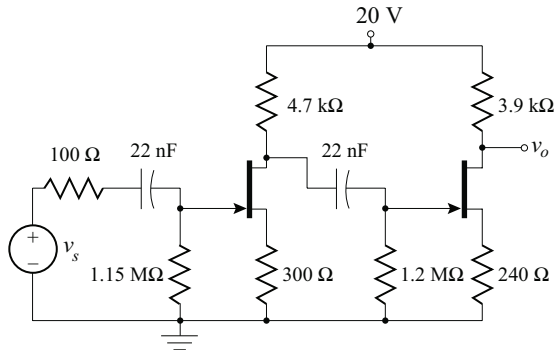

10.31. The circuit below was designed with identical transistors with the following characteristics:

$$I_{DSS} = 10\,\text{mA}, \; V_{PO} = -2\,\text{V}, \; V_A = 100\,\text{V}, \; C_{rss} = 7.3\,\text{pF}, C_{iss} = 26.5\,\text{pF}.$$

Determine:

(a) the midband voltage gain.

(b) low 3-dB frequency.

(c) high 3-dB frequency.

(d) Verify the results using SPICE.

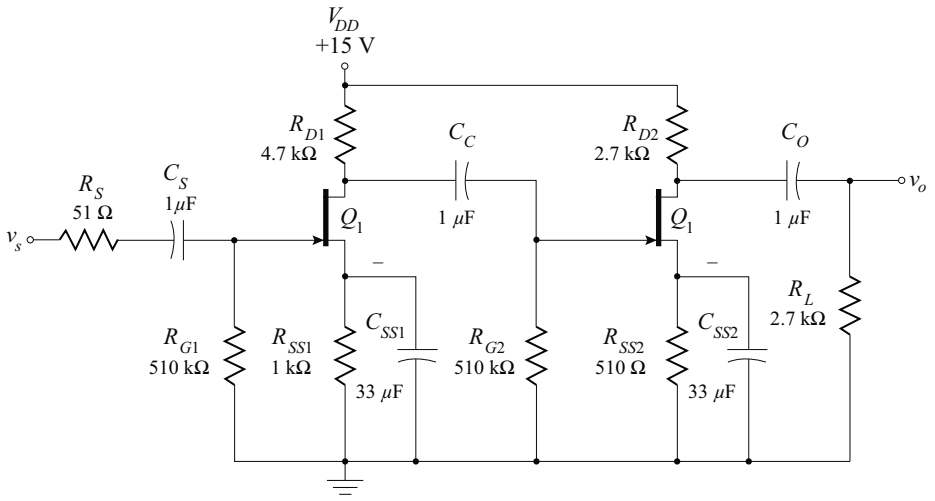

10.32. Complete the design of the circuit shown by determining a value for R_d that will achieve a quiescent output voltage of 5 V. Determine the high and low 3-dB frequencies for the completed circuit. The transistors are described by:

JFET:	BJT
$I_{DSS} = 2\,\text{mA}$	$\beta_F = 120$
$V_{PO} = -2\,\text{V}$	$V_A = 135\,\text{V}$
$V_A = 120\,\text{V}$	
$C_{obo} = 6\,\text{pF}$ at $V_{BC} = 5\,\text{V}$	
$C_{gso} = 4\,\text{pF}$	$C_{ibo} = 15\,\text{pF}$ at $V_{BE} = 0.5\,\text{V}$
$C_{gdo} = 1.5\,\text{pF}$	$f_T = 180\,\text{MHz}$ at $I_{CT} = 2.5\,\text{mA}$

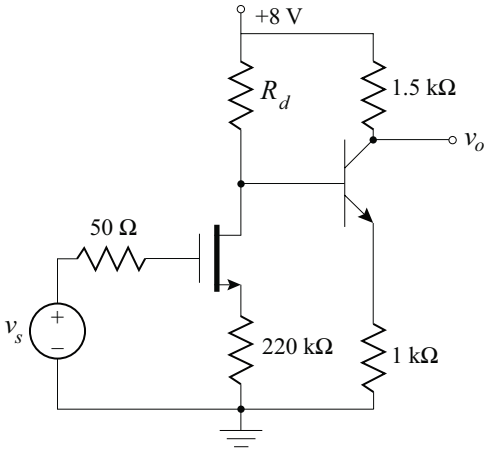

10.33. Design a three stage *npn* BJT amplifier with an overall gain which is greater than 500 with a high 3-dB frequency of 10 MHz and a low 3-dB frequency under 100 Hz. The transistors are identical with the following characteristics:

$$\beta_F = 200,\ f_T = 400\,\text{MHz},\ V_A = 200\,\text{V},\quad \text{and}\quad C_{obo} = 2\,\text{pF}.$$

A 15 V power supply is available. Confirm the design with SPICE.

10.34. Given the circuit shown below with transistor parameters:

JFET: $I_{DSS} = 10\,\text{mA},\ V_{PO} = -3.1\,\text{V},\ V_A = 100\,\text{V},\ C_{rss} = 6.5\,\text{pF},\ C_{iss} = 33.5\,\text{pF},$
BJT: $\beta_F = 200,\ f_T = 500\,\text{MHz},\ V_A = 200\,\text{V},\quad \text{and}\quad C_{obo} = 5\,\text{pF}.$

Determine the high and low 3-dB frequencies.

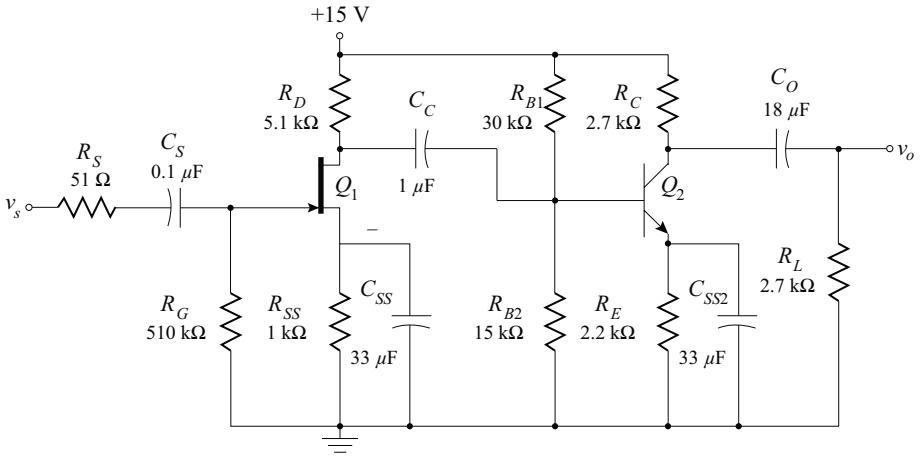

10.35. Determine the high and low 3-dB frequencies for the circuit shown. The JFET has parameters,

$$\begin{aligned} V_{PO} &= -2\,\text{V},\\ I_{DSS} &= 2\,\text{mA},\\ V_A &= 200\,\text{V},\\ C_{gso} &= 3\,\text{pF},\\ C_{gdo} &= 1\,\text{pF}. \end{aligned}$$

The BJT has parameters:

$\beta_F = 150,$
$V_A = 200\,\text{V},$
$C_{obo} = 7\,\text{pF}$ at $V_{CB} = 5\,\text{V},$
$C_{ibo} = 16\,\text{pF}$ at $V_{BE} = 0.5\,\text{V},$
$f_T = 160\,\text{MHz}$ at $I_{CT} = 3\,\text{mA}.$

Compare results to SPICE simulation.

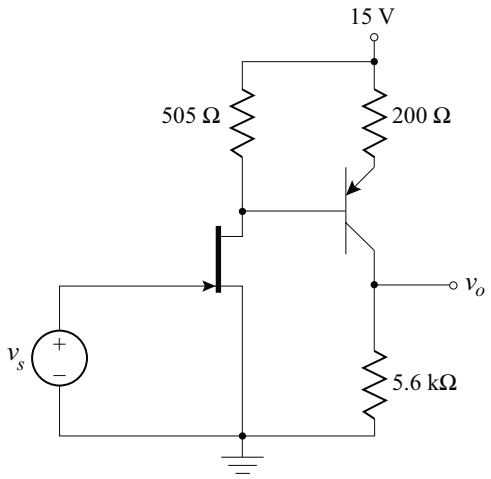

10.36. For the Common-collector circuit shown, the BJT is described by:

$\beta_F = 150, \quad r_b = 30\,\Omega,$
$V_A = 200\,\text{V},$
$C_\mu = 0.5\,\text{pF}, \quad f_T = 200\,\text{MHz}.$

(a) Complete the design by determining the coupling capacitors so that the low 3-dB frequency is $10\,\text{Hz} \pm 2\,\text{Hz}$.

(b) What is the midband gain?

(c) Determine the high 3-dB frequency.

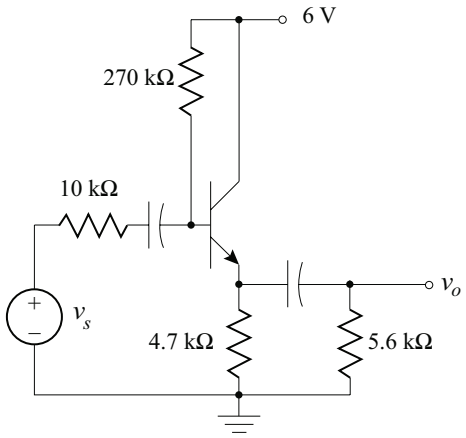

10.37. In the emitter-coupled amplifier circuit shown, it has been decided to ground one of the inputs and only use a single-ended output. The transistor parameters are:

$\beta_F = 120,$
$V_A = 250\,\text{V},$
$r_b = 15\,\Omega,$
$C_\mu = 2\,\text{pF},$
$f_T = 150\,\text{MHz}.$

(a) Determine the quiescent conditions on all transistors.

(b) Determine the midband voltage gain of the circuit.

(c) Determine the high and low 3-dB frequencies.

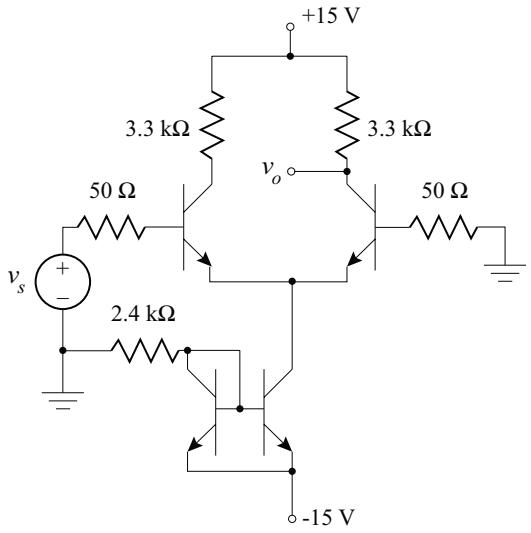

10.38. The BJT cascode amplifier shown uses identical transistors with parameters:

$\beta_F = 200$, $V_A = 200\,\text{V}$,
$f_T = 600\,\text{MHz}$, and $C_{obo} = 2\,\text{pF}$.

(a) Complete the design of the amplifier for $I_E = -3\,\text{mA}$, and $V_{CE1} = V_{CE2} = 3.5\,\text{V}$. Find the quiescent point of all of the transistors.

(b) Determine the high and low 3-dB frequencies.

(c) Confirm the results using SPICE.

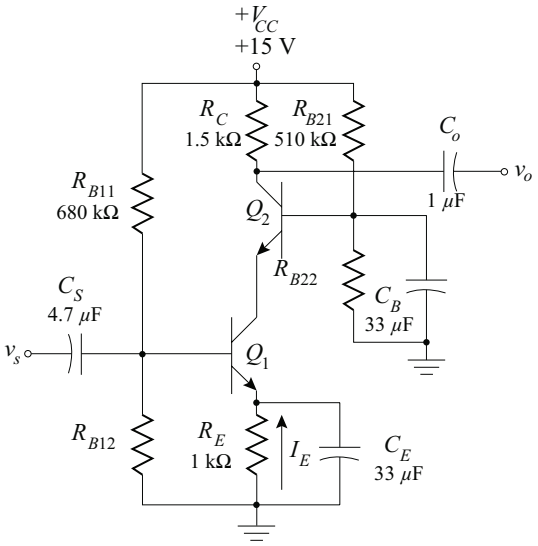

10.39. The transistors in the differential amplifier shown below are identical and have the following characteristics:

$$I_{DSS} = 10\,\text{mA},\ V_{PO} = -4.5\,\text{V},$$
$$C_{rss} = 7.3\,\text{pF},\ C_{iss} = 26.5\,\text{pF},\ C_{oss} = 8.3\,\text{pF},$$
and $V_A = 100\,\text{V}$.

Determine the high and low 3-dB frequencies.

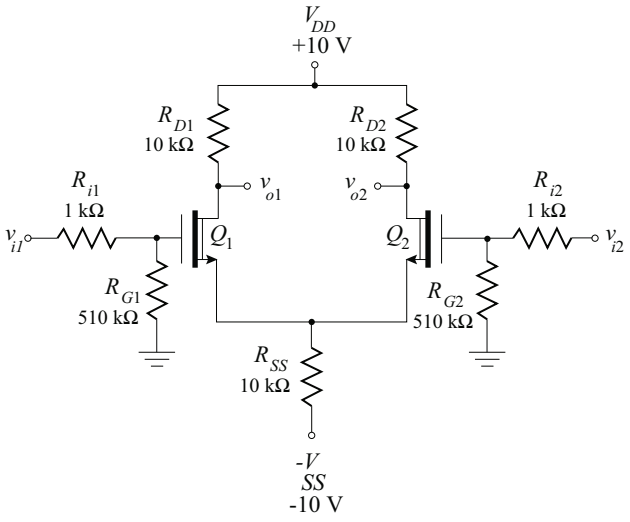

10.40. For the single-input differential amplifier shown, find the low and high 3-dB frequencies Assume identical transistors with

$$\beta_F = 120,$$
$$f_T = 600\,\text{MHz},$$
$$V_A = 200\,\text{V}, \text{ and}$$
$$C_{obo} = 2\,\text{pF}.$$

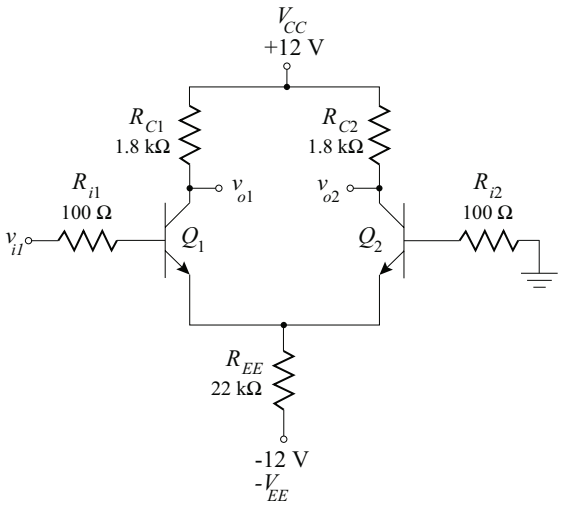

REFERENCES

[1] Antognetti, P. and Massobrio, G., *Semiconductor Device Modeling with SPICE*, McGraw-Hill, New York, 1988.

[2] Ghausi, M. S., *Electronic Devices and Circuits: Discrete and Integrated*, Holt, Rinehart and Winston, New York, 1985.

[3] Gray, P. R. and Meyer, R. G., *Analysis and Design of Analog Integrated Circuits*, 3rd ed., John Wiley & Sons, Inc., New York, 1993.

[4] Millman, J., *Microelectronics: Digital and Analog Circuits and Systems*, McGraw-Hill Book Company, New York, 1979.

[5] Millman, J. and Halkias, C. C., *Integrated Electronics: Analog and Digital Circuits and Systems*, McGraw-Hill Book Company, New York, 1972.

[6] Savant, C. J., Roden, M. S., and Carpenter, G. L., *Electronics Design: Circuits and Systems*, 2nd ed., Benjamin/Cummings Publishing Company, Redwood City, 1991.

[7] Sedra, A. S. and Smith, K. C., *Microelectronic Circuits*, 3rd ed., Holt, Rinehart, and Winston, Philadelphia, 1991.

[8] Seymour, J., *Electronic Devices & Components*, 2nd ed., Longman Scientific & Technical, Essex, U.K., 1988.

[9] Tyagi, M. S., *Introduction to Semiconductor Materials and Devices*, John Wiley & Sons, New York, 1991

CHAPTER 11

Feedback Amplifier Frequency Response

The basic topology of a feedback amplifier, as previously described is shown in Figure 11.1.

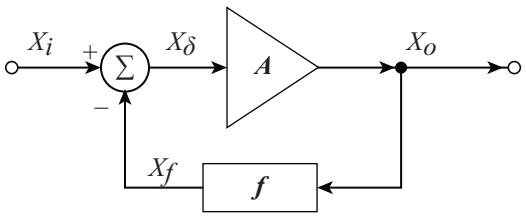

Figure 11.1: Basic negative feedback topology.

In Chapter 8 (Book 2) several of the benefits of negative feedback were presented and analyzed. The mixing of a portion of the output signal with the input signal was shown to provide several benefits:

- The gain of the amplifier is stabilized against variation in the characteristic parameters of the active devices.
- The input and output impedances of the amplifier can be selectively increased or decreased.
- Non-linear signal distortion is reduced.

An additional benefit of negative feedback is the general increase in the midband frequency range. Previously described as a reduction in the variation of the gain *due to changes in frequency*, this increase in midband frequency range is exhibited by *both* an increase in the high 3 dB frequency, f_H, and a decrease in the low 3 dB frequency, f_L.[1]

The above listed benefits were shown to be accompanied by a drawback:

- The gain of the circuit is reduced.

[1]Amplifiers for which $f_L = 0$ will, with the application of negative feedback, continue to operate with no low-frequency deterioration.

An additional drawback is the possibility of oscillations. Amplifiers for which the high- and low-frequency response is described by either single or double pole expressions are shown to be inherently stable and not subject to oscillations. If the amplifier high- or low-frequency response is described by three or more poles, the application of feedback brings forth the possibility of instability in the form of oscillations. This possibility of instability can be controlled by either limiting the range of applied feedback or with the addition of a compensation network to the amplifier.

In this chapter the benefit of increased bandwidth and the possibility of oscillations related to negative feedback are explored in electronic amplifiers. As in Chapter 10, the frequency response of an amplifier is broken into three regions: low-frequency, midband, and high-frequency regions. The effect of feedback on the midband region was discussed thoroughly in Chapter 8 (Book 2). Of interest here is the effect of feedback on the poles that determine the amplifier response in the low- and high-frequency regions. After deriving the pole location change in single-pole systems, the analysis is expanded to two-pole, three-pole, and many-pole systems. The concept of dominant poles is utilized to simplify system characterization when applicable.

While the early sections of this chapter focus on analysis techniques, the later sections focus on design techniques to ensure stable amplifier operation. Stability against oscillation is explored through the use of Bode diagrams and computer simulation, as well as other standard stability criteria. Several common compensation networks that can alter the pole-zero characterization of the basic forward amplifier and, thereby ensure amplifier stability are also explored.

11.1 THE EFFECT OF FEEDBACK ON AMPLIFIER BANDWIDTH (SINGLE-POLE CASE)

It has been previously shown that the gain, A_f, of a feedback amplifier is simply related to the forward gain, A, of a loaded basic forward amplifier and the feedback ratio, f:

$$A_f = \frac{A}{1 + Af}. \tag{11.1}$$

As in the derivations and demonstrations of Chapter 8 (Book 2), the amplifier gain can be expressed as a transresistance, a current gain, a voltage gain, or a transconductance depending on the topology of the mixing and sampling processes. The frequency response derivations presented here are not dependent the mixing or sampling topology.

As was seen in Chapter 10, the small-signal sinusoidal forward gain of an amplifier is dependent on the frequency of the input. The high-frequency response of an amplifier that is characterized by a single high-frequency pole, ω_H, and a mid-band gain, A_o, is given by:

$$A = \frac{A_o}{1 + \dfrac{j\,\omega}{\omega_H}}. \tag{11.2}$$

When the feedback gain relationship, Equation (11.1), is applied to this single-pole frequency-dependent gain expression, the resultant feedback gain is given by:

$$A_f = \frac{\dfrac{A_o}{1+\dfrac{j\omega}{\omega_H}}}{1+\left(\dfrac{A_o}{1+\dfrac{j\omega}{\omega_H}}\right)f} = \frac{A_o}{1+A_o f+\dfrac{j\omega}{\omega_H}} = \frac{A_o}{1+A_o f}\left(\frac{1}{1+\dfrac{j\omega}{(1+A_o f)\,\omega_H}}\right). \quad (11.3)$$

This gain is of the same form as that of a single-pole amplifier with reduced gain and increased pole frequency:

$$A_{of} = \frac{A_o}{1+A_o f} \quad \text{and} \quad \omega_{Hf} = (1+A_o f)\omega_H. \quad (11.4)$$

The gain has been reduced, as expected, by the return ratio ($D = 1 + A_o f$) and *the high-frequency pole value has also been increased by the return ratio*.

Similarly, if the low-frequency response of an amplifier is characterized by a single pole:

$$A = \frac{A_o}{1+\dfrac{\omega_L}{j\omega}}, \quad (11.5)$$

the feedback gain can be derived to be:

$$A_f = \frac{\dfrac{A_o}{1+\dfrac{\omega_L}{j\omega}}}{1+\left(\dfrac{A_o}{1+\dfrac{\omega_L}{j\omega}}\right)f} = \frac{A_o}{1+A_o f+\dfrac{\omega_L}{j\omega}} = \frac{A_o}{1+A_o f}\left(\frac{1}{1+\dfrac{\omega_L}{(1+A_o f)\,j\omega}}\right). \quad (11.6)$$

This gain is again of the same form as that of a single low-frequency pole amplifier. The feedback amplifier low-frequency pole magnitude is given by:

$$\omega_{Lf} = \frac{\omega_L}{1+A_o f}. \quad (11.7)$$

The gain has been reduced, as expected, by the return ratio ($D = 1 + A_o f$) and *the low-frequency pole value has been decreased by the return ratio*.

Frequency Response

The magnitude of the gain function of a general amplifier with (A_f) and without (A) feedback is shown in Figure 11.2a with frequency on a logarithmic scale. The increase in the width of

the midband frequency range is evident. In Figure 11.2b, the Bode straight-line approximate amplitude plot is shown. It is interesting to note that the intersection of the two Bode plots occurs at $\omega = \omega_{Lf}$ and $\omega = \omega_{Hf}$. Outside the midband region of the feedback amplifier, the Bode plots are coincident. This property is a useful aid in the design of feedback amplifiers described by simple poles.

Step Response

The time-domain response of a single-pole amplifier to unit step is a simple exponential decay to the final value:

$$X_o(t) = X_{o(final)} + \left(X_{o(initial)} - X_{o(final)}\right) e^{-t/\tau}, \tag{11.8}$$

where

$$\tau = \frac{2\pi}{\omega_H}. \tag{11.9}$$

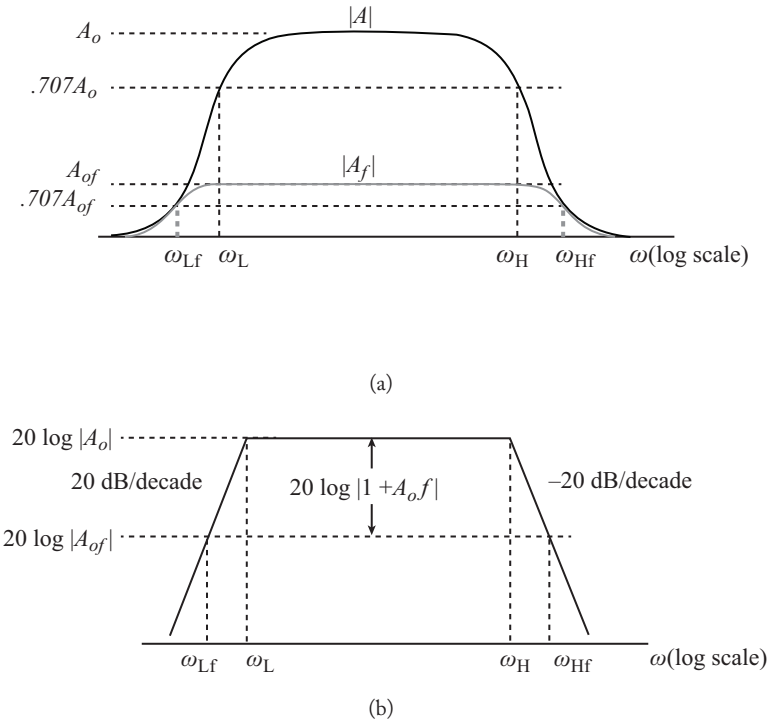

Figure 11.2: Changes to gain with the application of feedback: (a) Gain on a linear scale; (b) Idealized Bode plot.

Application of feedback increases the high-frequency pole, ω_H, and consequently reduces the time constant of the exponential decay for the step response:

$$\tau_f = \frac{2\pi}{\omega_{Hf}}. \tag{11.10}$$

The amplifier responds more quickly to step inputs. The tilt or sag of the amplifier is measured with a pulse train of frequency, ω, and is dependent on the low-frequency pole:

$$sag = \frac{\pi\omega_L}{\omega} \times 100\% = \frac{\pi f_L}{f} \times 100\%. \tag{11.11}$$

The application of feedback reduces ω_L and consequently reduces the tilt or sag of the pulse train response.

11.2 DOUBLE POLE FEEDBACK FREQUENCY RESPONSE

The high-frequency response of an amplifier that is characterized by two high-frequency poles, ω_1 and ω_2, and a mid-band gain, A_o, is given by:

$$A = \frac{A_o}{\left(1 + \frac{j\omega}{\omega_1}\right)\left(1 + \frac{j\omega}{\omega_2}\right)}. \tag{11.12}$$

In order to more appropriately study the change in pole location for multiple-pole amplifiers, a change in the notation to describe frequency will be used:

$$j\omega \Rightarrow \ s = j\omega + \sigma. \tag{11.13}$$

This notation is common as one progresses from Fourier analysis to Laplace analysis and should be familiar to the reader. Under this change of variables, Equation (11.12) becomes:

$$A = \frac{A_o}{\left(1 + \frac{s}{\omega_1}\right)\left(1 + \frac{s}{\omega_2}\right)}. \tag{11.14}$$

When the feedback gain relationship, Equation (11.2), is applied to this double-pole frequency-dependent gain expression, the resultant feedback gain is given by:

$$A_f = \frac{A_o}{\left(1 + \frac{s}{\omega_1}\right)\left(1 + \frac{s}{\omega_2}\right) + A_o f} \tag{11.15}$$

which is more commonly written in the form:

$$A_f = \frac{A_o}{1 + A_o f}\left(\frac{1}{1 + \frac{s}{1 + A_o f}\left(\frac{1}{\omega_1} + \frac{1}{\omega_2}\right) + \frac{s^2}{1 + A_o f}\left(\frac{1}{\omega_1 \omega_2}\right)}\right). \tag{11.16}$$

As expected, the low-frequency gain is reduced by the return ratio. However, the new locations of the two poles is not obvious. One heuristic approach to visualizing the general pole location change due to various amounts of feedback is through a plot of the denominator of Equation (11.15):

$$P(s) = \left(1 + \frac{s}{\omega_1}\right)\left(1 + \frac{s}{\omega_2}\right) + A_o f. \tag{11.17}$$

The plot of the denominator, $P(s)$, is shown in Figure 11.3 for four values of the loop gain, A_{of}. With unity return ratio (no feedback), the curve intersects the horizontal axis at the two poles, $-\omega_1$ and $-\omega_2$, of the basic amplifier gain, A. Increasing the feedback raises the curve, $P(s)$, by A_{of} and results in a translation of the two poles, seen as the intersection of the curve with the horizontal axis, toward each other. With sufficiently large loop gain, the curve, $P(s)$, no longer crosses the horizontal axis and the poles become a complex conjugate pair.

A more rigorous approach to determining the migration of the pole locations with varying feedback casts Equation (11.16) into the general form:

$$A_f = \frac{A_o}{(1 + A_o f)\left(1 + 2\zeta\frac{s}{\omega_o} + \frac{s^2}{\omega_o^2}\right)}. \tag{11.18}$$

This format was initially presented in Chapter 9 and is standard for a two-pole system with resonant frequency,

$$\omega_o = \sqrt{\omega_1 \omega_2 (1 + A_o f)}; \tag{11.19}$$

and damping coefficient,

$$\zeta = \frac{\omega_1 + \omega_2}{2\sqrt{(1 + Af)}\omega_1 \omega_2} = \frac{\omega_1 + \omega_2}{2\omega_0}. \tag{11.20}$$

The resonant frequency *and* the damping coefficient depend on the original pole location and return difference, $D = 1 + A_o f$. The resonant frequency *increases* as the square root of the return difference, while the damping coefficient *decreases* by the same factor. With the use of the quadratic formula, the two poles can be found to be located at:

$$s = -\frac{\omega_1 + \omega_2}{2} \pm \frac{\omega_1 + \omega_2}{2}\sqrt{1 - \frac{1}{\zeta^2}}. \tag{11.21}$$

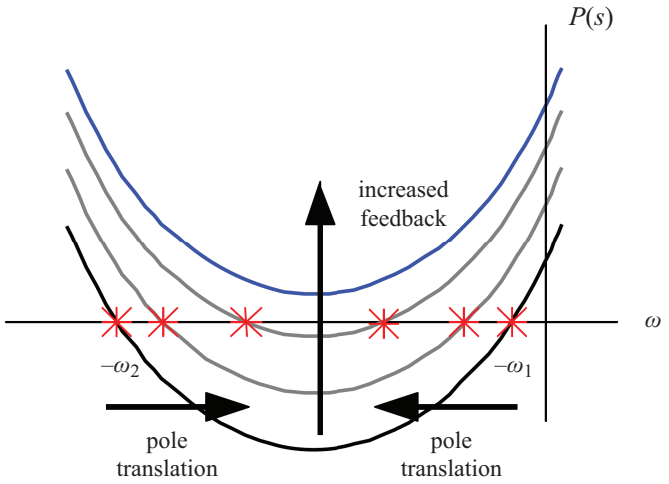

Figure 11.3: Heuristic interpretation of pole migration with increasing loop gain.

As predicted by the heuristic approach, when there is a large damping coefficient, $\zeta > 1$, (small amounts of feedback) there are two distinct, real poles: for small damping coefficient, $\zeta < 1$, (large amounts of feedback) the argument of the square root becomes negative and the poles become a complex conjugate pair.

It is common to display the locus of pole locations with varying damping coefficient on the complex s plane. This plot, called a *root-locus plot*, is shown in Figure 11.4. As the damping coefficient decreases (return difference increases) the poles converge along the real axis and then split vertically. Notice that when the poles of this two-pole gain function become a complex conjugate pair, the real part of the pole location remains a constant. This constancy of the real part of the complex pair pole location indicates that the poles are always located in the left-half of the complex plain: the resonant frequencies, e^{st}, contain an exponential decay. Consequently, resonances do not experience uncontrolled growth and the two-pole feedback amplifier is always stable.

11.2.1 FREQUENCY RESPONSE

The frequency response of a two-pole system has been discussed extensively in Section 9.1. A normalized plot the frequency response of a two high-frequency pole system in the general neighborhood of ω_o with the damping coefficient as a parameter ($0.2 \leq \zeta \leq 1.0$ in increments of 0.1) is shown in Figure 11.5.

In Chapter 9, a peak in the frequency response was found to exist for damping coefficients less than $1/\sqrt{2}$. This characteristic is particularly important in the design of amplifiers: the design

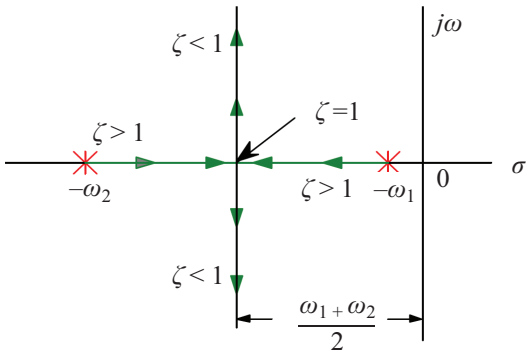

Figure 11.4: The root locus of a two-pole gain function.

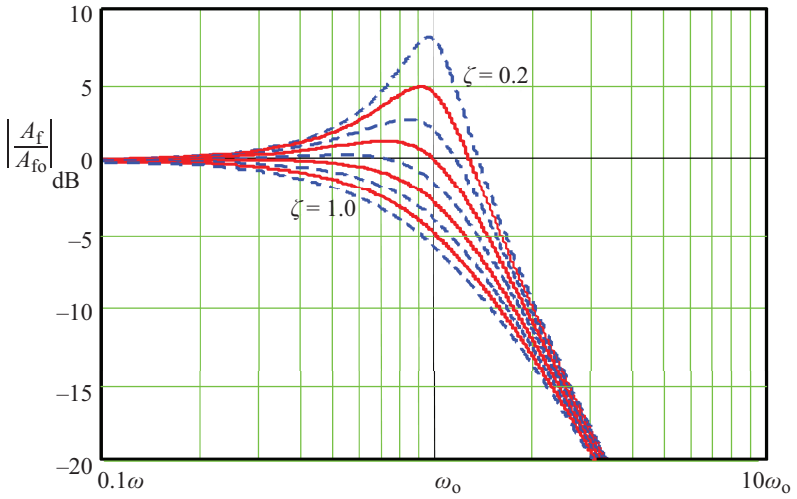

Figure 11.5: Normalized feedback amplifier gain.

requirements of good amplifiers rarely allows for significant peaks in the frequency response of the gain. The frequency at which this peak occurs is related to ω_o:

$$\omega_{peak} = \omega_o \sqrt{1 - 2\zeta^2}, \tag{11.22}$$

and has magnitude:

$$|A_f(\omega_{peak})| = \frac{|A_{of}|}{2\zeta\sqrt{1-\zeta^2}}. \tag{11.23}$$

The design specifications on the midband flatness will place an lower limit on the damping coefficient (and consequently the return difference). Good amplifiers rarely have damping coefficients less than 0.5.

In amplifier design it is important to find the change in the 3 dB frequency as feedback is applied to the amplifier. In two-pole systems, the high 3 dB frequency, ω_{Hf}, is dependent on the resonant frequency, ω_o, and the damping coefficient, ζ. Each of these quantities is, in turn, dependent on the original pole locations, ω_1 and ω_2, and the return difference, D. The calculation of the 3 dB frequency is therefore a complicated process. One approach to this process begins with the notational convention that the amplifier before the application of feedback is described by two simple poles with frequency ratio:

$$\omega_2 = k\omega_1. \tag{11.24}$$

It was previously shown in Section 10.2 that if $k > 4$, a dominant pole exists. After the application of feedback, it is also possible that a dominate pole exists. To determine the appropriate condition for a dominant pole with feedback, the ratio of the two feedback pole frequencies, k_f, given in Equation (11.21) is taken:

$$k_f = \frac{-\dfrac{\omega_1+\omega_2}{2}\left(1+\sqrt{1-\dfrac{1}{\zeta^2}}\right)}{-\dfrac{\omega_1+\omega_2}{2}\left(1-\sqrt{1-\dfrac{1}{\zeta^2}}\right)} > 4. \tag{11.25}$$

The condition necessary for a feedback dominant pole is the solution of Equation (11.25), given by:

$$\left(1+\sqrt{1-\frac{1}{\zeta^2}}\right) > 4\left(1-\sqrt{1-\frac{1}{\zeta^2}}\right) \tag{11.26}$$

or

$$\zeta > 1.25. \tag{11.27}$$

If this condition on the damping coefficient is met, the 3 dB frequency of the system can be obtained with the methods described in Section 10.2. While the dominant pole case is significant, in many cases the damping coefficient is smaller than the appropriate value ($\zeta < 1.25$) and other methods of determining the 3 dB frequency must be used. The 3 dB frequency must be obtained by analysis of the magnitude of the feedback gain equation (Equation (11.18)). If the parameter s is replaced by its sinusoidal equivalent, $s \Rightarrow j\omega$, the gain expression becomes:

$$\frac{A_f}{A_{of}} = \frac{1}{\left(1+2\zeta\dfrac{j\omega}{\omega_o}-\dfrac{\omega^2}{\omega_o^2}\right)}. \tag{11.28}$$

Which, when related to relative magnitudes, reduces to:

$$\left|\frac{A_f}{A_{of}}\right|^2 = \frac{1}{\left(1-\dfrac{\omega^2}{\omega_o^2}\right)^2 + 4\zeta^2\dfrac{\omega^2}{\omega_o^2}}. \tag{11.29}$$

The 3 dB frequency, ω_{Hf}, occurs when the gain power ratio is reduced to one-half its midband value or when the denominator of Equation (11.29) has value 2:

$$\left(1-\frac{\omega_{Hf}^2}{\omega_o^2}\right)^2 + 4\zeta^2\frac{\omega_{Hf}^2}{\omega_o^2} = 2. \tag{11.30}$$

Application of the quadratic formula leads to a solution for ω_{Hf}:

$$\frac{\omega_{Hf}^2}{\omega_o^2} = 1 - 2\zeta^2 + \sqrt{(1-2\zeta^2)^2 + 1}. \tag{11.31}$$

Equation (11.19) can be recast into a form to relate ω_o to the lowest non-feedback pole frequency:

$$\omega_o = \omega_1\sqrt{k(1+Af)} = \omega_1\sqrt{kD}. \tag{11.32}$$

Which leads to a relationship between the feedback 3 dB frequency and the lowest non-feedback pole:

$$\frac{\omega_{Hf}}{\omega_1} = \sqrt{\left(1-2\zeta^2+\sqrt{(1-2\zeta^2)^2+1}\right)kD}. \tag{11.33}$$

Because of the dependence of ζ on the initial pole spacing, k, and the return difference, D, the true significance of Equation (11.33) is disguised. One form of interpreting the significance of this expression is the ratio of 3 dB frequency to the product of the return difference and ω_1:

$$\omega_{Hf} = \left(\sqrt{\left(1-2\zeta^2+\sqrt{(1-2\zeta^2)^2+1}\right)\frac{k}{D}}\right)(D\omega_1). \tag{11.34}$$

Further insight can be obtained by replacing the return difference (inside the square root) with its equivalent expression in k and ζ:

$$D = \frac{(k+1)^2}{4k\zeta^2}.$$

Equation (11.34) now takes the form:

$$\omega_{Hf} = \left(\frac{2k\zeta}{k+1}\sqrt{\left(1-2\zeta^2+\sqrt{(1-2\zeta^2)^2+1}\right)}\right)(D\omega_1). \tag{11.34a}$$

The relationship is similar to the single pole case with an additional factor:

$$\omega_{Hf} = K(\zeta, k) \cdot D \cdot \omega_1 \tag{11.35}$$

where the factor, $K(\zeta, k)$, is given by:

$$K(\zeta, k) = \frac{2k\zeta}{k+1}\sqrt{\left(1 - 2\zeta^2 + \sqrt{(1-2\zeta^2)^2 + 1}\right)}. \tag{11.36}$$

This relationship is shown in Figure 11.6 for a variety of initial pole ratios, k.

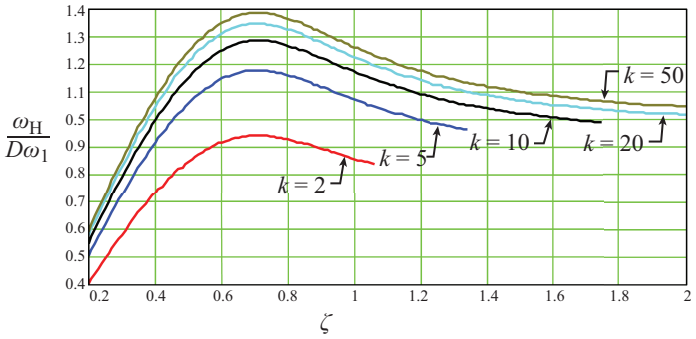

Figure 11.6: High 3 dB frequency as a function of ζ and non-feedback pole spacing.

Example 11.1

A two-pole amplifier with midband gain, $A_o = 1000$, and two high-frequency poles, $f_1 = 100\,\text{kHz}$ and $f_2 = 1\,\text{MHz}$, has feedback applied so that the midband gain is reduced to

$$A_{of} = 80.$$

Determine the location of the new poles and the high 3 dB frequency.

Solution

The ratio of the two pole frequencies is: $k = 10$. The return difference is the ratio of the two gains:

$$D = \frac{A_o}{A_{of}} = \frac{1000}{80} = 12.5.$$

The resonant frequency is found to be:

$$f_o = \sqrt{f_1 f_2 (1 + A_o f)} = \sqrt{100\,k\,(1M)\,12.5} = 1.118\ \text{MHz}$$

and damping coefficient,

$$\zeta = \frac{f_1 + f_2}{2f_o} = \frac{k+1}{2\sqrt{kD}} = \frac{10+1}{2\sqrt{10 \times 12.5}} = 0.492.$$

The high 3 dB frequency, f_H, can be found by obtaining $K(\zeta, 10)$ from Figure 11.6 (or Equation (11.36)) and by multiplying $K(\zeta, 10)$, D and f_1.

$$f_H = K(\zeta, 10)Df_1 = (1.146)(12.5)(100k) = 1.43\,\text{MHz}.$$

The two poles are a complex conjugate pair located at

$$s = 2\pi\left[-550k \pm j550k\left(\sqrt{3.1311}\right)\right] = -1.1\pi \pm j1.95\pi\ \text{Mrad/s}.$$

A plot of the amplifier gain (in dB) with and without feedback is shown below.

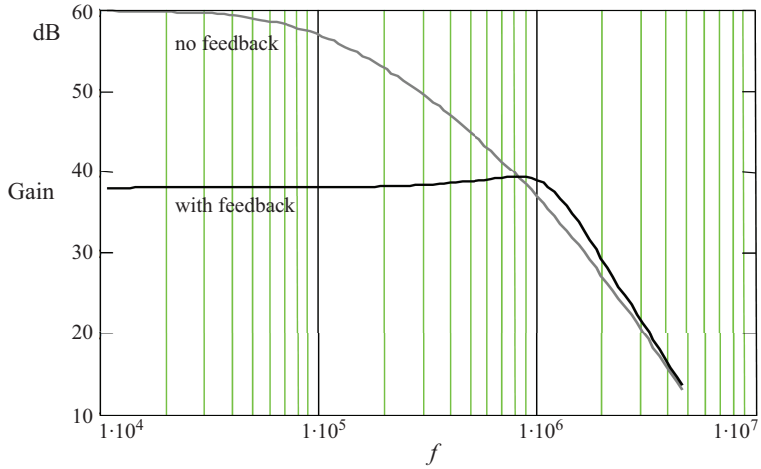

Low-frequency response

If the low-frequency response of an amplifier is described by two low-frequency poles, ω_{1L} and ω_{2L}, the gain function can be expressed as:

$$A = \frac{A_o}{\left(1 + \frac{\omega_{1L}}{s}\right)\left(1 + \frac{\omega_{2L}}{s}\right)}. \tag{11.37}$$

The application of feedback to the amplifier will produce a convergence of poles similar to that described for high-frequency poles. There are, however distinct differences. The low-frequency resonant frequency, ω_{oL} is given by:

$$\omega_{oL} = \sqrt{\frac{\omega_{1L}\omega_{2L}}{1 + Af}}, \tag{11.38}$$

and the expression for the damping coefficient is:

$$\zeta_L = \frac{\omega_{oL}}{2}\left(\frac{1}{\omega_{1L}} + \frac{1}{\omega_{2L}}\right) = \frac{k+1}{2\sqrt{kD}}. \tag{11.39}$$

The frequency response plots take the same form as for high-frequency poles with the single exception of being mirror images on the logarithmic frequency scale. The low 3 dB frequency, ω_{Lf}, can be determined in a similar manner as was the case for ω_{Hf}. For damping coefficients, ζ, greater than 1.25, a dominant pole exists and the methods of Chapter 10 can be used to determine ω_{Lf}. If the damping coefficient is smaller than 1.25, the methods of this chapter are more appropriate.

If the two low-frequency poles are identified by ω_{1L} , the pole closest to the midband region, and

$$\omega_{2L} = \frac{\omega_{1L}}{k}, \tag{11.40}$$

the low 3 dB frequency is given by:

$$\omega_{Lf} = \frac{\omega_{1L}}{K\left(\zeta_L, k\right) \cdot D}, \tag{11.41}$$

where, $K(\zeta, k)$ is defined by Equation (11.36).

The frequency response curve will also exhibit a peak if the low-frequency damping coefficient is less than $1/\sqrt{2}$. Peaks in the low-frequency response are usually undesirable in amplifiers and good amplifiers rarely have damping coefficients less than 0.5. The frequency of this peak is related to ω_{oL}:

$$\omega_{peak} = \frac{\omega_{oL}}{\sqrt{1-2\zeta^2}}, \tag{11.42}$$

and has magnitude:

$$\left| A_f\left(\omega_{peak}\right)\right| = \frac{\left|A_{of}\right|}{2\zeta\sqrt{1-\zeta^2}}. \tag{11.43}$$

Example 11.2

A two-pole amplifier with midband gain, $A_o = 1000$, and two low-frequency poles, $f_1 = 100$ Hz and $f_2 = 10$ Hz, has feedback applied so that the midband gain is reduced to

$$A_{of} = 80.$$

Determine the low 3 dB frequency.

Solution:

Here the ratio of the two pole frequencies is 10. The return difference is the ratio of the two gains:

$$D = \frac{A_o}{A_{of}} = \frac{1000}{80} = 12.5.$$

The resonant frequency is found to be:

$$f_{oL} = \sqrt{\frac{f_{1L} f_{2L}}{1 + A_o f}} = \sqrt{\frac{100\,(10)}{12.5}} = 8.944 \text{ Hz}$$

and damping coefficient,

$$\zeta_L = \frac{k+1}{2\sqrt{kD}} = \frac{10+1}{2\sqrt{10 \times 12.5}} = 0.492.$$

The low 3-dB frequency, f_L, can be found by obtaining $K(\zeta_L, 10)$ from Figure 11.6 (or Equation (11.36)) and by dividing f_{1L} by the product of $K(\zeta_L, 10)$ and D.

$$f_L = \frac{f_{1L}}{K\,(\zeta_L, 10) \cdot D} = \frac{100}{1.146\,(12.5)} = 7.0 \text{ Hz}.$$

A plot of the amplifier gain (in dB) with and without feedback is shown below.

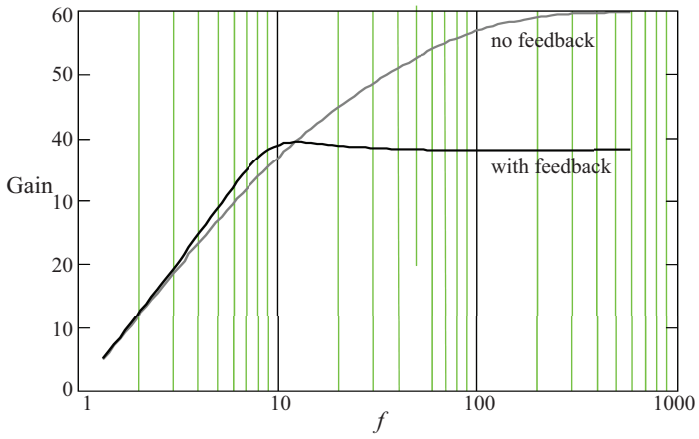

11.2.2 STEP RESPONSE

The step response for an amplifier with two real high-frequency poles was discussed in Section 10.1. Feedback amplifiers with greater than unity value damping coefficients behave is the

same manner: the step response is the sum of two exponential terms converging to a steady-state value. Damping coefficients less than unity value are underdamped systems and have a more complex step response.

The response of an underdamped feedback amplifier to a unit step is given by:

$$X(t) = A_{of}\left[1 - \left(\frac{\zeta\omega_o}{\omega_d}\sin\omega_d t + \cos\omega_d t\right)e^{-\zeta\omega_o t}\right], \tag{11.44}$$

where the damped frequency, ω_d, is given by the expression:

$$\omega_d = \sqrt{1-\zeta^2}\,\omega_o. \tag{11.45}$$

A plot of the normalized step response of a feedback amplifier is shown in Figure 11.7 for several values of the damping coefficient, ζ.

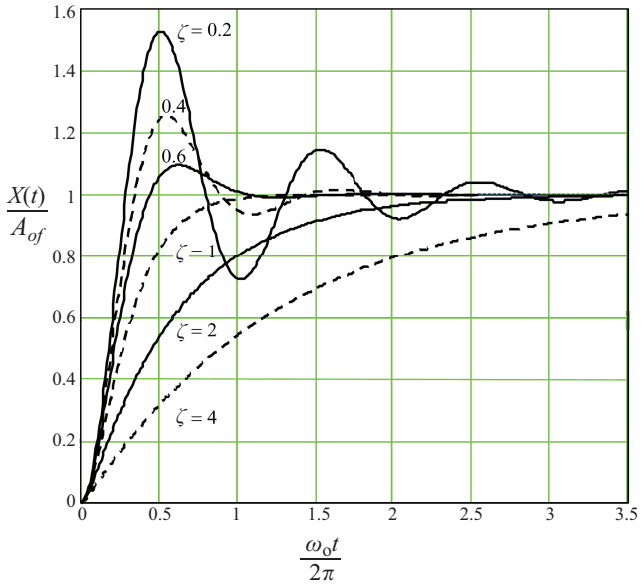

Figure 11.7: Step response of a two-pole feedback amplifier.

For small values of the damping coefficient, ζ, the step response of a feedback amplifier overshoots and oscillates about the final value before settling down to a steady-state condition. While a small amount of overshoot is often acceptable, large overshoot is often unsatisfactory for quality amplifiers. In order to quantify the response several quantities are defined as follows:

Rise time	≡ time to rise from 10% to 90% of the final value
Delay time	≡ time to rise to 50% of the final value
Overshoot	≡ peak excursion above the peak value
Damped period	≡ time interval for one cycle of oscillation
Settling time	≡ time for response to settle to within $\pm P\%$ of the steady-state value

These parameters are displayed for a typical underdamped step response in Figure 11.8.

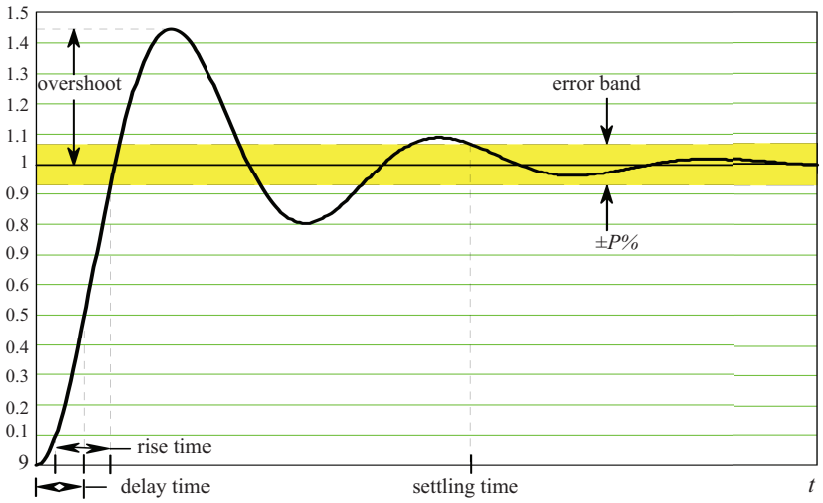

Figure 11.8: Step response for $\zeta = 0.25$.

The quantifying parameters can be obtained through careful analysis of Equation (11.43). One significant parameter, the overshoot, is obtained by setting the first derivative of Equation (11.43) to zero: the resultant time of the first peak is:

$$t_{peak} = \frac{2\pi}{\omega_d} = \frac{2\pi}{\sqrt{1-\zeta^2}\omega_o}. \tag{11.46}$$

The peak value of the step response is given by $X(t_{peak})$:

$$X\left(t_{peak}\right) = A_{of}\left(1 + e^{\frac{-\pi\zeta}{\sqrt{1-\zeta^2}}}\right). \tag{11.47}$$

Which is equivalent to an overshoot of

$$overshoot = e^{\frac{-\pi\zeta}{\sqrt{1-\zeta^2}}} \times 100\%. \tag{11.48}$$

A good amplifier will have small rise, delay and settling times and a small overshoot. Rise and delay time decrease with increased return ratio (D) while overshoot and settling time increase once the system becomes underdamped. The design process balances the conflicting requirements.

Tilt or Sag

It has previously be shown the low-frequency poles tilt the constant portion of a square wave. Amplifiers described by underdamped low-frequency poles also exhibit tilted square wave response. The response of a low-frequency underdamped amplifier to a unit step is given by:

$$X_L(t) = A_{of}\left\{\cos(\omega_{dL}t) - \frac{\zeta\omega_{oL}}{\omega_{dL}}\sin(\omega_{dL}t)\right\}e^{-\zeta\omega_{oL}t}. \tag{11.49}$$

While this response is oscillatory, it can be approximated as

$$X_L(t) \approx A_{of}\{1 - 2\zeta\omega_{oL}t\}, \tag{11.50}$$

for small values of $\omega_{oL}t$. Under these approximations, the percent tilt of a square wave of frequency ω is given by

$$sag \approx \frac{2\zeta\pi\omega_{oL}}{\omega} \times 100\% = \frac{2\zeta\pi f_{oL}}{f} \times 100\%. \tag{11.51}$$

Notice that increasing feedback reduces the resonant frequency and the damping coefficient: the percent tilt will be decreased by each of these reductions.

11.3 MULTIPOLE FEEDBACK FREQUENCY RESPONSE

It has been shown that the frequency response of an amplifier is dependent the pole locations. The application of feedback alters the pole locations and therefore the frequency response. In first and second order systems, the migration of poles is relatively simple to describe: the poles move in a predictable manner and remained in the left-hand plane. As a consequence, single-pole or double-pole feedback amplifiers are always stable. In systems with three or more poles, hereafter identified as *Multipole Amplifiers*, some of the poles migrate into the right-hand plane if sufficiently large quantities of feedback (large return difference) are applied. Multiple amplifiers can become unstable.[2] If, however, the feedback is moderate, multipole amplifiers are stable and extremely useful.

[2]Stability criteria and compensation are discussed in the Sections 11.4 and 11.5.

The high-frequency response of an amplifier that is characterized by three high-frequency poles, ω_1, ω_2, and ω_3, and a mid-band gain, A_o, is given by:

$$A = \frac{A_o}{\left(1 + \frac{s}{\omega_1}\right)\left(1 + \frac{s}{\omega_2}\right)\left(1 + \frac{s}{\omega_3}\right)}. \tag{11.52}$$

When the feedback gain relationship, Equation (11.2), is applied to this triple-pole frequency-dependent gain expression, the resultant feedback gain is given by:

$$A_f = \frac{A_o}{\left(1 + \frac{s}{\omega_1}\right)\left(1 + \frac{s}{\omega_2}\right)\left(1 + \frac{s}{\omega_3}\right) + A_o f}. \tag{11.53}$$

As expected, the midband gain is reduced by the return difference: the new pole locations are obscure. The heuristic approach to pole location migration is shown in Figure 11.9. As can be seen in the figure, the two lower-frequency poles, ω_1 and ω_2, converge and, with sufficient feedback, become a complex conjugate pair. With increased feedback, the highest magnitude pole frequency, ω_3, increases in magnitude and *becomes more distant from the two lower-frequency poles*. This separation of the poles is of particular interest as it indicates that the lower-frequency poles become more dominant poles as feedback increases.

As with the two-pole case, the heuristic approach gives no insight into pole migration once poles become a complex conjugate pair. A root-locus plot is necessary to show the pole migration in the complex plane: Figure 11.10 shows the migration of poles for a third-order system.

The lower-frequency pole pair converge until the damping coefficient associated with the pair is of unity value. At this point, the pair diverges vertically: this migration mimics the two-pole case. However, as feedback is increased and the damping coefficient is reduced further, the pole-pair migrates toward the right-hand plane. With large amounts of feedback, the pole-pair crosses the axis into the right-hand plane and the system becomes unstable. Since small damping coefficients are, in general, undesirable in amplifiers, a quality amplifier with a relatively flat midband region will not sufficiently displace the pole pair to cause instability.

As the number of poles increases, it becomes more difficult to intuitively understand the migration of poles with changes in feedback. Continued application of the heuristic interpretation shows that the lowest pole pair will converge in all cases. Each successive pole pair thereafter will also converge. In odd-order systems, the final highest magnitude frequency pole will move to even higher frequencies. The migration of the poles once they have become complex conjugate pairs is, as usual, determined through the use of a root-locus plot.

There are three simple rules to aid in the construction of an approximate root-locus plot for an amplifier described by high-frequency poles:

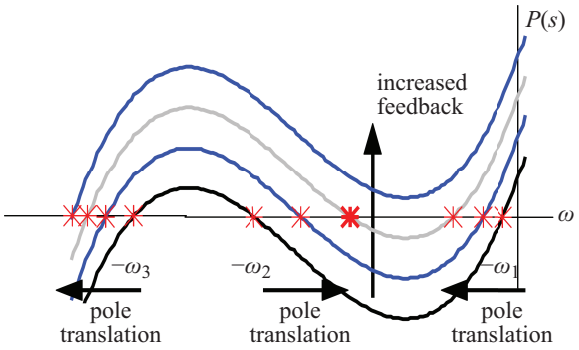

Figure 11.9: Heuristic interpretation of pole migration: third-order system.

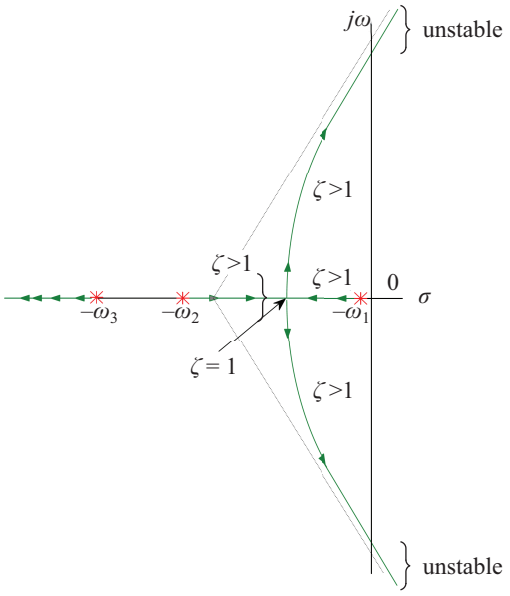

Figure 11.10: Root-locus of a three-pole gain function.

1. The average of the pole frequencies remains unchanged with the application of feedback. It is given as:

$$\sigma_o = \frac{1}{n_p}\sum_{c=1}^{n_p} p_c. \tag{11.54}$$

2. When a pole pair becomes underdamped ($\zeta < 1$) the root-locus for that pair departs from the real axis at an angle of 90°. The location of the departure point is at a zero of the slope of the denominator function, $P(s)$.

3. Each pole-pair root-locus approaches an asymptote that intersects the real axis at σ_o and diverges from the real axis at an angle of:

$$\phi = \pm\frac{180° + m360°}{n_p} \qquad m = 1, 2, \ldots, n_p/2. \tag{11.55}$$

For example, the asymptotes for a third order system are at ±60° and at 180° (seen as dotted lines on Figure 11.10): for a fourth-order system, they are at ±45° and ±135°: for a fifth-order system, at ±36°, ±108°, ±180°.
Some conclusions that can be drawn from these construction rules are:

- The two lowest-frequency poles form a pole pair that will have the greatest significance in determining amplifier high-frequency response.

- Poles that are at higher frequencies than the lowest-frequency pole pair will migrate farther away from the pole pair. For example, in a third-order system, the second and third poles migrate away from each other.

- If the lowest-frequency pole pair is dominant before the application of feedback, it will remain dominant.

The consequence of these conclusions is the treatment of multipole amplifiers as if they were two-pole amplifiers as long as the second and third poles are at least two octaves apart:

$$\left|\frac{\omega_3}{\omega_2}\right| \geq 4. \tag{11.56}$$

The low-frequency response of a feedback amplifier is also approximately determined by its dominant poles: the pole pair that is closest to the midband region.

Example 11.3
A three-pole amplifier with midband gain, $A_o = 1000$, and three high-frequency poles, $f_1 = 100\,\text{kHz}$, $f_2 = 1\,\text{MHz}$, and $f_3 = 6\,\text{MHz}$ has feedback applied so that the midband gain is reduced to

$$A_{of} = 80.$$

Determine the high 3 dB frequency.

Solution

This amplifier is the same as the amplifier of Example 11.1 with the addition of an additional pre-feedback pole at 6 MHz. The ratio of the second and third pole frequencies is given by:

$$\left|\frac{\omega_3}{\omega_2}\right| = \left|\frac{f_3}{f_2}\right| = \frac{6\,\text{MHz}}{1\,\text{MHz}} = 6 \geq 4.$$

The pole pair is dominant and the results of Example 11.1 are approximately valid:

$$f_H \approx 1.43\,\text{MHz}.$$

A computer simulation of the exact response (including all three poles) found the 3 dB frequency to be at $f_H = 1.489\,\text{MHz}$. The approximate result is entirely satisfactory with less than −4% variation in the 3 dB frequency from the exact result. The three feedback amplifier poles can be numerically found to be:

$$p_1 = -0.4332 + j1.054\,\text{MHz} \qquad p_2 = -0.4332 + j1.054\,\text{MHz}$$
$$p_3 = -6.233\,\text{MHz}.$$

Notice that the sum of the feedback poles is −7.1 MHz: the same as the sum of the non- feedback poles.

11.4 STABILITY IN FEEDBACK CIRCUITS

It was shown in Chapter 8 (Book 2) that the benefits of negative feedback were obtained at the expense of reduction in gain by the reduction factor, D. An additional drawback to using feedback in circuits is the possibility of self-oscillation: that is, the amplifier may become an unstable system. In general, a stable electronic system has an output response, that decays to zero with time when excited by any initial energy in the system. The initial energy can take the form of random noise in the power supply rails. A stable system in steady state does not have a time-varying output when the input is zero. An unstable or marginally stable electronic system will have some form of output when the input is zero.

Instability in electronic circuits stems from the fact that the forward gain of the amplifier and reverse gain from the feedback elements may be frequency sensitive. At low and high frequencies, the output voltage may be shifted in phase and changed in magnitude relative to the midband frequencies. At the mixing point in the feedback circuit, the input signal to the circuit and the output signal of the feedback network may, because of this additional phase shift, add rather than subtract which can result in possible oscillation.

Unstable circuit behavior can be visualized by studying Equation 8.5 (Book 2), which is repeated here:

$$A_f(s) = \frac{A(s)}{1 + A(s)\,f}. \tag{11.57}$$

When $A(s)f = -1$, the total gain of the circuit $A_f(s) \to \infty$: a condition that is intolerable in amplifiers and represents an output that is essentially limited by the power rails.[3]

For the loop gain, $A(s)f$, to be negative, the combination of phase shifts by the forward gain and the feedback ratio must cause a summation of in-phase signals at the mixing point of the feedback amplifier. Stable amplifier operation requires that the magnitude of the loop gain, $|A(s)f|$, to be less than unity when its phase angle approaches 180°.[4]

11.4.1 GAIN AND PHASE MARGINS

Amplifier stability can be analyzed using the magnitude and phase verses frequency plots of the loop gain. Figure 11.11 shows the magnitude and phase verses frequency plots of a three- pole loop gain function. The *gain margin* is the difference in gain (in dB) between the 0 dB loop gain (unity magnitude) and the loop gain magnitude at a phase angle, $\angle A(s)f$, of 180° from the midband: that is, $Gain\ Margin = -|A(s)f|_{180^\circ}$ in dB. *A positive value for the gain margin indicates stable amplifier operation*; if the gain margin is near zero, the amplifier is unstable and its output will oscillate without regard to its input.

The *phase margin* is the difference between the loop gain phase angle, $\angle A(s)f$, at $|A(s)f| = 0$ dB (unity magnitude) and $\angle A(s)f = -180^\circ$: that is,

$$Phase\ Margin = \angle A(s)f|_{0\,\mathrm{dB}} + 180^\circ. \tag{11.58}$$

For stable operation, the phase margin must be greater than 0°.

Alternately, the stability of a feedback amplifier can be determined from the difference between the magnitude and phase verses frequency plots of the open-loop gain and the feedback ratio. If the feedback ratio is frequency independent (resistive), $20\log|1/f|$ is a straight horizontal line on the open-loop gain magnitude verses frequency plot. The phase of f is constant for a resistive feedback network. In the midband region, $A(s)$ and f both have the same sign: their phases must be identical at either 0° or 180°. The magnitude of the loop gain (in dB) can be expressed as the difference of the magnitude of the open-loop gain and the magnitude of the inverse of the feedback ratio,

$$20\log|A(s)f| = 20\log|A(s)| - 20\log\left|\frac{1}{f}\right|. \tag{11.59}$$

Equation (11.59) can be used to plot the magnitude and phase verses frequency characteristics for the open-loop gain and the feedback ratio to determine amplifier gain and phase margins for varying values of the feedback ratio, f. Figure 11.12 shows how the plots of the open-loop gain and feedback ratio can be used to determine the gain and phase margins. The phase of the open loop amplifier is plotted as a relative phase difference to the midband phase of $A(s)$. The Figure shows a straight horizontal line (for a resistive network) representing the feedback ratio,

[3]The output voltage is actually limited by the nonlinear regions of the transistor characteristics.
[4]Recall that a 180° phase shift causes a sign change in the signal.

$20\log|1/f|$, superimposed on the magnitude verses frequency plot of the open-loop gain. The loop gain is the difference between the open-loop gain and the inverse of the feedback ratio. The *gain margin* is the difference (in dB) of the inverse of the feedback ratio to the open-loop gain magnitude (in dB) at a phase angle, $\angle A(s)$, of 180°: that is,

$$Gain\ Margin\ (in\ \text{dB}) = 20\log|1/f| - 20\log|A(s)|_{180°}. \tag{11.60}$$

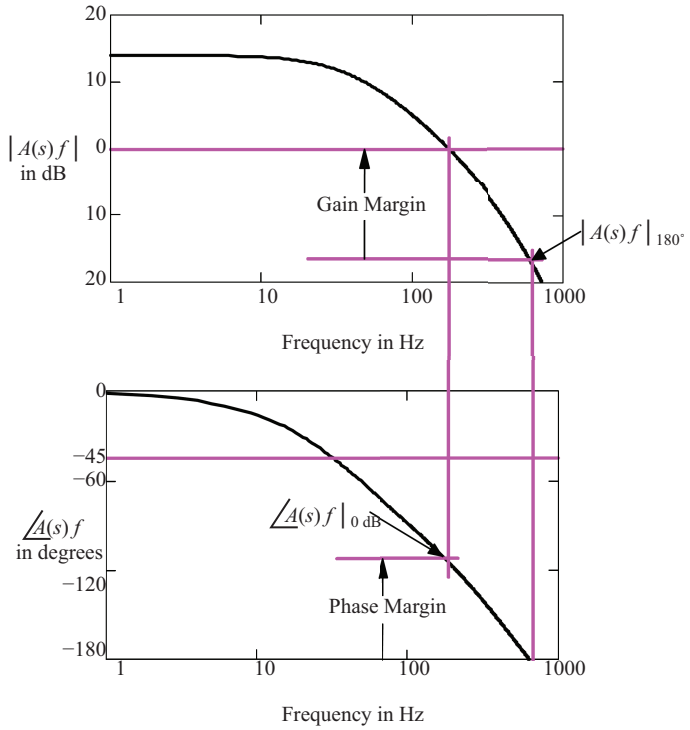

Figure 11.11: Definition of (a) Gain margin and (b) Phase margin.

The *phase margin* is the difference of the phase angle at the intersection of the magnitudes of the open-loop gain and inverse of the feedback ratio to $\angle A(s) = -180°$.
It is common to specify the design of feedback amplifiers with gain and phase margins of greater than 10 dB and 50°, respectively. This assures stable amplifier operation over variations in component parameter values.

The amount of phase margin has a significant effect on the shape of the closed-loop magnitude response of the feedback amplifier. Using the definitions of gain and phase margin, the frequency ω_1 where the loop gain is unity is,

$$A(j\omega_1)\, f = 1 \times e^{-j\theta}, \tag{11.61}$$

where

$$\theta = 180^\circ - (\textit{phase margin}). \tag{11.62}$$

The closed-loop gain at ω_1 is,

$$A_f(j\omega_1) = \frac{A(j\omega_1)}{1 + A(j\omega_1)f} = \frac{\frac{1}{f}e^{-j\theta}}{\left|1 + e^{-j\theta}\right|}. \tag{11.63}$$

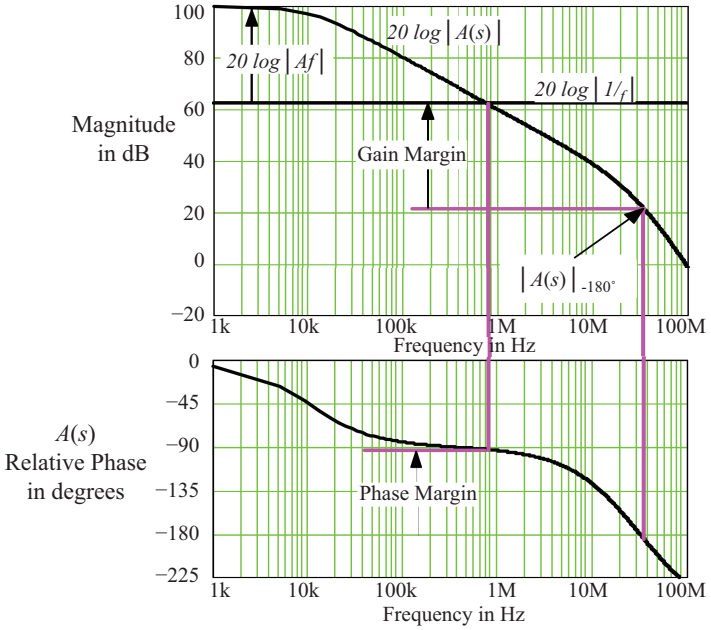

Figure 11.12: Alternate stability analysis technique.

The magnitude of the closed-loop gain is therefore,

$$\left|A_f(j\omega_1)\right| = \frac{\frac{1}{f}}{\left|1 + e^{-j\theta}\right|} = \frac{\frac{1}{f}}{\sqrt{(1+\cos\theta)^2 + \sin^2\theta}}. \tag{11.64}$$

Using Equation (11.64), the magnitude of the closed-loop gain for a 50° phase margin, or $\theta = 180° - 50° = 130°$, is

$$\left|A_f\left(j\omega_1\right)\right| = \frac{\frac{1}{f}}{\sqrt{(1+\cos 130°)^2 + \sin^2 130°}} = \frac{1.18}{f}. \tag{11.65}$$

Equation (11.65) indicates that the magnitude plot of the closed-loop gain will peak by a factor of 1.18, or 1.4 dB, above the midband gain value of $1/f$. For lower phase margins, the peaking in the magnitude plot increases. For example, for a 10° phase margin, the closed-loop gain magnitude plot will peak by 5.7, or 15.1 dB, above the midband gain at frequency at ω_1. For a 90° phase margin, the magnitude plot of the closed-loop gain at ω_1 is 0.707, or −3 dB, of the midband gain.

For a two pole system or a three pole system that is dominated by the two lowest pole frequencies, the phase margin is related to the damping coefficient in Equation (9.17) which is repeated here:

$$\left|A_f\left(\omega_{peak}\right)\right| = \left|A_f\left(\omega_1\right)\right| = \frac{1}{2\zeta\sqrt{1-\zeta^2}}. \tag{11.66}$$

An equation solver may be used to determine ζ in Equation (11.66) for a given phase margin.

Example 11.4

A feedback amplifier has an open loop transfer function,

$$A\left(s\right) = \frac{100\times 10^3}{\left(1+\frac{s}{2\pi\left(10\times 10^3\right)}\right)\left(1+\frac{s}{2\pi\left(200\times 10^3\right)}\right)\left(1+\frac{s}{2\pi\left(20\times 10^6\right)}\right)}$$

and resistive feedback ratio $f = 1/100$.

1. Find the gain and phase margins.
2. Is the amplifier stable?
3. Plot the closed loop gain response.

Solution:

1. The Gain and Phase margins are found by plotting (either asymptotic or computer) the open loop transfer function and the feedback ratio as shown below:

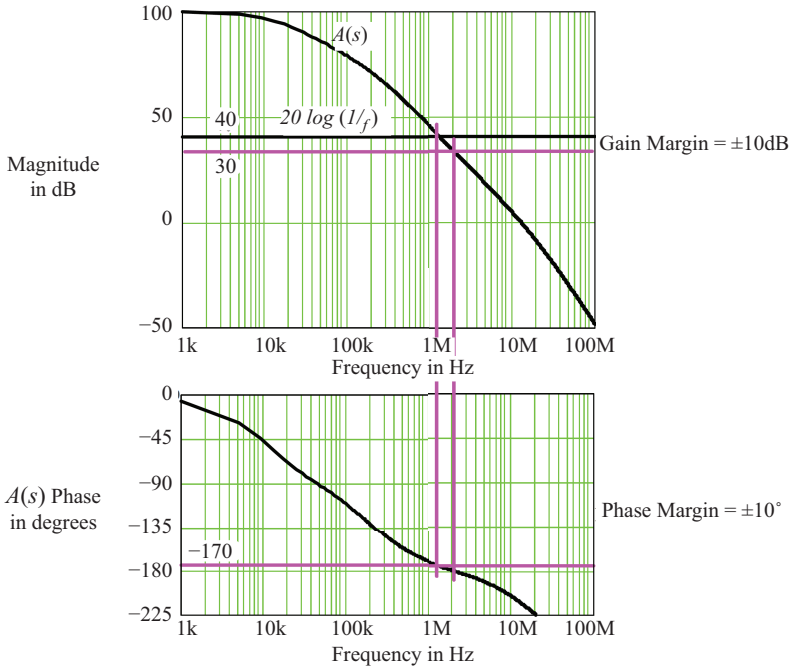

From the frequency plots, the Phase Margin $= +10°$ and Gain Margin $= +10$ dB.

2. The feedback amplifier is just stable since Gain Margin > 0 and Phase Margin > 0. However, since the Phase Margin is less than $+50°$, variations in temperature and component parameters may cause the amplifier to become unstable.

   Since the circuit frequency response has dominant pole characteristics, the approximate analysis discussed in this section may be used to determine the amount of peaking. It was shown in this section that a 10° phase margin corresponded to an amplitude peak of 15.1 dB relative to the midband gain.

3. The closed loop response exhibits peaking of slightly greater than 15 dB above the midband gain.

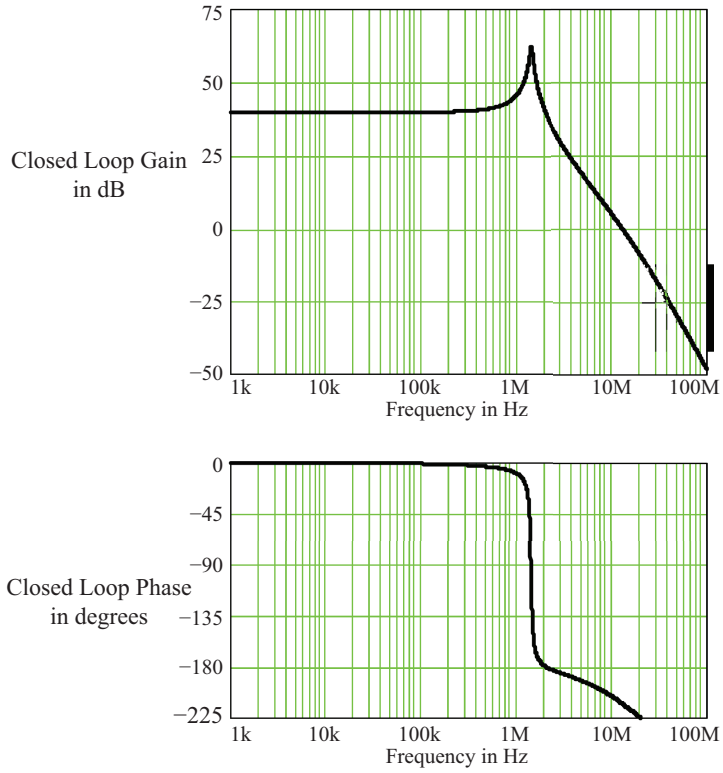

11.4.2 NYQUIST STABILITY CRITERION

An alternate method for analyzing feedback amplifiers was developed by H. Nyquist in 1932. The Nyquist criterion can determine whether a linear amplifier is stable.

A closed-loop feedback amplifier with gain, $A_f(s)$, is stable if it has no poles with positive or zero real parts. Assuming that the open-loop gain and the feedback ratio are stable,[5] only the loop gain $A(s)f$ need be inspected for poles with positive or zero real parts.

The Nyquist diagram is simply a polar plot of $A(s)f$ for s on the contour shown in Figure 11.13a.

The Nyquist diagram maps the right half of the s-plane, shown in Figure 11.13a, into the interior of the contour in the Af plane (Figure 11.13b). If there are zeros of $D(s)$ in the RHP, the Af plane contour will enclose the point $-1\angle 0°$, which is called the critical point. The number of times that the Af plane contour encircles the critical point in a counterclockwise direction is equal to the number of zeros of $D(s)$ with positive real parts.

[5]The open-loop gain in electronic amplifiers are assumed to be stable. However, if the open-loop amplifier contains feedback elements, the open-loop gain must be analyzed for stability. Passive component feedback ratios are stable.

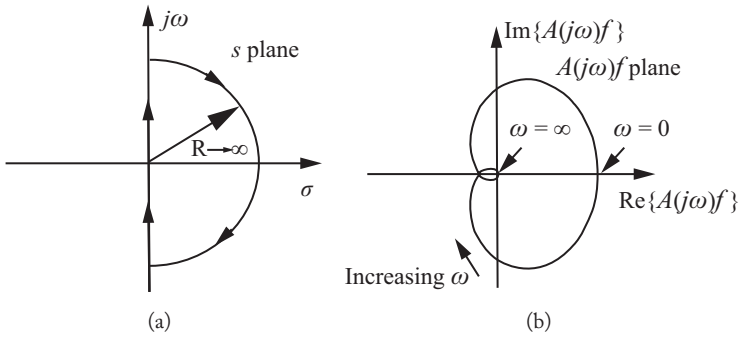

Figure 11.13: (a) Nyquist s-plane contour; (b) $A(j\omega)f$ plane contour for a loop gain with three identical poles.

The behavior of the closed-loop response is determined largely by the nearness of the plot of $A(j\omega)f$ to the -1 point on the Nyquist diagram. Figure 11.14a is a plot of a loop gain response that encircles the critical point and is unstable by the Nyquist criterion. Figure 11.14b is a plot of a stable amplifier whose loop gain response does not encircle the critical point.

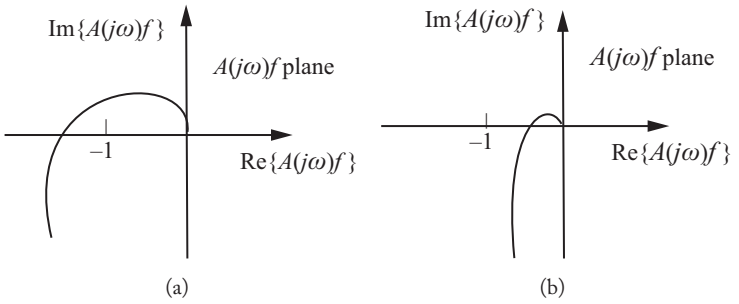

Figure 11.14: (a) Nyquist diagram for a stable loop gain; (b) Nyquist diagram for an unstable loop gain.

The Nyquist diagram can be used to find the gain and phase margins of a feedback amplifier. Since stability is related to the amplifier gain at $-180°$ phase shift, the gain margin and phase margin are defined in a Nyquist diagram as follows (Figure 11.15):

Gain margin: For a stable amplifier, the ratio $1/\alpha$ in dB, where α is the distance from the $-180°$ crossover on the Nyquist diagram (where the plot of $A(j\omega)f$ crosses the negative real axis) to the origin, corresponds to the gain margin: that is, gain margin [dB] $= 20\log|1/\alpha|$. If the Nyquist diagram has multiple $-180°$ crossovers, the gain margin is determined by that point that lies closest to the critical point.

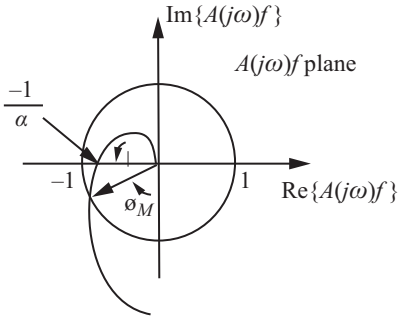

Figure 11.15: Gain margin and phase margin for Nyquist diagram.

Phase margin: For a stable amplifier, the phase margin is the magnitude of the minimum angle ϕ_M between a line from the origin to the point where the Nyquist diagram of $A(j\omega)f$ intersects a circle of unit radius with the center at the origin and the negative real axis.

Example 11.5
A three stage transistor amplifier with feedback was found to have a loop gain frequency response that is approximately

$$A(j\omega)\, f = \frac{5}{\left(1 + \dfrac{j\omega}{2\pi\,(10^4)}\right)^3}.$$

(a) Plot the loop gain on the complex plane.

(b) Is the amplifier stable?

(c) At what frequency does a 180° phase shift occur for the amplifier?

(d) What is the maximum magnitude of the loop gain for stable operation for networks having this form of transfer function?

(e) What are the gain and phase margins?

Solution:

(a) Using MathCAD, the following Nyquist plot was drawn:

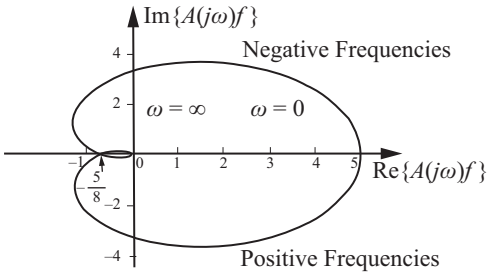

(b) The amplifier is stable since the Nyquist plot does not encircle the $-1 + j0$ point.

(c) From the expression of the loop gain, the intersection of the plot with the negative real axis occurs when the imaginary part of the loop gain is zero. The denominator of the loop gain is expanded to solve for the frequency where the imaginary part of the loop gain is zero,

$$\left[1 + \frac{j\omega}{\omega_o}\right]^3 = \left(1 - 3\frac{\omega^2}{\omega_o^2}\right) + j\left[3\frac{\omega^2}{\omega_o^2} - \frac{\omega^3}{\omega_o^3}\right],$$

where $\omega_o = 2\pi \times (10 \times 10^3)$. This expression is real when,

$$\left[3\frac{\omega^2}{\omega_o^2} - \frac{\omega^3}{\omega_o^3}\right] = 0$$

at the frequency, $\omega_o = 108.8\,\text{krad/s} \Rightarrow 17,320\,\text{Hz}$.

At 17, 320 Hz, the loop gain is,

$$|A(j\omega)\,f|_{\omega=108.8\,\text{krad/s}} = \frac{5}{1 - 3\dfrac{\omega^2}{\omega_0^2}} = \frac{5}{1 - 3\left(\dfrac{108.8 \times 10^3}{2\pi\,(10 \times 10^3)}\right)} = -\frac{5}{8}.$$

This value is greater than -1, and as is evident from the plot of the loop gain, no encirclement of $-1 + j0$ occurs at this value of gain.

(d) The gain can be increased by 8/5 before $-1 + j0$ is intersected. Therefore, the condition for absolute stability for amplifiers having this form of loop gain transfer function is,

$$|A(j\omega)\,f| < \left(\frac{8}{5}\right)5 = 8.$$

However, by doing so, there will no longer be any margin for stability and the amplifier transient response will become increasingly oscillatory as this limiting value of gain is approached.

(e) From part (c), $\alpha = 5/8$ and $20\log(5/8)^{-1} = 4.08\,\text{dB}$ is the gain margin. Data from the Nyquist plot shows $A(j\omega)f = 1$ at $\omega = 87.5\,\text{krad/s} \Rightarrow 13.88\,\text{kHz}$ and $\angle A(j\omega)f = 17.3°$. The phase margin is $|\angle A(j\omega)f - 180°| = 168°$.

11.5 COMPENSATION NETWORKS

Feedback amplifiers have been shown to be unstable if they are characterized by negative phase margins. In negative feedback amplifiers, the potential for instability is present when the amplifier open-loop (loaded basic forward) transfer function has three or more poles. Unstable amplifiers can be stabilized by:

- Decreasing the loop gain, Af, of the amplifier
- Adding a compensation network to the amplifier to shape the loop gain frequency response characteristic so that the phase and gain margins are positive and in the acceptable range (desirable phase margin $\geq 50°$ and gain margin ≥ 10 dB).

Careful design is required in each of these cases to ensure stable amplifier operation over temperature and parameter variations.

In many cases, decreasing the loop gain to achieve stability is not acceptable due to bias or amplifier gain constraints. Alternately, the designer many not have control over f, as in the case of OpAmp circuits. Here the amplifier must operate over a wide range of feedback ratios determined by the user rather than the designer of the OpAmp. In such cases, compensation networks are added to the amplifiers to increase gain and phase margins.

The placement of compensation networks in feedback amplifiers is of some importance. The basic topology of the negative-feedback amplifier of Figure 8.1 (Book 2) is repeated in Figure 11.16a. The triangle symbol is a linear amplifier of gain A, and the rectangular symbol is the feedback network of feedback ratio f. *The compensation network must be placed in the signal path of the linear amplifier and the feedback network,* as shown in Figure 11.16b. Depending on the feedback topology, the compensation network could be placed between amplifier stages internal to a multi-stage linear amplifier or at the output of a linear amplifier. It is necessary that the signal pass through the amplifier, compensation network, and the feedback network.

Compensation networks add poles or a combination of poles and zeros to the loop gain transfer characteristic to achieve desired gain and phase margins. The following compensation techniques and their passive-component circuit implementations are presented in this section:

- Dominant Pole,
- Lag-Lead,
- Lead,
- Phantom Zero.

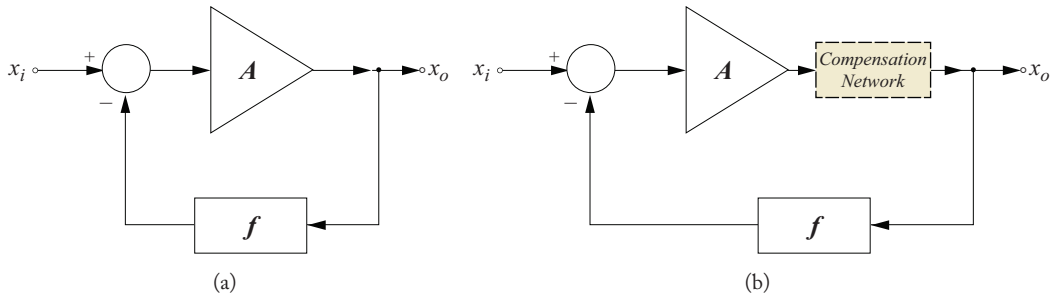

Figure 11.16: (a) Basic negative feedback topology; (b) Compensation network added to the negative feedback topology.

11.5.1 DOMINANT POLE (LAG) COMPENSATION

The simplest form of compensation adds an additional dominant (real) pole in the transfer characteristic of the open-loop amplifier gain. The transfer function of the dominant pole compensation network is,

$$H_{DP}(s) = \frac{1}{1 + \dfrac{s}{\omega_p}},$$

where the pole location of the network, ω_p, is significantly smaller than the poles of the uncompensated amplifier: $\omega_p << \omega_{p1}, \omega_{p2}$.

When this compensation network is added to the circuit, the open-loop gain becomes

$$A_{comp}(s) = A(s) H_{DP}(s) = \frac{A(s)}{1 + \dfrac{s}{\omega_p}}. \tag{11.67}$$

The dominant pole added by the compensation network is chosen so that the loop gain, $|A_{comp}(s) f|$ is 0 dB at a frequency where the poles of the uncompensated open-loop gain $A(s) f$ contribute negligible phase shift. Typically, the compensation network adds a dominant pole that reduces the compensated loop gain to unity (0 dB gain) at the lowest high-frequency pole, ω_{p1}, of the open-loop amplifier. The compensation network causes a phase "lag" in the signal path. Therefore, the phase of the compensated loop gain is shifted lower in frequency which results in increased gain and phase margins.

The method for finding the frequency of the dominant pole can be visualized as in Figure 11.17. The dominant pole of the compensation network is designed so that its transfer function has a gain of 0 dB at the first pole frequency of the uncompensated loop gain, with a slope of −20 dB/decade. The dominant pole frequency of the compensation network, ω_p, is found through

the following relationship:

$$0 = 20\log|A_{midband}\,f| - 20\log\left(\frac{\omega_{p1}}{\omega_p}\right), \tag{11.68a}$$

or simply

$$\omega_p = \frac{\omega_{p1}}{A_{midband}\,f}. \tag{11.68b}$$

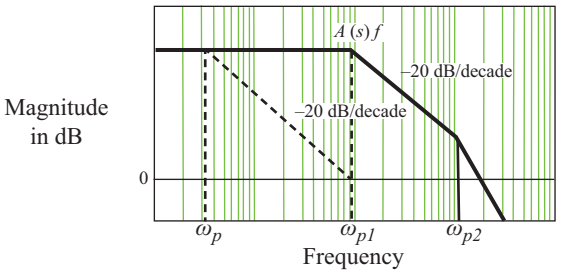

Figure 11.17: Construction technique for dominant-pole location.

A small-signal model of the amplifier can be used to determine the (loaded basic forward) open-loop transfer function. However, the transfer function of an open-loop amplifier becomes increasingly cumbersome for open-loop characteristics with more than three poles. Therefore, it may be preferable to use SPICE computer simulations to provide a graphical output of the compensated loop gain transfer characteristic from which the new pole locations can be found.

A simple dominant-pole compensation network, shown in the shaded area of Figure 11.18, is added to the open-loop amplifier. As stated previously, the compensation network could, depending on the feedback topology, reside within the open-loop amplifier so that the signal passes through the linear amplifier, compensation network, and feedback network. Here, the dominant pole of the compensated open-loop amplifier transfer function is

$$\omega_p \approx \frac{1}{(R_p + R_o)\,C_p}, \tag{11.69}$$

where R_o is the output resistance of the open-loop amplifier.
The procedure for designing a dominant pole compensation network is as follows:

1. Determine the midband loop gain.
2. Find the dominant high-frequency pole, f_{p1}, or high 3-dB bandwidth of the loop gain transfer characteristic.

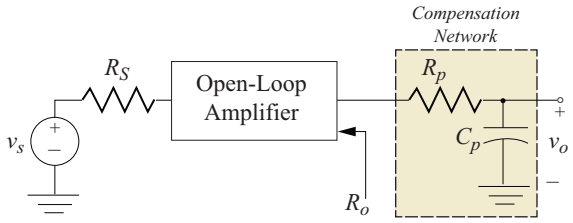

Figure 11.18: Dominant pole compensation network at output terminal of open-loop amplifier.

3. Design the dominant pole of the compensation network such that the compensated loop gain drops to 0 dB, with a slope of −20 dB/decade, at the uncompensated high 3-dB cutoff frequency.

The dominant-pole compensation network is a simple low-pass filter with a cutoff frequency, f_{p1}, that is significantly lower than the 3-dB frequency (f_H) of the open-loop amplifier. Therefore, the dominant-pole compensation network yields *greater phase margin at the expense of bandwidth.*

Example 11.6

Consider the OpAmp inverting amplifier shown. The open-loop gain of the amplifier is:

$$R_M(s) = \frac{-10^4}{\left(1+\frac{s}{2\pi\,(10^6)}\right)\left(1+\frac{s}{2\pi\,(10\times 10^6)}\right)\left(1+\frac{s}{2\pi\,(40\times 10^6)}\right)}.$$

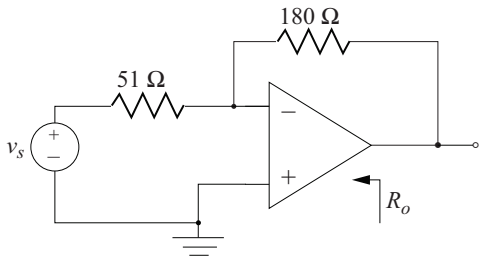

The input and output resistances of the OpAmp are $R_o = 75\,\Omega$ and $R_i = 1\,\text{M}\Omega$, respectively.

Find the gain and phase margins and, if necessary, compensate the circuit using a dominant-pole compensation network.

Solution

Since the feedback topology of the amplifier is a shunt-shunt configuration, the feedback ratio is $f = -1/R_2 = -1/180$. The gain and phase versus frequency plots of the loop gain, $R_M f$, shown essentially zero gain and phase margins. Therefore, the amplifier is unstable in its current configuration.

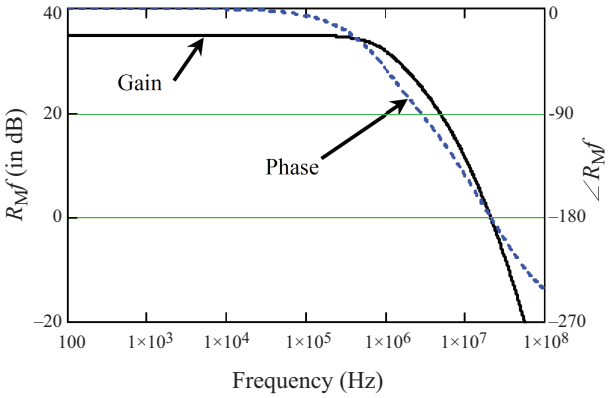

A dominant-pole compensation network is used to stabilize the amplifier. The pole location of the compensation network is found by following the suggested dominant-pole compensation network design procedure in this section.

The dominant-pole frequency of the uncompensated loop gain, equal to the dominant pole of the open-loop amplifier, is 1 MHz. The midband loop gain is 34.9 dB. The compensation network is designed so that the magnitude of the loop gain at 1 MHz is 0 dB. Since the compensation network has a slope of −20 dB/decade, the location of the dominant pole, f_p, of the compensation network is easily found by using the following formula:

$$0 = 20\log|R_{M,midband}\, f| = 20\log\left(\frac{10^6}{f_p}\right),$$

where $R_{M,midband} = 34.9\,\text{dB}$. Solving for f_p yields $f_p = 18.0\,\text{kHz}$.

The compensation circuit has a dominant pole at $f_p = 18.0\,\text{kHz}$. The component values of the compensation network are found for $R_p = 0$ and $R_o < R_2$ to ensure that the feedback resistor does not influence the dominant pole of the compensation network. The capacitance of the compensation network is therefore

$$C_p = \frac{1}{2\pi f_p R_o} = \frac{1}{2\pi\left(18\times 10^3\right)75} = 0.12\,\mu\text{F}.$$

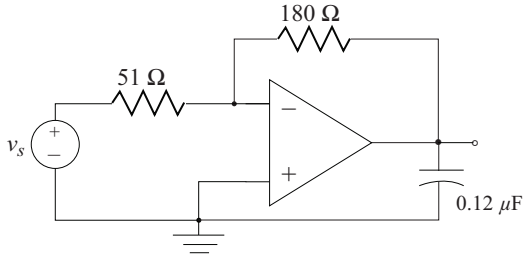

The compensated amplifier is as shown above. The gain and phase response plots for the feedback amplifier before and after compensation are also shown below. The *uncompensated amplifier oscillation at* 21 MHz of is easily observed. The compensated amplifier has a much smoother gain profile and is clearly stable; however, the high 3-dB frequency is significantly reduced: for this example to 1.33 MHz. Also noticeable in the compensated frequency is a "bump." Such bumps are difficult to predict exactly in multipole system, but, if necessary, can be completely eliminated by further reducing the compensation pole frequency, f_p. In this example, the bump is eliminated by reducing f_p by a factor of approximately two which results in a high 3-dB frequency $\approx$ 750 kHz.

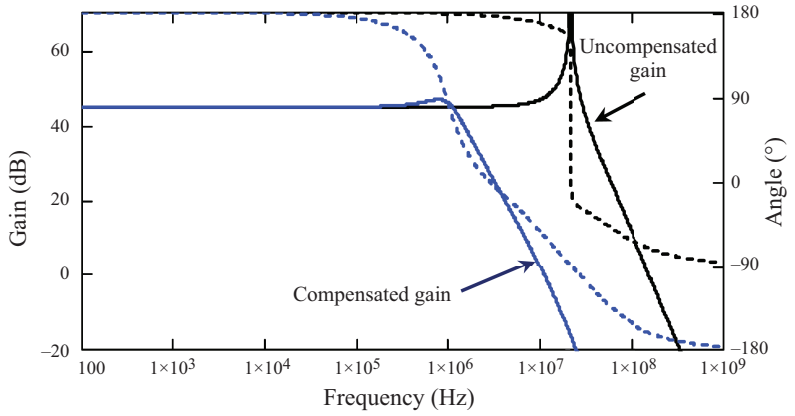

Example 11.7

Given the two-stage shunt-series feedback amplifier shown, find the gain and phase margins. If necessary, compensate the circuit using a dominant-pole compensation network. The capacitors C_S, C_p, C_{E1}, and C_{E2} are very large and contribute only to the lower 3-dB frequency.

The BJT SPICE model parameters are $BF = 200, CJE = 35.5$ pF, $CJC = 19.3$ pF, and $TF = 477$ ps.

Solution

DC analysis results in the quiescent values for the circuit: $I_{CQ1} = 1.8$ mA, $V_{CEQ1} = 2.0$ V, $I_{CQ2} = 2.3$ mA, and $V_{CEQ2} = 5.7$ V.

The loop gain frequency characteristics are found with SPICE using the following circuit shown. The circuit is modified to take into account the loading due to the feedback elements. The input voltage source has been converted to a Norton source as required for shunt-series amplifier analysis.

The input and output loading effects due to the feedback network are $R_{F1} = R_F + R_{E2} = 3\,\text{k}\Omega$ and $R_{F2} = 1\,\text{k}\Omega$, respectively. The large capacitor C_F is used to block the DC voltages in order to maintain the bias conditions.

11.5.2 LAG-LEAD (POLE-ZERO) COMPENSATION

Although dominant-pole (lag) compensation is successful in reducing the loop gain to 0 dB before the phase shift of the open-loop amplifier becomes excessive, the amplifier bandwidth is significantly reduced. In many cases, design specifications may call for maximum bandwidth and a specified closed-loop gain. The lag-lead compensation network, which introduces both a pole and a zero, will usually yield a wider bandwidth amplifier than a dominant-pole network. The transfer function of the lag-lead network is

$$H_{LL}(s) = \frac{1 + \dfrac{s}{\omega_z}}{1 + \dfrac{s}{\omega_p}}, \qquad \omega_p < \omega_z, \tag{11.70}$$

where ω_z is the zero location and ω_p is the pole location of the lag-lead network.

The lag-lead compensated open-loop gain is then

$$A_{comp}(s) = H_{LL}(s)\,A(s) = A(s)\,\frac{1 + \dfrac{s}{\omega_z}}{1 + \dfrac{s}{\omega_p}}. \tag{11.71}$$

The zero is chosen to be at the same frequency as the smallest high-frequency pole of the open-loop amplifier transfer function. This choice has the effect of increasing the compensated bandwidth over the simple dominant-pole compensated amplifier. For example, given an open loop gain transfer function

$$A(s) = \frac{A_{midband}}{\left(1 + \dfrac{s}{\omega_{p1}}\right)\left(1 + \dfrac{s}{\omega_{p2}}\right)\left(1 + \dfrac{s}{\omega_{p3}}\right)}. \tag{11.72}$$

Here ω_{p1} is the smallest high-frequency pole. The lag-lead compensated transfer function becomes

$$A_{comp}(s) = H_{LL}(s)\,A(s) = A(s)\,\frac{1 + \dfrac{s}{\omega_z}}{\left(1 + \dfrac{s}{\omega_{p1}}\right)\left(1 + \dfrac{s}{\omega_{p2}}\right)\left(1 + \dfrac{s}{\omega_{p3}}\right)}. \tag{11.73}$$

The smallest pole of $A(s)$ is canceled by setting the zero of the lag-lead network at the same point; that is,

$$\omega_z = \omega_{p1}. \tag{11.74}$$

The open-loop gain becomes a three-pole transfer function with a new dominant pole, ω_p:

$$A(s) = \frac{A_{midband}}{\left(1 + \frac{s}{\omega_p}\right)\left(1 + \frac{s}{\omega_{p2}}\right)\left(1 + \frac{s}{\omega_{p3}}\right)}. \tag{11.75}$$

Figure 11.19 is a graphical visualization of the method for finding the dominant pole of the lag-lead compensation network. The dominant pole of the compensation network is designed so that its transfer function has a gain of 0 dB at the second pole frequency of the uncompensated loop gain, with a slope of −20 dB/decade. The dominant pole frequency of the compensation network, ω_p, is found through the following relationship:

$$0 = 20\log|A_{midband}\, f| - 20\log\left(\frac{\omega_{p2}}{\omega_p}\right), \tag{11.76a}$$

or

$$\omega_p = \frac{\omega_{p2}}{A_{midband}\, f}. \tag{11.76b}$$

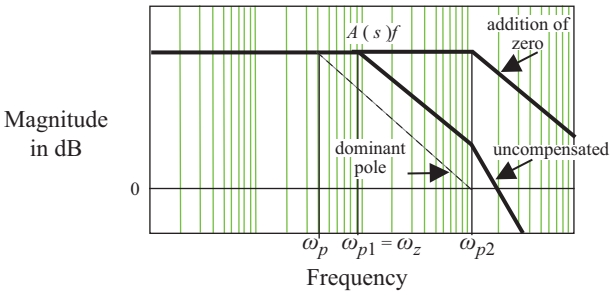

Figure 11.19: Construction technique for finding lag-lead compensation pole and zero location.

The result of the introduction of a zero, in addition to the dominant pole, in the lag-lead compensation network, is an increase in open-loop (and therefore in the closed-loop) bandwidth.

A lag-lead compensation network implementation is shown in Figure 11.20. As stated previously, the compensation network could, depending on the feedback topology, reside within the open-loop amplifier so that the signal passes through the linear amplifier, compensation network,

and feedback network. The dominant pole of the compensated open-loop amplifier transfer function is,

$$\omega_p = \frac{1}{(R_a + R_b + R_o)\, C_c}, \tag{11.77}$$

where R_a is the output resistance of the open-loop amplifier. The zero of the compensation network is located at the lowest pole of the open-loop amplifier to increase the loop gain bandwidth,

$$\omega_z = \omega_{p1} = \frac{1}{R_b C_c}. \tag{11.78}$$

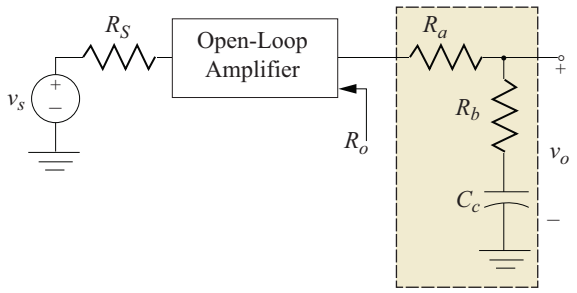

Figure 11.20: Lag-lead compensation network at the output terminal of the open-loop amplifier.

The Bode diagrams for the transfer function of the lag-lead compensation network are shown in Figure 11.21.
The procedure for designing a lag-lead compensation network is:

1. Find the midband loop gain.
2. Find the dominant high frequency pole, ω_{p1}, or high 3 dB bandwidth of the loop gain transfer characteristic.
3. Find the second to the lowest pole, ω_{p2} .
4. Design the compensation network so that the compensated loop gain drops to 0 dB, with a slope of −20 dB/decade, at ω_{p2} of the uncompensated loop gain characteristics.
5. Design the compensation network so that the zero of the network is at ω_{p1} of the uncompensated loop gain characteristic.
6. In some cases, the zero location may have to be changed due to interactions with the reactive components of the open-loop amplifier.

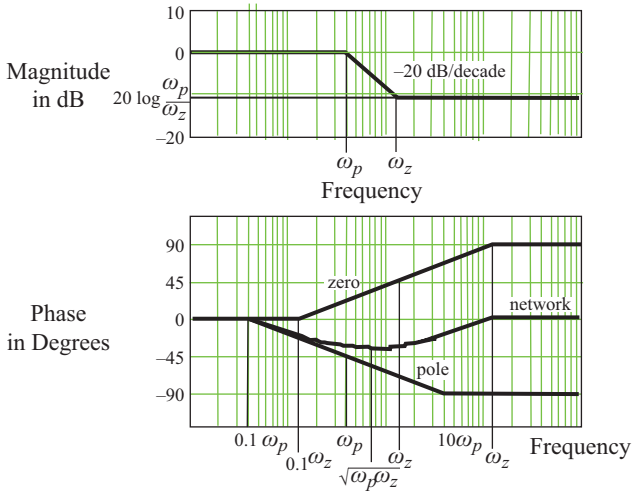

Figure 11.21: Bode diagrams for the lag-lead compensation network.

There is no loop gain magnitude penalty when using a lag-lead compensation network.

Example 11.8
Compensate the unstable OpAmp inverting amplifier of Example 11.6 using a lag-lead compensation network.

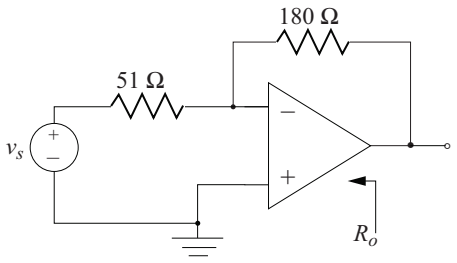

Solution:

The open-loop gain of the amplifier was given as:

$$R_M(s) = \frac{-10^4}{\left(1+\frac{s}{2\pi\left(10^6\right)}\right)\left(1+\frac{s}{2\pi\left(10\times10^6\right)}\right)\left(1+\frac{s}{2\pi\left(40\times10^6\right)}\right)},$$

and the input and output resistances of the OpAmp are $R_o = 75\,\Omega$ and $R_i = 1\,\text{M}\Omega$, respectively.

Lag-lead compensation introduces a zero at the first pole of the open-loop gain and a pole at a fraction of the second pole frequency.

$$f_z = f_{p1} = 1\,\text{MHz} \quad \text{and} \quad f_{pc} = \frac{f_{p2}}{A_{midband}\, f} = \frac{10 \times 10^6}{(55.56)} = 180\,\text{kHz}.$$

If one makes the design decision, $C_c = 3\,\text{nF}$, the compensation network resistors can be calculated to be:

$$R_b = \frac{1}{(2\pi \times 10^6)\, C_c} = 53.0\,\Omega \quad \text{and} \quad R_a = \frac{1}{(2\pi \times 180 \times 10^3)\, C_c} - R_b - R_o = 167\,\Omega,$$

both of which are standard values. Shown below is the circuit diagram for the compensated amplifier. Note that the compensation network lies within the feedback loop.

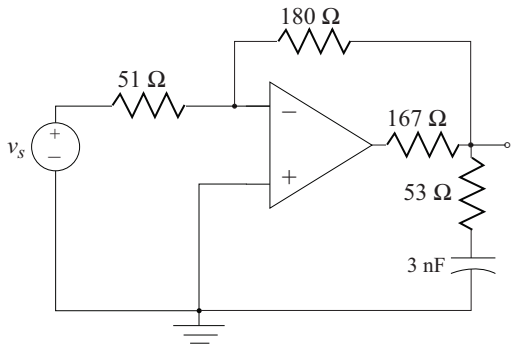

Shown below are the Bode response plots for the uncompensated amplifier and the compensated amplifier. As was the case in Example 11.6, the compensated amplifier has a much smoother gain profile and is clearly stable; however, the high 3-dB frequency is significantly higher than for dominant-pole compensation. For this example the high 3-dB frequency is 13.3 MHz: approximately a factor of ten higher.

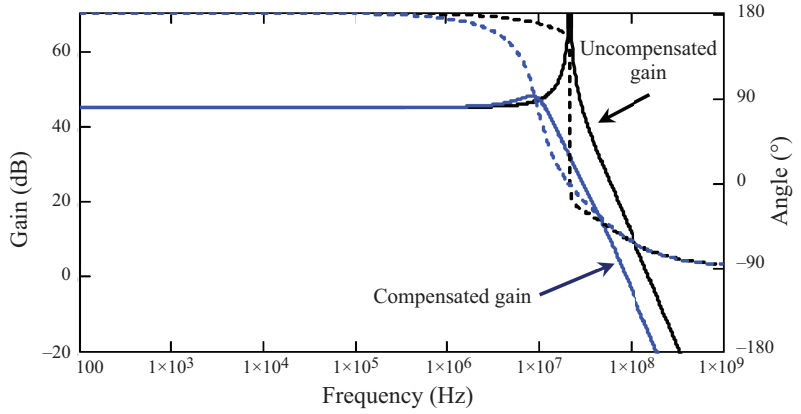

11.5.3 LEAD COMPENSATION (EQUALIZER)

The midband loop gain is often fixed by the specifications on the closed-loop gain and bandwidth of an amplifier. If a dominant pole (or a lag-lead) network results in a bandwidth that is too narrow, an alternate solution must be found. Since stability depends only on the phase margin, a compensation network that would introduce phase *lead* at this point would be the desired alternate solution. A simple lead network, or equalizer, has a transfer function,

$$H_{EQ}(s) = \frac{s + \omega_{eqz}}{s + \omega_{eqp}}, \qquad \omega_{eqp} >> \omega_{eqz}. \tag{11.79}$$

Note that the transfer function of the lead compensation network is similar to the lag-lead compensation characteristics in Equation (11.69), except that here the pole occurs at a higher frequency than the zero.

Using Equation (11.76), the lag-lead compensated open-loop gain is,

$$A_{comp}(s) = H_{EQ}(s)\, A(s) = A(s)\, \frac{s + \omega_{eqz}}{s + \omega_{eqp}}. \tag{11.80}$$

The zero is chosen *at the second high-frequency pole location* of the loop gain transfer function, $\omega_{eqz} = \omega_{p2}$. The pole location is chosen to be significantly large so that ω_{eqp} does not affect the bandwidth of the loop-gain. This choice has the effect of increasing the compensated bandwidth over both the dominant pole and lag-lead compensated amplifiers. However, there is a gain penalty that is incurred when using lead compensation networks. The midband gain yields,

$$H_{EQ}(0) = \frac{\omega_{eqz}}{\omega_{eqp}}. \tag{11.81}$$

This attenuation must be taken into account since it directly impacts midband gain.

Figure 11.22 is a graphical visualization of the method for finding the zero of the lead compensation network. The zero of the compensation network is designed so that its transfer function has zero at the second pole frequency of the uncompensated loop gain, with a slope of −20 dB/decade, $\omega_{eqz} = \omega_{p2}$. The zero frequency of the compensation network is found through the following relationship:

$$0 = 20\log|A_{midband}| - 20\log\left(\frac{\omega_{p1}}{\omega_z}\right), \tag{11.82a}$$

or simply,

$$\omega_z = \frac{\omega_{p1}}{A_{midband}}. \tag{11.82b}$$

For example, if an open-loop transfer function has the form,

$$A(s) = \frac{A_{midband}}{\left(1 + \frac{s}{\omega_{p1}}\right)\left(1 + \frac{s}{\omega_{p2}}\right)\left(1 + \frac{s}{\omega_{p3}}\right)}, \tag{11.83}$$

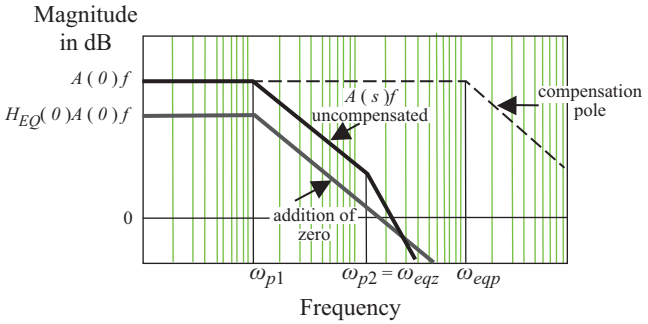

Figure 11.22: Construction technique for finding the lead compensation pole and zero locations.

where ω_{p1} is the smallest pole, the lead compensated loop-gain transfer function becomes,

$$A_{comp}(s)\, f = \frac{A_{midband} H_{EQ}(0)\, f \left(1 + \dfrac{s}{\omega_{eqz}}\right)}{\left(1 + \dfrac{s}{\omega_{eqp}}\right)\left(1 + \dfrac{s}{\omega_{p1}}\right)\left(1 + \dfrac{s}{\omega_{p2}}\right)\left(1 + \dfrac{s}{\omega_{p3}}\right)}. \tag{11.84}$$

The second lowest pole of $A(s)$ is canceled by setting the zero of the lead network at the same point; that is,

$$\omega_{eqz} = \omega_{p2}. \tag{11.85}$$

The lead network cancels the second-lowest amplifier pole. The pole in the lead compensation network is chosen to be large enough so that it has little effect on the phase margin. The open-loop gain becomes the three-pole transfer function,

$$A_{comp}(s)\, f = \frac{A_{midband} H_{EQ}(0)\, f}{\left(1 + \dfrac{s}{\omega_{eqp}}\right)\left(1 + \dfrac{s}{\omega_{p1}}\right)\left(1 + \dfrac{s}{\omega_{p3}}\right)}, \tag{11.86}$$

where $\omega_{eqp} >> \omega_{p3} > \omega_{p1}$ or if ω_{p1} is dominant, $\omega_{p3} >> \omega_{eqp} >> \omega_{p1}$. The introduction of a zero in the lead compensation network results in an increase in open-loop (and therefore in the closed-loop) bandwidth.

A lead compensation network implementation is shown in Figure 11.23. As stated previously, the compensation network could, depending on the feedback topology, reside within the open-loop amplifier so that the signal passes through the linear amplifier, compensation network, and feedback network. The zero of the compensation network is located at the second lowest pole frequency of the open-loop amplifier characteristics to increase bandwidth,

$$\omega_{eqz} = \frac{1}{R_a C_c}. \tag{11.87}$$

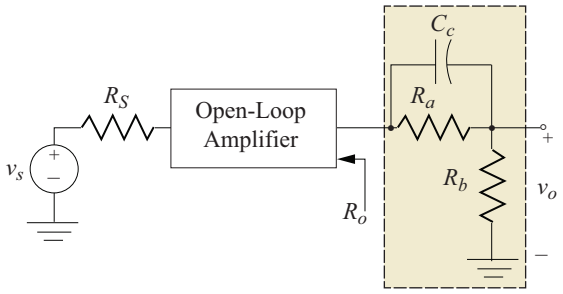

Figure 11.23: Lead compensation network at output terminal of open-loop amplifier.

The pole location of the compensation network,

$$\omega_{eqp} = \frac{1}{(R_a // R_b)\, C_c} \tag{11.88}$$

is chosen to be significantly large so as to have minimal effect the loop gain crossover point (0 dB point). Using Equations (11.81), (11.87), and (11.88), yields the expression for the attenuation due to the compensation network,

$$H\,(0) = \frac{R_b}{R_a + R_b}. \tag{11.89}$$

The actual output signal attenuation taking into account the output resistance of the open-loop amplifier is,

$$H'\,(0) = \frac{R_b}{R_o + R_a + R_b}. \tag{11.90}$$

The resistor values must be carefully selected so that the closed-loop amplifier gain is acceptable.

The Bode diagrams for the transfer function of the lead compensation network are shown in Figure 11.24.

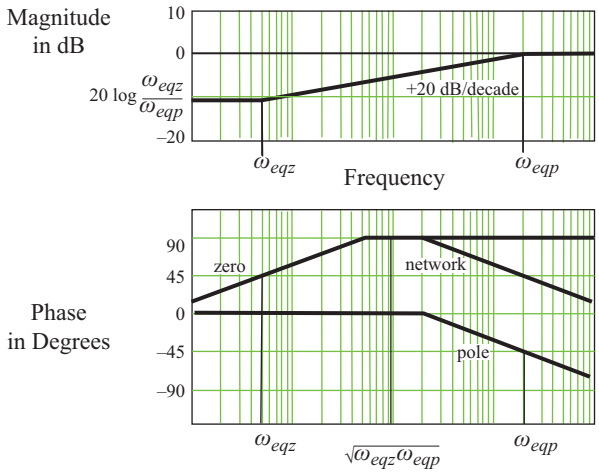

Figure 11.24: Bode diagrams for the lead compensation network.

Example 11.9

Compensate the unstable OpAmp inverting amplifier of Example 11.6 using a lead compensation network.

Solution

The open-loop gain of the amplifier was given as:

$$R_M(s) = \frac{-10^4}{\left(1+\frac{s}{2\pi\,(10^6)}\right)\left(1+\frac{s}{2\pi\,(10\times 10^6)}\right)\left(1+\frac{s}{2\pi\,(40\times 10^6)}\right)},$$

with output resistance, $R_o = 75\,\Omega$.

Lead compensation requires that a zero be inserted at the second pole frequency and a pole at a frequency higher than the third pole frequency. The significant equations are:

$$f_z = f_{p2} = \frac{1}{2\pi R_a C_c} \quad \text{and} \quad f_{pc} = \frac{1}{2\pi\,(R_a // R_b)\,C_c}.$$

With the design choice $C_c = 0.2\,\text{pF}$ and $f_{pc} = 2f_{p3} = 80\,\text{MHz}$, the resistor values in the circuit of Figure 11.23 are determined to be:

$$R_a = 79.6\,\text{k}\Omega \quad \text{and} \quad R_b = 11.4\,\text{k}\Omega.$$

Shown below are the Bode response plots for the uncompensated amplifier and the compensated amplifier. The compensated amplifier has a very smooth gain profile and is clearly stable.

The high 3-dB frequency is approximately the same as for lag-lead compensation: it is approximately 10.5 MHz for this case. The gain reduction suffered by the design choices for the lead compensation network was approximately 1 dB: a reduction from 44.95 dB to 43.94 dB.

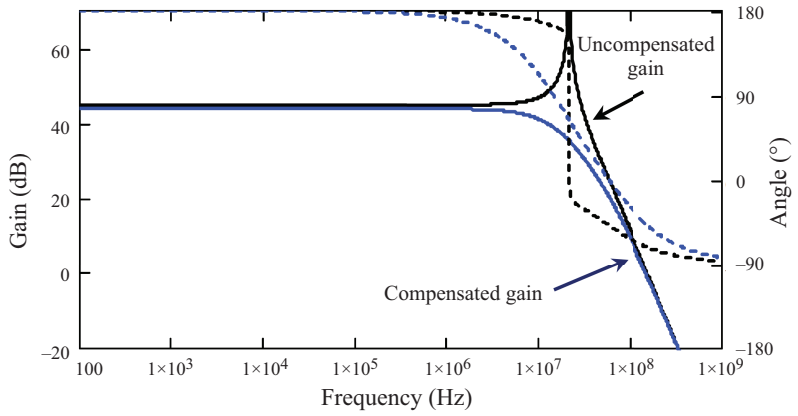

11.5.4 PHANTOM ZERO COMPENSATION

Instead of shaping the open-loop transfer characteristics of an amplifier, the loop gain may be altered by the addition of reactive elements in the feedback network, f, for compensating a feedback amplifier. The use of the reactive elements in the feedback circuit is essentially equivalent to adding lead compensation: the locations of the zero and the pole for a phantom compensation network are the same as that of the lead compensation network. Figure 11.25 shows phantom zero compensation for a shunt-shunt feedback amplifier. The shaded area in the figure constitutes the phantom compensation network. Note that removal of the capacitor, C_f, results in a simple resistive shunt-shunt feedback amplifier.

Another slightly different version of phantom zero compensation is the Miller compensation method shown in Figure 11.26. In the Miller compensation method, a capacitor, C_f, is placed in shunt between the collector and base (drain and gate for FETs) of an internal transistor amplifier stage that establishes the amplifier's lowest high frequency pole, ω_{p1}. The effect will be an increase in the input capacitance due to Miller's effect, which in turn, reduces ω_{p1} and results in a dominant pole.

The advantage of Miller's compensation is the reduction of the capacitance value compared to the techniques shown in Sections 11.5.1–11.5.3. The small value of C_f is multiplied by the Miller-effect factor (amplifier gain) resulting in a much larger capacitance value. Since small values of C_f can be used, Miller's compensation may be used in integrated circuit design.

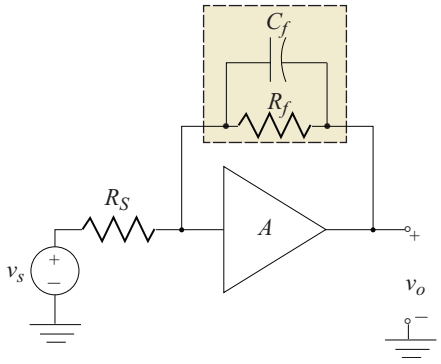

Figure 11.25: Phantom zero compensation for a shunt-shunt feedback amplifier.

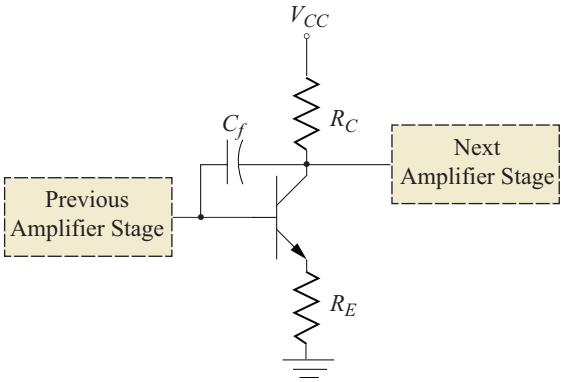

Figure 11.26: Miller's compensation method using shunting capacitor.

11.6 CONCLUDING REMARKS

Frequency response of feedback amplifiers is discussed in this chapter. The effects of feedback on the poles in the low and high frequency regions were investigated. It was shown that pole locations changed with feedback. In particular, the low frequency pole decreased with increased return ratio and the high frequency pole increased with increased return ratio. This "pole-splitting" phenomenon was discussed for single, double, and multipole feedback frequency responses.

Time domain effects of feedback were also shown to be dependent on the return ratio. The rise and delay times (with step inputs) decrease with increased return ratio, while overshoot and settling times increase once the amplifier becomes underdamped. Increased feedback proved to reduce the damping coefficient in double pole feedback amplifiers resulting in a decrease in the percent tilt.

The root-locus method was introduced as a tool to analyze the pole behavior with feedback. A simple set of rules was established to aid in the construction of approximate root-locus plots of amplifiers described by high-frequency poles. The concept of dominant poles was used to simplify amplifier frequency characteristics when applicable.

The stability of amplifiers was investigated. Stable systems were defined and the conditions for instability discussed. Design goals for stability were related to frequency response analysis (or Bode plots). Gain and phase margins were defined and used to quantify stability. An alternate method, developed by Nyquist, for determining stability was also discussed.

Methods to compensate for unstable amplifiers were established. These methods include the addition of electrical networks to shift the pole locations of the amplifiers. The trade-offs for each compensation technique were presented.

Summary Design Example: Fiber-Optic Transimpedance Preamplifier

Fiber-optic receivers consist of a photodiode, which can be modeled as a current source and a parallel capacitor, and amplifying electronics. The first stage of amplification, which is often called the preamplifier is critical in determining the performance of a fiber-optic receiver. A moderately low input resistance amplifier is often used as the preamplifier. The low input resistance allows for the RC time constant of the amplifier and the photodiode shunt capacitance to be small, allowing for large bandwidth operation. Since the input signal can be modeled as a current source, output voltages are desired, and large transresistances are required to amplify the low input currents, a transimpedance (transresistance) amplifier is often used.

Low cost transistor components can be used for low bandwith applications. Low data rate (corresponding to moderate bandwidth) fiber-optic links are often used in simple computer networks. For a 32 kbit/s link, a high frequency cutoff of approximately 22.4 kHz is required. With proper digital encoding, the low cutoff frequency is approximately 1 kHz. The minimum mid-band transresistance requirement is -2000. A photodiode with a 10 pF shunt capacitance and responsivity of 0.9 A/W is used. A $+6$ V power supply is available. The *npn* BJT parameters are:

$$\beta_F = 150, \quad V_A = 160\,\text{V}, \quad r_b = 30\,\Omega,$$
$$C_{ibo} = 8\,\text{pF} \quad \text{at} \quad V_{EB} = 0.5\,\text{V}, \quad C_{obo} = 4\,\text{pF} \quad \text{at} \quad V_{CB} = 5\,\text{V}, \quad \text{and} \quad f_T = 300\,\text{MHz}.$$

Design the fiber-optic preamplifier to meet the required specifications.

Solution:

The transimpedance amplifier topology is shown below:

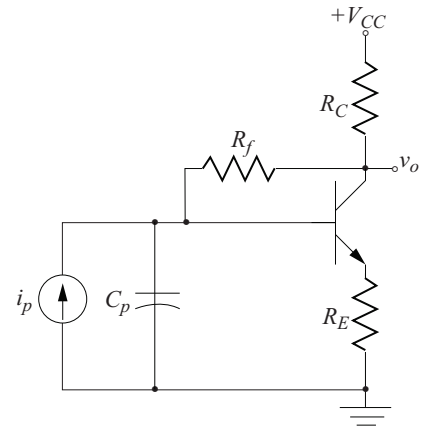

Since the transresistance must be at least $-2000\,\Omega$, let $R_f = 3.3\,\text{k}\Omega$, which will allow the amplifier to exceed the required specifications.

Also let $I_C = 3.8\,\text{mA}$ and $V_{CE} = 0.785\,\text{V}$. This allows for a small value for $r_\pi = 1.02\,\text{k}\Omega$ and $g_m = 0.146$.

Let the value of the emitter degenerative resistor $R_E = 27\,\Omega$, then the collector resistor is $R_C = 3.9\,\text{k}\Omega$.

The midband loaded forward amplifier is shown below:

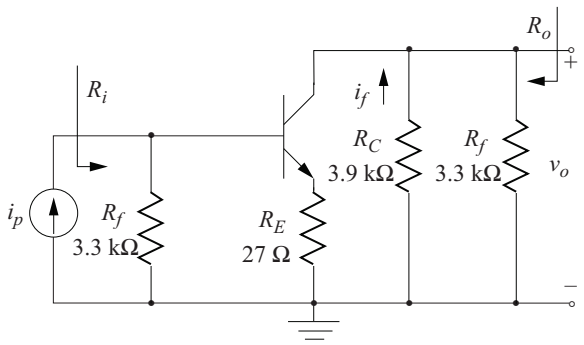

The feedback quantity is,

$$f = \frac{i_f}{v_o} = \frac{-1}{3300}.$$

The input resistance is,

$$R_i = 3300 \,\|\, [r_\pi + r_b + (1 + g_m r_\pi)\, 27] = 2\,\text{k}\Omega.$$

The output resistance is,

$$R_o = 3.9\,\text{k}//3.3\,\text{k} = 1.79\,\text{k}\Omega.$$

The amplifier forward transresistance is,

$$R_M = \frac{v_o}{i_p} = A_v R_i = -105.2\,\text{k}\Omega.$$

The feedback quantities of interest are:

$$D = 1 + Af = 32.9$$
$$R_{if} = \frac{R_i}{D} = 60.8\,\Omega \qquad R_{of} = \frac{R_o}{D} = 54.3\,\Omega$$
$$R_{Mf} = \frac{R_M}{D} = -3.2\,\text{k},$$

which meets the midband transresistance specification.

One finds the frequency response of the transimpedance amplifier by determining the capacitances for the BJT and the frequency response of the loaded forward amplifier.

$$CJC = C_{obo}\left(1 + \frac{V_{CB}}{0.75}\right)^{0.33} = 7.83\,\text{pF},$$
$$CJE = C_{ibo}\left(1 + \frac{V_{EB}}{0.75}\right)^{0.33} = 9.47\,\text{pF},$$
$$TF = \frac{1}{2\pi f_T} - \frac{\eta V_t}{|I_{CT}|}\left[\frac{CJE}{\left(1 - \frac{0.7}{0.75}\right)^{0.33}} + C_{obo}\right] = 460\,\text{ps},$$

and

$$C_\mu = \frac{CJC}{\left(1 + \frac{V_{CB}}{0.75}\right)^{0.33}} = 7.6\,\text{pF}.$$
$$C_\pi = \frac{g_m}{\omega_T} - C_\mu = 70\,\text{pF}.$$

The high-frequency response is found using the equations found in Table 9.3 for a Common-emitter with emitter-degeneration amplifier:

$$\omega_H = \frac{\left[R'_S + r_\pi + (1+\beta_F)\,R_E\right]}{\left[(1+\beta_F)\left(R'_S R_C + R'_S R_E + R_C R_E\right) + r_\pi\left(R'_S + R_C\right)\right]C_\mu + r_\pi\left(R'_S + R_E\right)C_\pi}$$
$$= 1.16\,\text{Grad/sec} \quad \Rightarrow \quad 184\,\text{kHz}.$$

Therefore, the high frequency cutoff of the feedback amplifier is,

$$\omega H = D \times 184\,\text{kHz} = 6.0\,\text{MHz}.$$

Which easily fulfills the specification for the high frequency cutoff.

Since the preamplifier does not use external capacitors, the low frequency response extends to DC.

11.7 PROBLEMS

11.1. The voltage gain of an amplifier is described by the following quantities:

midband gain - 1000

low 3 dB frequency - 100 Hz

high 3 dB frequency - 50 kHz

(a) Assume that the high- and low-frequency responses are characterized by single poles. Feedback is to be applied to increase the bandwidth of the amplifier by a factor of ten (10). Assuming the feedback network does not load the initial amplifier, what return difference is necessary to accomplish the design goal? Determine the new midband gain and the high and low 3 dB frequencies after the application of feedback.

(b) Upon a more careful analysis of the original amplifier (prior to application of feedback) it was discovered that a second high-frequency pole exists at 1 MHz. What effect will this second pole have on the feedback amplifier specified by the results of part a)?

11.2. An audio amplifier is described by two high-frequency poles at 25 kHz and 60 kHz. It is desired to increase the bandwidth with the application of feedback without significantly destroying the step response of the amplifier. A design goal of no more than 2% overshoot is established. Assuming that the feedback network will not change the pole location of the original amplifier, determine the following:

(a) the maximum high 3 dB frequency that can be obtained.

(b) the rise time before and after the application of feedback.

11.3. The response to an OpAmp non-inverting amplifier to a unit step voltage input is shown. Assume the amplifier frequency response is characterized by a single high-frequency pole.

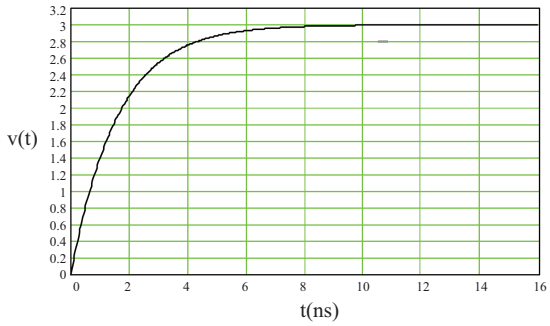

(a) Determine the high 3 dB frequency.

(b) Determine the gain bandwidth product (GBP) of the amplifier.

(c) If the OpAmp has an open loop gain of 110 dB, what is the 3 dB frequency of the OpAmp open loop gain?

11.4. An amplifier is described by two low-frequency poles at

$$f_{L1} = 50\,\text{Hz} \qquad f_{L2} = 4\,\text{Hz}.$$

(a) Determine the low 3 dB frequency of this amplifier.

(b) Estimate the sag that a 1 kHz square wave will experience passing through this amplifier.

(c) It is desired to reduce the sag to 1% with the application of feedback. What return ratio, D, will result in that amount of sag?

(d) What is the new 3 dB frequency of the resultant feedback amplifier?

11.5. The current gain of an amplifier is described by the following quantities:

midband gain - 10 A/mA

low 3 dB frequency - 120 Hz

high 3 dB frequency - 2.4 MHz

(a) Assume the high- and low-frequency responses are characterized by single poles. Feedback is to be applied to increase the high 3 dB frequency to 20 MHz. Assuming the feedback network does not load the initial amplifier, what return difference is necessary to accomplish the design goal? Determine the new midband gain and the low 3 dB frequency after the application of feedback.

(b) Upon a more careful analysis of the original amplifier (prior to the application of feedback) it was discovered that a second low-frequency pole exists at $f_{L2} = 10\,\text{Hz}$ and a second high-frequency poles exists at $f_{H2} = 48\,\text{MHz}$. What effect will these initially non-dominant poles have on the feedback amplifier specified by the results of part a)?

11.6. An audio amplifier is described by a midband gain of 420, a single low-frequency pole at:

$$f_{L1} = 100\,\text{Hz},$$

and two high-frequency poles at:

$$f_{H1} = 14\,\text{kHz} \quad \text{and} \quad f_{H2} = 26\,\text{kHz}.$$

The amplifier is to be redesigned as a feedback amplifier so that the midband region will be extended to at least cover the frequency range $40\,\text{Hz} \leq f \leq 20\,\text{kHz}$. Assuming that the application of feedback does not alter the original amplifier, determine the following properties of the redesigned amplifier:

(a) the minimum feedback ratio, f, that will accomplish the new design goals.

(b) the feedback return difference, D.

(c) the high and low 3 dB frequencies.

(d) the midband gain.

(e) are there any peaks in the frequency response? If so, determine the peak characteristics.

11.7. An audio amplifier is described by a midband gain of 251, two low-frequency poles at

$$f_{l1} = 60\,\text{Hz} \quad \text{and} \quad f_{l2} = 20\,\text{Hz},$$

and two high-frequency poles at

$$f_{h1} = 40\,\text{kHz} \quad \text{and} \quad f_{h2} = 100\,\text{kHz}.$$

The amplifier is to be redesigned as a feedback amplifier so that the midband region will be as large as possible without introducing any peaks in the frequency response. Assuming that the application of feedback does not alter the original amplifier, determine the following properties of the redesigned amplifier:

(a) the minimum feedback ratio, f, that will accomplish the new design goals.

(b) the feedback return difference, D.

(c) the high and low 3 dB frequencies.

(d) the midband gain.

11.8. A designer is attempting to create a feedback amplifier with a midband voltage gain of 40. The basic forward gain elements of this amplifier are two amplifier stages (each described by single high- and low-frequency poles) with properties:

	#1	#2
midband voltage gain	15	20
high 3 dB frequency	30 kHz	20 kHz
low 3 dB frequency	40 Hz	30 Hz

Assume that series interconnection of the amplifier stages does not change the above stated properties.

(a) Apply global feedback to the amplifier so that a gain of 40 is obtained and determine the resultant frequency response.

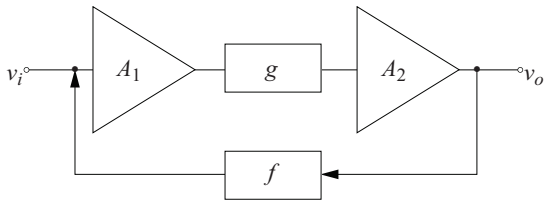

(b) Unfortunately the technique of part a results in significant peaks in the frequency response. An alternate approach is proposed whereby an attenuator is placed in the forward gain path as shown. Determine the values of the attenuation factor, g, and feedback ratio, f, that will result in maximum bandwidth, no peaks in the frequency response, and a voltage gain of 40. Note, for this configuration, the feedback gain is given by:

$$A_f = \frac{A_1 g A_2}{1 + f\ A_1 g A_2}.$$

(c) What are the high and low 3 dB frequencies for the amplifier designed in part b)?

11.9. Another circuit topology that might be used to accomplish the design goals of the previous problem incorporates both local and global feedback. For the topology shown, determine the local and global feedback ratios, f_{Local}, and f_{Global}, that will maximize the bandwidth and produce a voltage gain of 40 without introducing any peaks in the frequency response. The individual, non-interacting amplifier stages are described by:

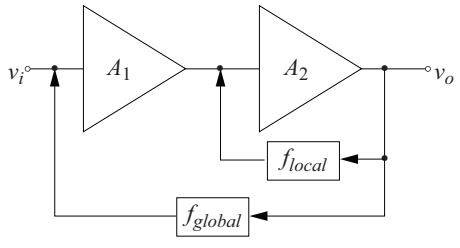

	#1	#2
midband voltage gain	15	20
high 3 dB frequency	30 kHz	20 kHz
low 3 dB frequency	40 Hz	30 Hz

11.10. A macromodel for a μA741 Bipolar OpAmp is provided in most SPICE-based circuit simulators.

(a) Use SPICE to determine the frequencies of the first two high-frequency poles of the μA741 OpAmp. Assume a resistive load of 820 Ω.

(b) Design a simple inverting amplifier with a voltage gain of −10. Use SPICE to determine the high 3 dB frequency of this amplifier.

(c) Compare the results of part b) to those predicted by feedback theory.

11.11. A macromodel for an LM324 Bipolar OpAmp is provided in most SPICE-based circuit simulators.

(a) Use SPICE to determine the frequencies of the first two high-frequency poles of the LM324 OpAmp. Assume a resistive load of 560 Ω.

(b) Design a simple non-inverting amplifier with a voltage gain of +8. Use SPICE to determine the high 3 dB frequency of this amplifier.

(c) Compare the results of part b) to those predicted by feedback theory.

11.12. A macromodel for an LF411 JFET input OpAmp is provided in most SPICE-based circuit simulators.

(a) Use SPICE to determine the frequencies of the first two high-frequency poles of the LF411 OpAmp. Assume a resistive load of 1 kΩ.

(b) Design a simple non-inverting amplifier with a voltage gain of +15. Use SPICE to determine the high 3 dB frequency of this amplifier.

(c) Compare the results of part b) to those predicted by feedback theory.

11.13. The transistors in the given feedback amplifier circuit are 2N2222. The quiescent conditions have been previously determined to be:

$$I_{c1} \approx I_{c2} \approx 2.0\,\text{mA}.$$

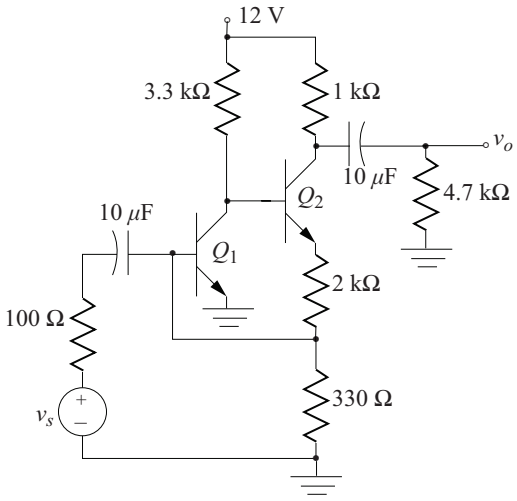

(a) Determine the midband voltage gain and approximate 3 dB frequencies of the amplifier.

(b) Compare hand calculations to PSpice simulation.

11.14. For the single stage feedback amplifier shown, determine the high and low 3 dB frequencies.

The FET parameters are:

$$K = 1\,\text{mA/V}^2 \qquad C_{rss} = 1.3\,\text{pF}$$
$$V_T = 1.5\,\text{V} \qquad C_{iss} = 5.0\,\text{pF}$$
$$V_A = 160\,\text{V}.$$

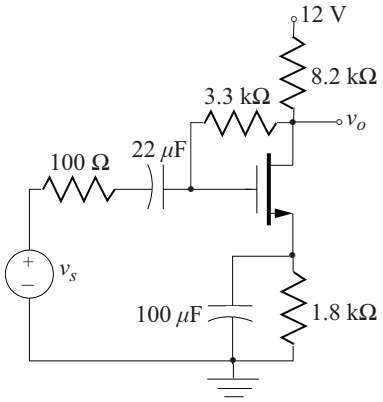

11.15. The transistors in the given feedback amplifier circuit are 2N3904. The quiescent conditions have been previously determined to be:

$$I_{c1} \approx I_{c2} \approx 1.32\,\text{mA}.$$

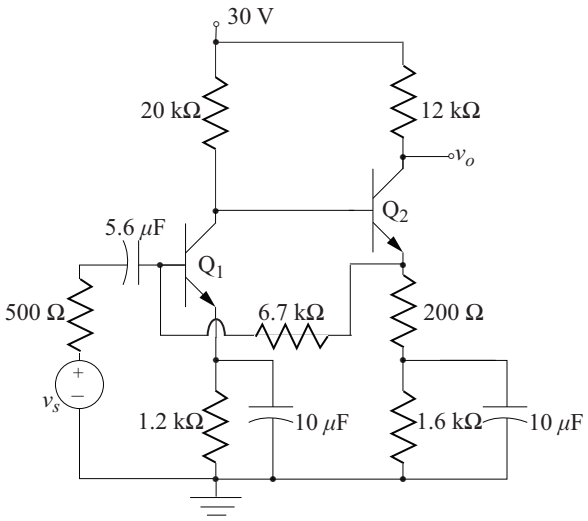

(a) Determine the midband voltage gain and approximate 3 dB frequencies of the amplifier.

(b) Compare hand calculations to PSpice simulation.

11.16. For the amplifier shown, determine the high and low 3 dB frequencies. The JFETs are described by:

$$V_{PO} = -2\,\text{V} \quad I_{DSS} = 4\,\text{mA} \quad V_A = 200\,\text{V}$$
$$C_{rss} = 1.0\,\text{pF} \quad C_{iss} = 5.0\,\text{pF}.$$

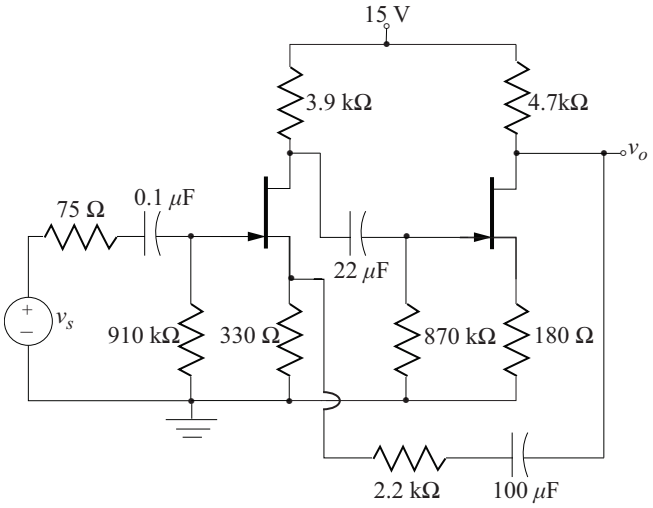

Verify the analysis using SPICE.

11.17. The transistor in the given feedback amplifier circuit is a 2N3904 (description is given in the PSpice libraries).

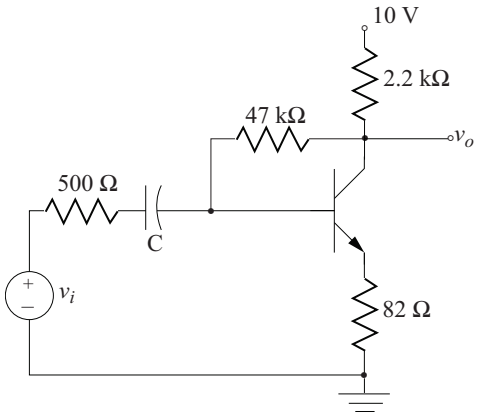

(a) Complete the amplifier design by determining a realistic value for the capacitor, C, that will result in a low 3 dB frequency $\approx$ 100 Hz.

(b) Determine the high 3 dB frequency of the amplifier.

(c) Use SPICE to determine the high and low 3 dB frequencies of the final design: compare the simulation results to hand calculations. Comment.

11.18. Determine the high and low 3 dB frequencies for the feedback amplifier shown. Assume the following circuit parameters:

BJTs - 2N2222

Coupling capacitors - 10 μF

Bypass capacitor - 1000 μF

Feedback capacitor - 1000 μF .

Compare results to SPICE simulation.

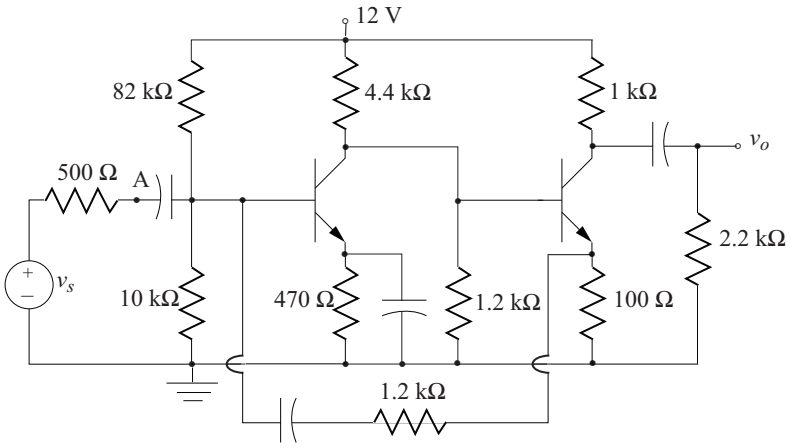

11.19. Compute the high and low 3 dB frequencies for the amplifier of the previous problem if the mixing point is moved to location "A." Compare results to SPICE simulation.

11.20. Determine the high and low 3 dB frequencies for the feedback amplifier shown. Assume the following circuit parameters:

BJTs - 2N2222

Coupling capacitors - 20 μF

Bypass capacitor - 2200 μF

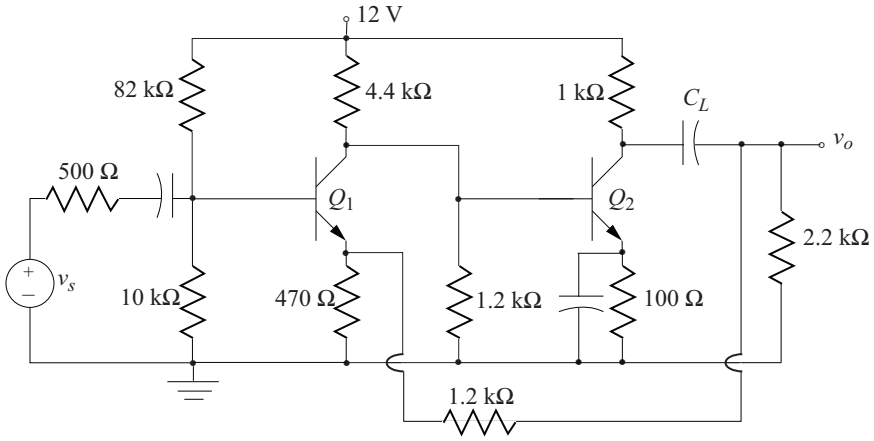

(a) Compare results to SPICE simulation.

(b) The frequency response for this circuit is not flat in the midband. Modify the circuit so that the midband region is flat. Use SPICE to verify that the design modifications improve the midband region.

11.21. In the previous problem the load capacitor, C_L, is included within the feedback amplifier due to the sampling point of the feedback network. Assume the sampling point is moved to the collector of Q_2 and a 100 μF capacitor is inserted in series with the 1.2 kΩ feedback resistor: this change essentially removes C_L from the feedback amplifier.

(a) Determine the high and low 3 dB frequencies of the modified circuit.

(b) Compare results to SPICE simulation.

11.22. A particular series-shunt feedback amplifier can be described as having a midband voltage gain of 10,000 with three high-frequency poles at the following frequencies:

$$f_{p1} = 1\,\text{MHz} \quad f_{p2} = 4\,\text{MHz} \quad f_{p3} = 25\,\text{MHz},$$

(a) Write an expression for A_v as a function of frequency.

(b) Draw the idealized Bode magnitude and phase plots. On the graph label all slopes and use a small circle to indicate where the slope changes.

(c) At what frequency will this feedback amplifier oscillate (if it oscillates at all)?

(d) In order to have at least 45° phase margin, what is the amount of feedback that can be added? Is this a maximum or a minimum for stable amplifier operation?

(e) What is the gain margin for the amount of feedback determined in part c)?

11.23. An amplifier can be described by a midband gain of 251, two low-frequency poles at

$$f_{l1} = 60\,\text{Hz} \quad \text{and} \quad f_{l2} = 20\,\text{Hz},$$

and four high-frequency poles at

$$f_{h1} = 40\,\text{kHz} \quad f_{h2} = 100\,\text{kHz} \quad f_{h3} = 200\,\text{kHz} \quad \text{and} \quad f_{h4} = 1\,\text{MHz}.$$

(a) Draw the idealized Bode magnitude and phase plots. On the graph label all slopes and use a small circle to indicate where the slope changes. Compare these straight-line approximate curves to exact curves (use a software package to generate the exact curves).

(b) At what frequency will this feedback amplifier oscillate (if it oscillates at all)?

(c) In order to achieve a gain margin of at least 5 dB, what is the amount of feedback that can be added? Is this a maximum or a minimum for stable amplifier operation?

(d) What is the phase margin for the amount of feedback determined in part c)?

11.24. If the loop gain of an inverting amplifier is

$$A(j\omega)\,f = \frac{-250}{(1+j\omega)(1+j0.01\omega)^2}.$$

Determine whether the amplifier is stable using:

(a) the Nyquist plot

(b) the gain and phase plot of the loop gain.

11.25. The loop gain of an inverting amplifier is

$$A(j\omega)\,f = \frac{-K}{(1+j0.01\omega)^3}.$$

(a) If $K = 5$, is the amplifier stable?

(b) What value of K defines a gain margin of greater than 10 dB and phase margin of greater than 50°?

11.26. The loop gain of an amplifier is

$$A(j\omega) = \frac{24000}{\left(1+\dfrac{j\omega}{2\times 10^5}\right)^2\left(1+\dfrac{j\omega}{10^5}\right)}.$$

with a feedback factor $f = -5$,

(a) plot the magnitude and phase of the loop gain

(b) determine whether the amplifier is stable. If the amplifier is stable, determine the gain and phase margins.

11.27. An OpAmp with an open loop gain of

$$A(j\omega) = \frac{10^5}{\left(1 + \frac{j\omega}{10^5}\right)^2 \left(1 + \frac{j\omega}{10^2}\right)}.$$

is used to design an inverting amplifier with a gain of -125. Determine the gain and phase margins of the inverting amplifier using:

(a) the Nyquist plot

(b) the gain and phase plot of the loop gain.

11.28. Sketch the Nyquist plot of the loop gain for a three pole amplifier with a DC open loop gain of $A_o = -1100$, and open-loop poles at 500 kHz, 1.1 MHz, and 1.8 MHz. Determine whether the amplifier is stable with the following feedback factors:

(a) $f = -0.005$

(b) $f = -0.02$

(c) Determine the maximum value of f for which the amplifier is stable.

11.29. A three pole amplifier has an open-loop DC gain of -1000 and poles located at 1.1 MHz, 12 MHz, and 28 MHz. Dominant pole compensation is applied to the amplifier.

(a) Find the proper location of the dominant pole.

(b) Determine the maximum value of the feedback factor f for which this compensated amplifier is marginally stable.

(c) Determine the maximum value of the feedback factor f for which this compensated amplifier has a gain margin greater than 10 dB and phase margin of at least 50°?

11.30. Lag-lead compensation is used with an amplifier with a DC gain of -1200 and poles at 1 MHz, 10 MHz, and 220 MHz. The zero of the compensation network is selected to cancel the 1 MHz pole of the uncompensated amplifier.

(a) Find the pole of the lag-lead compensation network so that the amplifier is stable with a phase margin of 50° when the feedback factor is $f = -0.01$.

(b) Determine the bandwidth of the compensated feedback amplifier.

11.31. An inverting OpAmp inverting amplifier is to be stabilized using lead compensation, as shown. The OpAmp input and output resistances are $R_i = 1\,\text{M}\Omega$ and $R_o = 75\,\Omega$. The open-loop gain of the OpAmp is

$$A(j\omega) = \frac{24000}{\left(1 + \dfrac{j\omega}{2 \times 10^5}\right)^2 \left(1 + \dfrac{j\omega}{10^5}\right)}.$$

(a) Complete the design for a phase margin of 50°.

(b) Confirm the result with SPICE.

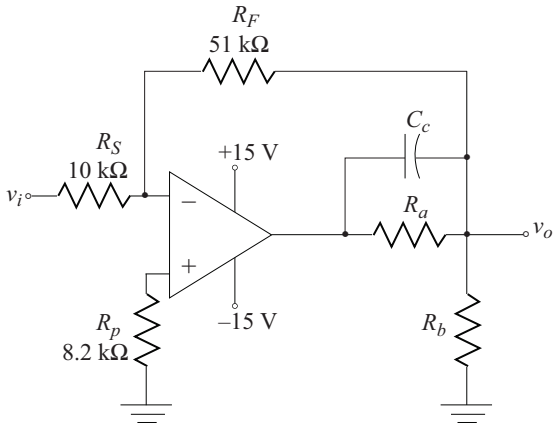

11.32. An inverting OpAmp inverting amplifier is to be stabilized using dominant pole compensation, as shown. The OpAmp input and output resistances are:

$$R_i = 1\,\text{M}\Omega \quad \text{and} \quad R_o = 75\,\Omega.$$

The open-loop gain of the OpAmp is:

$$A(j\omega) = \frac{24000}{\left(1 + \dfrac{j\omega}{2 \times 10^5}\right)^2 \left(1 + \dfrac{j\omega}{10^5}\right)}.$$

(a) Complete the design for a phase margin of 50°.

(b) Confirm the result with SPICE.

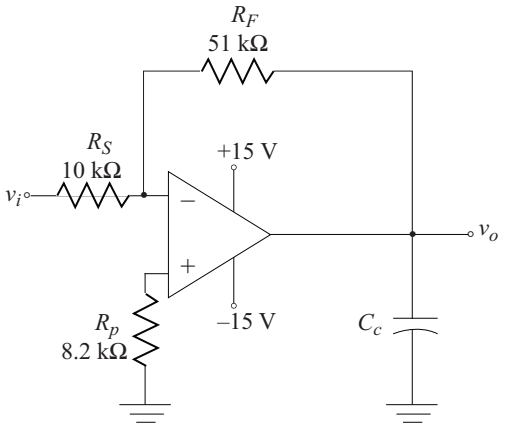

11.33. The lag-lead compensated amplifier shown uses an OpAmp with input and output resistances of $R_i = 1\,\text{M}\Omega$ and $R_o = 75\,\Omega$, respectively. The open-loop gain of the OpAmp is

$$A(j\omega) = \frac{1000}{\left(1 + \dfrac{j\omega}{2\pi \times 10^6}\right)\left(1 + \dfrac{j\omega}{2\pi \times 10^6}\right)}.$$

(a) Complete the design for a phase margin of 50°.

(b) Confirm the result with SPICE.

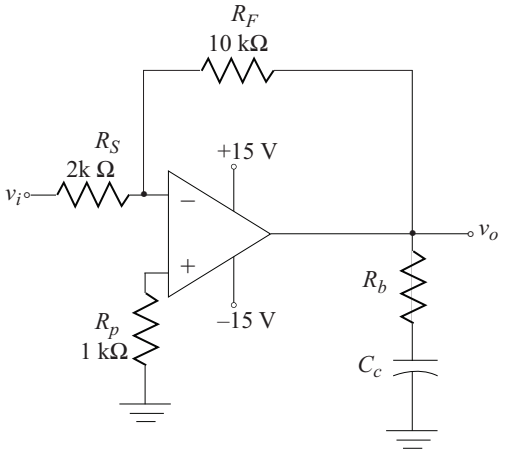

11.34. For the shunt-series feedback amplifier shown below, the transistor characteristics are:

NPN: $\beta_F = 200$, $V_A = 120$ V, CJC = 7.31 pF, CJE = 22.01 pF, and TF = 411 ps

PNP: $\beta_F = 200$, $V_A = 100$ V, CJC = 14.76 pF, CJE = 19.82 pF, and TF = 603.7 ps.

(a) Determine the value of the feedback resistor, R_f, for unstable amplifier operation.

(b) Using the value of R_f found in a), design a stable dominant pole compensated amplifier.

(c) Confirm the results using SPICE.

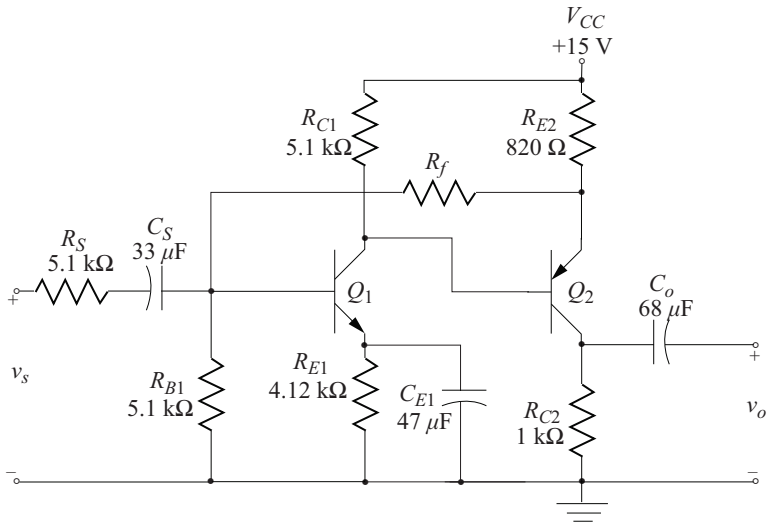

11.35. Design a lead compensated amplifier using the result found in part a) of Problem 11.34. Confirm the results using SPICE.

11.36. Design a lag-lead compensated amplifier using the result found in part a) of Problem 11.34. Confirm the results using SPICE.

11.37. For the differential amplifier shown, assume identical transistors with

$$\beta_F = 120, \quad V_A = 175\,\text{V}, \quad \text{CJE} = 19\,\text{pF}, \quad \text{CJE} = 36\,\text{pF}, \quad \text{and} \quad \text{TF} = 3.3\,\text{ns}.$$

(a) Determine the value of the feedback resistor, R_{f1}, for unstable amplifier operation.

(b) Using the value of R_{f1} found in a), design a stable dominant pole compensated amplifier.

(c) Confirm the results using SPICE.

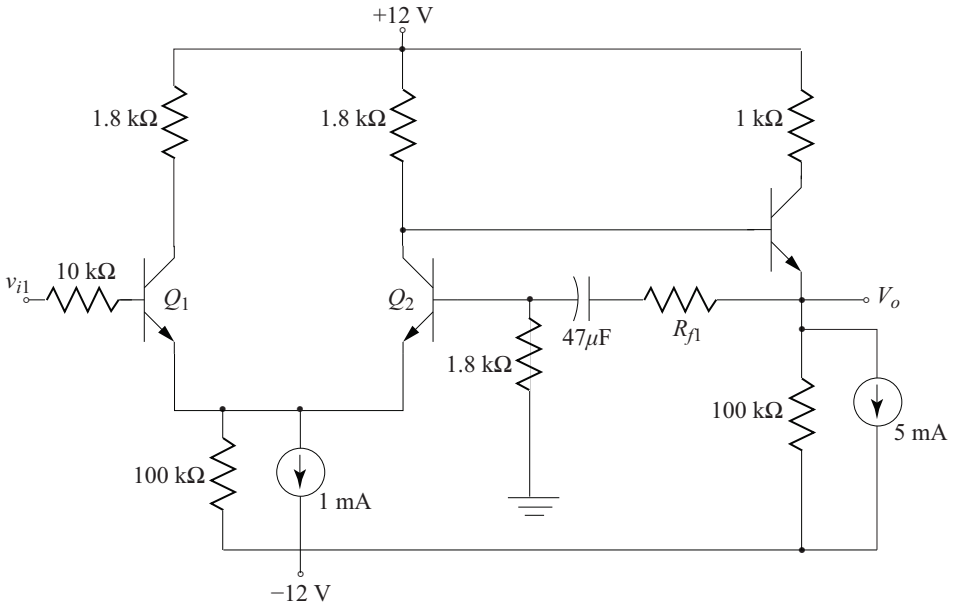

11.38. Design a lead compensated amplifier using the result found in part a) of Problem 11.37. Confirm the results using SPICE.

11.39. The amplifier shown uses identical NMOSFETs with the following characteristics:

$$K = 1.25\,\text{mA/V}^2, \quad V_T = 2\,\text{V}, \quad V_A = 150\,\text{V}, \quad C_{iss} = 12\,\text{pF}, \quad C_{rss} = 2\,\text{pF}.$$

(a) Determine the value of the feedback resistor, R_f, for unstable amplifier operation.

(b) Using the value of R_f found in a), design a stable dominant pole compensated amplifier.

(c) Confirm the results using SPICE.

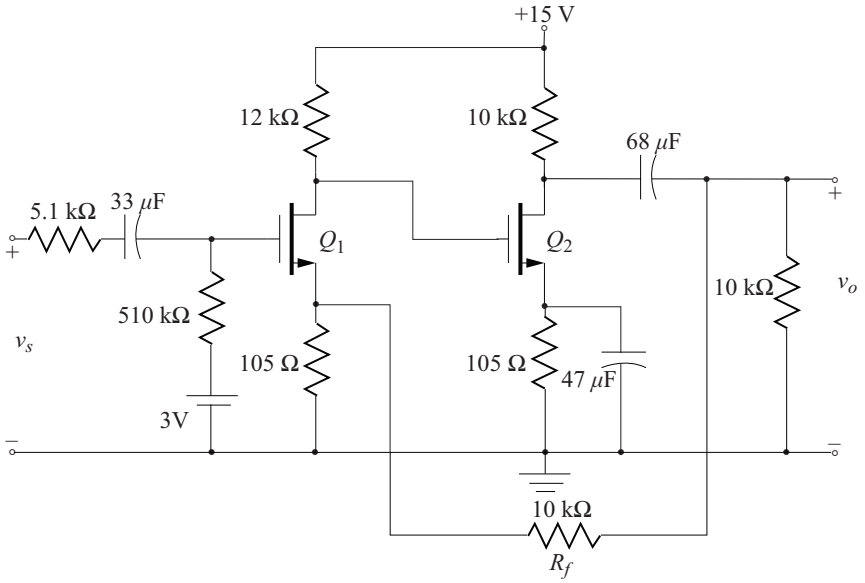

11.40. Design a lead compensated amplifier using the result found in part a) of Problem 11.39. Confirm the results using SPICE.

11.41. Design an analog amplifier to meet the following specifications:

- Input - a differential amplifier
- Input voltage - at least ± 1 mV
- Midband voltage gain - 1000 $\pm$ 10
- Midband input resistance - at least 1 MΩ
- Midband output resistance - less than 100 Ω
- Low 3 dB frequency - 100 Hz, maximum
- High 3 dB frequency - 1 MHz, minimum

Design limitations are:

- Coupling capacitors are to be limited to 1 μF, maximum
- Bypass capacitors are to be limited to 1000 μF, maximum
- *At least* one BJT *and* one JFET must be used .

Active devices are limited to the following types:

- 2N2222A NPN bipolar transistor

- 2N2907A PNP bipolar transistor
- 2N3904 NPN bipolar transistor
- 2N3906 PNP bipolar transistor
- 2N3819 N-channel Junction field effect transistor
- 2N4393 N-channel Junction field effect transistor

A report on the design is required. Minimum requirements for the report include:

- A complete theoretical analysis of the design
- SPICE verification of design specifications
- Comparisons, conclusions, and comments

11.42. Design an analog feedback amplifier to meet the following specifications:

- Midband voltage gain - 100 $\pm$ 5 (driving a 1 kΩ load)
- Midband input resistance - at least 40 kΩ
- Midband output resistance - less than 50 Ω
- Low 3 dB frequency - 30 Hz, maximum
- High 3 dB frequency - 10 MHz, minimum
- Output voltage swing - $\pm$4 V (from Q point), minimum

Design limitations are:

- Coupling capacitors are to be limited to 1 μF, maximum
- Bypass capacitors are to be limited to 1000 μF, maximum

Active devices are limited to the following types:

- 2N2222A NPN bipolar transistor
- 2N2907A PNP bipolar transistor
- 2N3904 NPN bipolar transistor
- 2N3906 PNP bipolar transistor
- 2N3819 N-channel JFET
- 2N4393 N-channel JFET

A report on the design is required. Minimum requirements for the report include

- A complete theoretical analysis of the design
- SPICE verification of design specifications
- Comparisons, conclusions, and comments.

REFERENCES

[1] D'Azzo, J. J. and Houpis, C. H., *Linear Control System Analysis and Design: Conventional and Modern,* 3rd ed., McGraw-Hill Book Company, New York, 1988.

[2] Fitchen, F. C., *Transistor Circuit Analysis and Design*, Van Nostrand Company, Princeton, 1966.

[3] Ghausi, M. S., *Electronic Devices and Circuits: Discrete and Integrated*, Holt, Rinehart and Winston, New York, 1985.

[4] Gray, P. R. and Meyer, R. G., *Analysis and Design of Analog Integrated Circuits,* 3rd ed., John Wiley & Sons, Inc., New York, 1993.

[5] Millman, J., *Microelectronics: Digital and Analog Circuits and Systems*, McGraw-Hill Book Company, New York, 1979.

[6] Millman, J. and Halkias, C. C., *Integrated Electronics: Analog and Digital Circuits and Systems*, McGraw-Hill Book Company, New York, 1972.

[7] Nise, N. S., *Control Systems Engineering*, Benjamin/Cummings Publishing Company, Redwood City, 1992.

[8] Rosenstark, S., *Feedback Amplifier Principles*, Macmillan Publishing Company, New York, 1986.

[9] Sedra, A. S. and Smith, K. C., *Microelectronic Circuits,* 3rd ed., Holt, Rinehart, and Winston, Philadelphia, 1991.

[10] Schilling, D. L. and Belove, C., *Electronic Circuits,* 3rd ed., McGraw-Hill Book Company, New York, 1989.

Authors' Biographies

Thomas F. Schubert, Jr., and Ernest M. Kim are colleagues in the Electrical Engineering Department of the Shiley-Marcos School of Engineering at the University of San Diego.

THOMAS F. SCHUBERT, JR.

Thomas Schubert received BS, MS, and PhD degrees in Electrical Engineering from the University of California at Irvine (UCI). He was a member of the first engineering graduating class and the first triple-degree recipient in engineering at UCI. His doctoral work discussed the propagation of polarized light in anisotropic media.

Dr. Schubert arrived at the University of San Diego in August, 1987 as one of the two founding faculty of its new Engineering Program. From 1997–2003, he led the Department as Chairman, a position that became Director of Engineering Programs during his leadership tenure. Prior to coming to USD, he was at the Space and Communications Division of Hughes Aircraft Company, the University of Portland, and Portland State University. He is a Registered Professional Engineer in the State of Oregon.

In 2012, Dr. Schubert was awarded the Robert G. Quinn Award by the American Society of Engineering Education "in recognition of outstanding contributions in providing and promoting excellence in engineering experimentation and laboratory instruction."

ERNEST M. KIM

Ernest Kim received his B.S.E.E. from the University of Hawaii at Manoa in Honolulu, Hawaii in 1977, an M.S.E.E. in 1980 and Ph.D. in Electrical Engineering in 1987 from New Mexico State University in Las Cruces, New Mexico. His dissertation was on precision near-field exit radiation measurements from optical fibers.

Dr. Kim worked as an Electrical Engineer for the University of Hawaii at the Naval Ocean Systems Center, Hawaii Labs at Kaneohe Marine Corps Air Station after graduating with his B.S.E.E. Upon completing his M.S.E.E., he was an electrical engineer with the National Bureau of Standards in Boulder, Colorado designing hardware for precision fiber optic measurements. He then entered the commercial sector as a staff engineer with Burroughs Corporation in San Diego, California developing fiber optic LAN systems. He left Burroughs for Tacan/IPITEK Corporation as Manager of Electro-Optic Systems developing fiber optic CATV hardware and systems. In 1990 he joined the faculty of the University of San Diego. He remains an active consultant in radio frequency and analog circuit design, and teaches review courses for the engineering Fundamentals Examination.

Dr. Kim is a member of the IEEE, ASEE, and CSPE. He is a Licensed Professional Electrical Engineer in California.